MIT-2344-1
MITNE-49

STUDIES OF REACTIVITY AND RELATED PARAMETERS IN SLIGHTLY ENRICHED URANIUM, HEAVY WATER LATTICES

by

B. K. Malaviya,

I. Kaplan, D. D. Lanning, A. E. Profio, T. J. Thompson

Contract AT (30-1) 2344

U. S. Atomic Energy Commission

May 25, 1964

Department of Nuclear Engineering
Massachusetts Institute of Technology
Cambridge, Massachusetts

MASSACHUSETTS INSTITUTE OF TECHNOLOGY
DEPARTMENT OF NUCLEAR ENGINEERING
Cambridge 39, Massachusetts

STUDIES OF REACTIVITY AND RELATED PARAMETERS IN SLIGHTLY ENRICHED URANIUM, HEAVY WATER LATTICES

by

B. K. MALAVIYA,
I. KAPLAN, D. D. LANNING, A. E. PROFIO, T. J. THOMPSON

May 25, 1964

MIT - 2344 - 1
AEC Research and Development Report
UC - 34 Physics
(TID - 4500, 31st Edition)

Contract AT(30-1)2344
U. S. Atomic Energy Commission

DISTRIBUTION

MIT-2344-1

AEC Research and Development Report

UC - 34 Physics

(TID - 4500, 31st Edition)

1. USAEC, New York Operations Office (D. Richtmann)
2. USAEC, Division of Reactor Development (P. Hemmig)
3. USAEC, New York Patents Office (H. Potter)
4. USAEC, Division of Reactor Development, Reports and Statistics Branch
5. USAEC, Maritime Reactors Branch
6. USAEC, Civilian Reactors Branch
7. USAEC, Army Reactors Branch
8. USAEC, Naval Reactors Branch
9. Advisory Committee on Reactor Physics (E. R. Cohen)
10. ACRP (G. Dessauer)
11. ACRP (D. de Bloisblanc)
12. ACRP (M. Edlund)
13. ACRP (R. Ehrlich)
14. ACRP (I. Kaplan)
15. ACRP (J. Chernick)
16. ACRP (F. C. Maienschein)
17. ACRP (R. Avery)
18. ACRP (P. F. Zweifel)
19. ACRP (P. Gast)
20. ACRP (G. Hansen)
21. ACRP (S. Krasik)
22. ACRP (L. W. Nordheim)
23. ACRP (T. M. Snyder)
24. ACRP (J. J. Taylor)

25. - 27. O.T.I.E., Oak Ridge, for Standard Distribution, UC-34, TID-4500 (31st Edition)

28. - 49. B. K. Malaviya

50. - 150. Internal Distribution

ABSTRACT

The kinetic behavior of a neutron transport medium which is irradiated by a burst of fast neutrons has been investigated on the basis of several theoretical models. Expressions have been derived for the prompt neutron decay constant of the asymptotic thermal flux in a subcritical multiplying system. These expressions relate the decay constant of a subcritical assembly to various parameters of interest.

Pulsed neutron experiments were made with subcritical assemblies in the M.I.T. Lattice Facility to measure lattice parameters. The pulsed neutron method has also been applied to the measurement of absolute reactivity and the reactivity worth of control rods in far subcritical assemblies. Concurrently with the pulsed neutron studies, steady-state exponential experiments with control rods have also been undertaken.

Die-away experiments on pure moderator assemblies in the M.I.T. Lattice Facility were made to measure the thermal neutron diffusion parameters of heavy water at room temperature and the effect of thermally black rods inserted axially in a cylindrical moderator assembly. Pulsed neutron runs on unperturbed lattices were used to evaluate such lattice parameters as k_∞, L^2, k, f_m, B_m^2, etc. These values are in agreement, within experimental uncertainties, with the results of steady-state exponential experiments and of calculations based on the THERMOS code.

Pulsed neutron experiments on perturbed lattices were made to find prompt neutron lifetime and the absolute negative reactivity of the assembly. The worths of control rods have also been measured. The pulsed neutron and steady-state experiments for the measurement of the reactivity effect of control rods give results which agree within the experimental uncertainties. Two-group theory, with no allowance for absorption in the fast group, is found to underestimate the worth of the rod by a few per cent. The conditions for the validity of control rod experiments in exponential assemblies have been considered. Suggestions for extending the techniques developed in this work and for refining the results have also been included.

ACKNOWLEDGMENTS

The experimental aspect of a project of this magnitude, involving diversified experimental equipment and a variety of specialized techniques is, of necessity, predicated upon the advice and coöperation of a number of individuals and groups. The present report and the results presented herein are due to the work of the principal author, Bimal Kumar Malaviya, who has submitted substantially this same thesis in partial fulfillment of the requirements of a Ph.D. degree from Harvard University. He wishes to acknowledge the encouragement and kindness of Dean H. Brooks of Harvard.

The over-all direction of the M.I.T. Heavy Water Lattice Project is shared by Professors I. Kaplan, T. J. Thompson and D. D. Lanning. Dr. A. E. Profio (now at General Atomic) was, at an earlier time, associated with the Project.

The technical staffs of the Lattice Project, the M.I.T. Reactor, the Reactor Machine Shop, the Reactor Electronics Shop and the Radiation Protection Office have provided assistance and advice during the experimental phase of this work. Mr. D. Gwinn especially has been of very material help in designing the pulsed neutron equipment and with the electronics. The secretarial work involved in producing this report was very ably handled by Mrs. M. Bosco.

Much of the reduction of data has been done with the aid of the IBM 7090 electronic computer, and the willing coöperation of the staff of the M.I.T. Computation Center is gratefully acknowledged.

TABLE OF CONTENTS

TABLE OF CONTENTS (Continued)

TABLE OF CONTENTS (Continued)

TABLE OF CONTENTS (Continued)

TABLE OF CONTENTS (Concluded)

LIST OF FIGURES

LIST OF FIGURES (Continued)

LIST OF FIGURES (Concluded)

LIST OF TABLES

INTRODUCTION

One of the general aims of research in Reactor Physics is the application and development of a variety of methods of studying the physics of subcritical neutron multiplying assemblies. The difficulty of obtaining information about reactor physics from reactors operating at power has led to the development of more economical methods involving the use of zero-power critical assemblies and exponential assemblies (1, 2, 3). These have now been supplemented by "miniature" lattices (4), PCTR-type assemblies (5), two-region substitution experiments (2) and, in the limit, single rod experiments (6) for the investigation of reactor parameters. The M.I.T. Lattice Research Project is trying to extend the use of independent, economical methods of obtaining information about assemblies moderated with heavy water. Lattices of uranium rods in heavy water are being studied in steady-state exponential experiments, in miniature assemblies, and in experiments with single rods or a few rods. The pulsed neutron technique has also been applied to lattices far below critical, and the present report is the first extensive summary of the work done at M.I.T. with the technique.

The pulsed neutron technique has the practical advantage (7) that it can be used in small systems, is comparatively simple and yet capable of yielding results with satisfactory accuracy even for the reactivity, which has generally necessitated an operating reactor or a critical assembly. The exploration of ways in which this technique can be used in subcritical assemblies is desirable, not only for its practical usefulness but also for the increased understanding that it affords of the relations among the various lattice parameters.

The present investigation has for its primary experimental goal the exploration of the pulsed neutron technique as a means of measuring lattice parameters and large absolute reactivities in subcritical assemblies. To make such a study self-contained, a number of related pulsed neutron studies on non-multiplying pure moderator systems and on non-perturbed multiplying systems are necessary. The diffusion parameters of heavy water at room temperature have been measured in die-away

pulsed neutron experiments over a wide range of values of the geometrical buckling. These parameters have been used in the interpretation of measurements of the geometrical buckling of moderator assemblies with different size absorbing rods inserted along the axis. Die-away experiments have been made in a lattice of uranium rods in heavy water, with the heavy water at different heights, to study the relationship between the prompt neutron decay constant and the geometrical buckling for a simple multiplying system, and to explore the potential of this correlation in yielding values of the various lattice parameters, including k_∞ and L^2 (the thermal diffusion area). These parameters and the measured geometrical bucklings from moderator experiments have been used to evaluate the prompt neutron lifetime in the lattice without and with the control rods; together with a calculated value of $\bar{\beta}$ (the effective yield of delayed neutrons), the prompt neutron lifetime then provides the proportionality constant relating the prompt neutron decay constant with the reactivity without and with the individual absorbing rods inserted. The change in geometrical buckling produced by the control rods in the lattice assembly has been obtained from the measured decay constants and lattice parameters. Other pulsed neutron reactivity methods, e.g., the $k\beta/\ell$ method, have also been examined. Concurrently with these pulsed neutron experiments, steady-state experiments, involving foil activation methods, have been made with control rods in the exponential assembly to measure the reactivity effect of the control rods. The extrapolation distance of black cylinders has been measured in steady-state exponential experiments in the moderator. Flux distributions in the radial direction have been measured (with the control rods in the assembly) to investigate the conditions under which measurements in exponential experiments are applicable to critical systems. Intercomparisons between stationary and pulsed neutron methods, and also with theory, have been made in an attempt to evaluate the different approaches.

Chapter I traces some of the basic concepts relating to reactor kinetics parameters and discusses the importance of reactivity studies and some of the common methods of reactivity measurement. A detailed theoretical treatment of a neutron transport medium, especially a subcritical multiplying system, bombarded by a fast neutron burst, is

undertaken in Chapter II, and expressions are derived for the decay constant of the asymptotic thermal flux under different conditions. These expressions are examined for possible experimental applications and a literature survey is attempted in Chapter III. Chapter IV relates to the theoretical basis and applications of exponential experiments with control rods which produce changes in reactivity. The design, construction and operation of the experimental equipment are the subject of Chapter V. Chapter VI presents a brief review and some aspects of control rod theory. The results of the measurements are presented and discussed in Chapter VII. Finally, in the last chapter, the main conclusions from this study are sought and recommendations are made for future work, indicating the lines along which this investigation can be continued. The Appendices provide supplementary information about notation, special computer codes prepared for this work, the theoretical calculations of lattice parameters, accelerator operation, and some of the special methods used in the analysis of data for the subcritical pulsed neutron reactivity determination.

REFERENCES

1. A. M. Weinberg and E. P. Wigner, The Physical Theory of Neutron Chain Reactors, The University of Chicago Press, Chicago (1958).

2. J. A. Thie, Heavy Water Exponential Experiments, Pergamon Press, New York (1961).

3. I. Kaplan, NYO-10,207; MITNE-25 (1962).

4. J. Peak, I. Kaplan and T. J. Thompson, NYO-10,204 (1962).

5. R. E. Heineman, Proc. Int. Conf. on Peaceful Uses of Atomic Energy, Geneva, Vol. 12, 15P/1929, p. 650 (1958).

6. L. W. Zink and G. W. Rodeback, NAA-SR-5392 (1960).

7. A. V. Antonov et al., Proc. Int. Conf. on Peaceful Uses of Atomic Energy, Geneva, Vol. 5, P/661, p. 3 (1955).

Chapter I

REACTIVITY: CONCEPT AND MEASUREMENT

A physical system can be conveniently described in terms of a mathematical formulation that states a basic requirement of continuity. From such a formulation, the concepts relating to the system and the parameters defining it are best understood. For a chain-reacting system, the basic equation is a Boltzmann-type equation of continuity[1] which describes the conservation of the neutron population in a closed region. The equation in its general form[2] can be written as

$$\frac{\partial}{\partial t} N(\vec{r},\vec{\Omega},u,t) + \vec{v} \cdot \nabla N(\vec{r},\vec{\Omega},u,t) + \Sigma_t(\vec{r},u)\, vN(\vec{r},\vec{\Omega},u,t)$$

$$= \int_{u-\epsilon_e}^{u} du' \int d\vec{\Omega}'v'\Sigma_e(\vec{r},u')\, N(\vec{r},\vec{\Omega}',u',t)\, g_e(\vec{\Omega}',u';\vec{\Omega},u)$$

$$+ \int_{u-\epsilon_i}^{u} du' \int d\vec{\Omega}'v'\Sigma_i(\vec{r},u')\, N(\vec{r},\vec{\Omega}',u',t)\, g_i(\vec{\Omega}',u';\vec{\Omega},u)$$

$$+ g_f(u) \int_0^{\infty} du' \int d\vec{\Omega}'v'\nu(u')\, \Sigma_f(\vec{r},u')\, N(\vec{r},\vec{\Omega},u',t)$$

$$+ S^{ext}(\vec{r},\vec{\Omega},u,t)\ , \qquad (1.1)$$

where

$N(\vec{r},\vec{\Omega},u,t)\, d\vec{r}\, d\vec{\Omega}\, du$ = the number of neutrons whose position vectors lie in the volume element $d\vec{r}$ about $\vec{r}$, whose velocities lie in the solid angle $d\vec{\Omega}$ about $\vec{\Omega}$ and whose lethargies are between u and u+du, all measured at time t;

$\Sigma_t(\vec{r},u)$ = the macroscopic total cross-section
$= \Sigma_e(\vec{r},u) + \Sigma_i(\vec{r},u) + \Sigma_a(\vec{r},u)$, Σ_e, Σ_i, and Σ_a being, respectively, the macroscopic elastic scattering, inelastic scattering and absorption cross-sections;

$g_e(\vec{\Omega}',u';\vec{\Omega},u)$ = relative probability of a neutron being left with velocity parameters $(\vec{\Omega},u)$ as a result of an elastic collision before which its velocity parameters were $(\vec{\Omega}',u')$;

$g_i(\vec{\Omega}',u';\vec{\Omega},u)$ = a similar quantity for inelastic collision;

$u - \epsilon_e$ = lowest lethargy from which neutrons may be elastically scattered into u;

$u - \epsilon_i$ = a similar quantity for inelastic scattering;

$g_f(u)$ = the relative probability that a fission neutron is born with lethargy u;

Σ_f = macroscopic fission cross-section;

ν = the number of prompt neutrons produced per fission;

S^{ext} = an external source, including sources of delayed neutrons.

The vector or directional neutron flux is given by

$$\phi(\vec{r},\vec{\Omega},u,t) = vN(\vec{r},\vec{\Omega},u,t) .$$

Equation 1.1 may, in general, be written in the form

$$\frac{\partial}{\partial t} N = HN + S^{ext} , \tag{1.2}$$

where N is the neutron density, and H is an operator which is generally independent of N and, therefore, linear. H can be split into two parts:

$$H \equiv I - K , \tag{1.3}$$

where I and K are, respectively, the production and destruction operators (in the language of Field Theory), such that IN gives the rate of production of fission neutrons per unit volume and KN gives the rate of loss of neutrons. If ν, the average number of neutrons per fission, is taken to be independent of lethargy, it is possible to write

$$I = \nu J , \tag{1.4}$$

so that

$$H \equiv \nu J - K . \tag{1.5}$$

For the critical or self-sustained steady state, we must have

$$\frac{\partial N}{\partial t} = 0 \ , \tag{1.6}$$

without the external source ($S^{ext} = 0$). Thus, the eigenvalue ν_c must satisfy the equation

$$\nu_c JN - KN = 0 \ . \tag{1.7}$$

The lowest value ν_c is then the value of ν required to maintain a steady chain reaction. The parameter ν_c is a fictitious value of the number of neutrons per fission that would render the actual system critical; ν, the actual number of neutrons per fission, must be proportional to ν_c; i.e.,

$$\nu = k\nu_c \qquad \text{or} \quad k = \frac{\nu}{\nu_c} \ , \tag{1.8}$$

where k is a constant characteristic of the system. It is seen from Eq. 1.7 that k is an eigenvalue of the equation

$$\nu JN = kKN \ . \tag{1.9}$$

The corresponding adjoint equation is

$$\nu J^{\dagger} M = kK^{\dagger} M \ , \tag{1.10}$$

where M is the adjoint of N. If dt is the volume element with respect to which the adjointness is defined, so that $\int N d\tau$ is the total number of neutrons in the reactor, we may write:

$$k = \nu \frac{\int MJN \ d\tau}{\int MKN \ d\tau} \ . \tag{1.11}$$

Before proceeding further, we must state the physical content and interpretation of these equations. The adjoint function $M(\vec{r},\vec{\Omega},u)$ represents the importance of a neutron toward maintaining the chain reaction and may be defined as the neutron content of the system resulting from a unit, point, monoenergetic, unidirectional neutron source at $\vec{r}$ with lethargy u and direction $\vec{\Omega}$. Then, for any general neutron distribution N – not necessarily satisfying Eq. 1.9 – the quantity $\nu \int MJN \ d\tau$ is the rate of production of neutrons (via fission), weighted by the importance function,

and integrated over the entire volume of the reactor. Similarly, $\int MKN\, d\tau$ is the net destruction rate due to scattering, absorption and leakage. Thus, the adjoint function $M(\vec{r},\vec{\Omega},u,t)$, which has been introduced above as a mathematical recipe, indicates, physically, that an importance function must be used to give the proper relative weights to neutrons in different parts of the reactor.

The constant k defined by Eq. 1.8 is a measure of the departure of the system from criticality – a state representing the exact balance between the neutrons born in the system and those lost by and in it; k is unity for a critical system $\left(\frac{\partial N}{\partial t} = 0\right)$, greater than unity for a supercritical system $\left(\frac{\partial N}{\partial t} > 0\right)$ and less than unity for a subcritical system $\left(\frac{\partial N}{\partial t} < 0\right)$. This constant k is called* the effective multiplication factor or the criticality factor of the system. According to Eq. 1.11 and the above interpretation,

$$k = \frac{\text{Production rate of neutrons through fissions}}{\text{Net destruction rate due to scattering, absorption and leakage}} . \tag{1.12}$$

The rates in the numerator and denominator are weighted by the importance function. Equation 1.11 has the stationary property so that the effective multiplication factor depends only on the reactor characteristics ν, J, K and is independent of changes in neutron distribution within the reactor.

The advantage in defining k from this fundamental point of view is that this concept is readily applicable to any general chain-reacting system. For systems in which most of the fissions occur in a particular, limited, energy range, the usual life-cycle point of view defining k in terms of successive generations, is probably more easily understood.

---

*The usual practice of designating the infinite medium multiplication factor by k_∞ and the effective multiplication factor by k_{eff} seems somewhat clumsy. It seems appropriate to designate the infinite medium multiplication factor by k_o and the criticality factor of the finite system simply by k. This notation is consistent and in line with such designations as ℓ_o, ℓ etc. However, perhaps the most elegant notation is that of Weinberg and Wigner[3] who use the term criticality factor as distinct from the infinite medium multiplication factor k and denote it by C.

In such cases, however, the two points of view are equivalent and yield identical definitions. A distinction can be made between the static and the dynamic criticality factors, and a detailed discussion of these will be found in Ref. (3).

With the criticality factor k and its constituent rates defined, the other kinetic parameters can be defined in terms of these. One such parameter is the reactivity ρ of the system, given by

$$\rho = \frac{k - 1}{k} \quad . \tag{1.13}$$

For most systems of interest, $k \approx 1$ and sometimes reactivity is defined as

$$\rho = k - 1 \equiv k_{ex} \quad .$$

We adopt the first definition so that

$$\rho = \frac{\text{Production rate} - \text{net destruction rate}}{\text{Production rate}}$$

$$= \frac{\text{Net rate of increase of neutron population}}{\text{Production rate}} \quad . \tag{1.14}$$

Thus, the reactivity is a measure of the rate of change of the neutron population, being zero, positive or negative according as the system is critical, supercritical or subcritical. The quantities k, k_{ex} and ρ are three equivalent measures of the neutron multiplying properties of the system.

From Eqs. 1.8 and 1.13, we can write

$$\rho = \frac{\nu - \nu_c}{\nu} \quad . \tag{1.15}$$

Equations 1.8 and 1.15 are very useful and of general applicability. When ν_c/ν, the ratio of the fictitious to the true yield of fission is used, those relations may be applied to reactors containing mixtures of fissionable materials and to multigroup calculations in which fission neutrons are produced in several groups. Through perturbation theory, they may be extended to reactors with non-uniform fuel loading.

A measure of the dynamic behavior of the system is the effective mean prompt neutron lifetime ℓ – usually referred to simply as the

neutron lifetime — given by:

$$\ell = \frac{\int MN\, d\tau}{\int MKN\, d\tau} = \frac{I}{\int MKN\, d\tau}\ , \tag{1.16}$$

where $I = \int MN\, d\tau$ is the neutron density N, weighted by the importance function and integrated over the entire volume of the reactor, i.e., the weighted total neutron population; the denominator is, as before, the weighted total consumption rate of neutrons. The lifetime ℓ is then the average turnover time of importance or physically, the weighted average of the time required by a fission neutron to produce another fission.

A kindred parameter is the generation time Λ introduced by Hurwitz[4] and given by

$$\Lambda = \frac{\int MN\, d\tau}{\nu \int MJN\, d\tau} = \frac{I}{\nu \int MJN\, d\tau}\ . \tag{1.17}$$

It may be noted that

$$k = \frac{\ell}{\Lambda}\ . \tag{1.18}$$

The actual formulation of the various rates depends on the particular theoretical model employed. The quantities ℓ and Λ arise in a natural way in the treatment of reactor kinetics; historically, reactor kinetics equations were first derived from one-group diffusion theory and such a treatment affords an insight into the meaning and role of these parameters. The starting point for reactor kinetics, in this case, is a balance between the destruction and production probabilities of neutrons and precursors[5]:

$$\begin{aligned} \frac{dn}{dt} &= v[\nu\Sigma_f - \Sigma_a - DB^2]\, n - v\beta\nu\Sigma_f n + \sum_i \lambda_i C_i\ , \\ \frac{dC_i}{dt} &= v\beta_i\nu\Sigma_f n - \lambda_i C_i\ , \end{aligned} \tag{1.19}$$

where the various symbols have their usual definitions. It is to be observed that neither production nor destruction can be determined independently by the kinetic behavior. The definition of each is arbitrary.

to the extent of an additive term and the only operationally determinable characteristic of a reactor is its period, the direct consequence of the difference between the rates of production and destruction.

The kinetics equations can be cast in a form involving either ℓ or Λ; there seems to be some confusion in the literature, and the terms, lifetime and generation time, are often used interchangeably. This confusion arises from the fact that ℓ and Λ are equal at the steady state ($k = \frac{\ell}{\Lambda} = 1$); in most kinetics problems, ℓ and Λ are calculated for the steady state and treated as constant in the solution of the time-dependent problem. The argument has sometimes been made[6] that, since $\ell = \ell(\Sigma_a)$, one should use the kinetics equations with ℓ whenever the absorption cross-section is nearly constant in the transient, i.e., if one makes changes in the scattering or fission cross-sections. On the other hand, $\Lambda = \Lambda(\Sigma_f)$ and should be used whenever there is a large change in the absorption cross-section, e.g., in experiments with control rods.

Attempts to clarify the operational and conceptual significance of reactor kinetics parameters have been made by Hurwitz[4], Ussachoff[8], Henry[6], Lewins[5] and Gozani[7] among others. Lewins has shown that the formulation of the reactor kinetics equations in a form parametric in the generation time, is more accurate and simpler to solve than the corresponding form in the lifetime. The general concept and elementary expressions for the various reactor kinetics parameters are summarized in Table 1.1, taken from Ref. (5).

1.2 PHYSICAL SIGNIFICANCE OF REACTOR KINETICS PARAMETERS

The reactivity (as also the criticality factor k and k_{ex}) provides a measure of the over-all neutron economy of a chain-reacting system and, in this sense, it is a global parameter characterizing the state of the system as a whole. It is an indicator of the degree of criticality and hence of the response of the system to external and internal perturbations. The effect on the multiplying properties of the system, of control rods, of individual fuel elements, of changes in moderator or reflector configuration, of external probes or external samples, as well as of internal changes such as temperature variation, fuel depletion or void formation, is most conveniently expressed in terms of change in the

TABLE 1.1

REACTOR KINETICS PARAMETERS

Parameter	Concept	Elementary Value
(a) Normalized to destruction:		
k_{eff} effective multiplication	$\frac{\text{production probability}}{\text{destruction probability}}$	$\frac{v\nu\Sigma_f}{v(\Sigma_a+DB^2)}$
k_{ex}, excess multiplication	$\frac{\text{production-destruction}}{\text{destruction}}$	$\frac{v(\nu\Sigma_f-\Sigma_a-DB^2)}{v(\Sigma_a+DB^2)}$
ℓ, neutron effective lifetime	$\frac{1}{\text{destruction}}$	$\frac{1}{v(\Sigma_a+DB^2)}$
(b) Normalized to production:		
ρ, reactivity	$\frac{\text{production-destruction}}{\text{production}}$	$\frac{v(\nu\Sigma_f-\Sigma_a-DB^2)}{v\nu\Sigma_f}$
β_i, fractional precursor yield	$\frac{\text{precursor production}}{\text{production}}$	$\frac{v\beta_i\nu\Sigma_f}{v\nu\Sigma_f}$
Λ, generation time	$\frac{1}{\text{production}}$	$\frac{1}{v\nu\Sigma_f}$

reactivity. A knowledge of these effects is vital to the safe operation of the reactor, and the study of reactivity is, therefore, a basic aspect of reactor safety. Moreover, a knowledge of the reactivity may be used to determine other parameters of the reactor itself or the material properties of external samples. Theoretically, reactivity may be related to both the static (e.g., the multiplication factor and its component ingredients) and dynamic parameters (e.g., the reactor period) and provides a bridge between reactor statics and reactor dynamics. The study of reactivity is, therefore, also basic from the point of view of theoretical understanding.

The magnitude of the reactivity can be specified in several ways. As a mnemonic aid in fixing the magnitude of ρ for which delayed neutrons cease to play a predominant part in determining the reactor period, the condition known as "prompt criticality" is defined by the relation:

$$\rho = \overline{\beta} , \tag{1.20}$$

where $\overline{\beta}$ is the effective delayed neutron fraction for the particular system. A unit of reactivity based upon this relationship is called the "dollar":

$$\$ = \frac{\rho}{\overline{\beta}} , \tag{1.21}$$

so that a reactivity of 1 dollar (positive) represents the condition of prompt criticality. Reactivity may also be expressed as a percentage — one hundred times the numerical value of (k-1). It is frequently more convenient to use a reactivity expression more closely related to the reactor period, particularly for small reactivities. For this purpose, the inverse hour or inhour unit has been defined. A reactivity of 1 inhour is that value of ρ for a given reactor which yields a stable period of 1 hour. For any period, the reactivity in inhours is

$$\rho = \frac{\dfrac{\ell}{T+\ell} + \dfrac{T}{T+\ell}\displaystyle\sum_{1}^{m}\frac{\beta_i}{1+\lambda_i T}}{\dfrac{\ell}{3600+\ell} + \dfrac{3600}{3600+\ell}\displaystyle\sum_{1}^{m}\frac{\beta_i}{1+3600\lambda_i}} = \frac{R(T)}{R(3600)} \text{ inhours} . \tag{1.22}$$

In general, ℓ and β_i depend on the constitution of the reactor.

The true effective lifetime of prompt neutrons in a reactor is made up of the effective thermal lifetime and the effective fast lifetime. First-order, two-group perturbation theory gives the following expression for the prompt neutron lifetime in a finite reactor:

$$\ell = \frac{\int \left[\frac{\phi_1^\dagger \phi_1}{v_1} + \frac{\phi_2^\dagger \phi_2}{v_2} \right] d\tau}{\int \phi_1^\dagger [\nu\Sigma_{f1}\phi_1 + \nu\Sigma_{f2}\phi_2]\, d\tau} , \tag{1.23}$$

where ϕ_1 and ϕ_2 are respectively the fast and thermal group fluxes and other symbols have their usual meaning. This expression can be derived from the basic Eq. 1.16. If the reactor is bare and its properties are uniform, then Eq. 1.23 can be shown to reduce to

$$\ell = \frac{1}{v_2\Sigma_{a2}(1+L^2B^2)} + \frac{1}{v_1\Sigma_{a1}(1+\tau B^2)} , \tag{1.24}$$

where Σ_{a1} is the macroscopic "slowing-down cross-section." The time required for the neutrons to slow down is usually neglected in thermal reactors and then we have the simple expression:

$$\ell = \frac{1}{v\Sigma_a(1+L^2B^2)} = \frac{\ell_o}{1 + L^2B^2} , \tag{1.24a}$$

which appears in Table 1.1.

The effective prompt neutron lifetime is an index of the stability of the system and is an important parameter in judging the safety of a reactor in case a large increase in reactivity should be introduced accidentally. For reactivity increments greater than the delayed neutron fraction $\overline{\beta}$, the inverse period $\omega\left(= \frac{1}{T}\right)$ is given approximately by

$$\omega \approx \frac{\rho - \overline{\beta}}{\ell} , \tag{1.25}$$

and the rate of change in such a prompt-critical accident is inversely proportional to the lifetime ℓ. It is seen from Eq. 1.25 that ℓ depends on the concentration of fissionable material (Σ_f); a relatively large value of ℓ can be obtained by having this concentration low with a good

moderator (e.g., heavy water or graphite). It can also be shown that a longer lifetime can result if a reactor is surrounded by a large reflector.

Values of the effective neutron lifetime in representative reactors have been computed, for example, by Pigford et al.[9]. A more precise expression than Eq. 1.24, based on two-group perturbation theory, has been derived by Arnold[10]:

$$\ell = \frac{1}{v_1}\left(\frac{1}{1+\tau B^2}\right)\frac{1}{D_{1/\tau}} + \frac{1}{v_2}\left(\frac{\nu-1}{\epsilon\nu-1}\right)\left(\frac{1}{1+L^2B^2}\right)\frac{1}{\Sigma_{a2}} \; ; \qquad (1.26)$$

here ℓ is taken to be the sum of the time required for a neutron to slow down from fission to thermal energies and the time spent in diffusion before capture as a thermal neutron.

1.3 NEED FOR THE CONTROL OF REACTIVITY AND METHODS OF CONTROL

The need for the control of reactivity arises basically in three ways: (1) as a safety measure; (2) as a design requirement to insure steady operation against transient and long-term perturbing effects; and (3) to cause the system to respond to changes in power demand. Any chain-reacting system that is potentially critical must be provided with means of controlling the rate of the chain reaction. As the system comes into operation, it heats up thermally, fissile material is consumed and the fission products, some of which have high neutron capture cross-sections, accumulate. The latter two effects, and preferably the first one also, tend to decrease the probability that a neutron will produce fission. In some cases, pressure changes, voids and the conversion of fertile to fissile fuel must also be considered. To compensate for these changes, the reactor must contain enough fissionable material to ensure criticality when it is in the hot, poisoned, depleted condition. Hence, at the start-up when the reactor is cold, clean and undepleted, a degree of potential supercriticality must be present which must be offset by the control mechanisms.

It is evident that reactivity control may be brought about in many ways. The basic methods may be broadly termed "fuel control," "moderator control," "absorber control," or "configuration or reflector

control." Specifically, some of the possible methods are: variation of the fission cross-section by adjustment of the fuel content of the core; variation of moderator atom density; change in the neutron capture cross-section by the introduction or removal of highly absorbing non-fissionable nuclides called "poisons;" increasing the effective surface-to-volume ratio, e.g., by reflector movement. The ultimate choice of methods for control depends upon many factors: reactor type, purpose of the reactor, physical state of fuel and moderator etc. However, absorber control is the most commonly used method for maintaining safe, mechanically efficient control of thermal reactors, while allowing flexibility for programmed control.

The poison is generally present in lumped form – control "rods" which are located so as to traverse a major dimension of the core and which may be positioned at any point between complete removal and complete insertion. These "rods" may be solid or hollow cylinders, thin slabs or symmetrical Y-shaped or cross-shaped pieces.

Reactivity control is required (a) when the reactor is not operating, in order to insure a subcritical condition; (b) during start-up, shutdown and changes in power level, when small changes in reactivity are required for the transition to new steady states; (c) during constant power operation, when all the short- and long-term effects that tend to change the reactivity must be counterbalanced so as to maintain criticality. In a reactor operating at high power levels, at least three types of control are normally necessary: (1) emergency shutdown (scramming); (2) coarse or shim control; and (3) fine control. These categories are roughly indicative of the order of magnitude of the reactivity changes which must be provided for.

The worth of a control rod is defined in terms of the change in the criticality factor k, which the rod is capable of causing. If the criticality factors without and with the rod inserted be k and k_1, the corresponding reactivities are

$$\rho = 1 - \frac{1}{k}, \qquad \rho_1 = 1 - \frac{1}{k_1}. \tag{1.27}$$

Customs for specifying worth vary: the worth might be $k - k_1$, $\rho - \rho_1$, or the deviation of k/k_1 or k_1/k from unity. These are nearly equivalent when small (i.e., $\rho \ll 1$, $\rho_1 \ll 1$) reactivity changes are involved; but when large reactivity changes are treated, it is important to specify which definition is used.

1.4 IMPORTANCE OF REACTIVITY STUDIES

The measurement of reactivity is one of the most important measurements in reactor physics and technology. Whether the chief concern is reactor safety, design, or operation, experimental research or theoretical understanding, it is necessary to know how to measure different forms and varying amounts of reactivity at some stage or another. Reactivity monitoring is required to assure the safety of certain operations with reactor fuel, such as reactor loading, approach to critical and storage under unevaluated conditions.

If the amount, δk, by which a reactor is subcritical, or the value of k when it is less than unity, could be determined accurately, the information would be valuable for use in fuel loading, reloading, and control-rod calibration. This measurement has recently assumed added importance because of the accidental occurrence of supercriticality in SL-1 (ALPR). In general, reactivity measurements arise in conjunction with criticality or start-up experiments on new systems, calibration of control rods, estimation of the worth of fuel rods, the comparative study of different control materials for use as shim or safety devices, the studies of the dynamic coefficients describing the response of the system to specific forms of perturbation, changes in the composition of the system, or to changes introduced from outside.

Apart from the need for measuring the reactivity in connection with specific problems, the reactivity provides an index of the over-all neutron behavior in the system and can be used to correlate analytical results with quantities that are directly measurable. For this reason, the measurement of reactivity is an interesting and instructive experiment in pure research and constitutes a significant tool for the test of theoretical models, such as the results of control rod theory, calculations of prompt neutron lifetime and effective delayed neutron fraction, results of perturbation theory, and so on.

1.5 THE MEASUREMENT OF REACTIVITY

Since reactivity is a property of a reactor assembly as a whole, its measurement involves a change in the assembly which affects it in a characteristic way. The change is a perturbation which is equivalent to the addition of a positive or negative reactivity. The measurement of reactivity is then based either on a differential study of the system with and without the perturbation or on a study of the transient response to the perturbation. The first class of methods includes the static or steady-state methods, while the second includes the transient or dynamic methods.

1.5.1 Static Methods

The static method involves measurements in one or more steady states which may be critical or subcritical.

1.5.1.1 The Compensation Method[11-13]. The compensation method is based on maintaining criticality by counteracting any change in the reactivity by means of control rods or by introducing uniform poison into the core. Compensation by control rods is useful for the relative calibration of control rods. The compensation with an absorber distributed uniformly throughout the reactor can be interpreted in terms of the change in thermal utilization:

$$\rho = \frac{\delta k}{k} \approx \frac{\Delta f}{f} \approx \frac{\Delta \Sigma_a}{\Sigma_a} . \tag{1.28}$$

The poison calibration can be supplemented by the more direct period method. The compensation method can also be applied in an exponential assembly by using a measurement of the subcritical multiplication constant as a reference point.

1.5.1.2 The Subcritical Inverse-Multiplication Method[14,15]. The subcritical inverse-multiplication method, which is especially adapted to reactivity monitoring, is based on measuring the neutron multiplication or a quantity roughly proportional to it. The basic requirements for this type of measurement are a neutron source — either inherent in the fuel assembly or externally applied to it — and a neutron

detector with an adequate and reliably scaled response to neutrons from fission. In the absence of photoneutrons, the detector response rate under equilibrium conditions is proportional to neutron multiplication, and its reciprocal approaches zero as the fuel assembly is made to approach delayed critical. If the ratio of the response rate to neutron multiplication is known, then a single measurement may be sufficient to provide an index of reactivity.

1.5.1.3 Critical Height Measurement[16]. This method consists in starting with the reactor in a critical state with the moderator (liquid) level below the level of active fuel in the core. The control rod is then inserted and the moderator level raised to restore criticality; the material buckling of the core remains unchanged. The resulting change in geometrical buckling is related to the reactivity worth of the control rod: on two-group theory, for a bare cylindrical reactor core of extrapolated height H,

$$\frac{d\rho}{dH} = \frac{2\pi^2}{H^3} \frac{M^2 + 2\tau L^2 B^2}{k_\infty} . \qquad (1.29)$$

The same type of experiment may be performed in an exponential assembly by changing a dimension of the assembly so as to yield the same multiplication constant after rod insertion as before, the assembly remaining subcritical.

1.5.1.4 Buckling Measurement. For simple control rod configurations, the change in geometrical buckling produced by the insertion of the rod in a critical or exponential assembly can be measured directly by mapping the flux distribution. This geometrical buckling change can then be related to the reactivity worth of the control rod if the reactor parameters of the unperturbed system are known.

1.5.2 Kinetic Methods

The kinetic methods are based on a measurement of the temporal response of the neutron population to some change in the system. Basically, the time behavior of the neutron population is given by a solution of the reactor kinetics equations. A general form of this solution is[17,18]:

$$n(t) = \frac{S\ell}{1-k_{eff}} + \sum_{j=0}^{m} \left\{ \frac{n_o + \sum_{i=1}^{m} \frac{\lambda_i C_{io}}{p_j + \lambda_i}}{1 + \frac{k_{eff}}{\ell} \sum_{i=1}^{m} \frac{\beta_i \lambda_i}{(p_j+\lambda_i)^2}} + \frac{S}{p_j \left(1 + \frac{k_{eff}}{\ell} \sum_{i=1}^{m} \frac{\beta_i \lambda_i}{(p_j+\lambda_i)^2} \right)} \right\} e^{p_j t} \quad (1.30a)$$

for $k_{eff} \neq 1$, and

$$n(t) = \frac{S\ell}{\ell + \sum \frac{\beta_i}{\lambda_i}} t + \sum_{j=0}^{m} \left\{ \frac{n_o + \sum_{i=1}^{m} \frac{\lambda_i C_{io}}{p_j + \lambda_i}}{1 + \frac{1}{\ell} \sum_{i=1}^{m} \frac{\beta_i \lambda_i}{(p_j+\lambda_i)^2}} e^{p_j t} + \frac{S}{p_j \left(1 + \frac{1}{\ell} \sum_{i=1}^{m} \frac{\beta_i \lambda_i}{(p_j+\lambda_i)^2} \right)} \left(e^{p_j t} - 1 \right) \right\}, \quad (1.30b)$$

for $k_{eff} = 1$,

where the p_j are the roots of the characteristic equation

$$\rho = \frac{1}{1 + \ell p} \left(\ell p + \sum \frac{p}{p+\lambda_i} \right) . \quad (1.31)$$

Initially, the reactor may be in the near critical state, the positive prompt critical region, or in the subcritical state. A positive or negative reactivity change is effected rapidly by some external means and the reactivity to be measured is deduced from the response of a suitable detector.

1.5.2.1 Stable Reactor Period Method[19,20,21,22,23]. The basic technique for the calibration of a control rod is based on the measurement of the positive period resulting from the positive reactivity introduced by the withdrawal of the rod. The reactor is made critical with the rod inserted; the rod is then moved out a short distance and after the transients die out, the stable period is measured. The inhour equation relates this period to the reactivity introduced during the rod bump, i.e., the differential reactivity at the initial position of the rod. To obtain a calibration curve, it is necessary to determine the differential worth at other points, and the motion of the rod must be compensated for, in some way. This experiment cannot be made in an exponential assembly.

1.5.2.2 Pile Oscillator Method[23,24,25,26]. The control rod is oscillated in and out of the core at a frequency of about one cycle per second, and the oscillating signal generated in an ion chamber is amplified, rectified and integrated. Since the neutron equations are linear, the amplitude of the signal is directly proportional to the absorption introduced. The oscillating component Δn and the steady-state neutron density n are related as

$$\frac{\Delta n}{n} = W(j\omega)\,\frac{\Delta k}{\beta}\,, \tag{1.32}$$

where $\frac{\Delta k}{\beta}$ is the reactivity in dollars and $W(j\omega)$ is the reactor transfer function. The latter can be calculated from the kinetics equations (if the constants involved are known), or determined experimentally by observing the frequency response to reactivity oscillation of known amplitude.

Other less important methods which depend on measurements in the near-critical state are the rod-drop-bump (square-wave) method[25,27], the trapezoid-wave method[27,28] and the electronic simulator method[29,13]. The positive prompt transient method[30,31] is limited to a few special reactors.

1.5.2.3 The Statistical Method[32,33,34,35]. The most important among the statistical methods is the Rossi-α technique which makes use of the time dependence of detector counts observed in a chain-reacting assembly at low power. This method is discussed more fully in Chapter III. The reactivity \$, in dollars, is obtained from the experimentally determined, prompt neutron decay constant α, according to the relation

$$\alpha = \alpha_{d.c.}(1 - \$)\,, \tag{1.33}$$

where $\alpha_{d.c.}$ is established by a single measurement at delayed critical.

A recently described[36] method makes use of a fast neutron source, electronically modulated by a pseudo-random, i.e., "noise-like" waveform. Reactivity is estimated by examining the impulse response of the reactor, which is measured by cross-correlating input (source strength) and output (neutron population). A new means of continuously determining the

"shutdown margin" reactivity via statistical analysis of reactor noise has recently been suggested[37,35].

1.5.2.4 Rod-Drop Technique[22,23,25,38]. The rod-drop method provides a convenient measurement of negative reactivity (the integral worth of a rod). With the reactor exactly critical, the rod is withdrawn over the range for which the reactivity worth is desired. The control rod is then rapidly inserted into the core and the resultant power transient recorded. The results can be analyzed in several ways. One way is to extrapolate the transient following the rod drop back to the time of the drop, neglecting the fast transient which dies out in a fraction of a second. The reactivity worth (in dollars) is then given by

$$\$ = \frac{1 - R}{R} , \tag{1.34}$$

where R is the ratio of the power level after the rod drop to the power level before the drop.

Modifications of the standard rod-drop technique include the integral count method[39] in which total neutron count following the rod drop is measured rather than the post-drop level. In this case,

$$\rho = - \frac{n(0)}{\int_0^\infty n(t)\, dt} \sum \frac{\overline{\beta}_i}{\lambda_i} , \tag{1.35}$$

where the initial neutron density n(0) can be measured by accumulating counts from a suitable detector from the time of rod drop until the neutron level becomes constant.

1.5.2.5 The Source-Jerk Technique[25,23]. A neutron source is placed in the subcritical core of the reactor with the rod inserted, and the neutron level is noted on the detectors. The source is then removed in a time that is short compared to the mean life of the shortest delayed neutron group, and the transient neutron level following the removal is observed. The analysis of the results is similar to that in the rod-drop method; when the extrapolation method is used, the reactivity in dollars is given by

$$\$ = \frac{n_1 - n_o}{n_1} .$$

1.5.2.6 The Pulsed Neutron Method[40,41,42]. In this method, a burst of fast neutrons is injected into a subcritical multiplying system, and the decay of the thermal neutron population is recorded as a function of time. After neutron thermalization and decay of the higher modes of the neutron flux, the decay constant α of the fundamental mode can be measured. The result can be analyzed in several ways which will be discussed in Chapter III. One way is to obtain the reactivity \$ in dollars from the relation

$$\alpha = \alpha_{d.c.}(1-\$) , \tag{1.36}$$

where the proportionality constant $\alpha_{d.c.}\left(=\frac{\bar{\beta}}{\ell}\right)$ can be determined by a pulse decay measurement at delayed critical.

1.6 CRITIQUE OF THE METHODS FOR THE MEASUREMENT OF REACTIVITY

The merit and validity of any particular method of reactivity measurement depend on the nature and range of reactivity to be measured and the degree of precision demanded. A general, but brief, critique of the individual methods will be attempted in this section.

Among the static methods, the simplest is the subcritical multiplication method. This method depends strongly on a knowledge of the harmonic content, at the measuring point, which is introduced by the source that maintains the constant neutron flux in the subcritical assembly. Estimating the effect of harmonics in an actual system may be difficult. The compensation method is often used for the relative calibration of control rods. The precision of this method depends either on the absence of interaction between the different components or the degree to which these effects are known. It is usually difficult to estimate the interaction effects. The compensation of reactivity with local absorber is, therefore, limited to the measurement of small amounts of reactivity.

The stable period method is the most common technique for reactivity measurement. It suffers from the disadvantage that in order to start with a critical reactor at each position of the control rod, the motion of the rod being calibrated must be compensated for in some way; this changes the other parameters and affects the criticality

analysis. Moreover, quite long wait-times are required to insure that the asymptotic period is being observed. In fact, the determination of a detailed multipoint control rod calibration curve by the period method may require several hours. The pile oscillator method is much faster because the steady power remains nearly constant and no time is lost in waiting for the delayed neutrons to return to equilibrium. Comparison of the rod oscillator method with the period method and the rod-drop method has demonstrated that good agreement is possible[25]. However, the pile-oscillator method requires special apparatus for oscillating the rod and improved instrumentation for detecting the power oscillations. The method also suffers from the dependence of the signal on detector location[43]. This method is useful for comparing control rods.

Of the statistical methods, the Rossi-α technique is the only one which has been applied to actual measurements to a significant extent. This method is generally capable of very good (errors of a few per cent) precision in determining the prompt neutron decay constant, but is practical only when small amounts of negative reactivity are to be measured. The Rossi-α method gives good results in fast systems and can be extended to somewhat slower systems. However, this method is not considered practical for thermal reactors. Other statistical methods are still in early stages of development and cannot be properly evaluated.

Although reactivities ranging from zero at delayed critical to about -2 dollars can be measured by the inhour method, this method is not applicable for large multidollar reactivities. For a large negative reactivity, the period is almost independent of the reactivity, while for large positive reactivities, the periods are too short to be measurable by an unrefined method. Large negative reactivities can be measured by the rod-drop or the source-jerk technique. Both these methods, however, involve difficulties associated with the measurement of the flux during the transient produced by dropping the rod or removing the external source. The difficulty is compounded in the source-jerk method because at the low flux level present in a subcritical system, the detector output may be erratic[39]. In the rod-drop method, if the motion of the rod changes the flux-distribution in all directions, the

accuracy of the results may be in doubt. The source-jerk method is just the converse of the rod-drop method.

The pulsed-neutron-source technique affords a simple, straightforward, and accurate method of reactivity measurement which is valid over a wide range of reactivities. This method can give reliable results from very close to critical to several dollars below critical. In highly subcritical assemblies, modal and thermalization-time effects may impose an effective lower limit. In the measurement of very large reactivity changes (several dollars), it is necessary to correct for the variation in neutron lifetime. Detailed comparisons[42,43] of the pulsed source technique with asymptotic period, rod-drop and rod-oscillator methods have shown good agreement (within a few per cent) for reactivities down to a dollar below delayed critical. For large values of subcriticality, the pulsed method has been found to be definitely superior and, in nearly all cases, it appears to be "more convenient, rapid and straightforward." Furthermore, the pulsed neutron method is self-contained in the sense that it provides its own reactivity calibration, usually via a delayed critical measurement, and does not depend upon supplementary measurements to yield absolute reactivities. As a "by-product" of the reactivity measurement, one gets a measurement of the prompt neutron lifetime which is, in itself, a kinetic parameter of major importance. In the present work, the theoretical basis of the pulsed neutron method is explored in detail, and the method is applied to the measurement of reactivities in far subcritical heterogeneous systems.

References

1. L. S. Ornstein and G. E. Uhlenbeck, Physica, Haag 4, 478 (1937).
2. H. Soodak (Ed.), Reactor Handbook, Vol. III, Part A, Physics, (2nd Edn.), Interscience Publishers, New York, 1962.
3. A. M. Weinberg and E. P. Wigner, The Physical Theory of Neutron Chain Reactors, The University of Chicago Press, Chicago, 1958.
4. H. Hurwitz, Jr., Nucleonics 5, 61 (1949).
5. J. Lewins, Nucl. Sci. and Eng. 7, 122 (1960).
6. A. F. Henry, Nucl. Sci. and Eng. 3, 52 (1958).
7. von T. Gozani, Nukleonik, Band 5, Heft 2, S55 (1963).
8. L. N. Ussachoff, Proc. Inter. Conf. on the Peaceful Uses of Atomic Energy, Geneva, P/656 (1955).
9. T. H. Pigford, M. Troost, J. R. Powell and M. Benedict, A.I.Ch.E. Journal, 2, 219 (1956).
10. W. H. Arnold, Jr., Nucl. Sci. and Eng. 4, 598 (1958).
11. G. R. Hopkins and C. P. Jamieson, WAPD-BT-8, 90-103 (6, 1958).
12. Annual Progress Report, ORNL-1871 (September 1955).
13. P. Liewers, Kernenergie 4, 593-618 (1961).
14. Martin Company, Nuclear Division, MND-MPR-1646 (1958).
15. J. Bernot and V. Raievski, CEA Report No. 310 (1954).
16. P. F. Gast, Proc. Int. Conf. on the Peaceful Uses of Atomic Energy, Geneva, Vol. 5, P/612 (1955).
17. H. Grümm and K. H. Höcker, Erg. exakt. Naturwiss. 30, S. 134 (1958).
18. B. J. Toppel, Nucl. Sci. Eng. 5, 88 (1959).
19. H. L. Garabedian, AECD-3666 (1950).
20. B. S. Finn, Nucl. Sci.Eng. 7, 396 (1960).
21. E. Fast and D. A. Millsap, IDO-16610 (1957).

22. J. M. Harrer, Nuclear Reactor Control Engineering, D. Van Nostrand Company, Inc., New York (1963).

23. W. K. Anderson and J. S. Theilacker (Ed.), Neutron Absorber Materials for Reactor Control, USAEC (1962).

24. V. Raievski, CEA Report No. 1095 (1959).

25. F. J. Jankowski, D. Klein and T. M. Miller, Nucl. Sci. Eng. 2, 288 (1957).

26. A. M. Weinberg and H. C. Schweinler, Phys. Rev. 74, 851 (1948).

27. M. N. John, AEEW-M193 (1, 1962).

28. H. D. Brown and W. E. Loewe, Nucl. Sci. Eng., 5, 376 (1959).

29. C. A. Sastre, Nucl. Sci. Eng. 8, 443 (1961).

30. T. F. Wimett et al., Nucl. Sci. and Eng. 8, 691 (1960).

31. F. Schroeder (Ed.), IDO-16640 (4, 1961).

32. G. S. Brunson et al., Nucleonics, 15, 132 (1957).

33. J. Bengston et al., Proc. 2nd Geneva Conf. on the Peaceful Uses of Atomic Energy, 15/P/1783 (1958).

34. J. D. Orndoff, Nucl. Sci. Eng. 2, 450 (1957).

35. J. A. Thie, Reactor Noise, Rowman and Littlefield, Inc., New York, (1963).

36. T. E. Stern, A. Blaquiere and J. Valat, React. Sc. and Techn. 16, 499 (1962).

37. R. E. Uhrig, Proc. of Symp. on React. Kinetics and Control, Univ. of Arizona, March 1963.

38. H. L. McMurry, IDO-16241 (1955).

39. W. S. Hogan, Nucl. Sci. and Eng. 8, 518 (1960).

40. B. E. Simmons and J. S. King, Nucl. Sci. and Eng. 3, 595 (1958).

41. K. H. Beckürts, Nucl. Instr. and Methods, 11, 144 (1961).

42. O. C. Kolar and F. C. Kloverstrom, Nucl. Sci. and Eng. 10, 45 (1961).

43. W. C. Ballowe, W. R. Morgan and J. L. Russell, Jr., GEAP-3639 (1961).

Chapter II

THE PULSED NEUTRON TECHNIQUE: THEORETICAL TREATMENT OF THE KINETICS OF AN ASSEMBLY IRRADIATED BY A FAST NEUTRON PULSE

INTRODUCTION

By the Pulsed Neutron Technique is generally meant the body of methods which utilize short, repetitive bursts of fast neutrons for the study of the interaction of neutrons with nuclei in a medium. The source of pulsed neutrons is usually a charged particle accelerator with an appropriate target. The first pulsed accelerator to be used for neutron research was the 36-inch Berkeley Cyclotron, as reported by Alvarez,[1] who produced neutron bursts from the (d,n) reaction with a beryllium target, by the modulation of the cyclotron acceleration voltage and studied the validity of the inverse velocity law down to 30°K for the case of boron. Since then, the technique has been greatly extended and refined, and applied to such diverse problems as low and intermediate energy neutron spectroscopy, the investigation of the diffusion properties of moderating materials, reactivity measurements in neutron-multiplying systems, and measurements of the neutron spectra of multiplying and non-multiplying systems by the time-of-flight method. A brief history of the development of the technique and some of its ramifications is to be found in Refs. (2, 3), while Refs. (4, 5, 6) review articles introducing the "state of the art" and its applications. The relevant volumes of the Proceedings of the Brookhaven Conference on Neutron Thermalization[7] form a comprehensive survey of the current status of pulsed neutron research.

The lifetime of the neutrons which comprise a burst of fast neutrons injected into an assembly can be divided into three more-or-less overlapping regions. During the first region, the moderation or fast-resonance period, the neutrons are slowed down from the source energy E_o to about

0.25 ev and the average energy is high enough, compared to the energies of the chemical bonds and to the thermal energy, so that the neutrons interact individually with the atoms of the moderator as if the atoms were free and at rest. This region is followed by the thermalization or the transition phase involving slowing down below about 0.25 ev; the atoms of the medium have a distribution of velocities and, in solids and liquids, are bound so that neutrons may gain as well as lose energy in collisions with the atoms. The thermalization process continues until the neutrons reach an asymptotic energy distribution whose characteristics are governed by the energy exchange scattering kernel and by the absorption and leakage in the medium. Finally, in the diffusion or thermal region, the shape of the asymptotic energy distribution remains unchanged but the amplitude decreases in time, and the sequence is terminated by absorption or by leakage of neutrons (thermal) from the medium.

In line with the sequence of events just outlined, pulsed neutron studies can be broadly classified into the fields of "Asymptotics" and "Transients." The field of "asymptotics" has to do with the rate at which the amplitude of the asymptotic neutron distribution (i.e., the thermal flux) decays with time during the diffusion period. This rate is characterized by the lowest (zeroth) eigenvalue associated with the decaying pulse and yields information about the thermal diffusion properties of the medium including the diffusion cooling coefficient. The field of "transients" deals with the approach to this asymptotic distribution and the conditions under which it is attained; this approach is characterized by the first eigenvalue which is related to the "thermalization time constant." The main interest centers around the neutron flux and spectrum during the thermalization process and the investigation of the thermalization properties of the medium.

A large part of the applications of the pulsed neutron technique pertains to the asymptotic thermal region and is based on the study of the time-dependent behavior of the thermal neutron population which dies away at a fixed rate characteristic of the size (geometrical buckling) and nature (nuclear properties) of the system studied. A knowledge of the spatial and temporal neutron distribution in a medium following the injection of a short burst of fast neutrons is of interest in the analysis and

interpretation of experiments purporting to measure the neutron transport and reactor parameters by the pulsed neutron technique. The theoretical effort in the field has been largely stimulated by the discovery of diffusion cooling and the related phenomena which throw light on certain neutronic interactions in systems. The early work on the theory of the slowing down of neutrons by elastic collisions with atomic nuclei was reviewed by Marshak;[8] he considered the description of neutrons in time and energy by means of a spatially independent transport equation with an instantaneous monoenergetic fast source. The general treatment of the time-dependent Boltzmann equation with a generalized time varying source is reviewed in the comprehensive work of Amaldi.[2] Sykes,[9] who used a polynomial expansion method applied to the time-dependent transport equation, treated the time-spread of neutrons of thermal and intermediate energies at various distances from a pulsed source of fast neutrons in an infinite moderating and diffusing medium.

Hurwitz and Nelkin[10] used perturbation theory to evaluate the lowest (zeroth) eigenvalue associated with the asymptotic neutron distribution during the diffusion period for a heavy gas. Singwi and Kothari[11] studied this problem by means of the Rayleigh-Ritz variational method with the assumption of a modified Maxwellian asymptotic energy distribution. Nelkin[12] carried out a similar analysis and introduced the thermalization parameter M_2, the mean-square energy transfer. Singwi[13] developed a general theory of diffusion cooling without recourse to the concept of neutron temperature, while Häfele and Dresner[14] applied a similar analysis for the calculation of the diffusion cooling coefficient in a monoatomic heavy gas. These studies, as also that of Kazarnovsky et al.[15] for the neutron thermalization, were based on the diffusion approximation and referred to finite media. Nelkin[16] later studied the non-diffusion effects by considering the decay of a thermalized pulse according to transport theory. Singwi[13] and Sjöstrand[17] also obtained the non-diffusion corrections. Time-dependent studies of neutron moderation have also been undertaken by Waller[18] and Eriksson.[19]

Krieger and Zweifel[20] discussed the extension of "asymptotic reactor theory"[21] to the time-dependent case and obtained the solution of the time-dependent diffusion equation for a multiplying medium by using

an arbitrary slowing-down kernel. Fultz[22] made a two-group analysis of the transient behavior of the thermal flux in a subcritical assembly and applied it to the analysis of experiments on graphite-uranium systems. Purohit[23] has developed a general mathematical formalism, based on a method similar to that of Singwi[13], for determining the lower eigenvalues associated with the energy eigenfunctions of a decaying pulse of neutrons in a general finite medium; his formalism is based on the expansion of each energy eigenfunction in a complete sum of associated Laguerre polynomials of the first order. Boffi, Molinari and Parks[24] have applied Nelkin's[16] analysis of a decaying thermalized neutron pulse in a non-multiplying system to the discussion of certain aspects of the persisting neutron distribution in a large subcritical assembly. Dyad'kin and Batalina[25] have discussed the time dependence of the space-energy distribution of the neutrons from a pulsed source for certain geophysical applications.

In the present work, the main emphasis is on the study of the decay constant of the fundamental mode of the thermal neutron population following the injection of a fast neutron burst – especially in a subcritical multiplying system. The different expressions for the basic decay constant, according to the different generalized theoretical models for the slowing down and diffusion of neutrons, will be studied, as will the effects of such factors as the delayed neutrons in multiplying systems. An attempt will, therefore, be made to investigate the problem from several different theoretical standpoints and to develop the basic expressions for the analysis and interpretation of pulsed neutron experiments on subcritical assemblies. The spatial distributions will also be treated for the investigation of harmonics.

2.1 NON-MULTIPLYING SYSTEMS

2.1.1 Generalized Age-Diffusion Theory Treatment

The space and time-dependent thermal neutron flux in a pure moderator assembly, following the injection of a short burst of fast neutrons, has been treated by means of one-group[4] and two-group[26] elementary diffusion theories, and the basic expressions for the decay constant of the fundamental persisting mode of the thermal flux have been obtained. Here,

a generalized, time-dependent age equation will be used to obtain the slowing-down density at thermal energies, which gives the source term for the diffusion equation governing the subsequent thermal neutron decay. Such a treatment brings out more clearly the details of the neutron behavior during the slowing-down phase and yields a complete expression for the time-dependent thermal neutron population in terms of the original source intensity. The assumptions which generally underlie an age-theory treatment and the range and limits of validity of such a theory are well known and are discussed, for example, in Ref. (27).

The Fermi-age model of neutron transport gives the balance equation for neutrons of lethargy between u and u+du for an absorbing, non-multiplying medium as:

$$D(u)\nabla^2\phi(\vec{r},u,t) - \Sigma_a(u)\phi(\vec{r},u,t) - \frac{\partial}{\partial u}\chi(\vec{r},u,t) + S(\vec{r},u,t) = \frac{1}{v(u)}\frac{\partial}{\partial t}\phi(\vec{r},u,t) \ , \tag{2.1}$$

where D(u) is the diffusion coefficient of the medium for neutrons of lethargy u:

$$D(u) = \frac{1}{3}\lambda_{tr}(u) \ ,$$

$\chi(\vec{r},u,t)$ is the slowing-down density, $S(\vec{r},u,t)$ is the external neutron source, and the other symbols have their usual meaning. The following relation holds between ϕ and χ:

$$\chi(\vec{r},u,t) = \xi(u)\Sigma_t(u)\phi(\vec{r},u,t) \ . \tag{2.2}$$

Substituting Eq. 2.2 in Eq. 2.1, we obtain:

$$D(u)\nabla^2\chi(\vec{r},u,t) - \Sigma_a(u)\chi(\vec{r},u,t) - \xi(u)\Sigma_t(u)\frac{\partial}{\partial u}\chi(\vec{r},u,t) + \xi(u)\Sigma_t(u)S(\vec{r},u,t)$$

$$= \frac{1}{v}\frac{\partial}{\partial t}\chi(\vec{r},u,t) \ . \tag{2.3}$$

The linear term in this equation can be eliminated by means of the transformation,

$$q(\vec{r},u,t) = p(0,u)\,\chi(\vec{r},u,t) \ , \tag{2.4}$$

where

$$p(0,u) = \exp\left[- \int_0^u \frac{\Sigma_a(u')}{\xi(u')\Sigma_t(u')}\,du' \right] ; \tag{2.5a}$$

or, in terms of the energy,

$$p(E_o,E) = \exp\left[- \int_E^{E_o} \frac{\Sigma_a(E')}{\xi(E')\Sigma_t(E')} \frac{dE'}{E'} \right] ; \tag{2.5b}$$

p is just the infinite-medium resonance escape probability as given by the Fermi slowing-down theory.[28] If there is no absorption (i.e., $\Sigma_a = 0$), then $q = \chi$.

With the transformation of Eq. 2.4 and some simplification, Eq. 2.3 becomes:

$$\nabla^2 q(\vec{r},u,t) - \frac{\xi(u)\Sigma_t(u)}{D(u)} \frac{\partial}{\partial u} q(\vec{r},u,t) + \frac{\xi(u)\Sigma_t(u)}{D(u)p(0,u)} S(\vec{r},u,t)$$

$$= \frac{1}{vD(u)} \frac{\partial}{\partial t} q(\vec{r},u,t) . \tag{2.6}$$

If we now introduce the Fermi-age τ given by

$$d\tau = \frac{D(u)}{\xi(u)\Sigma_t(u)} du ,$$

or (2.7)

$$\tau(0,u) = \int_0^u \frac{D(u')}{\xi(u')\Sigma_t(u')} du' ;$$

[in terms of neutron energy, E,

$$d\tau = \frac{D(E)}{\xi(E)\Sigma_t(E)} \frac{dE}{E} ,$$

$$\tau(E_o,E) = - \int_{E_o}^{E} \frac{D(E')}{\xi(E')\Sigma_t(E')} \frac{dE'}{E'} \quad] .$$

We can rewrite Eq. 2.6 as

$$\nabla^2 q(\vec{r},u,t) - \frac{\partial}{\partial t} q(\vec{r},u,t) + \frac{1}{p(0,\tau)} S(\vec{r},\tau,t) = \frac{1}{vD(\tau)} \frac{\partial}{\partial t} q(\vec{r},\tau,t) , \tag{2.8}$$

where

$$S(\vec{r},\tau,t) = \frac{\xi(u)\Sigma_t(u)}{D(u)} S(\vec{r},u,t) .$$

Equation 2.8 is the generalized, time-dependent age-equation. For our problem, we particularize the source function as an impulse:

$$S(\vec{r},\tau,t) = S_o \delta(\vec{r}-\vec{r}_o)\,\delta(\tau)\,\delta(t)\ . \tag{2.9}$$

Thus we have to solve Eq. 2.8 with the source term given by Eq. 2.9. To this end, we multiply Eq. 2.8 throughout by e^{-st}, integrate with respect to t from 0 to ∞, and define the Laplace Transform pair[29, 32]

$$\bar{f}(s) = \int_0^\infty e^{-st} f(t)\,dt\ ,$$

$$f(t) = \frac{1}{2\pi i} \lim_{\omega\to\infty} \int_{\nu-i\omega}^{\nu+i\omega} e^{st}\,\bar{f}(s)\,ds\ . \tag{2.10a,b}$$

Using the physically obvious initial condition $q(r,\tau,0) = 0$, we obtain the transformed equation:

$$\nabla^2\bar{q}(\vec{r},\tau,s) - \frac{\partial}{\partial\tau}\,\bar{q}(\vec{r},\tau,s) - \frac{s}{vD}\,\bar{q}(\vec{r},\tau,s) = \frac{S_o}{p(0,\tau)}\,\delta(\vec{r}-\vec{r}_o)\,\delta(\tau)\ . \tag{2.11}$$

We wish to express the spatial dependence of the functions $\bar{q}(\vec{r},\tau,s)$ and $S_o\delta(\vec{r}-\vec{r}_o)$ in terms of an infinite series of eigenfunctions which form a complete orthogonal set. The choice of such a set is, in general, arbitrary;[30] but great simplification results if we choose the set generated by the Helmholtz equation

$$\nabla^2 Q(\vec{r}) + B^2 Q(\vec{r}) = 0\ . \tag{2.12}$$

Only those solutions are physically meaningful which vanish at the extrapolated surface of the assembly. The resulting eigenfunctions $Q_{mnp}(\vec{r})$ corresponding to the eigenvalues B^2_{mnp} form a complete orthogonal set. Hence, we can write, for any arbitrary geometrical shape,

$$\bar{q}(\vec{r},\tau,s) = \sum_{mnp} \bar{A}_{mnp}(\tau,s)\,Q_{mnp}(\vec{r})\ , \tag{2.13}$$

$$\delta(\vec{r}-\vec{r}_o) = \sum_{mnp} C_{mnp}\,Q_{mnp}(\vec{r})\ , \tag{2.14}$$

where

$$C_{mnp} = \frac{\int_v \delta(\vec{r}-\vec{r}_o)\, Q_{mnp}(\vec{r})\, d\vec{r}}{\int_v Q^2_{mnp}(\vec{r})\, d\vec{r}} \quad . \tag{2.15}$$

For instance, in cylindrical geometry, with the extrapolated surface defined by $r=R$, $z=\pm H$ and the source located at $(R_o,0,z_o)$, the eigenfunctions are

$$Q_{mnp}(r,\phi,z) = J_m\left(\beta_{mn}\frac{r}{R}\right)\cos m\phi \sin\frac{p\pi}{H} z \ , \tag{2.16}$$

with

$$C_{mnp} = \frac{\int_0^R \frac{1}{r}\delta(r-r_o)\, J_m\left(\beta_{mn}\frac{r}{R}\right) r\, dr \int_0^{2\pi}\delta(\phi)\cos m\phi\, d\phi \int_{-H}^{H}\delta(z-z_o)\sin\frac{p\pi}{H} z\, dz}{\int_0^R J_m^2\left(\beta_{mn}\frac{r}{R}\right) r\, dr \int_0^{2\pi}\cos^2 m\phi\, d\phi \int_{-H}^{H}\sin^2\frac{p\pi}{H} z\, dz}$$

$$= \frac{4}{\pi R^2(2H)}\,\frac{1}{1+\delta_{om}}\,\frac{J_m\left(\beta_{mn}\frac{R_o}{R}\right)}{\left[J'_m(\beta_{mn})\right]^2}\sin\frac{p\pi}{H} z_o \ , \tag{2.17}$$

where δ_{om} is the Kronecker delta:

$$\delta_{om} = \begin{cases} 1 & \text{for } m = 0 \\ 0 & \text{for } m \neq 0 \end{cases} \quad .$$

Now, substituting Eq. 2.13 in Eq. 2.11 and remembering that $\nabla^2 Q_{mnp}(\vec{r}) = -B^2_{mnp} Q_{mnp}(\vec{r})$, we obtain

$$\frac{\partial \overline{A}_{mnp}}{\partial\tau} + \left(B^2_{mnp} + \frac{s}{vD}\right)\overline{A}_{mnp} = \frac{S_o C_{mnp}}{p(0,\tau)}\,\delta(\tau) \ . \tag{2.18}$$

The solution of this linear differential equation in τ is:

$$\overline{A}_{mnp}(\tau,s) = H(\tau)\,\frac{S_o C_{mnp}}{p(0,\tau)}\exp\left\{-\int_0^\tau\left(B^2_{mnp}+\frac{s}{vD}\right)dt\right\} \ , \tag{2.19}$$

where $H(\tau)$ is the Heaviside function,[29]

$$H(\tau) = \begin{cases} 1 & \tau > 0 \\ 0 & \text{otherwise} \end{cases} \quad . \tag{2.20}$$

Substituting for $p(0,\tau)$ from Eq. 2.5 in terms of τ, we get:

$$\overline{A}_{mnp}(\tau,s) = H(\tau) S_o C_{mnp} \exp\left\{ - \int_0^\tau \left(B_{mnp}^2 + \frac{s}{vD} + \frac{\Sigma_a}{D} \right) d\tau \right\} . \tag{2.21}$$

If we define

$$\left\langle \frac{1}{vD} \right\rangle = \frac{1}{\tau} \int_0^\tau \frac{1}{vD(\tau)} \, d\tau ,$$

$$\left\langle \frac{\Sigma_a}{D} \right\rangle = \frac{1}{\tau} \int_0^\tau \frac{\Sigma_a(\tau)}{D(\tau)} \, d\tau , \tag{2.22}$$

then

$$\overline{A}_{mnp}(\tau,s) = H(\tau) S_o C_{mnp} \exp\left[- \left(B_{mnp}^2 + \left\langle \frac{\Sigma_a}{D} \right\rangle \right) \tau \right] e^{- \frac{\tau}{\langle vD \rangle} s} .$$

Inverting the last expression with respect to t and using the relation,[33]

$$2\pi i \delta(t-a) = \lim_{\omega \to \infty} \int_{\nu - i\omega}^{\nu + i\omega} e^{(t-a)s} \, ds ,$$

we get

$$A_{mnp}(\tau,t) = H(\tau) S_o C_{mnp} \exp\left[- \left(B_{mnp}^2 + \left\langle \frac{\Sigma_a}{D} \right\rangle \right) \tau \right] \delta\left(t - \frac{\tau}{\langle vD \rangle} \right) . \tag{2.23}$$

Hence, finally:

$$q(\vec{r},\tau,t) = H(\tau) S_o \, \delta\left(t - \frac{\tau}{\langle vD \rangle} \right) \sum_{m,n,p} C_{mnp} Q_{mnp}(\vec{r}) \, e^{- \left(B_{mnp}^2 + \left\langle \frac{\Sigma_a}{D} \right\rangle \right) \tau} , \tag{2.24}$$

where C_{mnp} and Q_{mnp} are given by Eqs. 2.17 and 2.16, respectively.

Equation 2.24 lends itself readily to a simple physical interpretation. The expression $\tau/\langle vD \rangle$ is the slowing-down time[31] T to age τ; thus, Eq. 2.24 states that for neutrons of any age, the slowing-down density is zero at all times except at t = T. Moreover, the exponential term in Eq. 2.24 is

$$e^{- \left(B_{mnp}^2 + \left\langle \frac{\Sigma_a}{D} \right\rangle \right) \tau} = e^{- \left[\left(B_{mnp}^2 + \left\langle \frac{\Sigma_a}{D} \right\rangle \right) \langle vD \rangle \right] T} .$$

In analogy with the thermal decay, the "slowing-down die-away" is also exponential in time with a decay constant:

$$\Lambda_{mnp} = \langle vD \rangle B^2_{mnp} + \langle vD \rangle \left\langle \frac{\Sigma_a}{D} \right\rangle , \tag{2.25}$$

which is composed of the absorption and leakage rates during slowing down; $\langle vD \rangle$ and $\langle \Sigma_a/D \rangle$ are given by Eqs. 2.22 with the appropriate value of τ. Equation 2.24 gives $q(\vec{r},\tau,t)$ in terms of the modal distribution of neutrons which escape leakage and absorption during slowing down. The thermal slowing-down density is

$$q(\vec{r},\tau_o,t) = S_o \delta(t-T_o) \Sigma C_{mnp} Q_{mnp}(\vec{r}) e^{-\Lambda_{mnp} T_o} , \tag{2.26}$$

where $T_o = \tau_o/\langle vD \rangle$, the slowing-down time to age τ_o.

Our primary interest is in the thermal die-away phase. The time-dependent thermal diffusion equation is:

$$D\nabla^2\phi(\vec{r},t) - \Sigma_a\phi(\vec{r},t) + q(\vec{r},\tau_o,t) = \frac{1}{v}\frac{\partial}{\partial t}\phi(\vec{r},t) , \tag{2.27}$$

and its Laplace Transform is:

$$D\nabla^2\bar{\phi} - \Sigma_a\bar{\phi} + \bar{q}(\vec{r},\tau_o) - \frac{s}{v}\bar{\phi} = 0 .$$

If we write

$$\bar{\phi}(\vec{r},s) = \Sigma \overline{F}_{mnp}(s) Q_{mnp}(\vec{r}) ,$$

we have

$$\left(DB^2_{mnp} + \Sigma_a + \frac{s}{v}\right)\overline{F}_{mnp} = \overline{A}_{mnp}(\tau_o,s) ;$$

or, if we write,

$$\lambda_{mnp} = vDB^2_{mnp} + v\Sigma_a , \tag{2.28}$$

then

$$\overline{F}_{mnp}(s) = \frac{v\,\overline{A}_{mnp}(\tau_o,s)}{s+\lambda_{mnp}} = vS_oC_{mnp} e^{-\Lambda_{mnp}T_o} \frac{e^{-T_o s}}{s+\lambda_{mnp}} .$$

Inverting the Laplace Transform and using the Convolution Theorem,[32, 33] we get:

$$F_{mnp}(t) = vS_oC_{mnp} e^{-\Lambda_{mnp}T_o} \int_0^t \delta(x-T_o) e^{-\lambda_{mnp}(t-x)} dx$$

$$= vS_oC_{mnp} e^{-\Lambda_{mnp}T_o} e^{-\lambda_{mnp}(t-T_o)}$$

$$= vS_oC_{mnp} e^{-(\Lambda_{mnp}-\lambda_{mnp})T_o} e^{-\lambda_{mnp}t} . \qquad (2.30)$$

Hence, the time-dependent thermal neutron flux is

$$\phi(\vec{r},t) = vS_o\Sigma C_{mnp}Q_{mnp}(\vec{r}) e^{-(\Lambda_{mnp}-\lambda_{mnp})T_o} e^{-\lambda_{mnp}t} . \qquad (2.31)$$

We thus also obtain the well-known result that the thermal population dies away exponentially with the decay constant λ_{mnp} of the particular mode given by Eq. 2.28.

2.1.2 Physical Treatment of The Thermal Neutron Decay

It is easy to understand physically why the decay of the thermal flux is exponential, and to derive from purely physical considerations a simple expression for the decay constant. Consider a finite assembly of moderator into which a burst of fast neutrons is injected. Suppose that at time $t = 0$ the neutrons have been moderated and thermalized, and that there are N_o thermal neutrons at $t = 0$. Then there are only two processes which can result in a loss of neutrons: absorption and leakage, and these two events are, to a first approximation, independent. Actually, leakage affects the spectrum and hence the absorption, but this is a second-order effect. The probability that a neutron survives absorption after travelling a distance x is $e^{-\Sigma_a x}$. And, since the leakage rate for any region is $-D\nabla^2\phi$, we can define an average global "leakage cross-section" typical of the geometrical dimensions of the assembly and given by:

$$\Sigma_\ell = \frac{-D\nabla^2\phi}{\phi} = DB^2 .$$

Then the probability for an individual neutron to escape leakage, on the average, while traversing a distance x is $e^{-\Sigma_\ell x}$. Since the two events are independent, the joint probability is the product of the individual probabilities, i.e., $e^{-\Sigma_a x} \cdot e^{-\Sigma_\ell x}$. If the thermal neutrons are considered monoenergetic with average velocity v, then at time t, x = vt and the thermal neutron population that survives after time t is given by

$$N(t) = N_o e^{-\Sigma_a vt} e^{-\Sigma_\ell vt}$$

$$= N_o e^{-(v\Sigma_a + vDB^2)t}$$

$$= N_o e^{-\lambda t}$$

with

$$\lambda = v\Sigma_a + vDB^2. \qquad (2.32)$$

Thus the decay constant is composed of the absorption rate and the leakage rate corresponding to the two possible mutually exclusive modes of neutron loss from the system.

2.1.3 Diffusion Cooling

A treatment such as the one just given, which relies on a description of thermal neutrons as monoenergetic and diffusing without exchanging energy with the medium, masks the effects due to the energy distribution of the neutrons in a finite assembly. Such effects were first brought to light by von Dardel's[34, 35] observation of a non-linearity in the dependence of λ on B^2 for small moderator assemblies. Qualitatively, this effect is readily understood on physical grounds. In a moderator assembly with small dimensions, the main effect which removes neutrons is leakage. If elementary diffusion theory were applicable, and if the asymptotic neutron spectrum were a Maxwellian with the moderator temperature, the effects of leakage would be correctly described by the term $D_o B^2$ where D_o is Maxwellian average of the energy-dependent diffusion coefficient D(E). However, neither of these conditions is strictly valid. A faster neutron has a greater probability of escaping from the moderator than a slower

one, and the moderator continuously and selectively loses neutrons which are "hotter" than the neutrons inside. This loss is partially compensated by the coupling through collisions between the neutron gas and the moderator.[5] These two conteracting processes result in a net shift of the neutron spectrum below the equilibrium Maxwellian distribution; this shift is larger for greater leakage effects and for poorer thermalization properties of the moderator. The resultant softening of the spectrum or "diffusion cooling" tends to reduce the leakage from its simple value $D_o B^2$.

Antonov et al.[26] have investigated the mechanism of this effect by means of a two-group analysis of the diffusion equations; other authors, referred to earlier, have given more sophisticated treatments. The result of careful experimental and theoretical work suggests that higher terms in B^2, especially a B^4 term, have to be considered for small dimensions of the moderator; a trial expression for the decay constant is of the form:

$$\lambda = v\Sigma_a + vDB^2 - CB^4 \pm FB^6 \pm \ldots \qquad (2.33)$$

The coefficient C represents the transport theory corrections to elementary diffusion theory and the effect of diffusion cooling.[12]

The phenomenon of diffusion cooling has opened up fresh approaches to the study of neutron thermalization and has stimulated a great deal of theoretical activity in the field.[7] The parameter C is related to such properties of the moderator as the thermalization time and thermalization power. Experimental studies of diffusion cooling, among other properties, of a moderator are becoming increasingly important in the understanding of the role of the moderator in a thermal reactor. The diffusion cooling effect is also important in multiplying media where spectral effects are more complicated. However, for multiplying media, as the dimensions get smaller, other considerations also arise and it becomes questionable whether the geometrical buckling is a suitable parameter for the description of non-escape probabilities.[36] A recent paper[36a] extends Nelkin's treatment of diffusion cooling to multiplying media.

2.2 MULTIPLYING SYSTEMS

The sequence of events following the injection of a fast neutron burst into a moderated multiplicative system is sketched in Fig. 2.1. Of the ΩS_o fast neutrons (where Ω is a geometrical factor) which enter the finite assembly in each burst, a fraction $\Omega S_o P_s(E_o \rightarrow E_{th})$ reaches thermal energies, constituting the "zeroth" generation of thermal neutrons (source-emitted). The fast neutrons resulting from these, as well as the neutrons produced in epithermal and fast fissions, lead after thermalization to the first generation of thermal neutrons ("lattice" born). Successive generations of thermal neutrons follow in rapid progression determined by the generation time for the system. At each generation, the thermal neutron population changes by a factor k_{eff} as shown in the figure. Hence, if the system is subcritical ($k_{eff} < 1$), there is an over-all progressive decay of the population.

It is easy to see that the gross qualitative time-behavior of the thermal neutron population in a moderated, multiplying, subcritical system following the injection of a fast neutron burst should be as in Fig. 2.2. As the source neutrons diffuse through the medium while slowing down (region I), a maximum is approached at a time depending on the slowing-down properties of the medium. The amplitude depends on the source strength and the multiplication factor of the system. Immediately following the maximum, there occurs a relatively short region (region II) during which the transients die away and the thermal flux stabilizes; the fundamental flux mode due to the prompt neutrons from fission then decays exponentially (region III). Typical values of the lifetime in moderated systems during this decay of the fundamental mode are in the millisecond range. This prompt neutron decay is finally followed by a much longer decay due to delayed neutron effects (region IV); on the time scale shown in Fig. 2.2, this delayed neutron tail is nearly flat because the delayed neutron groups have lifetimes of the order of seconds rather than milliseconds. At delayed critical, this tail is really flat (between bursts), for each neutron lost from the system is eventually replaced; the prompt neutron decay still occurs, however, since the prompt neutrons do not replace themselves immediately.

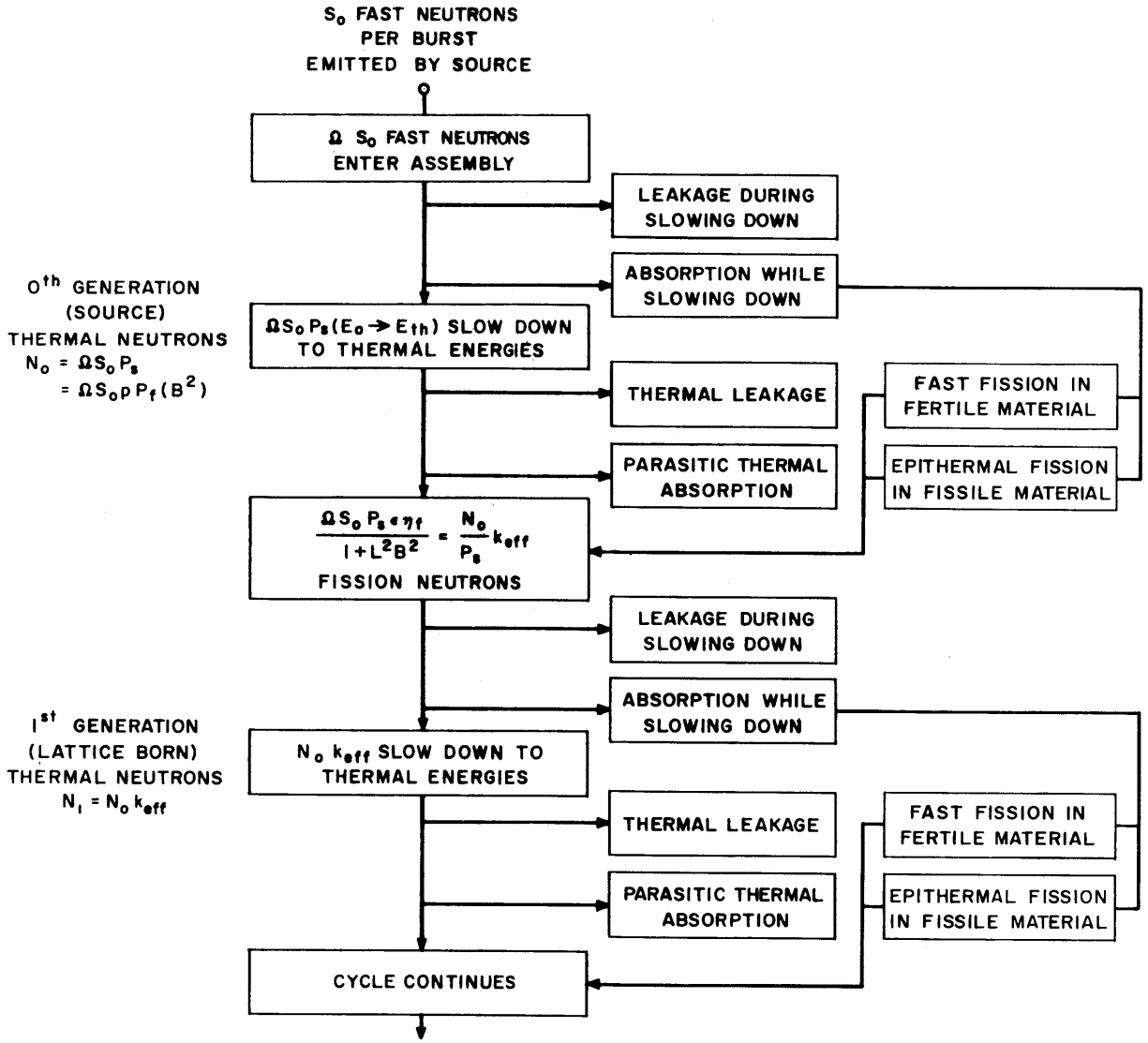

FIG. 2.1 THE SEQUENCE OF EVENTS FOLLOWING THE INJECTION OF A BURST OF FAST NEUTRONS IN A MODERATED SUBCRITICAL SYSTEM

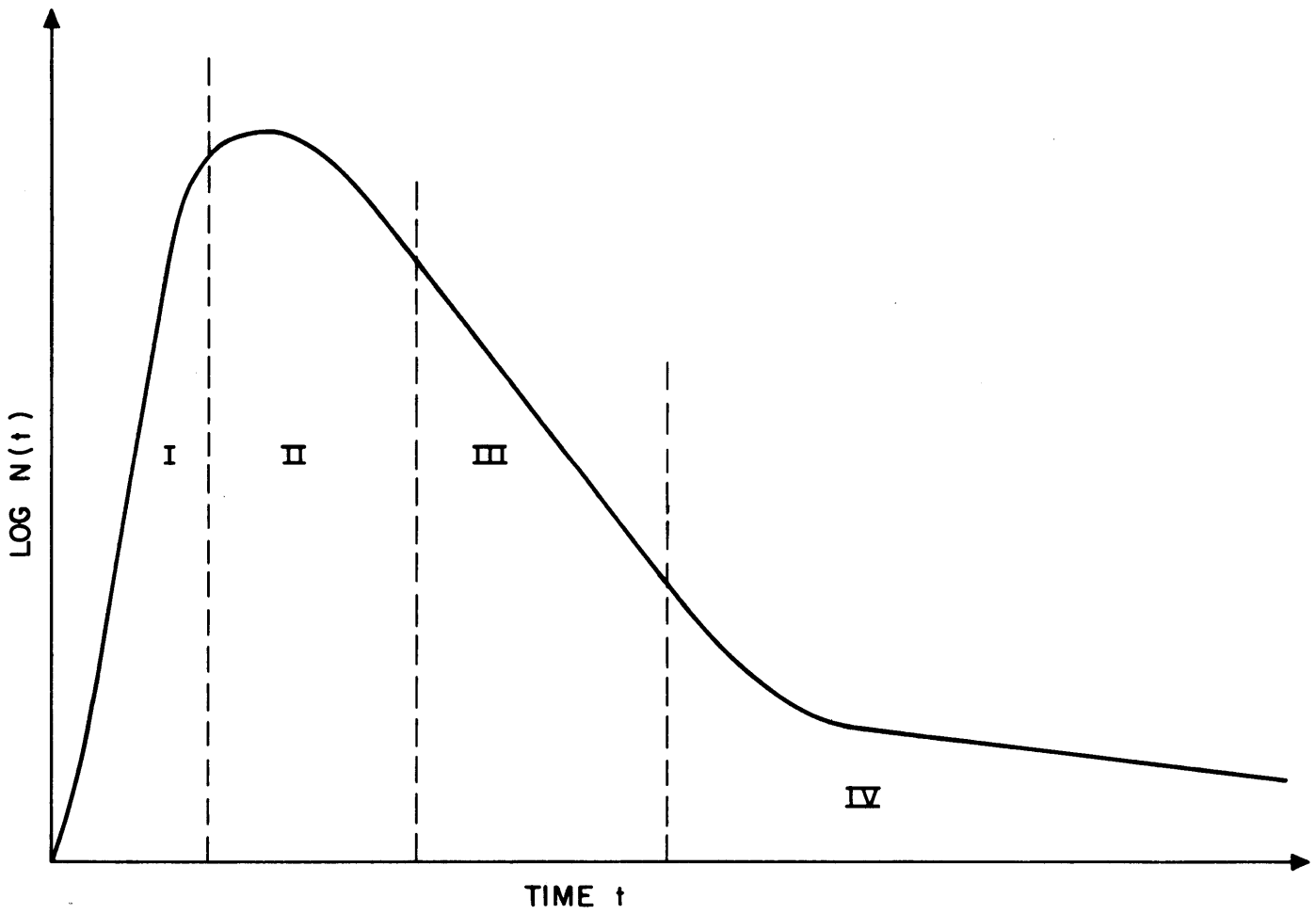

FIG. 2.2 TIME BEHAVIOR OF THE THERMAL NEUTRON POPULATION N(t) (COUNTS/TIME) IN A SUBCRITICAL SYSTEM FOLLOWING THE INJECTION OF A BURST OF FAST NEUTRONS AT t=0.

Spanning this gross behavior is the "fine structure" shown in Fig. 2.3.[36b] The decaying portion is actually represented by an irregular descending step function, with a constant step-width given by the prompt neutron lifetime ℓ. Each of the successive generations is less intense than its predecessor by a fractional decrement δ, so that the fractional rate of flux decay is δ/ℓ sec^{-1}. That the decay is exponential, can be shown in a simple-minded manner by reference to Fig. 2.3. At any stage, we have

$$\frac{dN_r}{dt} = \frac{N_{r+1} - N_r}{\ell} = \frac{(1-\beta)k - 1}{\ell} N_r \tag{2.35}$$

so that

$$N(t) = N_o \exp\left\{\frac{(1-\beta)k-1}{\ell}\right\} t .$$

Thus, the decay is exponential with a decay constant

$$\lambda = \frac{1}{\ell}(1-(1-\beta)k). \tag{2.36}$$

2.2.1 Time Behavior of the Slow Neutron Population; Derivation of the Basic Expression for the Decay Constant

The relationship between the decay constant and the reactor parameters will now be derived in a more rigorous manner without first going into the detailed spatial distribution. The following model of the neutron processes in the system is adopted:

(i) An instantaneous burst of S_o fast neutrons appears either outside or within the system at $t = 0$.

(ii) The fast neutrons undergo the sequence of events indicated in Fig. 2.1.

(iii) The slowing-down time in the system is negligible, so that a thermal flux distribution $\phi_o(\vec{r})$ is assumed to appear effectively at $t = 0$.

(iv) The time of flight from the neutron source to the assembly (when the source is outside) is assumed to be negligible.

(v) The effect of delayed neutrons is not taken into account except insofar as the prompt multiplication is taken to be $(1-\beta)k_o$.

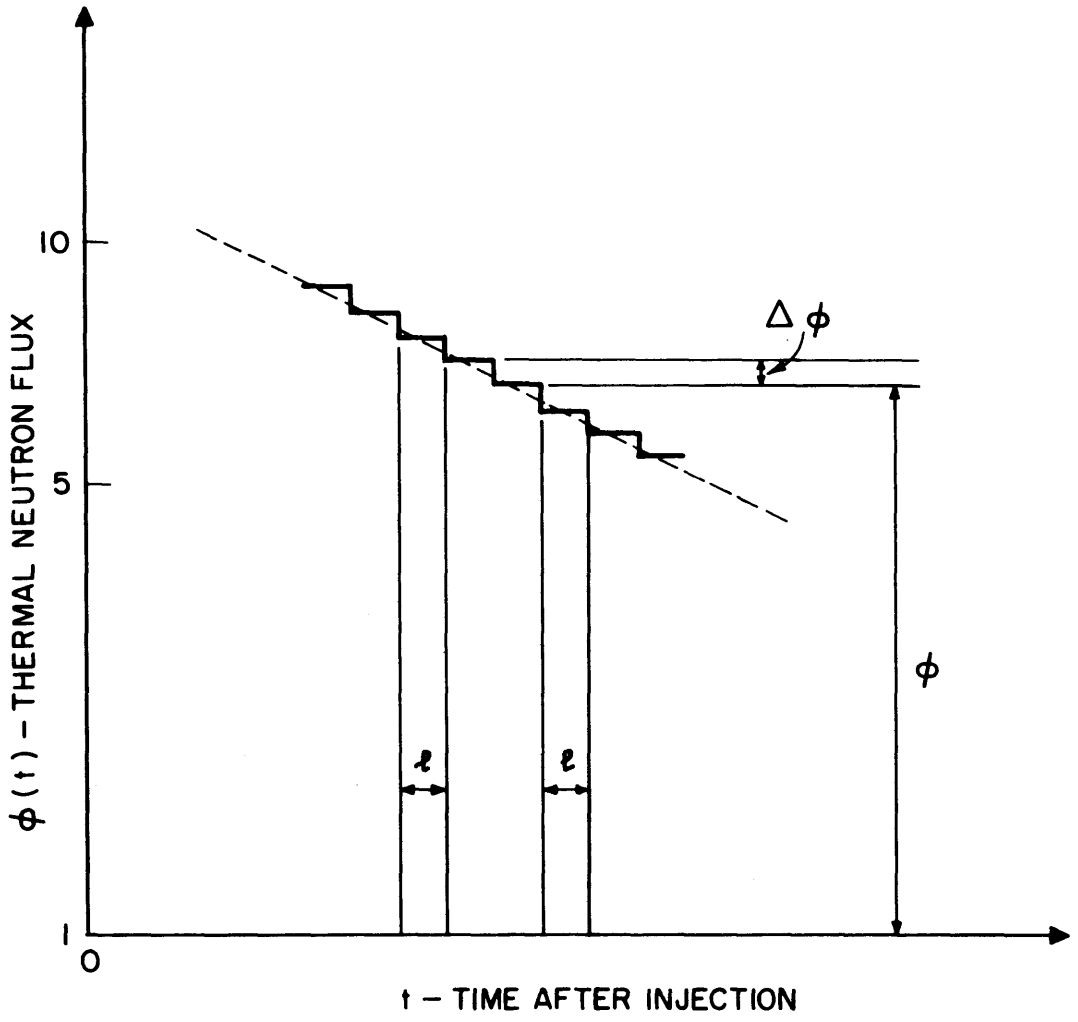

FIG. 2.3 PROMPT NEUTRON FLUX DECAY CURVE FOLLOWING NEUTRON BURST; $\phi(t)$ IS REPRESENTED BY STEP FUNCTION CORRESPONDING TO PROMPT NEUTRON LIFETIME ℓ

It is also assumed, for simplicity, that the assembly is a bare, homogeneous system of some elementary shape. We then wish to determine the thermal flux $\phi(\vec{r},t)$ for an arbitrary shape, given that the distribution at t = 0 is $\phi_o(\vec{r})$.

The appropriate time-dependent thermal neutron diffusion equation is:

$$D\nabla^2\phi(\vec{r},t) - \Sigma_a\phi(\vec{r},t) + (1-\beta)k_o\Sigma_a F(B^2)\,\phi(\vec{r},t) = \frac{1}{v}\frac{\partial}{\partial t}\phi(\vec{r},t)\ , \tag{2.37}$$

where the source term is assumed to be entirely due to prompt neutrons; $F(B^2)$ is the fast non-leakage probability. The boundary conditions are:

$$\begin{aligned} &\phi(S,t) = 0\ , \\ &\phi(\vec{r},0) = \phi_o(\vec{r})\ , \end{aligned} \tag{2.38}$$

where S represents the extrapolated outer surface of the assembly.

Rewriting Eq. 2.37 as

$$\nabla^2\phi(\vec{r},t) + \omega^2\phi(\vec{r},t) = \frac{1}{Dv}\frac{\partial}{\partial t}\phi(\vec{r},t)\ , \tag{2.39}$$

with

$$\omega^2 = \frac{(1-\beta)k_o\Sigma_a F(B^2)}{D} - L^2\ , \tag{2.40}$$

we seek solutions of the form

$$\phi_n(\vec{r},t) = R_n(\vec{r})\,T_n(t)\ . \tag{2.41}$$

Then

$$\frac{\nabla^2 R_n(\vec{r})}{R_n} = \frac{1}{Dv}\frac{T_n'(t)}{T_n} - \omega^2 = -B_n^2\ , \tag{2.42}$$

where B_n^2 is a separation constant. Thus we have

$$\nabla^2 R_n(\vec{r}) + B_n^2 R_n(\vec{r}) = 0\ , \tag{2.43}$$

with

$$R_n(S) = 0\ ,$$

and

$$\frac{d}{dt} T_n(t) + Dv\left(B_n^2-\omega^2\right) T_n(t) = 0 \ , \tag{2.44}$$

with $T_n(0) = T_n^o$. The choice of the separation constant B_n^2 is such as to ensure that the spatial dependence satisfies the Helmholtz equation (2.43). Equation 2.44 gives

$$T_n(t) = T_n^o \, e^{-Dv\left(B_n^2-\omega^2\right) t} \ , \tag{2.45}$$

and the general solution of Eq. 2.37 is:

$$\phi(\vec{r},t) = \sum_n A_n R_n(\vec{r}) \, e^{-Dv\left(B_n^2-\omega^2\right) t} \ , \tag{2.46}$$

where the A_n are determined from the initial conditions

$$\phi(\vec{r},0) \equiv \phi_o(\vec{r}) = \Sigma A_n R_n(\vec{r}) \ ,$$

i.e., (2.47)

$$A_n = \int_v \phi_o(\vec{r}) \, R_n(\vec{r}) \, d\vec{r} \ .$$

Here n is a generic symbolic index which stands for all the subscripts.

Now, substituting for ω^2 from Eq. 2.40, we obtain the time-dependent flux:

$$\phi(\vec{r},t) = \sum_n A_n R_n(\vec{r}) \, e^{-v[DB_n^2+\Sigma_a-(1-\beta)k_o\Sigma_a F(B^2)]\, t} \ . \tag{2.48}$$

The thermal flux in the assembly decays exponentially:

$$\phi_{\ell,m,n}(\vec{r},t) \sim e^{-\lambda_{\ell,m,n} t} \ , \tag{2.49}$$

and the decay constant of any mode is given by

$$\begin{aligned} \lambda_{\ell mn} &= v\Sigma_a + vDB_{\ell mn}^2 - v\Sigma_a(1-\beta)\, k_o F\left(B_{\ell mn}^2\right) \\ &= v\Sigma_a\left[\left(1+L^2B_{\ell mn}^2\right) - k_o(1-\beta)F\left(B_{\ell mn}^2\right)\right] \\ &= v\Sigma_a\left(1+L^2B_{\ell mn}^2\right)[1-(1-\beta)k] \ . \end{aligned} \tag{2.50}$$

For the fundamental mode ℓ=m=n=1, B^2_{111} is the geometric buckling B^2 and we have the equation:

$$\lambda = v\Sigma_a(1+L^2B^2)[1-(1-\beta)k] \ . \tag{2.51}$$

We may write this in several alternative forms:

$$\lambda = v\Sigma_a(1+L^2B^2)\ \frac{\beta-\rho}{1-\rho}\ , \tag{2.52}$$

where

$$\rho = \frac{k_{eff}-1}{k_{eff}} = \frac{k-1}{k} \text{ is the positive reactivity;}$$

$$\lambda = v\Sigma_a + vDB^2 - v\Sigma_a^{fuel}\,\eta\, p(1-\beta)\, F(B^2)$$

$$= v\Sigma_a^{mod} + vDB^2 + v\Sigma_a^{fuel}\{1-\eta(1-\beta)P(B^2)\}\ , \tag{2.53}$$

where $P(B^2)(= pF(B^2))$ is the "thermalization probability" or the three-dimensional Fourier transform of the slowing-down kernel for a point source in an infinite medium. In terms of the thermal neutron lifetime,

$$\ell = \frac{1}{v\Sigma_a(1+L^2B^2)}\ ,$$

$$\lambda = \frac{1}{\ell}[1-(1-\beta)k]$$

$$= \frac{1}{\ell}\cdot\frac{\beta-\rho}{1-\rho}\ . \tag{2.54}$$

Figure 2.4, taken from Ref. 4 with some modifications, illustrates the general variation of λ with B^2.

2.2.2 Space and Time Distribution of Thermal Neutrons in a Pulsed Subcritical System

We next derive an expression for the thermal neutron flux as a general function of both space and time. This treatment will be helpful in the planning and analysis of the pulsed neutron experiments. We shall use a cylindrical assembly as an illustration, but the results are of general validity. The slowing down is assumed to be on the continuous

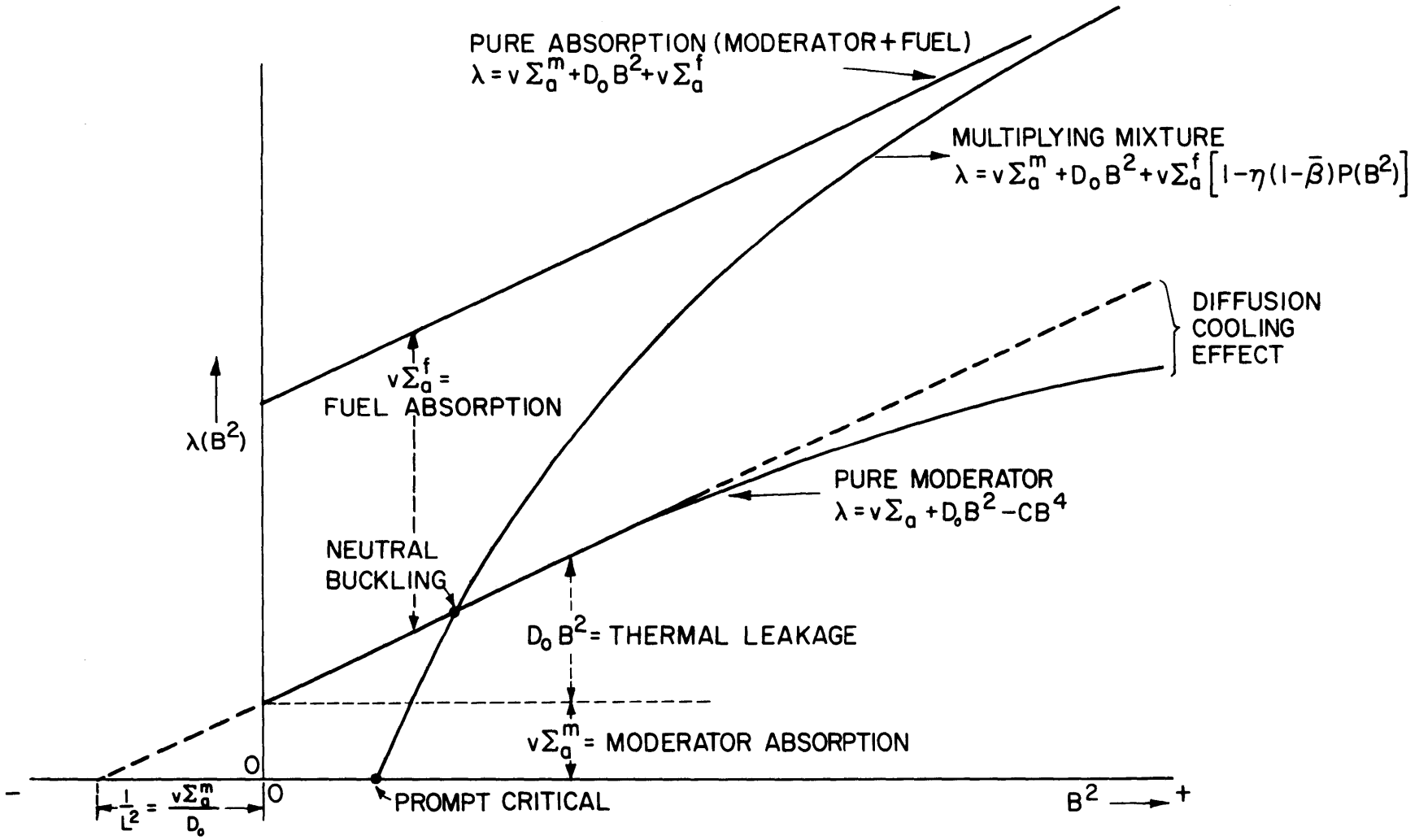

FIG. 2.4 VARIATION OF THE FUNDAMENTAL MODE DECAY CONSTANT λ, WITH THE GEOMETRICAL BUCKLING B^2, FOR SUBCRITICAL MULTIPLYING SYSTEM (EQ. 2.53)

slowing model and other assumptions are the same as in Section 2.2.1; the delayed neutron effects are ignored except for the designation of the prompt multiplication as $(1-\beta)k_o$.

A. Source Neutrons

The fast die-away of the source neutrons in the energy range, say, 14 Mev to 2 Mev, can be considered separately in terms of a removal cross-section Σ_o and the parameters D_o representing this range. The diffusion equation for the source flux ϕ_o is then:

$$D_o\nabla^2\phi_o(\vec{r},t) - \Sigma_o\phi_o(\vec{r},t) + S(\vec{r},t) = \frac{1}{v_o}\frac{\partial}{\partial t}\phi_o(\vec{r},t) \tag{2.55}$$

where

$$S(\vec{r},t) = S_o\frac{\delta(r-r_o)\,\delta(z-z_o)\,\delta(\theta)}{r}\,\delta(t)\ .$$

Equation 2.55 can be solved by a method similar to that used in Section 2.1.1. A Laplace Transformation gives:

$$D_o\nabla^2\bar{\phi}_o - \Sigma_o\bar{\phi}_o + \bar{S} = \frac{s}{v_o}\bar{\phi}_o\ ,$$

with (2.56)

$$\bar{S} = S_o\frac{\delta(r-r_o)\,\delta(z-z_o)\,\delta(\theta)}{r}\ .$$

In analogy with Eqs. 2.13 and 2.14, we set

$$\bar{\phi}_o(\vec{r},s) = \Sigma\,\bar{A}_{mnp}(s)Q_{mnp}(\vec{r})\ ,$$

and (2.57)

$$\delta(\vec{r}-\vec{r}_o) = \Sigma\,C_{mnp}Q_{mnp}(\vec{r})\ ,$$

where the $Q_{mnp}(\vec{r})$ are the eigenfunctions (Eq. 2.16) of Eq. 2.12 as before. Proceeding along the same lines, we obtain:

$$\bar{A}_{mnp}(s) = \frac{1}{s+\lambda_{m,n,p}}\frac{\int_v \delta(\vec{r}-\vec{r}_o)\,Q_{m,n,p}(\vec{r})\,d\vec{r}}{\int_v Q^2_{m,n,p}(\vec{r})\,d\vec{r}} \tag{2.58}$$

$$= \frac{4v_oS_o}{\pi R^2(2H)}\frac{1}{1+\delta_{o,m}}\frac{J_m\left(\beta_{mn}\frac{r_o}{R}\right)}{\left[J'_m(\beta_{mn})\right]^2}\sin\frac{p\pi}{H}z_o\frac{1}{s+\lambda_{m,n,p}}\ ,$$

where

$$\lambda_{m,n,p} = v_o\Sigma_o + v_oD_o\left[\left(\frac{\beta_{m,n}}{R}\right)^2 + \left(\frac{p\pi}{2H}\right)^2\right] . \tag{2.59}$$

Hence, the space-time dependent source flux is:

$$\phi_o(\vec{r},t) = \frac{4v_oS_o}{\pi R^2(2H)} \sum_{m,n,p} \frac{1}{1+\delta_{o,m}} \frac{J_m\left(\beta_{m,n}\frac{r_o}{R}\right)}{\left[J'_m(\beta_{mn})\right]^2} \sin\frac{p\pi}{H} z_o$$

$$\times J_m\left(\beta_{mn}\frac{r}{R}\right) \cos m\phi \sin\frac{p\pi}{H} z_o \, e^{-\lambda_{m,n,p}t} . \tag{2.60}$$

B. Lattice-Born Thermal Neutrons

The diffusion equation for the lattice-born thermal neutrons is

$$D\nabla^2\phi(r,z,t) - \Sigma_a\phi(r,z,t) + pq(r,z;\tau_2) = \frac{1}{v}\frac{\partial}{\partial t}\phi(r,z,t) , \tag{2.61}$$

where the diffusion parameters, D and Σ_a, are for thermal neutrons, τ_2 and p are the Fermi age to thermal energy and resonance escape probability, respectively; the slowing-down density q is for a system with no resonance absorption. For simplicity, azimuthal symmetry is assumed so that the ϕ-dependence is eliminated.

The slowing-down density is given by the Fermi-age equation:

$$\nabla^2 q(r,z,\tau) = \frac{\partial}{\partial\tau} q(r,z,\tau) . \tag{2.62}$$

The boundary conditions are:

$$\phi(S) = 0 = q(S) \tag{2.63}$$

on the extrapolated boundary and at the source energy (τ=0),

$$q(r,z,t;\tau=0) = (1-\beta)\frac{k_o}{p}\Sigma_a\phi(t-T) + S_o\delta(\vec{r}-\vec{r}_o)\,\delta(t) , \tag{2.64}$$

the slowing-down time T will be assumed to be negligible, the source is at (r_o,z_o):

$$S_o\delta(\vec{r}-\vec{r}_o) = S_o\frac{\delta(r-r_o)\,\delta(z-z_o)}{r} . \tag{2.65}$$

The above equations will be solved by means of transform techniques: a Laplace Transform in the time variable t; a finite Hankel Transform in the space variable r; and a finite Sine Transform in the space variable z. The Laplace Transform pair has already been defined in Eq. 2.10a,b. The Laplace Transformation, with respect to t applied to the above equations and boundary conditions, gives

$$D\nabla^2\bar{\phi}(r,z,s) - \left(\Sigma_a + \frac{s}{v}\right)\bar{\phi} + p\bar{q} = 0 \ , \tag{2.66}$$

$$\nabla^2\bar{q} = \frac{\partial}{\partial\tau}\bar{q} \ , \tag{2.67}$$

$$\bar{q}(\tau=0) = (1-\beta)\frac{k_o}{p}\Sigma_a\phi + S_o\delta(\vec{r}-\vec{r}_o) \ , \tag{2.68}$$

$$\bar{q}(S) = 0 = \bar{\phi}(S) \ . \tag{2.69}$$

A finite Hankel Transform[37] pair is defined as follows: if

$$\bar{f}(\xi_m) = \int_0^R rf(r)\, J_o(\xi_m r)\, dr \ , \tag{2.70}$$

where

$$J_o(\xi_m R) = 0 \ ,$$

then

$$f(r) = \frac{2}{R^2}\sum_{m=1}^{\infty}\bar{f}(\xi_m)\frac{J_o(\xi_m r)}{[J_1(\xi_m R)]^2} \ . \tag{2.70a}$$

Now, in cylindrical coördinates with no angular dependence, the Laplacian Operator is:

$$\nabla^2 \equiv \frac{\partial^2}{\partial r^2} + \frac{1}{r}\frac{\partial}{\partial r} + \frac{\partial^2}{\partial z^2} \ ,$$

and the Hankel Transform of $\nabla^2 f$ is:

$$\int_0^R r[\nabla^2 f(r,z)]\, J_o(\xi_m r)\, dr = R\xi_m f(R,z) J_1(\xi_m r) - \xi_m^2 \bar{f}(\xi_m,z) + \frac{\partial^2}{\partial z^2}\bar{f}(\xi_m z) \tag{2.71}$$

If then, we take the finite Hankel Transform of Eqs. 2.66-2.68, by virtue of the boundary condition,

$$\bar{\phi}(R,z) = 0 ,$$

the first term on the right side of Eq. 2.71 vanishes and the transformed equations are (double bars indicate transformed functions after the application of Laplace and Hankel transforms):

$$-\xi_m^2 \bar{\bar{\phi}}(\xi_m,z) + \frac{\partial^2}{\partial z^2}\bar{\bar{\phi}} - \frac{\Sigma'_a}{D}\bar{\bar{\phi}} + \frac{p\bar{\bar{q}}}{D} = 0 , \tag{2.72}$$

$$-\xi_m^2 \bar{\bar{q}}(\tau,\xi_m,z) + \frac{\partial^2}{\partial z^2}\bar{\bar{q}} = \frac{\partial}{\partial \tau}\bar{\bar{q}} , \tag{2.73}$$

$$\bar{\bar{q}}(\tau=0) = (1-\beta)\frac{k_o}{p}\Sigma_a\bar{\bar{\phi}} + S_o\delta(z-z_o)\,J_o(\xi_m r_o) , \tag{2.74}$$

where we have written for simplicity,

$$\Sigma'_a = \Sigma_a + \frac{s}{v} . \tag{2.75}$$

Finally, we use the finite Sine Transform with respect to z. This transform pair[37] is defined as

$$\bar{\bar{\bar{f}}}(n) = \int_0^H \bar{\bar{f}}(z)\sin\left(\frac{n\pi z}{H}\right) dz , \tag{2.76}$$

$$\bar{\bar{f}}(z) = \frac{2}{H}\sum_{n=1}^{\infty} \bar{\bar{\bar{f}}}(n)\sin\frac{n\pi}{H}z . \tag{2.77}$$

Observing that

$$\int_0^H \left(\frac{\partial^2 \bar{\bar{f}}(z)}{\partial z^2}\right)\sin\left(\frac{n\pi}{H}\right)z \; dz = -\frac{n^2\pi^2}{H^2}\bar{\bar{\bar{f}}}(n) , \tag{2.78}$$

we obtain the finite Sine Transformation of Eqs. 2.72-2.74:

$$-\left(\xi_m^2 + \frac{n^2\pi^2}{H^2} + \frac{\Sigma'_a}{D}\right)\bar{\bar{\bar{\phi}}}(\xi_m,n) + \frac{p}{D}\bar{\bar{\bar{q}}}(\tau_2,\xi_m,n) = 0 , \tag{2.79}$$

$$-\left(\xi_m^2 + \frac{n^2\pi^2}{H^2}\right)\bar{\bar{\bar{q}}}(\tau,\xi_m,n) = \frac{\partial}{\partial\tau}\bar{\bar{\bar{q}}}(\tau,\xi_m,n) , \tag{2.80}$$

$$\overline{\overline{\overline{q}}}(\tau=0) = (1-\beta)\frac{k_o}{p}\Sigma_a\overline{\overline{\overline{\phi}}} + S_o J_o(\xi_m r_o)\sin\frac{n\pi}{H}z_o \,. \tag{2.81}$$

Now, Eq. 2.80 is linear in τ and its solution – in conjunction with the "initial condition" (2.81) – is:

$$\overline{\overline{\overline{q}}}(\tau,\xi_m,n) = \left[(1-\beta)\frac{k_o}{p}\Sigma_a\overline{\overline{\overline{\phi}}} + S_o J_o(\xi_m r_o)\sin\frac{n\pi}{H}z_o\right] e^{-B^2_{m,n}\tau} \,, \tag{2.82}$$

where we have written

$$B^2_{m,n} = \xi^2_m + \frac{n^2\pi^2}{H^2} \,. \tag{2.83}$$

Substituting from Eqs. 2.82, 2.83 and 2.75 in Eq. 2.79, we get:

$$\left(DB^2_{m,n} + \Sigma_a + \frac{s}{v}\right)\overline{\overline{\overline{\phi}}} = p\left[(1-\beta)\frac{k_o}{p}\Sigma_a\overline{\overline{\overline{\phi}}} + S_o J_o(\xi_m r_o)\sin\frac{n\pi}{H}z_o\right] e^{B^2_{m,n}\tau} \tag{2.84}$$

whence

$$\overline{\overline{\overline{\phi}}}(\xi_m,n,s) = \frac{vpS_o J_o(\xi_m r_o)\sin\left(\frac{n\pi}{H}z_o\right) e^{-B^2_{m,n}\tau 2}}{s+\lambda_{m,n}} \,, \tag{2.85}$$

with

$$\lambda_{m,n} = v\Sigma_a + vDB^2_{m,n} - (1-\beta)k_o v\Sigma_a e^{-B^2_{m,n}\tau 2} \,. \tag{2.86}$$

If we invert the various transforms, using their respective inversion properties, we finally have:

$$\phi(r,z;t) = S_o pv\frac{4}{R^2 H}\sum_{m,n}\frac{J_o(\xi_m r_o)}{[J_1(\xi_m R)]^2}\sin\frac{n\pi}{H}z_o\, e^{-B^2_{m,n}\tau}$$

$$\cdot\, J_o(\xi_m r)\sin\frac{n\pi}{H}z\, e^{-\lambda_{m,n}t} \,. \tag{2.87}$$

Also, substituting Eq. 2.85 in Eq. 2.82, we get:

$$\overline{\overline{\overline{q}}}(\tau,\xi_m,n,s) = \left[\frac{(1-\beta)k_o v\Sigma_a e^{-B^2_{m,n}\tau 2}}{s+\lambda_{m,n}} + 1\right] S_o J_o(\xi_m r_o)\sin\left(\frac{n\pi z_o}{H}\right) e^{-B^2_{m,n}\tau} \,, \tag{2.88}$$

and, on inverting the transforms,

$$q(\tau,r,z,t) = \frac{4}{R^2 H} S_o \sum_{m,n} \frac{J_o(\xi_m r_o)}{[J_1(\xi_m R)]^2} \sin\frac{n\pi}{H} z_o \, J_o(\xi_m r) \sin\frac{n\pi}{H}$$

$$\cdot e^{-B_{mn}^2 \tau} \left\{ (1-\beta) k_o v \Sigma_a \, e^{-B_{m,n}^2 \tau} \cdot e^{-\lambda_{m,n} t} + \delta(t) \right\} . \qquad (2.89)$$

The appearance of the delta function $\delta(t)$ is a consequence of neglecting the slowing-down time.

2.2.3 Generalized Age Treatment with m-Groups of Delayed Neutrons

The differential equation expressing the conservation of thermal neutrons with the source term given by the Fermi-age model is:

$$D\nabla^2\phi(\vec{r},t) - \Sigma_a\phi(\vec{r},t) + pq(\vec{r},t,\tau_2) = \frac{1}{v}\frac{\partial}{\partial t}\phi(\vec{r},t) , \qquad (2.90)$$

where τ_2 is the age to the thermal group and the slowing-down density $q(\vec{r},t,z)$ obeys the age equation:

$$\nabla^2 q(\vec{r},t,\tau) = \frac{\partial}{\partial\tau} q(\vec{r},t,\tau) . \qquad (2.91)$$

The balance equation for fast neutrons, including delayed neutron production, is:

$$q(\vec{r},t,0) = (1-\beta)\frac{k_o}{p}\Sigma_a\phi(\vec{r},t-T)\,H(t-T) + \sum_{j=1}^{m} \omega_j C_j(\vec{r},t) + S_o\delta(\vec{r})\,\delta(t) , \qquad (2.92)$$

where ω_j is the decay constant of the j^{th} delayed neutron precursor, C_j is the concentration of the j^{th} precursor, T is the slowing-down time and H(t) is the unit Heaviside function which is zero for negative argument and unity otherwise; the pulsed source of strength S_o neutrons per burst is assumed to be located at the origin. The conservation of each of the m-delayed neutron precursors is expressed by the equation:

$$\beta_j \frac{k_o}{p}\Sigma_a\phi(\vec{r},t) - \omega_j C_j(\vec{r},t) = \frac{\partial}{\partial t} C_j(\vec{r},t) . \qquad (2.93)$$

In addition, the boundary conditions at the extrapolated boundary S are:

$$\phi(S,t) = 0 = q(S,t,\tau) = C_j(S,t) \ . \tag{2.94}$$

In solving the above equations, we are mainly interested in the time behavior of the thermal flux. We assume that the slowing-down density is separable in its variables and can be expressed as:

$$q(\vec{r},t,\tau) = \Sigma \ Q_n R_n(\vec{r}) \ \theta_n(\tau) \ \psi_n(t) \ , \tag{2.95}$$

where Q_n are constant coefficients, $R_n(\vec{r})$ are the eigenfunctions of the Helmholtz equation vanishing on the extrapolated boundary as before; $\theta_n(\tau)$ and $\psi_n(t)$ have to be determined; the subscript n is a symbolic composite subscript which stands for three subscripts in three spatial dimensions, so that actually,

$$\begin{aligned} R_n(\vec{r}) &\equiv R_{mnp}(\vec{r}) \ , \\ \psi_n(t) &\equiv \psi_{mnp}(t) \ , \\ &\text{etc.} \end{aligned} \tag{2.96}$$

Now, substituting Eq. 2.95 in Eq. 2.90 and making use of the orthogonality property of the $R_n(\vec{r})$, we get

$$\frac{d\theta_n(\tau)}{d\tau} = -B_n^2 \theta_n(\tau) \ ,$$

so that

$$\theta_n(\tau) = e^{-B_n^2 \tau} \ , \tag{2.97}$$

if it is assumed that

$$\theta_n(0) = 1 \ .$$

We further assume the space-time separability of the thermal flux and each precursor concentration

$$\begin{aligned} \phi(\vec{r},t) &= \sum_n R_n(\vec{r}) \ \psi_n(t) \ , \\ C_j(\vec{r},t) &= \sum_n R_n(\vec{r}) \ C_{jn}(t) \ . \end{aligned} \tag{2.98}$$

We also use the relation:

$$\delta(\vec{r})\,\delta(t) = \delta(t) \sum_n D_n R_n(\vec{r}) \,, \tag{2.99}$$

where the constant coefficients D_n can be evaluated from the orthogonality of the eigenfunctions $R_n(\vec{r})$, as in Eq. 2.14.

Substituting Eqs. 2.95, 2.97 and 2.98 into Eq. 2.90 and setting the coefficient of R_n to zero, we get:

$$\left[-DB_n^2 - \Sigma_a + pQ_n\, e^{-B_n^2\tau_2}\right]\psi_n(t) = \frac{1}{v}\frac{\partial}{dt}\psi_n(t) \,. \tag{2.100}$$

Again, substituting Eqs. 2.95, 2.97, 2.98 and 2.99 into Eq. 2.92, we obtain in the same manner:

$$Q_n\psi_n(t) = (1-\beta)\frac{k_o}{p}\Sigma_a H(t-T)\,\psi_n(t-T) + \sum_j \omega_j C_{jn}(t) + S_o D_n \delta(t) \,. \tag{2.101}$$

We can now eliminate the Q_n between Eqs. 2.100 and 2.101, so as to get:

$$-\Sigma_a(1+L^2B^2)\psi_n(t) + (1-\beta)k_o\, e^{-B_n^2\tau_2}\,\Sigma_a H(t-T)\,\psi_n(t-T) + p\, e^{-B_n^2\tau_2}\sum_j \omega_j C_{jn}(t)$$

$$+ S_o p D_n\, e^{-B_n^2\tau_2}\,\delta(t) = \frac{1}{v}\frac{d}{dt}\psi_n(t) \,. \tag{2.102}$$

If we define the effective multiplication factor and the prompt neutron lifetime for the finite system

$$\frac{k_o\, e^{-B_n^2\tau_2}}{1 + L^2B_n^2} \equiv k_n \,,$$

$$\frac{1}{v\Sigma_a(1+L^2B_n^2)} = \ell_n \,, \tag{2.103}$$

and divide Eq. 2.102 throughout by $\Sigma_a(1+L^2B_n^2)$, we get:

$$-\psi_n(t) + (1-\beta)k_n\, H(t-T)\psi_n(t-T) + \frac{p\, e^{-B_n^2\tau_2}}{\Sigma_a(1+L^2B_n^2)} \sum_j \omega_j C_{jn}(t)$$

$$= \ell_n \frac{d}{dt}\psi_n(t) - \frac{pS_o\, e^{-B_n^2\tau_2}}{\Sigma_a(1+L^2B^2)}\, D_n\delta(t) \ . \qquad (2.104)$$

So far, Eq. 2.93 has not been used; if we substitute in it the expression (2.98), we also get

$$\beta_j \frac{k_o}{p}\Sigma_a\psi_n(t) - \omega_j C_{jn}(t) = \frac{d}{dt} C_{jn}(t) \ . \qquad (2.105)$$

Thus, the original set of equations has been reduced to Eqs. 2.104 and 2.105, in $\psi_n(t)$ and $C_{jn}(t)$. We next apply the Laplace Transformation and then eliminate the C_{jn}. The Laplace-transformed equations are (assuming $\psi_n(0) = 0 = C_{jn}(0)$):

$$\left[(1-\beta)k_n\, e^{-sT} - 1 - s\ell_n\right]\bar{\psi}_n(s) + \frac{p\, e^{-B_n^2\tau_2}}{1+L^2B_n^2} \sum_j \omega_j \bar{C}_{jn}(s) = -\frac{S_o p\, e^{-B_n^2\tau_2}}{\Sigma_a(1+L^2B_n^2)}\, D_n \ , \qquad (2.106)$$

and

$$\beta_j \frac{k_o}{p}\Sigma_a\bar{\psi}_n(s) - (\omega_j + s)\bar{C}_{jn}(s) = 0 \ . \qquad (2.107)$$

The result of the elimination of $\bar{C}_{jn}(s)$ between Eqs. 2.106 and 2.107 is

$$\left\{(1-\beta)k_n\, e^{-sT} - 1 - s\ell_n + k_n \sum_j \frac{\beta_j\omega_j}{\omega_j + s}\right\}\bar{\psi}_n(s) = -\frac{S_o p\, e^{-B_n^2\tau_2}}{\Sigma_a(1+L^2B_n^2)}\, D_n \ . \qquad (2.108)$$

Hence

$$\bar{\psi}_n(s) = \frac{\dfrac{S_o p\, e^{-B_n^2\tau_2}}{\Sigma_a(1+L^2B_n^2)} D_n}{1 - (1-\beta)k_n\, e^{-sT} + s\ell_n - k_n \sum_j \dfrac{\beta_j\omega_j}{\omega_j + s}} \ . \qquad (2.109)$$

We are interested in the persisting mode of the flux and, therefore, in the behavior of $\psi_n(t)$ after long times. Now, according to the Tauberian Theorem,[33] the asymptotic behavior of $\psi_n(t)$ is determined by the pole of $\bar{\psi}_n(s)$ with the largest real part. Hence, we must investigate the singularities of $\bar{\psi}_n(s)$; these are given by the zeros of

$$1 - k_n(1-\beta)e^{-sT} + s\ell_n - k_n \sum \frac{\beta_j \omega_j}{\omega_j + s} = 0 , \tag{2.110}$$

or, if the slowing-down time is negligible, $T \to 0$, and

$$1 - k_n + s\ell_n + sk_n \sum \frac{\beta_j}{\omega_j + s} = 0 , \tag{2.111}$$

which is a polynomial equation of degree (m+1) in s and has (m+1) zeros. Furthermore, $s \sum \frac{\beta_j}{\omega_j + s}$ decreases continuously as s increases along the real axis $\left(\frac{\partial}{\partial s} \left\{ s \sum \frac{\beta_j}{\omega_j + s} \right\} = - \sum \frac{\omega_j \beta_j}{(\omega_j + s)^2} < 0 \right)$, while $(1-k_n) + s\ell_n$ continuously increases linearly as s increases. Consequently, there must exist one and only one real simple root $s = \lambda_n$ of Eq. 2.111 and, therefore, a single real simple pole of $\bar{\psi}_n(s)$. Moreover, it can be shown that this is also the pole with the largest real part; i.e., the real part of any complex root of Eq. 2.111 is less than λ_n. Hence, it follows from the Tauberian Theorem,[33] that the asymptotic behavior of $\psi_n(t)$ is given by:

$$\psi_n(t) \sim A_n e^{-\lambda_n t} , \tag{2.112}$$

where A_n is the residue of $\bar{\psi}_n(s)$ at the simple pole $s = \lambda_n$:

$$A_n = \lim_{s\to-\lambda_n} \{(s+\lambda_n)\bar{\psi}_n(s)\}$$

$$= \lim_{s\to-\lambda_n} \left\{ \frac{\dfrac{S_o p e^{-B_n^2\tau_2}}{\Sigma_a(1+L^2B_n^2)} D_n}{\dfrac{d}{ds}\left\{1 - k_n + s\ell_n + sk_n \sum \dfrac{\beta_j}{(\omega_j+s)}\right\}_{s=-\lambda_n}} \right\}$$

$$= \frac{\dfrac{S_o p e^{-B_n^2\tau_2}}{\Sigma_a(1+L^2B_n^2)} D_n}{\ell_n + k_n \sum_j \dfrac{\beta_j\omega_j}{(\omega_j-\lambda_n)^2}} \quad . \tag{2.113}$$

Hence we conclude that the thermal flux is given by:

$$\phi(\vec{r},t) = \sum_n R_n(\vec{r})\, \psi_n(t) \ , \tag{2.95}$$

where

$$\psi_n(t) = \frac{\dfrac{S_o p e^{-B_n^2\tau_2}}{\Sigma_a(1+L^2B_n^2)} D_n}{\ell_n + k_n \sum \dfrac{\beta_j\omega_j}{(\omega_j-\lambda_n)^2}} e^{-\lambda_n t} \ , \tag{2.114}$$

and λ_n is the real root of the equation

$$1 - k_n - \lambda_n\ell_n - \lambda_n k_n \sum \frac{\beta_j}{\omega_j - \lambda_n} = 0 \ . \tag{2.115}$$

The $R_n(\vec{r})$ are, as before, the eigenfunctions of the Helmholtz equation which vanish at the extrapolated boundary of the system. The coefficients D_n are determined from

$$\delta(\vec{r}-\vec{r}_o) = \sum_n D_n R_n(\vec{r}) \ , \tag{2.116}$$

if the source of pulsed neutrons is located at $\vec{r} = \vec{r}_o$.

The decay constant λ of the fundamental mode (n=1) of the thermal flux is given as a root of the equation

$$1 - k - \lambda\ell - \lambda k \sum \frac{\beta_j}{\omega_j - \lambda} = 0 \ . \tag{2.117}$$

If we define the positive reactivity of the system as

$$\rho = \frac{k - 1}{k} \ , \tag{2.118}$$

the above equation becomes

$$\rho + \lambda \frac{\ell}{k} + \lambda \sum \frac{\beta_j}{\omega_j - \lambda} = 0 \tag{2.119}$$

or, after a slight manipulation,

$$-\beta + \rho + \lambda \frac{\ell}{k} + \sum \frac{\omega_j \beta_j}{\omega_j - \lambda} = 0 \ .$$

Hence we have the iterative formula for λ:

$$\lambda = \frac{1}{\ell^*} \left[\beta - \rho + \sum_j \frac{\omega_j \beta_j}{\lambda - \omega_j} \right], \tag{2.121}$$

where ℓ^* is the modified thermal neutron lifetime

$$\ell^* = \frac{\ell}{k} = \frac{1}{k} \cdot \frac{1}{v\Sigma_a(1+B^2L^2)} \ . \tag{2.122}$$

We can also write just in terms of ρ:

$$\lambda = \frac{1}{\ell} \cdot \frac{1}{\ell - \rho} \left\{ \beta - \rho + \sum_j \frac{\omega_j \beta_j}{\lambda - \omega_j} \right\} . \tag{2.123}$$

2.2.4 Two-Group Treatment with m-Groups of Delayed Neutrons

In this section, the neutrons will be divided into two energy groups - fast (denoted by subscript 1) and thermal (denoted by subscript 2). The fast group comprises the energy span from fission energy (with an effective

upper limit of 10 Mev) to thermal:

$$\phi_1(\vec{r},t) = \int_{E_2}^{E_{fiss}} \phi(E,\vec{r},t)\, dE \ . \tag{2.124}$$

The source neutrons, which are usually in the neighborhood of 14 Mev, are slowed down to the fast group; this slowing down of the source neutrons was considered in Section 2.2.2A in terms of a source-removal cross-section Σ_o yielding a source term $\Sigma_o\phi_o$ for the fast group.

The two-group balance equations with m-groups of delayed neutrons can be written in matrix notation:

$$\begin{pmatrix} D_1\nabla^2 - \Sigma_1 & 0 \\ p\Sigma_1 & D_2\nabla^2 - \Sigma_a \end{pmatrix}\begin{pmatrix}\phi_1\\ \phi_2\end{pmatrix} + (1-\beta)k_o\begin{pmatrix} 0 & \frac{\Sigma_a}{p} \\ 0 & 0\end{pmatrix}\begin{pmatrix}\phi_1\\ \phi_2\end{pmatrix}$$

$$+ \sum_j \omega_j \begin{pmatrix} C_j \\ 0\end{pmatrix} + \Sigma_o\begin{pmatrix}\phi_o\\ 0\end{pmatrix} = \begin{pmatrix} \frac{1}{v_1} & 0 \\ 0 & \frac{1}{v_2}\end{pmatrix}\begin{pmatrix}\frac{\partial\phi_1}{\partial t}\\ \frac{\partial\phi_2}{\partial t}\end{pmatrix}, \tag{2.125}$$

and

$$\frac{\partial}{\partial t}\begin{pmatrix} C_j \\ 0\end{pmatrix} = -\omega_j\begin{pmatrix} C_j \\ 0\end{pmatrix} + \beta_j k_o\begin{pmatrix} 0 & \frac{\Sigma_a}{p} \\ 0 & 0\end{pmatrix}\begin{pmatrix}\phi_1\\ \phi_2\end{pmatrix} . \tag{2.126}$$

They may also be written in the form:

$$\begin{aligned} D_1\nabla^2\phi_1 - \Sigma_1\phi_1 + (1-\beta)k_o\frac{\Sigma_a}{p}\phi_2 + \sum_j \omega_j C_j + \Sigma_o\phi_o &= \frac{1}{v_1}\frac{\partial}{\partial t}\phi_1 \ , \\ D_2\nabla^2\phi_2 - \Sigma_2\phi_2 + p\Sigma_1\phi_1 &= \frac{1}{v_2}\frac{\partial}{\partial t}\phi_2 \ , \end{aligned} \tag{2.127}$$

$$-\omega_j C_j + \beta_j\frac{k_o}{p}\Sigma_a\phi_2 = \frac{\partial}{\partial t}C_j \ . \tag{2.128}$$

In these equations, "up-scattering" (from group 2 to 1) is not considered.

The solution will be obtained with the aid of the Laplace Transformation. If the initial conditions,

$$\phi_{1,2}(t=0) = 0 = C_j(t=0) ,$$

are assumed, the spatial dependence is, as usual, determined by the Helmholtz equation, so that:

$$\nabla^2 \phi^n_{1,2} = -B_n^2 \phi^n_{1,2} .$$

Hence, the transformed equations give, after elimination of C_j,

$$-\left(D_1 B_n^2 + \Sigma_1 + \frac{s}{v_1}\right)\bar{\phi}_1 + \left(1 - \beta + \sum_j \frac{\omega_j \beta_j}{\omega_j + s}\right) k_o \frac{\Sigma_a}{p} \bar{\phi}_2 = -\Sigma_o \bar{\phi}_o ,$$

$$p\Sigma_1 \bar{\phi}_1 - \left(D_2 B_n^2 + \Sigma_a + \frac{s}{v_2}\right)\bar{\phi}_2 = 0 . \tag{2.129}$$

We now define:

$$\ell_1^n = \frac{1}{v_1 \Sigma_1 \left(1+\tau B_n^2\right)} , \qquad \left(\tau = \frac{D_1}{\Sigma_1}\right),$$

$$\ell_2^n = \frac{1}{v_2 \Sigma_2 \left(1+L^2 B_n^2\right)} , \qquad \left(L^2 = \frac{D_2}{\Sigma_a}\right), \tag{2.130}$$

$$k_n = \frac{k_o}{\left(1+L^2 B_n^2\right)\left(1+\tau B_n^2\right)} ,$$

and eliminate $\bar{\phi}_1$ so as to get:

$$\left\{ \left(1+s\ell_1^n\right)\left(1+s\ell_2^n\right) - \left(1 - \beta + \sum_j \frac{\beta_j \omega_j}{\omega_j + s}\right) k_n \right\} \bar{\phi}_2 = - \frac{p\Sigma_o}{\Sigma_a \left(1+L^2 B_n^2\right)\left(1+\tau B_n^2\right)} \bar{\phi}_o . \tag{2.131}$$

Following the same procedure as in the last section, we find that the decay constant λ of the fundamental mode of the thermal flux is given by the real root of the equation:

$$(1-\lambda\ell_1)(1-\lambda\ell_2) - \left(1-\beta+\Sigma\frac{\beta_j\omega_j}{\omega_j-\lambda}\right)k = 0 \ . \tag{2.132}$$

If the fast neutron lifetime is neglected, $\ell_1 \approx 0$,

$$1 - \lambda\ell_2 - (1-\beta)k + k\sum\frac{\beta_j\omega_j}{\lambda-\omega_j} = 0 \ , \tag{2.133}$$

or, in terms of the reactivity, $\rho = \frac{k-1}{k}$,

$$\beta - \rho - \lambda\frac{\ell_2}{k} + \sum\frac{\omega_j\beta_j}{\lambda-\omega_j} = 0 \ . \tag{2.134}$$

This result may also be written in the iterative form:

$$\lambda = \frac{1}{\ell_2^*}\left[\beta-\rho+\sum_j\frac{\omega_j\beta_j}{\lambda-\omega_j}\right], \tag{2.135}$$

where

$$\ell_2^* = \frac{\ell_2}{k} = \frac{1}{k}\cdot\frac{1}{\Sigma_a\left(1+B^2L^2\right)} \ . \tag{2.122}$$

Equation 2.135 is the same as Eq. 2.121 of the previous section. Thus, we see that if the fast neutron lifetime is neglected, the two-group analysis yields the same equation for the decay constant λ as the age-theory treatment.

2.2.5 Decay Constant for Systems with Significant Resonance Fission

For primarily thermal reactor systems with high fuel enrichment or low moderator-to-fuel ratio, the contribution to the reactivity of fissions induced by epithermal neutrons becomes significant. Such an effect can be taken into account by including a term due to resonance fission in the usual two-group formulation. It is customary in treating this effect to use the following definitions:[38]

$$\begin{aligned} k_2 &= \eta_2\epsilon f p_{28}p_{25} \ , \quad \text{thermal} \\ k_r &= \eta_r\epsilon p_{28}(1-p_{25}), \quad \text{resonance.} \end{aligned} \tag{2.136}$$

where p_{28} and p_{25} are the resonance escape probabilities for the fertile and fissile materials, respectively; the η's correspond to average thermal and resonance fissions, respectively, and other symbols have their usual meanings. If β_2 and β_r are the respective delayed neutron fractions, then we can write the two-group equations in the form:

$$D_1\nabla^2\phi_1 - \Sigma_1\phi_1 + (1-\beta_2)\epsilon\eta_2 f\Sigma_2\phi_2 + (1-\beta_r)\epsilon\eta_r\Sigma_1 p_{28}(1-p_{25})\,\phi_1 = \frac{1}{v_1}\frac{\partial}{\partial t}\phi_1$$

and (2.137)

$$D_2\nabla^2\phi_2 - \Sigma_2\phi_2 + p_{28}p_{25}\Sigma_1\phi_1 = \frac{1}{v_2}\frac{\partial}{\partial t}\phi_2 \,.$$

It is assumed here that the resonance captures in fertile material occur at higher energies than those in the fissile material. If this is not a good model of the actual process, then p_{28} in the expression for k_1 may be somewhat larger than in the expression for k_2.

We are interested in the decay constant of the thermal flux and write:

$$\phi_{1,2}(\vec{r},t) = \sum \phi^n_{1,2}(\vec{r})\, e^{-\lambda_n t}\,, \tag{2.138}$$

where, as usual,

$$\nabla^2\phi^n_{1,2}(\vec{r}) + B_n^2\phi^n_{1,2}(\vec{r}) = 0\,.$$

Substituting Eq. 2.138 in Eq. 2.137 and using the notation previously used, we get:

$$-\left(1+\tau B_n^2 - (1-\beta_r)k_r - \lambda_n\ell_1\right)\phi_1 + (1-\beta_2)\eta_2\epsilon f\,\frac{\Sigma_2}{\Sigma_1}\phi_2 = 0\,,$$

$$p_{28}p_{25}\,\frac{\Sigma_1}{\Sigma_2}\phi_1 - \left(1+L^2B_n^2-\lambda_n\ell_2\right)\phi_2 = 0\,. \tag{2.139}$$

For these equations to have non-trivial solutions, the determinant of the coefficients must vanish and λ_n is given by:

$$\left(1+\tau B_n^2 - (1-\beta_r)k_r - \lambda_n\ell_1\right)\left(1+L^2B_n^2-\lambda_n\ell_2\right) = (1-\beta_2)k_2\,. \tag{2.140}$$

If we suppose $\ell_1\lambda_n \approx 0$, then

$$\lambda_n = \frac{1}{\ell_2}\left[\frac{(1-\beta_2)k_2^o}{1-(1-\beta_r)k_r^o+\tau B_n^2} - \left(1+L^2B_n^2\right)\right]. \qquad (2.141)$$

This result may be compared with the result without taking account of the resonance fission effect:

$$\lambda_n = \frac{1}{\ell_2}\left[\frac{(1-\beta)k^o}{1+\tau B_n^2} - \left(1+L^2B_n^2\right)\right].$$

It is also possible to treat this case by the so-called "two-and-one-half-group" theory proposed by Gelanin[39,40] for stationary systems to take into account neutron capture and multiplication during the slowing-down phase.

Fast-group constants for the diffusion coefficients, removal cross-sections, and Fermi age as used in two-group theory are given in Ref. (41) for beryllium (with and without the n,2n reaction), graphite, water, heavy water and beryllium oxide. Sets of constants are also available for two-group theory in which the effect of fast capture is included for uranium and UO_2-water mixtures. More extensive two-group constants (extrapolation distances; diffusion coefficients; cross-sections for absorption, scattering, fission, slowing-down; absorption-escape probability, diffusion area, multiplication constant) have been evaluated[42] for reactor materials over a temperature range from 68°F to 3,000°F.

2.2.6 Multigroup Treatment Without Delayed Neutrons

The treatment which provides the greatest accuracy and universality of application is the one based on the multigroup method. In this method, the entire energy range of the neutron is divided into various energy intervals and an appropriate differential equation of the one-velocity diffusion type is used to describe the neutron balance in each group. The formulation of the multigroup method and examples of its use will be found in Refs. (41-45). In the following, the usual multigroup method will be extended to the time-dependent case with special reference to a pulsed multiplying system. The notation employed here is similar to that of Okrent.[46] The source neutrons are supposed to be in the highest energy (first) group; the total number of groups is N. The set of equation is then

of the form:

$$D_j \nabla^2 \phi_j(\vec{r},t) - \Sigma_{aj}\phi_j(\vec{r},t) + Q_{sj}(\vec{r},t) + \gamma_j \chi(\vec{r},t) + \delta_{1j} S(\vec{r},t) = \frac{1}{v_j}\frac{\partial}{\partial t}\phi_j(r,t)$$

$$j = 1, 2, \ldots N , \qquad (2.142)$$

where:

Σ_{aj} = total removal cross-section from group j
$= \Sigma_{cj} + \Sigma_{fj} + \Sigma_{ij} + \Sigma_{ej}$,

Σ_{cj}, Σ_{fj} = macroscopic capture and fission cross-sections, respectively, of group j;

Σ_{ij} = macroscopic inelastic removal cross-section from group $j = \sum_{k \neq j} \Sigma_{i,j\to k}$;

Σ_{ej} = macroscopic elastic removal cross-section from group $j = \sum_{k \neq j} \Sigma_{e,j\to k}$;

$Q_{sj} = \sum_{k \neq j} (\Sigma_{i,k\to j} + \Sigma_{e,k\to j})\phi_k(\vec{r},t) = \sum_{k \neq j} \Sigma_{s,k\to j}\phi_k(\vec{r},t)$: total number of neutrons per cm^3 per second scattered into group j from all higher energy groups;

$\chi(\vec{r},t) = \sum_{k=1}^{N} \nu_k \Sigma_{fk}\phi_k(\vec{r},t)$: fission source distribution;

γ_j = fraction of fission neutrons born in group j;

δ_{1j} = Kronecker delta $= \begin{cases} 1 & j = 1 \\ 0 & j \neq 1 \end{cases}$;

$S(\vec{r},t) = S_o \delta(\vec{r}-\vec{r}_o)\delta(t)$: source neutron pulse.

Other symbols have their usual meaning (Appendix I). The group constants are defined as in Ref. (41) and are given in Appendix I.

Equations 2.142 represent N simultaneous equations with appropriate cross-sections. When more than one region is considered, the usual flux continuity relations are set at the boundaries for each group. In

general, if the analysis is to involve more than one region, the problem becomes too complex for an analytical solution and high-speed electronic computers provide the only practical method of obtaining numerical solutions. For bare systems with certain simplifying assumptions, the equations are more tractable. One such assumption is that all of the energy groups have the same spatial distribution, which is equivalent to assigning a single extrapolation distance to all groups. Even though there is direct experimental evidence[46] to indicate that the energy spectrum is not space-independent in bare systems, this simplified multigroup method does give reasonably good results away from the boundaries. If, in addition, we assume the usual space-time separability, we can write

$$\phi_j(\vec{r},t) = \sum_n R_n(\vec{r})\,\psi_{jn}(t) \ , \tag{2.143}$$

where the spatial dependence satisfies the Helmholtz equation as before:

$$\nabla^2 R_n(\vec{r}) + B_n^2 R_n(\vec{r}) = 0 \ .$$

Again, we also let:

$$\delta(\vec{r}-\vec{r}_o) = \sum_n P_n R_n(\vec{r}) \ ,$$

so that the coefficients P_n are known as in Eq. 2.14.

Substituting Eqs. 2.143 in Eq. 2.142, we get:

$$-\left(D_j B_n^2 + \Sigma_{aj}\right)\psi_{jn}(t) + \sum_{k\neq j}^{N} \Sigma_{s,k\to j}\psi_{kn}(t) + \gamma_j \sum_{k=1}^{N} \nu_k \Sigma_{fk}\psi_{kn}(t) + \delta_{1j} S_o P_n \delta(t)$$

$$= \frac{1}{v_j}\frac{d}{dt}\psi_{jn}(t) \ , \tag{2.144}$$

The Laplace transform of these equations gives:

$$\left(D_j B_n^2 + \Sigma_{aj} + \frac{s}{v_j}\right)\bar{\psi}_{jn}(s) = \delta_{1j} P_n S_o + \sum_{k\neq j}^{N} \Sigma_{s,k\to j}\bar{\psi}_{kn}(s) + \gamma_j \sum_{k=1}^{N} \nu_k \Sigma_{fk}\bar{\psi}_{kn}(s) \tag{2.145}$$

Now, $\sum_{k=1}^{N} \nu_k \Sigma_{fk}\bar{\psi}_{kn}(s)$ is some known function of s. If we write:

$$\sum_{k=1}^{N} \nu_k \Sigma_{fk} \bar{\psi}_{kn}(s) \equiv f_n(s) ,$$

and (2.146)

$$v_j \Sigma_{aj} + v_j D_j B_n^2 \equiv \lambda_{jn} ,$$

then we can write successively:

$$\bar{\psi}_{1n}(s) = \frac{P_n S_o + \gamma_1 f_n(s)}{s + \lambda_{1n}} v_1 ,$$

$$\bar{\psi}_{2n}(s) = \frac{\gamma_2 f_n(s) + \Sigma_{s,1\to 2} \bar{\psi}_{1n}(s)}{s + \lambda_{2n}} v_2 , \qquad (2.147)$$

$$\bar{\psi}_{3n}(s) = \frac{\gamma_3 f_n(s) + \Sigma_{s,1\to 3} \bar{\psi}_n(s) + \Sigma_{s,2\to 3} \bar{\psi}_{2n}(s)}{s + \lambda_{3n}} v_3 ,$$

et cetera .

Inverting the Laplace transform step by step, we obtain the time-dependent flux distribution for each group.

To obtain the equation determining the decay constant for each group in a closed form, we proceed in a slightly different manner. Consider Eq. 2.144 for $t > 0$ so that the last term on the left vanishes. Let us write:

$$\psi_{jn}(t) \sim e^{-\lambda_n t} ,$$

and (2.148)

$$v_j \Sigma_{aj} + v_j D_j B_n^2 \equiv \lambda_{jn} .$$

Then Eq. 2.144 gives:

$$(\lambda_n - \lambda_{jn}) \psi_{jn}(t) + v_j \sum_{k\neq j}^{N} \Sigma_{s,k\to j} \psi_{kn}(t) + v_j \gamma_j \sum_{k=1}^{N} \nu_k \Sigma_{fk} \psi_{kn}(t) = 0 . \qquad (2.149)$$

Introducing the Kronecker delta $\delta_{jk} = \begin{cases} 1 & j = k \\ 0 & j \neq k \end{cases}$, and using the summation convention,[29] we can write Eq. 2.149 as:

$$\left[(\lambda_n-\lambda_{jn})\delta_{jk}+v_j\sum_{k\neq j}\Sigma_{s,k\to j}+v_j\gamma_j\sum_{k=1}\nu_k\Sigma_{fk}\right]\psi_{kn}(t)=0\ ,$$

$$j=1,\ 2,\ \ldots\ N\ , \qquad (2.150)$$

$$k=1,\ 2,\ \ldots\ N\ .$$

This is a set of N homogeneous simultaneous linear equations in the N unknowns $\psi_{kn}(t)$, and the condition for non-trivial solutions is that the determinant of their coefficients in Eqs. 2.150 must vanish:

$$\left\|(\lambda_n-\lambda_{jn})\delta_{jk}+v_j\sum_{\substack{k=1\\k\neq j}}^{N}\Sigma_{s,k\to j}+v_j\gamma_j\sum_{k=1}^{N}\nu_k\Sigma_{fk}\right\|=0\ . \qquad (2.151)$$

This characteristic determinantal equation is, in general, a polynomial of degree N in λ_n and yields N roots corresponding to the decay constants of the N energy groups. The functions $\psi_{kn}(t)$ are then given by Eqs. 2.149 and Eq. 2.143 gives the flux distributions.

Multigroup reactor codes, such as the PDQ, can be used to calculate the prompt neutron decay constant for specific systems.[47] The General Atomic Neutron Thermalization group has developed[48] codes for the computation of λ based on the slowing-down equation:

$$\frac{1}{v}\frac{\partial}{\partial t}\psi(E,t)=\int_0^\infty\psi(E',t)\,\Sigma(E'\to E)\,dE'-\psi(E)[\Sigma(E)+B^2D(E)]$$

$$+(1-\beta)f(E)\int_0^\infty\psi(E',t)\,\Sigma_f(E)\nu\,dE'\ , \qquad (2.152)$$

where f(E) represents the normalized fission spectrum. Equation 2.152 has an asymptotic solution of the form

$$\psi(E,t)=e^{-\lambda t}\phi(E)\ , \qquad (2.153)$$

so that

$$\int_0^\infty\phi(E')[\Sigma(E'\to E)+f(E)(1-\beta)\nu\Sigma_f(E')]\,dE'=\phi(E)\left[\Sigma(E)+B^2D(E)-\frac{\lambda}{v}\right]\ . \qquad (2.154)$$

Thus, λ can be interpreted as a negative 1/v absorber which makes the

system just critical. Integration of Eq. 2.154 over all energies, gives

$$\lambda = \frac{\int_0^\infty \phi(E)\left[\Sigma_a(E)+B^2D(E)-(1-\beta)\nu\Sigma_f(E)\right] dE}{\int \phi(E)\frac{dE}{v}} \quad . \tag{2.155}$$

Equations 2.154 and 2.155 are solved by iteration by splitting the spectrum into a fast and a thermal part, with an appropriate cut-off energy. The calculation of the fast spectrum is done by the code GAM[49] and the thermal spectrum is computed with the code GATHER.[48]

2.2.7 Four-Group Treatment with One Delayed Neutron Group

As an illustration of the multigroup method developed in the last section, we consider a four-group treatment including delayed neutron effects. The neutrons will be divided into four energy groups: source (0); fast (1) including fission and delayed neutrons; resonance or epithermal (2) including the slowing-down phase; and, finally, thermal (3). Such a treatment should be well suited to the analysis of under-moderated systems, which have significant epithermal absorption in the fissile material. For systems with high enrichment in U^{235}, for instance, the core size is quite small and the fission and capture of neutrons by U^{235} in the resonance region cannot be ignored.

The conservation equations for each of the four groups and for the delayed neutrons can be immediately written down:

$$D_o\nabla^2\phi_o(\vec{r},t) - \Sigma_o\phi_o + S(\vec{r},t) = \frac{1}{v_o}\frac{\partial}{\partial t}\phi_o \ ,$$

$$D_1\nabla^2\phi_1 - \Sigma_1\phi_1 + \Sigma_o\phi_o + (1-\beta_2)k_2^o(1-p)\Sigma_2\phi_2 + (1-\beta_3)k_3^o\Sigma_3\phi_3 + \omega C$$

$$= \frac{1}{v_1}\frac{\partial}{\partial t}\phi_1 \ , \tag{2.156}$$

$$D_2\nabla^2\phi_2 - \Sigma_2\phi_2 + \Sigma_1\phi_1 = \frac{1}{v_2}\frac{\partial}{\partial t}\phi_2 \ ,$$

$$D_3\nabla^2\phi_3 - \Sigma_3\phi_3 + p\Sigma_2\phi_2 = \frac{1}{v_3}\frac{\partial}{\partial t}\phi_3 \ ,$$

and

$$\frac{\partial}{\partial t} C(\vec{r},t) = -\omega C + \beta_2(1-p)\, k_2^o \Sigma_2 \phi_2 + \beta_3 k_3^o \Sigma_3 \phi_3 \ . \tag{2.157}$$

Here k_2^o and k_3^o are the infinite medium multiplication factors for the neutrons of respective groups. To solve these equations, we proceed as in the previous section. We write:

$$\begin{aligned} \phi_j(\vec{r},t) &= \sum_n R_n(\vec{r})\, \psi_{jn}(t) \ , \qquad j = 0,\ 1,\ 2,\ 3 \ , \\ C(\vec{r},t) &= \sum_n R_n(\vec{r})\, C(t) \ , \\ \delta(\vec{r}-\vec{r}_o) &= \sum_n P_n R_n(\vec{r}) \ , \end{aligned} \tag{2.158}$$

with

$$\nabla^2 R_n(\vec{r}) + B^2 R_n(\vec{r}) = 0 \ .$$

We substitute Eq. 2.154 into Eqs. 2.156 and 2.157 and take the Laplace transform with respect to t; let

$$\begin{aligned} \ell_j^o &= \frac{1}{v_j \Sigma_j} \ , \\ \ell_j &= \frac{1}{v_j \Sigma_j + v_j D_j B^2} = \frac{1}{\lambda_j} \ , \\ \lambda_j &= v_j \Sigma_j + v_j D_j B^2 \ . \end{aligned} \tag{2.158a}$$

Henceforth, we drop the modal suffix n for simplicity. The result of performing the stated operations on Eqs. 2.156 and 2.157 is to give:

$$\begin{aligned} &\frac{s+\lambda_o}{v_o} \bar{\psi}_o(s) = PS_o \ , \\ &-\frac{s+\lambda_1}{v_1} \bar{\psi}_1(s) + \Sigma_o \bar{\psi}_o(s) + (1-p)(1-\beta_2)\, k_2^o \Sigma_2 \bar{\psi}_2(s) \\ &\qquad + (1-\beta_3)\, k_3^o \Sigma_3 \bar{\psi}_3(s) + \omega \bar{C}(s) = 0 \ , \\ &\frac{s+\lambda_2}{v_2} \bar{\psi}_2(s) = \Sigma_1 \bar{\psi}_1(s) \ , \qquad \frac{s+\lambda_3}{v_3} \bar{\psi}_3(s) = p\Sigma_2 \bar{\psi}_2(s) \ , \end{aligned} \tag{2.159}$$

and

$$(\omega+s)\bar{C}(s) = (1-p)\beta_2 k_2^o \Sigma_2 \bar{\psi}_2(s) + \beta_3 k_3^o \Sigma_3 \bar{\psi}_3(s) \ . \tag{2.160}$$

Eliminating $\bar{C}(s)$ between the second of Eqs. 2.159 and 2.160, we get:

$$-\frac{s+\lambda_1}{v_1}\bar{\psi}_1(s) + \Sigma_o \bar{\psi}_o(s) + (1-p)\left(\frac{\omega+(1-\beta_2)s}{\omega+s}\right) k_2^o \Sigma_2 \bar{\psi}_2(s)$$

$$+\left(\frac{\omega+(1-\beta_3)s}{\omega+s}\right) k_3^o \Sigma_3 \bar{\psi}_3(s) = 0 \ .$$

Next, we eliminate $\bar{\psi}_1(s)$ and $\bar{\psi}_2(s)$ between the last equation and the remaining of Eqs. 2.159 so as to get:

$$\left[\frac{(s+\lambda_1)(s+\lambda_2)(s+\lambda_3)}{v_1 v_2 v_3 p \Sigma_1 \Sigma_2} - (1-p)\left(\frac{\omega+(1-\beta_2)s}{\omega+s}\right) k_2^o \frac{s+\lambda_3}{p v_3}\right.$$

$$\left. -\left(\frac{\omega+(1-\beta_3)s}{\omega+s}\right) k_3^o \Sigma_3\right] \bar{\psi}_3(s) = \frac{v_o \Sigma_o}{s+\lambda_o} PS_o \ . \tag{2.161}$$

If we define the effective multiplication factors:

$$k_2 = \frac{k_2^o}{\left(1+L_1 B^2\right)\left(1+L_2 B^2\right)} = v_1 v_2 \Sigma_1 \Sigma_2 \ell_1 \ell_2 k_2^o \ ,$$

$$k_3 = \frac{k_3^o}{\left(1+L_1 B^2\right)\left(1+L_2 B^2\right)\left(1+L_3^2 B^2\right)} = v_1 v_2 v_3 \ell_1 \ell_2 \ell_3 k_3^o \ , \tag{2.162}$$

we finally obtain

$$\left[(\omega+s)(1+\ell_1 s)(1+\ell_2 s)(1+\ell_3 s) - (1-p)(\omega+(1-\beta_2)s)k_2(1+\ell_3 s) - p(\omega+(1-\beta_3)s)k_3\right]\bar{\psi}_3(s)$$

$$= \frac{p v_o v_1 v_2 v_3 \Sigma_o \Sigma_1 \Sigma_2 \ell_o \ell_1 \ell_2 \ell_3}{1+\ell_o s}(\omega+s)\, PS_o \ . \tag{2.163}$$

Thus, the Laplace transform of the time-dependent part of the thermal flux is given by an expression of the form,

$$\bar{\psi}_3(s) = \frac{f(s)}{F(s)} PS_o \ . \qquad (2.164)$$

This equation can be treated in a manner similar to that used for Eq. 2.109 of Section 2.2.3.

2.2.8 Treatment Based on Time-Dependent Asymptotic Reactor Theory

An extension of the so-called "Asymptotic Reactor Theory" to the time-dependent case has been used by Krieger and Zweifel[20] to investigate the spatial and temporal distribution of thermal neutrons in a multiplying assembly. In this section, such an extension will be used to derive a general equation for the prompt neutron decay constant in terms of the generalized time-dependent slowing-down kernels including explicitly the effect of delayed neutrons in the system.

The space- and time-dependent thermal flux, in a multiplying medium under the diffusion approximation, is given by:

$$\frac{1}{v}\frac{\partial}{\partial t}\phi(\vec{r},t) - D\nabla^2\phi(\vec{r},t) + \Sigma_a\phi(\vec{r},t)$$

$$= \int (1-\beta)k(\vec{r}')\Sigma_a(\vec{r}')\phi(\vec{r}',t')q_p(|\vec{r}-\vec{r}'|,t-t')\,d\vec{r}'\,dt'$$

$$+ \int \omega_i C_i(\vec{r}',t')\,q_d(|\vec{r}-\vec{r}'|,t-t')\,d\vec{r}'\,dt'$$

$$+ S_o \int \delta(\vec{r}')\delta(t')\,q_s(|\vec{r}-\vec{r}'|,t-t')\,d\vec{r}'\,dt' \ , \qquad (2.165)$$

with

$$\frac{\partial}{\partial t} C_i(\vec{r},t) = -\omega_i C_i(\vec{r},t) + k(\vec{r})\,\beta_i\Sigma_a(\vec{r})\,\phi(\vec{r},t) \ . \qquad (2.165a)$$

Here, the time-dependent, slowing-down kernel $q(|\vec{r}-\vec{r}'|,t-t')$ is the probability per unit volume, per unit time, that a neutron born at $(\vec{r}',t')$ will become "thermalized" at $(\vec{r},t)$, and the suffixes p, d, s denote prompt, delayed and source neutrons, respectively. The other symbols have their usual meaning.

Let the system be homogeneous so that Σ_a and k are space-independent. Further, let the system be bare so that $\phi(\vec{r},t)$, etc. vanish at the extrapolated boundary, and let us write:

$$\phi(\vec{r},t) = \Sigma\, R_n(\vec{r})\phi_n(t) ,$$

$$C_i(\vec{r},t) = \Sigma\, R_n(\vec{r})\psi_{in}(t) , \qquad (2.166)$$

and

$$\delta(\vec{r})\,\delta(t) = \Sigma\, a_n R_n(\vec{r})\,\delta(t) .$$

We substitute Eqs. 2.166 in Eqs. 2.165 and make use of the results of fundamental theorems of asymptotic reactor theory to simplify the slowing-down kernels. These theorems are discussed in detail by Weinberg[21] and by Weinberg and Wigner.[50] After substitution and simplification, we obtain:

$$\frac{1}{v}\frac{d}{dt}\phi_n(t) + \left(\Sigma_a + DB_n^2\right)\phi_n(t) = (1-\beta)k\Sigma_a \int_0^\infty \phi_n(t')\,\bar{q}_p\left(B_n^2, t-t'\right) dt'$$

$$+ \int \Sigma\omega_i\psi_{in}(t')\,\bar{q}_d\left(B_n^2, t-t'\right) dt'$$

$$+ S_o a_n \int \delta(t)\,\bar{q}_s\left(B_n^2, t-t'\right) dt' \qquad (2.167)$$

with

$$\frac{d}{dt}\psi_{in}(t) = -\omega_i\psi_{in}(t) + \beta_i k\Sigma_a\psi_{in}(t) ,$$

where $\bar{q}(B_n^2, t-t')$ is the Fourier transform of the slowing-down kernel in the infinite medium, with B_n^2 as the Fourier transform variable.

If, now, we take the Laplace transform of Eqs. 2.167 with respect to t and denote the transformed functions by bars, we obtain:

$$\left(\frac{s}{v} + \Sigma_a + DB_n^2\right)\bar{\phi}_n = (1-\beta)k\Sigma_a\bar{\phi}_n(s)\,\bar{\bar{q}}_p\left(B_n^2, s\right)$$

$$+ \Sigma\omega_i\psi_{in}(s)\,\bar{\bar{q}}_d\left(B_n^2, s\right)$$

$$+ S_o a_n \bar{\bar{q}}_s\left(B_n^2, s\right) , \qquad (2.168)$$

and

$$s\bar{\psi}_{in}(s) = -\omega_i\bar{\psi}_{in}(s) + \beta_i k\Sigma_a\bar{\phi}_n(s) .$$

Now we eliminate $\bar{\psi}_{in}(s)$ between Eqs. 2.168 and get:

$$\bar{\phi}_n(s) = \frac{S_o a_n q_s\left(B_n^2,s\right)}{s + v\left(\Sigma_a + DB_n^2\right) - v\Sigma_a(1-\beta)\,k\bar{\bar{q}}_p\left(B_n^2,s\right) + v\Sigma_a k\bar{\bar{q}}_d\left(B_n^2,s\right)\sum \frac{\omega_i\beta_i}{\omega_i + s}} \quad . \tag{2.168}$$

We can now adopt the procedure used in Section 2.2.3 to treat Eq. 2.109. It is found that the asymptotic behavior of $\phi_n(t)$ is given by

$$\phi_n(t) \sim A_n\, e^{-\lambda_n t} \quad ,$$

where the decay constant λ_n is now a root of the equation

$$\lambda_n + v\left(\Sigma_a + DB_n^2\right) - v\Sigma_a(1-\beta)\,k\bar{\bar{q}}_p\left(B_n^2,\lambda_n\right) + v\Sigma_a k\bar{\bar{q}}_d\left(B_n^2,\lambda_n\right)\sum \frac{\beta_i\omega_i}{\omega_i + \lambda_n} = 0 \quad . \tag{2.169}$$

Equation 2.169 can be used with any particular form of the slowing-down kernel. For example, on the Fermi-age model,

$$\bar{q}\left(B_n^2,t\right) = p\, e^{-B_n^2\tau}\, \delta(t-T) \quad , \tag{2.170}$$

where T is the mean slowing-down time. In this case,

$$\bar{\bar{q}}\left(B_n^2,t\right) = p\, e^{-\left(B_n^2\tau + sT\right)} \quad ,$$

and the general equation, Eq. 2.169, leads to the result (2.111) of Section 2.2.3 for the age theory.

In this chapter, we have derived several expressions for the decay constant of the neutron population in an assembly irradiated by a burst of fast neutrons. These expressions are based on different theoretical models of the neutron processes in the assembly and can be used to study the effect of a variety of factors which determine the decay constant. The spatial and temporal distributions are useful in determining the experimental conditions suitable for the measurement of the decay constant in any situation. In the next chapter, some of these theoretical results, especially those based on age theory, will be examined for possible experimental applications.

References

1. L. W. Alvarez, Phys. Rev. 54, 609 (1938).
2. E. Amaldi, Handbuch der Physik, Vol. 38, Part 2, Springer Verlag, Berlin (1959).
3. A. E. Profio, Ph.D. Thesis, Dept. of Nuclear Engineering, M.I.T. (1962).
4. G. von Dardel and N. G. Sjöstrand, Progress in Nuclear Energy Series 1 - Vol. 2, Pergamon Press, New York (1958).
5. K. H. Beckurts, Nuclear Instruments and Methods, 11, 144 (1961).
6. G. R. Keepin, LAMS-2215 (1958).
7. Proceedings of the Brookhaven Conference on Neutron Thermalization, BNL719(C-32), Vols. I-IV (1962).
8. R. E. Marshak, Revs. Modern Phys. 14, 185 (1947).
9. J. B. Sykes, J. Nuclear Energy 2, 31 (1955).
10. H. Hurwitz, Jr., and M. S. Nelkin, Nuclear Sci. and Eng. 3, 1 (1958).
11. K. S. Singwi and L. S. Kothari, J. Nuclear Energy 8, 59 (1958).
12. M. S. Nelkin, J. Nuclear Energy, 8, 48 (1958).
13. K. S. Singwi, J. Nuclear Energy 11, 19 (1959); Arkiv Fysik 15, 147 (1960).
14. W. Häfele and L. Dresner, ORNL-2842, 124 (1959).
15. M. V. Kazarnovsky, A. V. Stepanov and F. L. Shapiro, Proc. 2nd Intern. Conf. Peaceful Uses of Atomic Energy, Geneva P/2148 (1958).
16. M. S. Nelkin, Nuclear Sci. and Eng. 7, 210 (1960).
18. I. Waller, Proc. 2nd Intern. Conf. Peaceful Uses of Atomic Energy, Geneva P/153 (1958).
19. K. E. Eriksson, Arkiv Fysik 16, 1 (1959).
20. T. J. Krieger and P. F. Zweifel, Nuclear Sci. and Eng. 5, 21 (1959).
21. A. M. Weinberg, Am. J. Phys. 20, 401 (1952).

22. S. C. Fultz, Nuclear Sci. and Eng. 6, 313 (1959).

23. S. N. Purohit, Nuclear Sci. and Eng. 9, 157 (1961).

24. V. C. Boffi, V. G. Molinari and D. E. Parks, Reactor Sci. and Techn. 16, 395 (1962).

25. I. G. Dyad'kin and E. P. Batalina, Reactor Sci. and Techn. 16, 103 (1962).

26. A. V. Antonov, A. I. Isakoff, I. D. Murin, B. A. Neupocoyev, I. M. Frank, F. L. Shapiro and I. V. Shtranich,(1956 a) Proc. Int. Conf. on Peaceful Uses of Atomic Energy, Geneva, Vol. 5, 3 and 82 (1955).

27. B. Davison, Neutron Transport Theory, Oxford University Press, London (1957).

28. H. Soodak (Ed.), Reactor Handbook, Vol. III, Part A - Physics, Interscience Publishers, New York (1962).

29. P. M. Morse and H. Feshbach, Methods of Theoretical Physics, Part I, McGraw-Hill Book Company, Inc., New York (1953).

30. R. Courant and D. Hilbert, Methoden der Mathematischen Physik, Julius Springer, Berlin (1924).

31. S. Glasstone and M. C. Edlund, The Elements of Nuclear Reactor Theory, D. Van Nostrand Company, Inc., New York (1952).

32. C. H. Page, Physical Mathematics, D. Van Nostrand Company, Inc., New York (1955).

33. B. van Der Pol and H. Bremmer, Operational Calculus, Cambridge Univ. Press, London (1950).

34. G. F. von Dardel, Trans. Roy. Inst. Techn. Stockholm, 75 (1954).

35. G. F. von Dardel and N. G. Sjöstrand, Phys. Rev. 96, 1245 (1954).

36. E. C. Campbell and P. H. Stelson, ORNL-2204, 34 (1956).

36a. Karl-Heinz Joest, Nukleonik, Band 6, Heft 1, 3 (1964).

36b. B. E. Simmons and J. S. King, Nuclear Sci. and Eng., 3, 595 (1958).

37. I. A. Sneddon, Fourier Transforms, McGraw-Hill Book Company, Inc., New York (1951).

38. P. F. Gast, Nuclear Sci. and Eng., 9, 131 (1961).

39. A. D. Gelanin, Soviet Journal of Atomic Energy, Part 1, Sect. 10, Supplement Nos. 2 and 3. English translation by Consultants Bureau, Inc., New York (1958).

40. A. D. Gelanin, Proc. Int. Conf. on Peaceful Uses of Atomic Energy, Geneva, Vol. 5, 448 (1955).

41. L. Templin (Coördinator), Reactor Physics Constants, ANL-5800, 2nd Ed., Secs. 3.5 and 7.1 (1963).

42. M. J. Stanley, APEX-369 (1958).

43. D. Okrent, R. Avery and H. H. Hummel, Proc. Int. Conf. on Peaceful Uses of Atomic Energy, Geneva, Vol. 5, 347 (1955).

44. W. B. Lowenstein and D. Okrent, Proc. Second U.N. Int. Conf. on Peaceful Uses of Atomic Energy, Geneva, 12, 16 (1959).

45. K. F. Hansen, NYO-10,206, MITNE-19 (1962).

46. H. Etherington (Ed.), Nuclear Engineering Handbook, pp. 6-88 to 6-94, McGraw-Hill Book Company, Inc., New York (1958).

47. G. H. Kear and M. H. Ruderman, GEAP-3937 (1962).

48. J. R. Beyster et al., GEAP-3542 (1963).

49. G. D. Joanou and J. S. Dudek, GA-1850 (1961).

50. A. M. Weinberg and E. P. Wigner, The Physical Theory of Neutron Chain Reactors, The University of Chicago Press, Chicago (1958).

Chapter III

THE PULSED NEUTRON TECHNIQUE; EXPERIMENTAL CONSIDERATIONS AND APPLICATIONS

The asymptotic response of a multiplying system below prompt critical to a sudden burst of fast neutrons is described by the prompt neutron decay constant. In the absence of delayed neutron precursors, the asymptotic neutron population, subsequent to the establishment of the normal mode, decays in an exponential manner with a decay constant - ALPHA - called the prompt neutron decay constant. Alpha is an important parameter for describing the neutronic behavior in the system. It provides a convenient and precise measure of the reactivity without the use of the inhour equation. Like the reactivity, it is a global parameter of the system, representing the behavior of the system as a whole. However, it has much wider applicability; unlike the reactivity, it is directly measurable and can also be calculated with the aid of multigroup codes. It thus represents an eigenvalue which can, in principle, be both calculated and measured directly and provides a significant correlation between experiment and theory. Moreover, it provides a bridge between the two basic aspects of reactor physics - reactor dynamics and reactor statics. Although it is basically a dynamical parameter having to do with the temporal response of the system, the prompt neutron decay constant can be related theoretically to the static nuclear parameters. It also relates the microscopic and macroscopic aspects of a heterogeneous chain reacting system. Further, a knowledge of the effective delayed neutron fraction $\overline{\beta}$ in a system and of α at delayed critical enables us to evaluate the prompt neutron lifetime directly, which is a useful parameter in safety considerations. Consequently, the prompt neutron decay constant is an extremely useful parameter in reactor kinetics and its study in any neutron transport medium is worthwhile and instructive.

The role and the goals of theory in this study were, in part, the subject of the last chapter. The experimentalist is concerned first, with the method or methods that can yield the decay constant of the system under consideration in the energy range of neutron transport in question and, secondly, to utilize the theoretical knowledge for relating the decay constant to other parameters of interest with a view to obtaining the maximum possible information about the system. Also included in the experimental domain is the clear definition of the conditions underlying the experiments and the factors which bear on the comparison of theory and experiment.

3.1 METHODS OF MEASUREMENT OF ALPHA

The characteristic prompt neutron decay constant or the eigenvalue "alpha" is based on the composite or average behavior of a large number of individual neutron fission chains and can thus be studied experimentally from two basically different approaches: (1) by observing the decay of individual chains in succession, and continuing this process until enough chains have been observed to provide a statistically reliable measure of alpha or (2) by observing the simultaneous decay of a large number of neutrons introduced into an assembly as a burst or pulse. The first of these approaches leads to the Rossi-α and the "variance-to-mean" (Feynman-α) techniques, while the second approach characterizes the pulsed neutron techniques.

The Rossi-Feynman α-technique was first suggested by B. Rossi, and its theory was developed by Feynman, deHoffmann and Serber[1, 2] and later extended and applied by Orndoff.[3] The method involves counting the time-distribution of pairs of counts, due to neutrons with a common ancestor, in coincidence. The probability of a neutron count occurring in a time interval $(t, t+\Delta t)$, in a detector sensitive to fissions, following the occurrence of a count at $t = 0$, is:

$$P(t)\Delta t = C\Delta t + \frac{\epsilon k_p^2}{2(\bar{\nu})^2(1-k_p)\ell_p}\left[\overline{\nu(\nu-1)} + \frac{2\bar{\nu}(1-k_p)\delta}{k_p}\right] e^{-\alpha t}\,\Delta t\,, \qquad (3.1)$$

where $k_p = (1-\bar{\beta})k_{eff}$ is the prompt neutron multiplication factor, $C\Delta t$ is the chance-coincidence probability, ϵ is the detector efficiency in counts per fission, and δ is the effective number of neutrons resulting from a detector count. The Rossi-α technique requires only a fast response, sensitive neutron detector, and some type of time analyzer with short (e.g., microsecond) time-channels to display the decay of prompt neutron population with time. With such circuits, Rossi-α studies have been carried out on a number of fast metal assemblies at Los Alamos by Orndoff;[3] at Argonne by Brunson et al;[4] at Oak Ridge by Mihalczo[5] and at the National Reactor Testing Station, Idaho, critical assemblies by Brunson et al.[6] The Rossi-α method has also been used for the measurement of reactivity in fast assemblies.[3, 10]

A related method which also relies on the correlation of neutron counts is the variance-to-mean measurement which utilizes a pulse counter to determine repeatedly the number of counts in intervals of duration τ in a multiplying system that is either at steady power or is subcritical with a source present. The ratio of the variance of the number of counts per interval to the mean is:

$$\frac{\sigma^2}{\bar{c}} = \frac{\overline{c^2} - (\bar{c})^2}{\bar{c}} = 1 + Y \,, \tag{3.2}$$

where Y is zero for a random source system with pure Poisson statistics and no correlation; in general, for a chain-reacting system:[2]

$$Y = \frac{\epsilon k_p^2}{(1-k_p)^2} \frac{\overline{\nu(\nu-1)}}{(\bar{\nu})^2} \left[1 - \frac{1 - e^{-\alpha\tau}}{\alpha\tau} \right] . \tag{3.3}$$

This expression has been used by Luckow and Churchill[7] to evaluate Y experimentally for different gate times τ, with k_p fixed, and then to determine α by a curve-fitting procedure; the method has been used to study the prompt neutron decay constant of ZPR-IV and ZPR-V at Argonne. An advantage of the method is the conventional nature of the equipment and counting technique.

The most direct method of measuring alpha in a subcritical assembly is by the application of the pulsed neutron technique. A short

burst of fast neutrons is introduced into the assembly and the emergent asymptotic flux is recorded as a function of time; to obtain sufficient counts for statistical accuracy, it is necessary to repeat the process, the length of an individual run depending upon the intensity of the source, the repetition rate and the level of accuracy desired. The essential units in the equipment are a source of neutron pulses, which is usually the target of a particle accelerator, a detector of thermal neutrons and a time-analyzer. This technique will be discussed in detail in the following pages.

The techniques mentioned have been applied to a large number of different systems, and the relative merits of the three methods have been found to depend on magnitudes of the prompt neutron lifetime and multiplication constant.[8] The Rossi-α method is at its best for systems quite near delayed critical. For slower or far-subcritical systems, the presence of the factor, $k_p^2/\ell_p(1-k_p)$, in Eq. 3.1 indicates that the background problems will become greater. The time required for sufficient data accumulation is thus proportional to the prompt lifetime, making the Rossi-α method prohibitively lengthy for systems with prompt neutron lifetime of the order of 50 μseconds.

The Feynman-α method relies on more conventional electronic circuitry, although a large number of gate-count readings must be processed to obtain a reliable result. The Feynman method is also best applicable to systems near delayed critical, as can be seen from the factor, $k_p^2/(1-k_p)^2$, in Eq. 3.3. Since $\alpha\tau$ must be near unity for certain gate times, extension of the method to faster systems would demand a precise gate-timer for short intervals, and counter dead time would become a serious problem.

Finally, the pulsed neutron method may be viewed as complementary to the Rossi-α method for fast systems, since the former is more easily applied to systems further from delayed critical. This can be seen from an approximate expression for the ratio of the maximum neutron flux in the pulsed neutron method, to the source-induced background,[9]

$$\text{"}\left(\frac{\text{signal}}{\text{noise}}\right)\text{"} = 1 + \frac{(1-k_p)^2}{2\beta k_p}\,\frac{T}{\ell_p}\,, \tag{3.4}$$

where T is the repetition period. This ratio also decreases for longer mean lives, but this effect can be counterbalanced by cutting down the repetition rate. The pulsed neutron method can, therefore, be used over a wide range of prompt lifetimes - from about 0.01 μsec for fast assemblies to about 1 msec for slower systems. The data processing in the pulsed neutron method is relatively simple. Against these advantages is to be weighed the cost of the pulsed neutron source. However, the pulsed neutron technique can be applied to a wide range and variety of studies in reactor physics.

Intercomparisons of the Rossi-α and pulsed neutron methods in their region of overlap, should be especially instructive, although few such studies have been reported. Passel et al.[9, 11] have measured the prompt neutron decay constants in highly enriched (93.18% U^{235}), unmoderated uranium systems based on methods developed for fast neutron time-of-flight spectroscopy: Bendt et al.[10] have studied prompt periods from the Godiva fast critical assembly and have obtained good preliminary agreement between the Rossi-α and pulsed neutron methods. A comparison of the Rossi-α and pulsed neutron method for a measurement of the neutron generation time in the Brookhaven Beam Research Reactor critical facility, an under-moderated, enriched uranium, heavy water system, has been made by Price.[12] The Rossi-α technique has also been applied recently[13] to the measurement of reactivity and neutron lifetime in a thermal reactor with a neutron lifetime of 173.6 μsec.

3.2 APPLICATIONS OF THE PULSED NEUTRON TECHNIQUE TO MULTIPLYING THERMAL SYSTEMS: A LITERATURE SURVEY

The pulsed neutron technique was conceived and first developed in relation to pure moderator materials, and most of its applications have been to the study of the neutron transport characteristics (thermalization and diffusion) of non-multiplying media. A wide variety of moderating materials under varying conditions has been treated experimentally. No attempt will be made to review the literature in this rather extensive field; the reader is referred to review articles by von Dardel and Sjöstrand[14] and Beckurts,[12] and Volume III of the Proceedings of the Brookhaven Conference on Neutron Thermalization.[15]

The application of the pulsed neutron method to multiplying systems is still in its early stages and its potential usefulness appears to be high; it should become a standard tool in the study of subcritical assemblies. The basic technique and the equipment are similar to those used for non-multiplying systems; the most important experiment is of the thermal die-away type in which the quantity determined directly is the prompt neutron decay constant α of the fundamental flux mode. The application, usefulness and interpretation depend on the purpose of the experiment and the theoretical model available for the correlation of alpha with other parameters of interest.

Perhaps the first application of the pulsed neutron experiment to multiplying systems was by Sjöstrand[16, 17], who introduced a pulsed neutron source into the Swedish heavy water reactor R-1 while it was subcritical and studied the prompt neutron lifetime and the reactivity equivalent of heavy water. He used an "Area" method based on the analysis of the entire thermal neutron decay curve with its prompt and delayed neutron counterparts. His work served mainly to introduce the pulsed neutron technique to the domain of subcritical reactor experiments. Campbell and Stelson[18] pulsed homogeneous aqueous solutions of enriched uranyl fluoride ($U^{235}O_2F_2$-H_2O) in cylindrical buckets containing 53.0 and 26.5 g U^{235} per liter, respectively. Simmons[19, 20] and Simmons and King[21] introduced a pulsed neutron method for the measurement of reactivity based on the relationship between the decay constant and the criticality factor of the assembly. The proportionality constant - the ratio of the effective delayed neutron fraction to the prompt neutron lifetime - was determined by pulsing the reactor at delayed critical and assuming this ratio to remain constant. Fultz[22] has compared the experimentally measured decay constants for enriched uranium-graphite systems with two-group calculations and obtained good agreement at high C:U ratios (9950:1); for lower C:U ratio, the system may no longer be "thermal" and the hardened energy spectrum changes the group constants, especially those of the thermal group. Following the experiments of Campbell and Stelson[18] at Oak Ridge, de Saussure, Henry and Parez-Belles[23, 24] have measured the reactivity worths of single and clustered fuel elements in the Bulk Shielding Reactor-I. De Saussure, Silver and Kingston[25] also

used this method to calibrate the control rods of the Tower Shielding Reactor-II and to compare it with other methods. Kolar and Kloverstrom[26] at the Lawrence Radiation Laboratory, Livermore, have made reactivity measurements with the pulsed neutron method, on a reactor composed of bare rectangular graphite plates with oralloy foils sandwiched between them and have compared their results with those obtained with the asymptotic period and rod-drop methods; good agreement (within a few per cent) has been achieved for reactivities down to a few dollars below delayed critical. Bach and coworkers[27] at KAPL have measured the decay constant for a series of polyethylene-moderated subcritical assemblies and compared them with the decay constant as determined by the 1/v poison removal method. They used a four-group diffusion calculation with group-dependent buckling; the agreement is to within 10%. They have also investigated the neutron spectra in the assembly during the decay of the persistent spatial mode. Recently, Meister[28] has reported the results of pulsed neutron experiments on heavy water, natural uranium lattices; he has compared the measured decay constant and changes in radial buckling due to insertion of absorbing rods, with the results of simple two-group calculations involving lattice parameters determined from previous exponential experiments; the agreement was good in the buckling range $B^2 < 25\ m^{-2}$. A new method has recently been proposed by Russell and Garelis[29] for the measurement of the subcriticality of an assembly by the pulsed neutron method. This method uses the complete decay response of a repetitively pulsed assembly after a quasi-equilibrium state has been reached to extract the parameter $k\beta/\ell$, thus obviating the necessity of carrying the assembly to delayed critical. The feasibility of using a pulsed neutron source in conjunction with detectors and wave analyzers as a continuous, analog reactivity monitor has recently been pointed out.[30]

3.3 EXPERIMENTS WITH NON-MULTIPLYING SYSTEMS

3.3.1 Diffusion Properties of Moderators

A commonly used application of the pulsed neutron die-away technique is concerned with the determination of the fundamental mode decay constant λ, for a moderator assembly of elementary shape characterized by its geometrical buckling B^2. This measurement is repeated for several

assemblies of different dimensions so as to obtain a set of (λ, B^2) points. The relationship

$$\lambda = \overline{v\Sigma}_a + D_o B^2 - CB^4 + FB^6 - \ldots , \tag{3.5}$$

is then used to extract the values of the coefficients $\overline{v\Sigma}_a$, D_o, C, etc., usually by means of a least-squares fitting procedure. The series in Eq. 3.5 can be truncated after as many terms as is warranted by the experimental data and the accuracy desired.

After the asymptotic decay constants for the fundamental flux modes have been determined, the main problem is the accurate calculation of the geometrical bucklings. The buckling for a cylindrical assembly of radius R and height H according to the commonly used prescription is:

$$B^2 = \left(\frac{2.405}{R + d}\right)^2 + \left(\frac{\pi}{H + 2d}\right)^2 , \tag{3.6}$$

where

$$d = \epsilon \lambda_t , \tag{3.7}$$

and

$$\lambda_t = \frac{3D}{\bar{v}} .$$

There is some uncertainty in the choice of the proper extrapolation distance, d. This ambiguity arises from the dependence of d on the size and shape (ϵ) of the assembly and also from its energy dependence (λ_t). For small assemblies with dimensions comparable to the transport mean-free path, even very small variations in d can lead to large discrepancies in the final values of the diffusion parameters.[31] For such cases, special methods[32-35] must be used in evaluating the extrapolation distance which take into account not only the dependence on the dimensions of the assembly but also on its shape. The energy dependence of d can, if necessary, be accounted for by calculating λ_t from experimentally measured scattering cross-section curves and averaging over the asymptotic spectrum in the pulsed assembly. This spectrum can be taken to be a Maxwellian at the moderator temperature although it actually departs from a true Maxwellian because of diffusion cooling and absorption. When

the linear dimensions of the assembly exceed five transport mean-free paths, the buckling values are relatively insensitive to slight variations in d and the use of Eq. 3.7 with $\epsilon = 0.71$ is adequate.

3.4 Geometrical Bucklings for Assemblies with Complex Shapes

This application of the pulsed neutron method is in some ways the reverse of the one described in the last section. Once the parameters $\overline{v\Sigma}_a$, D and C (in Eq. 3.5 truncated after the third term) are determined as described by experiments on assemblies of well-defined elementary shape, the same equation can be used to determine the geometrical buckling of an assembly with a complex shape by measuring the decay constant for it. The complex shape can be encountered either with a body of intrinsic irregular shape for which the solution of the wave equation vanishing on its periphery poses theoretical difficulties, or with a system of regular shape which has been distorted by practical requirements such as the introduction of control rods, coolant channels, thimbles, etc.

In particular, the effect of the insertion of absorbers such as control rods can be studied in moderator assemblies. The control rods effectively provide an additional (internal) boundary and thereby change the geometrical buckling; this change is a measure of the effectiveness of the control rod as an absorber. By measuring the decay constant of the assembly with and without the absorber, the change in geometrical buckling caused by it can be calculated and compared with theoretical predictions.

Consider a cylindrical assembly of extrapolated dimensions (R,H), of a moderator for which the diffusion parameters $\overline{v\Sigma}_a$, D and C have been previously measured by the (λ, B^2) method. The solution of the ordinary diffusion equation which vanishes on the boundary is:

$$\phi_o(r,z) = A_o \cos \frac{\pi z}{H} J_o(a_o r) , \tag{3.8}$$

where the geometrical buckling is given by

$$B_o^2 = a_o^2 + \left(\frac{\pi}{H}\right)^2 , \tag{3.9}$$

with

$$J_o(a_o R) = 0, \qquad \text{i.e.,} \quad a_o = \frac{2.405}{R} .$$

If a thermally black cylindrical control rod of effective radius, a, is fully inserted along the axis, the corresponding equations become (with the moderator height H maintained constant):

$$\phi(r,z) = A \cos \frac{\pi z}{H} \left[J_o(ar) - \frac{J_o(aR)}{Y_o(aR)} Y_o(ar) \right], \tag{3.10}$$

where

$$B^2 = a^2 + \left(\frac{\pi}{H}\right)^2 , \tag{3.11}$$

and a is now a root of the transcendental equation

$$J_o(aa) - \frac{J_o(aR)}{Y_o(aR)} Y_o(aa) = 0 ; \tag{3.12}$$

then $\Delta a = a - a_o$ can be calculated theoretically. It also follows from Eqs. 3.9 and 3.11 that:

$$\Delta B^2 = \Delta a^2 , \tag{3.13}$$

where

$$\Delta B^2 = B^2 - B_o^2 ,$$

and B^2 and B_o^2 are the roots of the respective equations,

$$\lambda = v\Sigma_a + DB^2 - CB^4 , \tag{3.14a,b}$$

$$\lambda_o = v\Sigma_a + DB_o^2 - CB_o^4 ,$$

so that

$$\Delta B^2 = \frac{\Delta\lambda}{D - C(2B_o^2 + \Delta B^2)} . \tag{3.15}$$

The use of the one-group diffusion theory on which Eqs. 3.8 and 3.10 are based should provide a reasonable first approximation for this thermal moderator system.

3.5 PULSED NEUTRON EXPERIMENTS ON UNPERTURBED MULTIPLYING SYSTEMS

A multiplying system differs from a non-multiplying one in having not only multiplication but also additional absorption and neutron interactions occurring over a wide range of neutron energies. The special features of the multiplying system are characterized by new parameters. The broad aim of the pulsed neutron experiments with subcritical systems is to obtain as much information as possible about the system – both qualitatively and quantitatively.

The most straightforward way is to relate the experimentally measured decay constant with quantities characterizing the subcritical system and to exploit this relationship for extracting the reactor parameters. Several such expressions were derived in the preceding chapter, some representing generalizations of the simple basic relationship while some were especially germane to particular systems. Since our main interest is in the study of bare subcritical systems, we invoke the basic Eq. 2.50 of the last chapter. For the fundamental mode:

$$\lambda = \overline{v\Sigma}_a + \overline{vD}B^2 - \overline{v\Sigma}_a(1-\bar{\beta})\, k_o F(B^2), \tag{3.16}$$

where $F(B^2)$ is the fast non-leakage probability; on the age-theory model, $F(B^2) = e^{-B^2\tau}$, so that

$$\lambda = \overline{v\Sigma}_a + \overline{vD}B^2 - \overline{v\Sigma}_a(1-\bar{\beta})\, k_o e^{-B^2\tau} . \tag{3.17}$$

Before developing some of its applications, it is well to recall the assumptions underlying the derivation of Eq. 3.17. The relation is strictly valid for a bare, thermal, homogeneous system in which the slowing-down phase is described by the Fermi-age model; the latter differs little from the result of the two-group model for large sizes ($e^{-B^2\tau} \approx 1/(1+B^2\tau)$). The delayed neutron effects are not taken into account except for the inclusion of the factor $(1-\bar{\beta})$ in the multiplicative term. The diffusion cooling term, which may be important for small systems, is also not included. Under these conditions, Eq. 3.17 gives λ in terms of the parameters Σ_a, D, k_o, etc.

The relation, Eq. 3.17, can be used in several ways. For small bucklings, $e^{-B^2\tau} \approx 1 - B^2\tau$, so that Eq. 3.17 can be rewritten as:

$$\lambda = \overline{v\Sigma}_a + \overline{vD}B^2 - \overline{v\Sigma}_a(1-\bar{\beta})\, k_o(1-B^2\tau) \tag{3.18}$$

$$= -m + nB^2 , \tag{3.19}$$

where

$$-m = \overline{v\Sigma}_a(1-(1-\bar{\beta})k_o) ,$$
$$n = \overline{vD} + \overline{v\Sigma}_a(1-\bar{\beta})\,\tau k_o . \tag{3.19a,b}$$

Of the various unknowns appearing in Eq. 3.18, τ and $\bar{\beta}$ can be calculated well enough for any multiplying system. If the volume fractions of U and Al are small in a lattice cell compared to D_2O, then, since the transport cross sections of U and D_2O are nearly equal, we must have $\Sigma_{tr} \approx \Sigma_{tr}^m$ for the moderator. And, since $D = \frac{1}{3}\lambda_{tr}$, we also have

$$D = D^m . \tag{3.20}$$

The parameter D^m is known from pulsed neutron die-away experiments on pure moderator. Hence, if m and n are obtained from a least-squares fit of the (λ vs. B^2) data for a subcritical system, Eqs. 3.19 a,b yield the values of the parameter, $v\Sigma_a$ and k_∞. The velocity v characteristic of the actual spectrum in the assembly can be evaluated on some assumed model of the spectrum. Then, since

$$\overline{v\Sigma}_a = \overline{v\Sigma}_a^m + \overline{v\Sigma}_a^f , \tag{3.20a}$$

and the moderator absorption cross section, Σ_a^m, is known from the moderator experiments, Σ_a^f for the fuel (this includes fission and capture) can be determined. In addition, the diffusion area L^2 for the lattice can be determined from the relation:

$$L^2 = \frac{\overline{vD}}{\overline{v\Sigma}_a} . \tag{3.21}$$

Since B^2 can be calculated from the dimensions, the effective multiplication factor,

$$k = \frac{k_o\, e^{-B^2\tau}}{1 + L^2B^2} , \tag{3.22}$$

can also be evaluated. Furthermore, for pure moderator,

$$L_m^2 = \frac{\overline{vD}}{\overline{v\Sigma_a}^m} \tag{3.21a}$$

and, if we use the relation

$$L^2 = f_m L_m^2 , \tag{3.21b}$$

we get a value for the thermal utilization, f_m, of the moderator. If a correction is made for the neutron absorption in the fuel rod cladding, a value of the thermal utilization f can be obtained. If the fuel concentration is significantly large, Eq. 3.21b is modified as follows:[42]

$$L^2 = L_m^2 f_m \left[1 - \frac{N_U \sigma_{tr\,U}}{N_m \sigma_{tr\,m}} + \left(\frac{N_U \sigma_{tr\,U}}{N_m \sigma_{tr\,m}} \right)^2 - \ldots \right], \tag{3.21c}$$

where N and σ_{tr} are, respectively, the atom density and the microscopic transport cross section. Also, in finite heterogeneous systems, a further correction can be made to account for the reduced density of the moderator resulting from the presence of fuel channels; this modification gives:[42]

$$L^2 = L_m^2 f_m \left(\frac{V_T}{V_m} \right)^2 \tag{3.21d}$$

where V_T is the total reactor volume and V_m is the moderator volume.

The above analysis shows that it may be possible to determine k_o and L^2 for the lattice from the pulsed neutron experiments. These two parameters are difficult to determine experimentally and, if they can be found with satisfactory precision, this result would be a further important application of the pulsed neutron method.

From the known values of k_o, L^2 and τ, one can also calculate by some theoretical model, other quantities of interest such as the material buckling B_m^2, the critical dimensions, the leakage probabilities, etc. The value of these parameters can then be compared with the values obtained with other methods and calculations. Thus, the value of k_o can be compared with the value calculated from the four-factor formula, and with the value obtained from the material buckling (from static exponential experiments), estimated values of τ and L^2 and a suitable reactor model

or from PCTR-type measurements. The value of the thermal utilization, f, can be compared with the results of exponential experiments and calculations based on THERMOS[36] or the Amouyal-Benoist-Hurwitz[37] method.

Finally, since the relevant parameters have been separately determined as indicated above, we can evaluate the prompt neutron lifetime ℓ, corresponding to a geometrical buckling B_g^2:

$$\ell = \frac{1}{v\Sigma_a\left(1+L^2B_g^2\right)} = \frac{1}{v\Sigma_a + vDB^2} .$$

This value can then be used to obtain the reactivity from the measured prompt neutron decay constant.

In the above analysis, the first-order approximation, $e^{-B^2\tau} \approx 1 - B^2\tau$, has been taken for the sake of illustration. If the measurements involve assemblies whose dimensions do not warrant such an approximation, it may be necessary to include other higher-order terms in B^2, or to retain the form $e^{-B^2\tau}$ in Eq. 3.16. The (λ vs. B^2) data can be analyzed in several ways and the validity of any particular method should be checked by examining the value of $B^2\tau$ and estimating the error involved in making the basic approximation. This point will be discussed in Chapter VII.

3.6 APPLICATION OF THE PULSED NEUTRON METHOD TO REACTIVITY STUDIES

We have seen that the reactivity and the prompt neutron decay constant are measures of the global characteristics of a multiplying system. Furthermore, the methods of measuring reactivity depend on the study of the temporal response of the system to an over-all perturbation. It is, therefore, to be expected that the pulsed neutron method would be especially applicable to the study of reactivity. Basically, the pulsed neutron experiment yields the decay curve of the thermal flux in the subcritical assembly. This curve can be characterized by a decay constant which can be related to the reactivity through some theoretical model; this treatment is the basis of the "delayed critical method." Alternatively, the complete decay curve, itself, can be subjected to an analysis which yields the reactivity;

this latter scheme leads to the "area" method or to the so-called $k\beta/\ell$ method.

3.6.1 The Delayed Critical Method

The use of the pulsed neutron technique for the measurement of reactivity has been based largely on the first approach.[9, 21, 24, 26] The relationship between the prompt neutron decay constant and reactivity involves arbitrary definitions. Henry[38] has expressed the reactor kinetics equations in a form such that the asymptotic decay constant in the absence of delayed neutrons is given by the relation:

$$\lambda = \frac{\overline{\beta} - \rho}{\ell} = \frac{\overline{\beta}}{\ell}\left(1 - \frac{\rho}{\beta}\right), \tag{3.24}$$

where the ratio of the effective delayed neutron fraction in the system to the prompt neutron lifetime is the value of $\lambda (= \lambda_c)$ when $\rho = 0$, i.e., at delayed critical; ρ/β is the reactivity in dollars, \$, so that Eq. 3.24 may be rewritten as:

$$\lambda = \lambda_c(1-\$) \tag{3.25}$$

where

$$\lambda_c = \frac{\overline{\beta}}{\ell}. \tag{3.25a}$$

Simmons and Bohl[8] at KAPL have made a "null test" of the validity of Eq. 3.25. Under the constraint of maintaining criticality with no fuel or moderator changes, they have made considerable rearrangement of lumped poisons and found no resulting change in λ_c (within an experimental accuracy of about 1%) in four different hydrogen-moderated critical assemblies containing at least partially enriched U^{235} fuel, and with bucklings of the order of 0.003 cm^{-2}. It is conceivable, however, that extreme poison rearrangement could alter λ_c. The simultaneous addition of fuel and poison under the constraint of maintaining criticality – such as the addition of control rod and sufficient additional fuel and moderator to restore delayed criticality – does change λ_c appreciably.[8]

Equation 3.25 can be used in two ways: if the value of the buckling at delayed critical is known or can be calculated, one can measure λ as a function of moderator level and plot the λ vs. B^2 curve for a slightly

subcritical reactor and determine λ_c by extrapolation. Then a measurement of λ without and with the perturbation will yield the reactivity equivalent of the perturbation. If, in each of the two separate cases, a (λ vs. B^2) curve is obtained, then the reactivity of the absorber – say, a control rod – may be obtained directly from the graphs, as shown in Figure 3.1. The accuracy of this method depends on the precision with which $B^2_{d.c.}$ is known.

The more commonly used method is to make the calibration measurement for λ_c at some known reactivity, usually by taking the system to delayed critical ($\rho = 0$) and measuring λ_c directly. Thereafter, λ_c is assumed to remain constant as the system composition is altered by the introduction of the perturbation. The reactivity in dollars is then given by:

$$\$ = \frac{\lambda - \lambda_c}{\lambda_c} \quad . \tag{3.26}$$

The characteristic lifetime $\ell^*(= 1/\lambda_c)$, defined as the ratio of the ratio of the prompt neutron lifetime to the effective delayed neutron fraction, and the reactivity in dollars, \$, are both of interest since their values affect the zero power reactor kinetics.

This method, which has become almost standard practice for the measurement of reactivity by the pulsed neutron technique, suffers from at least two disadvantages. First, it is necessary to take the system to delayed critical and the measurement cannot be made entirely in a subcritical assembly. Even in a critical assembly, practical considerations may preclude the possibility of making a direct λ_c-measurement. For example, near delayed critical, the running reactor produces a large background of neutrons over which only a small number of decaying neutrons from the pulsed source is superimposed. Second, the variation of λ_c with reactivity is not taken into account. As remarked earlier, λ_c is insensitive to the redistribution of lumped poisons in a reactor core as long as the reactor remains critical without fuel or moderator changes. But in measurements with reactivity changes of several dollars, a correction must be made for the variation of λ_c with reactivity which may be caused by variations in the neutron spectrum and flux shape due to the introduction of the lumped absorber.

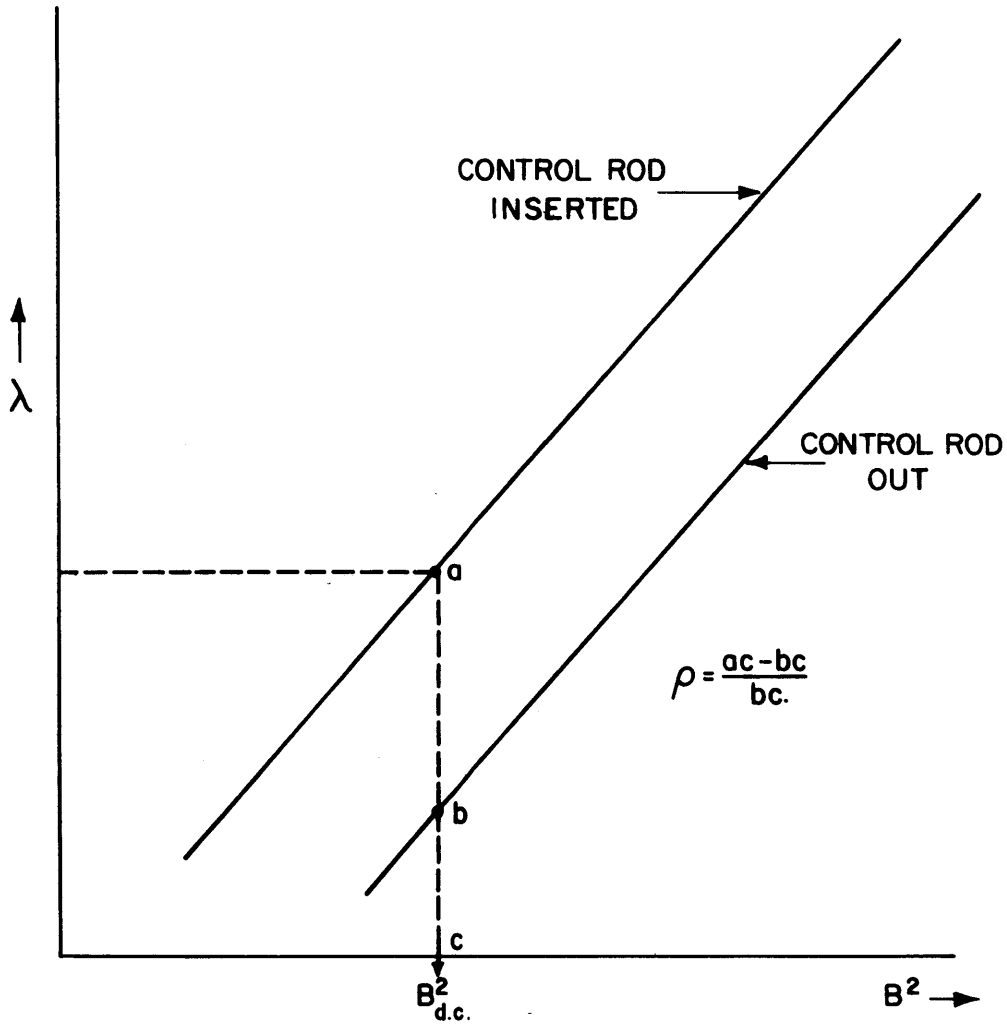

FIG. 3.1 DETERMINATION OF THE WORTH OF A CONTROL ROD FROM THE GRAPH OF THE PROMPT NEUTRON DECAY CONSTANT λ VS. THE GEOMETRICAL BUCKLING B^2; FOR A SUBCRITICAL ASSEMBLY WITH AND WITHOUT THE ROD.

When a critical assembly is made subcritical by the introduction of a control rod, the geometrical buckling is changed, and the lifetime ℓ also changes, as can be seen from the one-group expression for the neutron lifetime:

$$\ell = \frac{1}{v\Sigma_a(1+L^2B^2)} . \tag{3.27}$$

At delayed critical, this expression becomes:

$$\ell_c = \frac{1}{v\Sigma_a(1+L^2B_c^2)} , \tag{3.28}$$

and

$$\frac{\ell}{\ell_c} = \frac{1 + \frac{L^2}{M^2}(k_o-1)}{1 + \frac{L^2}{M^2}\{k_o(1-\rho)-1\}} ; \tag{3.29}$$

ℓ can differ from ℓ_c by as much as 15%. In order further to relate the change in lifetime with the change in reactivity, we write,

$$\ell = \frac{\ell_o}{1 + B^2L^2} , \tag{3.30}$$

$$k = \frac{k_o e^{-B^2\tau}}{1 + B^2L^2} . \tag{3.31}$$

From these equations, if we consider the change in each as being due to a change in the geometrical buckling B^2, then

$$\frac{\Delta \ell}{\ell} = \frac{1}{1 + \frac{\tau}{L^2}(1+B^2L^2)} \cdot \frac{\Delta k}{k} . \tag{3.32}$$

Thus, the fractional change in lifetime, which depends on the relative magnitudes of τ and L^2, may be significant.

One way of reducing the uncertainty due to the possible change in lifetime is to use the prompt neutron generation time Λ instead of the prompt neutron lifetime ℓ and to employ the relation:

$$\lambda = \lambda_c(1-\$) , \tag{3.33}$$

with

$$\lambda_c = \frac{\beta}{\Lambda} . \tag{3.34}$$

Then, since

$$\Lambda = \frac{\ell}{k} ,$$

and, since the prompt neutron lifetime ℓ changes with reactivity in the same way as k to a first approximation, Λ remains nearly constant. This is especially true if k is changed by a local variation of the absorption cross section as, for instance, the insertion of a control rod which affects ℓ and k in much the same way; if k is changed by varying B^2, e.g., by varying the moderator height, Λ remains constant according to one-group theory and varies only slightly in a two-group approximation.[39] However, when large absorption changes are affected, thereby disturbing the flux distribution appreciably, the changes in Λ may become significant.

3.6.2 The "Area" Method

This method has been used by Sjöstrand[16, 17] for measuring the reactivity equivalent of heavy water and the mean lifetime of thermal neutrons in the Swedish Heavy Water Reactor R-1. The method is based on an analysis of the complete decay curve of the neutron density with time and is useful for a reactor close to criticality when only the fundamental mode of the spatial neutron distribution is important. If the repetition time is much shorter than the shortest periods of the delayed neutrons and the time constant of the reactor is much shorter than the pulse length, then the neutron density in the reactor will vary with time as shown in Fig. 3.2. The curve consists of a part due to prompt multiplication of the same shape, roughly, as the source pulse (rectangular) and a delayed neutron portion which is nearly flat. If the area of a pulse above the constant value in the figure is denoted by A_1 and the area under the delayed neutron curve during one period, by A_2, and if the source strength is assumed to be a periodic function of time S(t), then, under certain simplifying assumptions, it can be shown that the prompt and total multiplication

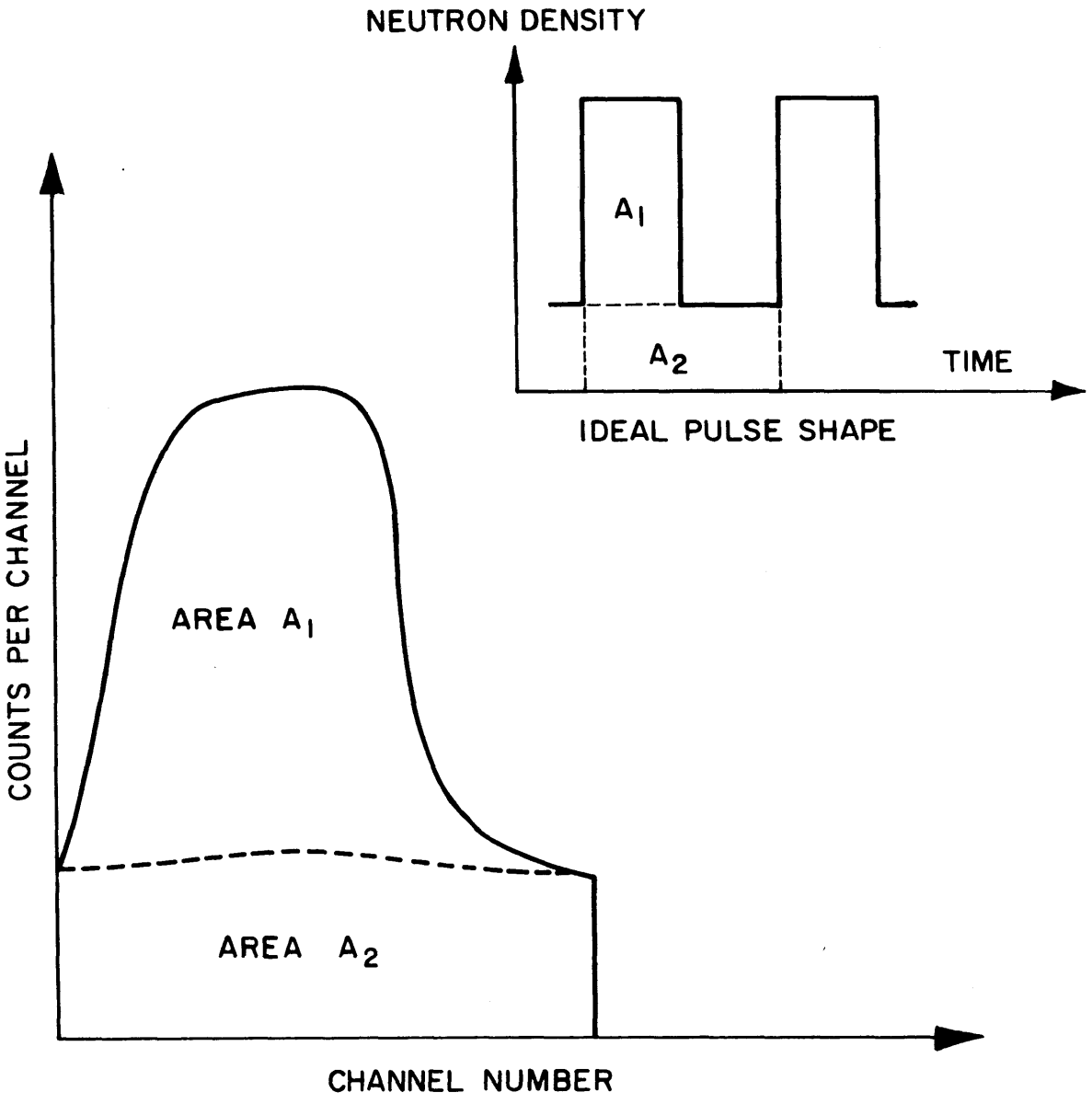

FIG. 32 ANALYSIS OF THE THERMAL NEUTRON DECAY CURVE IN A PULSED SUBCRITICAL ASSEMBLY, FOR THE MEASUREMENT OF REACTIVITY BY THE "AREA" METHOD (REF. 16)

are given by:

$$A_1 = \frac{aS}{1 - k(1-\beta)}, \tag{3.35}$$

$$A_1 + A_2 = \frac{aS}{1 - k}, \tag{3.36}$$

where a is a constant and β is the effective delayed neutron fraction. Equations 3.35 and 3.36 give directly:

$$\frac{A_1}{A_2} = \frac{1 - k}{\beta k} = \frac{\rho}{\beta} = \$, \tag{3.37}$$

where ρ is the negative reactivity ((1-k)/k) and \$ is the reactivity in dollars.

Thus, if the delayed neutron fraction β is known, the absolute reactivity of a subcritical assembly ρ can be determined, in principle, by this method.

This method has not been used much, partly because of the arbitrariness involved in the division of the curve into two parts. The errors arising from this uncertainty for certain reactor systems may be large enough to render the method unsuitable. Moreover, according to Keepin,[39a] the simplifying assumptions adopted by Sjöstrand do not hold in practice.

3.6.3 The $k\beta/\ell$ Method

A new method has recently been proposed by Garelis and Russell[29] for the determination of the subcriticality of an assembly directly in terms of dollars. The method determines the parameter $k\beta/\ell$ by using the complete response curve of a repetitively pulsed assembly after the quasi-equilibrium state has been attained. This value of $k\beta/\ell$, together with the usual prompt neutron decay constant measurement, yields the reactivity directly. The analytical model is based on a bare one-group diffusion treatment with m-delayed neutron precursors, but the applicability of the result appears to be broader.

Basically, the method is as follows. The equilibrium neutron density in a pulsed subcritical system, $N(\vec{r},t)$, is represented as the sum of two

contributions: the prompt distribution N_p and the delayed contribution N_d. It can then be shown that under certain conditions, the following relation holds:

$$\int_0^\infty N_p \exp\left[\left(\frac{k\beta}{\ell}\right)t\right] dt - \int_0^\infty N_p \, dt = \frac{N_d}{R}, \tag{3.38}$$

where R is the repetition rate. Thus, if the prompt neutron distribution is known, the above integral relationship determines $k\beta/\ell$ since N_d is an experimentally observable quantity. The delayed neutron contribution, N_d, is a constant provided $R \gg \omega$, where ω is the decay constant of the shortest lived important precursor. With a constant value of N_d, the prompt distribution can be determined simply by subtracting this constant value from the over-all equilibrium pulse shape. When the parameter $(k\beta/\ell)$ is thus known, the reactivity in dollars is given by

$$\$ = \frac{\left[\lambda - \left(\frac{k\beta}{\ell}\right)\right]}{\left(\frac{k\beta}{\ell}\right)}. \tag{3.39}$$

The above treatment is independent of the spatial modes since the latter are taken into account.

In general, the restriction on the pulse rate in this technique is such that $\omega \ll R \ll \lambda$, where λ is the prompt decay constant. The precise knowledge of the delay tail is crucial if meaningful results are to be obtained. Since the shape of the delayed contribution cannot be readily calculated in the general case for arbitrary pulse rates, the assembly is pulsed at a rate such that $R \gg \omega$ in order to yield a constant background. Preliminary experimental evidence[40] seems to indicate that a pulse rate of R = 10 pps is the lower limit for an assembly that is about a dollar subcritical. A simple pulsing technique[40] can be used to obtain the quasi-equilibrium neutron distribution without the necessity of a constant pulse strength.

In the actual application of the $(k\beta/\ell)$ technique, special methods of data reduction are needed, particularly for extracting the value of $(k\beta/\ell)$ from the integral relationship, Eq. 3.38. These methods are discussed in Appendix 4, and a computer code developed to facilitate the data reduction is also described.

3.7 PULSED NEUTRON EXPERIMENTS ON PERTURBED MULTIPLYING SYSTEMS

This section is, in fact, a continuation of Section 3.5 and seeks to explore the usefulness of the pulsed neutron technique in studying the effect of perturbations such as those caused by control rods in multiplying systems. The previous two sections were concerned with a specific aspect of this problem – the direct measurement of the reactivity of the perturbation. The effects of a perturbation can also be studied from other points of view, and the results obtained with the pulsed method can yield results which can be compared with the results obtained with other experimental methods or with theoretical calculations.

As an example, we consider the effect of control rods as being described by the change in geometrical buckling they produce in a multiplying assembly; this change can be related to the change in the prompt neutron decay constant. Thus, if we measure the decay constant of a lattice assembly with (λ) and without (λ_o) a control rod, then the difference,

$$\Delta\lambda = \lambda - \lambda_o ,$$

can be related to the corresponding difference ΔB^2 through the (λ vs. B^2) curve for the assembly. Alternatively, we can use the two-group expression derived in Chapter II:

$$\lambda = v\Sigma_a + vDB^2 - \frac{v\Sigma_a(1-\bar{\beta})\, k_o}{(1+\tau B^2-\lambda \ell_1)} ; \tag{3.40}$$

if the fast neutron lifetime ℓ_1 is such that $\lambda\ell_1 \ll 1$, we obtain:

$$\Delta B^2 = \frac{\Delta\lambda}{vD + \dfrac{v\Sigma_a(1-\bar{\beta})\, k_o \tau}{(1+\tau B^2)^2}} . \tag{3.41}$$

If the moderator level is maintained constant, then, since

$$B^2 = a^2 + \left(\frac{\pi}{H}\right)^2 ,$$

$$\Delta B^2 = \Delta a^2 . \tag{3.42}$$

Thus, Eq. 3.41 relates the change in radial buckling produced by the rod to the measurable change $\Delta\lambda$ in the prompt neutron decay constant. This result for Δa^2 can then be compared with the result obtained from exponential experiments as discussed in Chapter IV. Moreover, each of these can be compared with the calculated values of Δa^2. An expression based on the boundary condition defined in terms of the actual extrapolation distance for the rod has been derived (Chapter VI):

$$\frac{\Delta a^2}{a_o^2} = -0.820\left[Y_o(\mu a)+d\mu Y_1(\mu a)+\frac{2}{\pi}\frac{S_2}{S_1}(K_o(\nu a)+d\nu K_1(\nu a))\right]^{-1}, \qquad (3.43)$$

where μ^2, ν^2 are the roots of the two-group criticality equation and S_1, S_2 are the usual coupling coefficients.[41]

The nuclear parameters vD, $v\Sigma_a$, τ, k_o, etc., appearing in Eqs. 3.41 and 3.43 can be obtained by the pulsed technique by methods already outlined in Section 3.5.

3.7.1 Reactivity Measurements in Subcritical Assemblies by the Pulsed Neutron Method

We return to the problem of applying the pulsed neutron technique for the measurement of reactivity. The M.I.T. subcritical facility cannot be taken to delayed critical and most of the lattices are in the far-subcritical region so that the standard methods described in Sections 3.6.1 and 3.6.2 are not suitable. Moreover, it is desirable to have a technique which can be carried in its entirety in a subcritical assembly. Hence, special methods are needed to evaluate the thermal neutron lifetime and to relate the prompt neutron decay constant to the subcriticality of the lattice assembly.

We start with the basic relationship between λ and B^2 for a multiplying system which we have already used in Section 3.5:

$$\lambda = v\Sigma_a + vDB^2 - v\Sigma_a(1-\bar{\beta})\,k_o e^{-B^2\tau}. \qquad (3.44)$$

We rewrite this expression in the form:

$$\lambda = (v\Sigma_a + vDB^2)\left[1 - \frac{k_o e^{-B^2\tau}}{1 + L^2B^2}(1-\bar{\beta})\right], \tag{3.45}$$

and introduce the thermal neutron lifetime ℓ and the criticality factor k for the finite medium:

$$\ell = \frac{1}{v\Sigma_a + vDB^2}, \tag{3.46}$$

$$k = \frac{k_o e^{-B^2\tau}}{1 + L^2B^2}, \tag{3.47}$$

so as to obtain:

$$\lambda = \frac{1}{\ell}\left[1-(1-\bar{\beta})k\right]. \tag{3.48}$$

This equation relates λ to k. Now, if we define the negative reactivity or the degree of subcriticality as:

$$\rho = \frac{1 - k}{k}, \tag{3.49}$$

then we have:

$$\lambda = \frac{1}{\ell} \cdot \frac{\bar{\beta} + \rho}{1 + \rho}. \tag{3.50}$$

We notice that this expression can be written as

$$\lambda = \frac{k\beta}{\ell}(1+\$) = \frac{\bar{\beta}}{\Lambda}(1+\$) = \lambda_c(1+\$), \tag{3.51}$$

which is the relation used in the delayed-critical method described in Section 3.6.1. The sign before \$ in Eqs. 3.51, 3.33 or 3.25 depends on whether ρ is taken to be the positive or negative reactivity. Also, at delayed critical, k= 1 and the prompt neutron lifetime ℓ and the generation time Λ are equal so that λ_c may be written as $\frac{\bar{\beta}}{\ell}$ or $\frac{\bar{\beta}}{\Lambda}$.

Finally, we have from Eq. 3.50:

$$\rho = \frac{\lambda - \frac{\bar{\beta}}{\ell}}{\frac{1}{\ell} - \lambda}, \tag{3.52}$$

which is the basic relationship on which we shall base our method of reactivity measurement. Here, λ is the directly measured quantity in the experiment and $\overline{\beta}$ can be calculated for the assembly under investigation (Appendix 3). It remains to evaluate ℓ.

The parameter ℓ given by Eq. 3.46 may be evaluated from its component parts $v\Sigma_a$, vD and B^2, which can be measured by methods discussed in Sections 3.4 and 3.5. Since ℓ is evaluated directly in terms of the actual value of B^2 of the system, its variation with reactivity is taken into account. The lifetime ℓ as defined by Eq. 3.46 is the thermal neutron lifetime; the slowing-down time has been neglected in Eq. 3.44. For heavy water systems, the slowing-down times are of the order of 10^{-5} sec while the thermal lifetimes will be seen to be much greater, so that the approximation is quite good.

References

1. F. de Hoffmann, Statistical Aspects of Pile Theory, Chapter 9 of The Science and Engineering of Nuclear Power, Vol. II, Addison-Wesley, Reading, Massachusetts (1949).

2. R. P. Feynman, F. deHoffmann and R. Serber, J. Nuclear Energy, 3, 64 (1956).

3. J. D. Orndoff, Nuclear Sci. and Eng., 2, 450 (1957).

4. G. S. Brunson, R. Curran, S. G. Kaufmann, J. McMahon and L. Pahis, Nucleonics, 18, No. 11; 132 (1957).

5. J. T. Mihalczo, USAEC Report ORNL-TM-470 (1963).

6. G. S. Brunson, to be published.

7. W. K. Luckow, The Evaluation of Nuclear Reactor Parameters from Measurements of Neutron Statistics, Ph.D. Thesis, University of Michigan, Ann Arbor (1958); also Ref. 8.

8. J. Bengston et al., UCRL-5159, 1958.

9. J. Bengston et al., Proc. of Second Int. Conf. on the Peaceful Uses of Atomic Energy, Geneva, 1958, P/1783, 12, 63 (1958).

10. P. J. Bendt, H. J. Karr and F. R. Scott, Nuclear Sci. and Eng., 4, 703 (1958).

11. L. Passell, J. Bengston and D. C. Balir, UCRL-4808 (1957).

12. K. H. Beckurts, Nucl. Instr. and Methods, 11, 144 (1961).

13. von Theodor Striebel, Nukleonik, Band 5, Heft 4, p. 170 (1963).

14. G. F. von Dardel and N. G. Sjöstrand, Progr. Nucl. En., 1, 2, 183 (1958).

15. Proceedings of the Brookhaven Conference on Neutron Thermalization, BNL719(C-32), Vol. III (1962).

16. N. G. Sjöstrand, Arkiv För Fysik, Band 11, Nr. 13, 233 (1956).

17. N. G. Sjöstrand, Proc. Int. Conf. on Peaceful Uses of Atomic Energy, Geneva, Vol. 5, P/789 (1955).

18. E. C. Campbell and P. H. Stelson, ORNL-2204, 34 (1956).

19. B. E. Simmons, UCRL-5665, 127 (1958).

20. B. E. Simmons, KAPL-2000-4, 70 (1958).

21. B. E. Simmons and J. S. King, Nuclear Sci. and Eng., 3, 595 (1958).

22. S. C. Fultz, Nuclear Sci. and Eng., 6, 313 (1959).

23. G. de Saussure, K. M. Henry, Jr., and R. Perez-Belles, ORNL Annual Progress Report, p. 3, Sept. 1960.

24. G. de Saussure, K. M. Henry, Jr., and R. Perez-Belles, Nuclear Sci. and Eng., 9, 291 (1961).

25. G. de Saussure, E. G. Silver and J. D. Kingston, ORNL Annual Prog. Report, p. 54, Sept. 1960.

26. O. C. Kolar and F. C. Kloverstrom, Nuclear Sci. and Eng., 10, 45 (1961).

27. D. R. Bach, S. I. Bunch, R. J. Cerbone and R. E. Slovacek, Nuclear Sci. and Eng., 11, 199 (1961).

28. H. Meister, Reactor Sci. and Techn., 17, 97 (1963).

29. E. Garelis and J. L. Russell, Jr., Nuclear Sci. and Eng., 16, 263 (1963).

30. J. L. Shapiro, Trans. ANS, 5, 1, 180 (1962).

31. J. U. Koppel and W. M. Lopez, BNL-719(C32), Vol. III, p. 947 (1962).

32. E. M. Gelbard and J. A. Davis, Nuclear Sci. and Eng., 13, 237 (1962).

33. M. M. R. Williams, Reactor Sci. and Techn., 17, 55 (1963).

34. M. Nelkin, Nuclear Sci. and Eng., 7, 522 (1960).

35. S. K. Davis, J. A. DeJuren and M. Reier, Trans. ANS, Vol. 6, No. 2, p. 286 (1963).

36. H. C. Honeck, BNL-5826 (Sept. 1961).

37. A. Amouyal, P. Benoist and J. Horowitz, J. Nucl. En., 6, 79 (1957).

38. A. F. Henry, Nuclear Sci. and Eng., 3, 52 (1958).

39. M. Küchle, Symposium on Exponential and Critical Experiments, Amsterdam, Netherlands, Paper SM-42/6 (Sept. 1963).

39a. G. R. Keepin, LAMS-2215 (1958).

40. E. Garelis, Trans. Am. Nucl. Soci., Vol. 6, No. 2, p. 289 (1963).

41. S. Glasstone and M. C. Edlund, The Elements of Nuclear Reactor Theory, D. van Nostrand Company, Inc., New York (1952).

42. A. M. Weinberg and E. P. Wigner, The Physical Theory of Neutron Chain Reactors, The Univ. of Chicago Press (1958).

Chapter IV

THEORY AND APPLICATIONS OF EXPONENTIAL EXPERIMENTS WITH CONTROL RODS

The study of the physics of control in nuclear reactors should, ideally, involve two steps. First, theoretical methods for the calculation of the effectiveness of a control rod should be developed, based on clearly defined assumptions and boundary conditions. Second, paralleling the theoretical effort should be an experimental program for the measurement of control rod worths under conditions which make possible the critical comparison of the theoretical and experimental results.

Experimental control rod studies are usually undertaken in a critical facility, a PCTR-type assembly, a pulsed subcritical facility or an operating reactor. The type and scope of the experiments that can be made with an exponential assembly are limited. However, certain control rod measurements in exponential assemblies can be compared with theoretical predictions in a clearly defined way and also provide valuable supplemental information which can be used in control rod studies by other methods. These exponential measurements entail a considerable saving in time, effort and cost; and it is possible, in some cases, to extrapolate the results obtained to critical systems. In particular, for a bare exponential assembly with a single absorbing rod fully inserted parallel to the central axis, the effect of the rod can be interpreted in terms of the difference in axial buckling with and without the rod; this difference is related to the change in radial buckling for the particular assembly used. If the assembly is large enough so that the absorbing rod is far from the outer edge and is not, therefore, influenced by boundary transients (i.e., the extrapolation distance into the rod is independent of the size of the assembly), then the change of geometrical buckling caused by the rod in the exponential assembly can be related to the effect in a full-size reactor. In this chapter, an attempt

will be made to explore the potential usefulness of an exponential assembly in control rod studies and to develop the theoretical analyses which can be made the basis of meaningful experiments. The conditions under which the information obtained from exponential studies can be applied to a critical reactor are also examined.

Many of the control rod studies so far reported do not provide a basis for a well-defined comparison between calculated and measured rod worths. The measurements have usually been dictated by engineering design requirements and the information obtained is useful mainly for establishing the control criteria in the specific system under particular conditions. These measurements have largely been on control rods whose effectiveness could not be calculated accurately from basic principles because of complicated geometrical arrangements or for other reasons. Only rarely have measurements of control rod effectiveness been obtained under conditions amenable to rigorous theoretical treatment. Watson-Munro[1] and Persson[2] have reported preliminary measurements in heavy water systems. Price[3] has described control rod studies in water-moderated lattices, and Gast[4] has compared the results of single control rod experiments in rectangular uranium-graphite critical assemblies. Murray and Niestlie[5] have described the analysis of a set of control rod measurements in small, enriched hydrogen-moderated reactors and have examined the effect of fast neutron boundary conditions. The experiments have underscored the difficulty of predicting the control rod effectiveness accurately. In the usual two-group treatment, neglect of neutron absorption in the fast group tends to underestimate the worth of the rod, but the evaluation of a meaningful extrapolation length for fast neutrons is difficult. While pointing out the need for further work, Gast[4] notes that opportunities for such measurements seldom arise, because experimental determinations are usually carried out in critical systems which tend to be expensive and in great demand for other experiments. If, therefore, meaningful experiments can be performed in subcritical assemblies, the field of possible investigation becomes much broader.

Some isolated exponential experiments with control rods have been reported[2,6] but no detailed systematic studies have been undertaken.

Recently, Wood[7] and James and Till[8] have described control rod experiments with natural uranium-graphite systems. In the following sections, simple theoretical analyses of control rods in exponential assemblies will be presented and possible measurements suggested by these analyses will be considered.

4.1 ONE-GROUP ANALYSIS OF A MODERATOR ASSEMBLY; MEASUREMENT OF THE THERMAL EXTRAPOLATION LENGTH

Consider a bare cylindrical exponential assembly of pure moderator of extrapolated radius R with a full-length black cylindrical rod of actual physical radius, a, placed along its axis. The radial flux is then given as the solution of the radial part of the one-group, steady-state diffusion equation in the moderator region ($a < r < R$),

$$\nabla^2\phi + B_m^2\phi = 0 \ , \tag{4.1}$$

which satisfies the following boundary conditions: at the external boundary,

$$\phi(R) = 0 \ ; \tag{4.2}$$

at the internal boundary (control rod),

$$d_2 = \frac{\phi(a)}{\phi'(a)} \ , \tag{4.3}$$

where d_2 is the thermal extrapolation length into the rod and $\phi'(r)$ stands for the derivative.

The solution of the radial part of Eq. 4.1 which satisfies Eq. 4.2 is:

$$\phi(r) = A\left[J_o(\alpha r) - \frac{J_o(\alpha R)}{Y_o(\alpha R)} Y_o(\alpha r)\right] , \tag{4.4}$$

where α^2 is the radial buckling which is related to the inverse relaxation length γ (axial buckling γ^2) by the familiar equation,

$$B_m^2 = \alpha^2 - \gamma^2 \ . \tag{4.5}$$

Applying the second boundary condition, Eq. 4.3, we get:

$$d_2 = \frac{1}{a} \cdot \frac{Y_o(aR)\, J_o(aa) - Y_o(aa)\, J_o(aR)}{Y_1(aa)\, J_o(aR) - Y_o(aR)\, J_1(aa)} \,. \tag{4.6}$$

Thus, if we know a, Eq. 4.6 determines the thermal extrapolation length d_2 for a black control rod of radius a.

To determine a, consider the same assembly without the control rod. The boundary conditions on the flux are changed because the internal boundary has been removed. Consequently, the flux shape is modified so that the radial leakage (at both the internal and external boundaries) is reduced and the relaxation length increases, owing to reduced leakage. However, the material buckling of the moderator region is unchanged:

$$B_m^2 = a_o^2 - \gamma_o^2 \,, \tag{4.7}$$

where $a_o^2 \left(= \left(\frac{2.405}{R}\right)^2\right)$ and γ_o^2 are the new radial and axial bucklings. From Eqs. 4.5 and 4.7, we get:

$$\begin{aligned} a^2 &= \gamma^2 - \gamma_o^2 + a_o^2 \\ &= \Delta\gamma^2 + \left(\frac{2.405}{R}\right)^2 . \end{aligned} \tag{4.8}$$

The parameters γ and γ_o can be determined from the measured axial flux plots in the exponential tank of pure moderator (say, heavy water) with and without the rod in question.

4.2 TWO-GROUP TREATMENT OF A MULTIPLYING ASSEMBLY WITH CONTROL ROD

We apply two-group diffusion theory to a multiplying assembly with a black control rod along its central axis. The usual two-group equations in the core are:

$$D_1 \nabla^2 \phi_1 - \Sigma_1 \phi_1 + k_o \Sigma_2 \phi_2 = 0 \,, \tag{4.9}$$

$$D_2 \nabla^2 \phi_2 - \Sigma_2 \phi_2 + \Sigma_1 \phi_1 = 0 \,. \tag{4.10}$$

We seek solutions for ϕ_1 and ϕ_2 which satisfy:

$$\nabla^2\phi_1 + B^2\phi_1 = 0 \ ,$$
$$\nabla^2\phi_2 + B^2\phi_2 = 0 \ , \qquad (4.11a,b)$$

where the material buckling B^2 is taken to be the same for the two groups. Equations 4.9, 4.10 and 4.11 yield the consistency condition,

$$(1+\tau B^2)(1+L^2B^2) = k_o \ , \qquad (4.12)$$

where $\tau = D_1/\Sigma_1$ and $L^2 = D_2/\Sigma_2$. We then get the two possible values of the material buckling:

$$\mu^2 = \frac{1}{2}\left[-\left(\frac{1}{\tau}+\frac{1}{L^2}\right) + \left\{\left(\frac{1}{\tau}+\frac{1}{L^2}\right)^2 + \frac{4(k_o-1)}{\tau L^2}\right\}^{1/2}\right],$$
$$-\nu^2 = \frac{1}{2}\left[-\left(\frac{1}{\tau}+\frac{1}{L^2}\right) - \left\{\left(\frac{1}{\tau}+\frac{1}{L^2}\right)^2 + \frac{4(k_o-1)}{\tau L^2}\right\}^{1/2}\right], \qquad (4.13a,b)$$

which are related by

$$\mu^2 - \nu^2 = -\left(\frac{1}{\tau}+\frac{1}{L^2}\right) . \qquad (4.14)$$

Equations 4.11 can then be solved in cylindrical coördinates by separation of variables; separation constants a_1, γ_1 and a_2, γ_2 are obtained, given by:

$$\mu^2 = a_1^2 - \gamma_1^2 \ ,$$
$$-\nu^2 = a_2^2 - \gamma_2^2 \ . \qquad (4.15a,b)$$

The solutions are of the form:

$$R_1 = AJ_o(a_1\tau) + BY_o(a_1 r) \ ,$$
$$Z_1 \sim e^{-\gamma_1 z} \ ; \qquad (4.16)$$

and

$$R_2 = CI_o(a_2 r) + DK_o(a_2 r) ,$$
$$Z_2 \sim e^{-\gamma_2 z} . \qquad (4.17)$$

Since μ^2 and $-\nu^2$ are material bucklings, a^2 and γ^2 are analogous to radial and axial bucklings. For a system with no internal boundaries in the axial direction, there is a single relaxation length, $\gamma_1^2 = \gamma_2^2 = \gamma^2$.

The general solutions for the fast and thermal radial fluxes are of the form:

$$\theta_1(r) = R_1 + R_2 ,$$
$$\theta_2(r) = S_1 R_1 + S_2 R_2 . \qquad (4.18a,b)$$

We apply the boundary conditions at the external and internal boundaries:

$$\theta_1(R) = 0 = \theta_2(R) , \qquad (4.19a,b)$$

$$\frac{\theta_1(a)}{\theta_1'(a)} = d_1 , \qquad (4.20)$$

$$\frac{\theta_2(a)}{\theta_2'(a)} = d_2 . \qquad (4.21)$$

From these relations, we obtain:

$$S_1 \frac{\frac{X_1}{X_1'} - d_2}{\frac{X_1}{X_1'} - d_1} = S_2 \frac{\frac{X_2}{X_2'} - d_2}{\frac{X_2}{X_2'} - d_1} , \qquad (4.22)$$

where

$$X_1 = J_o(a_1 a) - \frac{J_o(a_1 R)}{Y_o(a_1 R)} Y_o(a_1 a) ,$$
$$X_2 = I_o(a_2 a) - \frac{I_o(a_2 R)}{K_o(a_2 R)} K_o(a_2 a) ; \qquad (4.23a,b)$$

S_1 and S_2, the coupling coefficients,[9] are related through the equation:

$$\frac{S_1}{S_2} = \frac{\frac{1}{L^2} - \nu^2}{\frac{1}{L^2} - \mu^2}, \tag{4.24}$$

and the primes denote differentiation with respect to a.

4.3 APPLICATIONS OF THE TWO-GROUP ANALYSIS

We now consider the usefulness of some of these results. In Eq. 4.22, d_2 can be taken as known from the moderator experiments described in Section 4.1. Other quantities, such as S_1, S_2, X, etc., involve the known values of a, R and the parameters L^2, τ, α which can be calculated or obtained from exponential experiments on unperturbed lattices; μ^2, ν^2 are given by Eqs. 4.13 and

$$\alpha_1^2 = \mu^2 + \gamma^2 ,$$
$$\alpha_2^2 = -\nu^2 + \gamma^2 . \tag{4.25a,b}$$

Thus, if we measure γ^2, the axial buckling in the lattice with the control rod, the other unknown in Eq. 4.22 is d_1 and we can, therefore, determine the fast extrapolation length into the rod. For example, when the control rod contains moderating material, there is a sink for fast neutrons and d_1 is finite and positive.

Further, if we let $d_1 \to d_2 (=d)$, we get, as expected, the result of one-group theory obtained earlier,

$$d_2 = \frac{X_1}{X_1'} = \frac{1}{\alpha_1} \frac{Y_o(\alpha R) J_o(\alpha a) - Y_o(\alpha a) J_o(\alpha R)}{Y_1(\alpha a) J_o(\alpha R) - Y_o(\alpha R) J_1(\alpha a)} . \tag{4.26}$$

A measure of the reactivity worth of the control rod is the change in radial buckling α_1^2 produced by the insertion of the rod in the lattice. We observe that

$$\alpha_{10}^2 = \mu^2 + \gamma_o^2 , \quad \text{without the rod;}$$
$$\alpha_1^2 = \mu^2 + \gamma^2 , \quad \text{with the rod in;} \tag{4.27a,b}$$

whence

$$\Delta a_1^2 = \Delta\gamma^2 \ . \tag{4.28}$$

Thus, Δa_1^2 can be obtained from a measurement of the change in axial buckling produced by the rod in the lattice. This result for Δa_1^2 can be compared with the theoretical results based on two-group theory in a critical reactor (Chapter VI).

The Swedish Reactor Physics Group[2] has utilized the two-group equation,

$$k = \frac{k_o}{(1+\tau B^2)(1+L^2B^2)} \ , \tag{4.29}$$

to obtain a measure of the reactivity effect of a control rod from an exponential assembly. If k_1 and k_2 are the values of the criticality factor before and after the insertion of the control rod, then

$$\frac{\Delta k}{k_1 k_2} = \frac{L^2(1+\tau B^2) + \tau(1+L^2B^2)}{k_o} \ \Delta B^2 \ , \tag{4.30}$$

where

$$B^2 = \tfrac{1}{2}(B_1^2+B_2^2) \ ,$$

$$\Delta B^2 = (B_2^2-B_1^2) \ ,$$

and

$$\Delta k = k_2 - k_1 \ .$$

Special analyses can be developed to apply the exponential experiments to the measurements with partially inserted rods, off-center eccentric rods and a combination of central and off-center rods to study the shadowing effect. However, in these cases, the interpretation of the results is more involved; the exponential assembly is basically unsuited for such studies and can, at most, provide information to supplement control rod studies on critical assemblies.

4.4 THE INTERPRETATION AND VALIDITY OF EXPONENTIAL EXPERIMENTS WITH CONTROL RODS

The usefulness of the control rod experiments in exponential assemblies depends on the extent to which these experiments can be meaningfully interpreted and correlated with similar measurements in critical assemblies. For this, we must examine the basis of the two measurements and investigate the conditions under which such correlation is possible. A control rod introduced in a critical assembly alters the critical buckling and hence the effective multiplication factor; the magnitude of this change is related to the effectiveness of the rod. This buckling change can be directly measured, for instance, by increasing the height of the moderator in the core to restore criticality and relating the change in height to the buckling change.

The major difference in an exponential assembly from a critical system is the negative axial buckling which arises from the balance of neutron production and leakage in the steady state with the deficit being made good from external sources. Since the form of the radial flux distribution is the same in the two cases ($J_o(ar)$), it seems logical to describe the effectiveness of the rod in terms of the change in radial buckling caused by the rod. This is the basis of the steady-state control rod experiments described earlier; the change in radial buckling is obtained by relating it to the change in the inverse relaxation length. The latter affords a suitable parameter for direct measurement because the introduction of the rod in an assembly leaves unaltered the form of the axial distribution ($e^{-\gamma z}$) although the rate of relaxation of the flux changes. This is similar to increasing the height of the core in a critical assembly to restore criticality.

In considering the transformation of the change in axial buckling from an exponential assembly to a full-size reactor, Eq. 4.26 can be used. Consider also the case where the fast flux is flat at the control rod surface; i.e., let $d_1 \to \infty$, so that Eq. 4.22 gives

$$S_1 = S_2 \frac{\frac{X_2}{X_2'} - d_2}{\frac{X_1}{X_1'} - d_2} . \qquad (4.31)$$

A knowledge of d_2 is not needed; it is only necessary to examine how the terms vary with the radius R of the core. The quantities d_1, d_2, a, S_1 and S_2 do not depend on R. The term which is most sensitive to the core radius is X_1/X_1'. The variation of X_2/X_2' is small since ν^2 is relatively insensitive to R. In a first approximation, therefore, we can use one-group theory – i.e., Eq. 4.26 – and investigate X_1/X_1' as a function of μR.

An important question concerns the difference in the neutron energy spectrum in the critical and the exponential cases and the effect due to the conditions at the external boundary. The latter are important because a significant part of the control rod worth arises from the increased outward leakage brought about by the change in flux shape due to the introduction of the rod. The exponential experiments are usually analyzed by the application of bare reactor theory in which a single buckling is assumed and identical boundary conditions are assigned to neutrons of all energies. This treatment is based on the assumption that the flux distribution is completely described by the asymptotic solution of the multigroup equations. Near boundaries, however, the use of infinite-medium kernels is no longer valid and the spectrum changes since the leakage rate of neutrons depends on energy. If the flux shape is changed – as, for instance, by the introduction of a central control rod – the extent of this departure from equilibrium spectrum could also change. This question has been discussed by James and Till[8] who argue that the effect should be negligible. If an exponential assembly is to give information relating to a critical assembly, it must be large enough for the weighted effect of the boundary regions to be very small compared with the region over which the asymptotic flux and spectrum are found. The introduction of the rod should, at most, change slightly this already small effect. The effect should be negligible compared with the major change in asymptotic buckling produced by the rod.

The absorption by the control rod is strongly dependent on neutron energy for most control rod materials; the insertion of the control rod, therefore, changes the neutron spectrum in its vicinity, and there is a resultant change in the multiplying properties of the lattice from the values characteristic of the asymptotic region of the unperturbed lattice. This change represents part of the effectiveness of the rod. In a critical

assembly, the asymptotic region spectrum is regained within a few mean-free paths from the perturbation and if the measurements in the exponential assembly are to correspond to the measurements in the critical system, the same condition must obtain. Hence, a necessary condition for the results of control rod experiments on exponential assemblies to be interpretable in terms of the properties of lattice by simple theory, is that the neutron spectrum which is disturbed in the vicinity of the rod, should regain its equilibrium (asymptotic region) distribution within the bounds of the assembly. This condition sets a limit to the size of the exponential assembly which is suitable for control rod experiments. A simple way to check this condition in an assembly is to examine the distribution of cadmium ratio (ϕ_2/ϕ_1) over the lattice in the unperturbed state and with a control rod along its axis.

References

1. C. N. Watson-Munro, AECL Report CRP-287 (1946).

2. R. Persson, A. B. Atonzenergi (Stockholm) Report AEF 86 (1957); also Geneva (1958), P/160.

3. G. A. Price, TID-7532, p. 150 (1957).

4. P. F. Gast, Geneva Conf. Proc. (1955), Vol. V, p. 389 (1955).

5. R. L. Murray and J. W. Niestlie, Nucleonics, 13, 18 (1955).

6. E. P. Wigner, A. M. Weinberg and R. R. Williamson, U.S. Metallurgical Project Report CR-1461 (1944).

7. D. E. Wood, HW-64866, p. 92 (1960).

8. C. G. James and C. E. Till, Proc. Roy. Soc., Vol. 269, p. 66 (1962).

9. S. Glasstone and M. C. Edlund, The Elements of Nuclear Reactor Theory, D. van Nostrand Company, Inc., New York (1952).

Chapter V

EXPERIMENTAL EQUIPMENT

The design and construction of the equipment and the planning of the experiments were guided by two broad objectives: first, to initiate control rod research with the M.I.T. exponential facility; and second, to start a program of pulsed neutron experiments on subcritical assemblies with emphasis on reactivity studies. The two objectives are, of course, interrelated, because the pulsed source method provides a reliable way to measure the reactivity effect of control rods. Exponential experiments involving the measurement of the material buckling and the microscopic reactor parameters on a variety of lattices have been in progress for some time at the Massachusetts Institute of Technology[1,2,3]. A few modifications were necessary to adapt the subcritical facility for control rod research. The pulsed neutron research program, on the other hand, was started ab initio and the whole experimental equipment was set up with a view to making the pulsed neutron lattice studies a permanent feature of the general lattice research program.

The experimental work described here falls into three areas, each of which depends upon a different arrangement and experimental set-up. The stationary experiments involved the use of the exponential facility with the operating M.I.T. reactor as the neutron source. The preliminary pulsed neutron experiments were made mostly in small moderator assemblies with a Cockcroft-Walton accelerator as the pulsed source. Finally, the main pulsed neutron experiments were undertaken in the subcritical facility with a small, compact sealed tube as the pulsed neutron source. The equipment used in these different areas will be described separately.

5.1 STATIONARY EXPERIMENTS: EQUIPMENT

5.1.1 The M.I.T. Subcritical Facility. The M.I.T. subcritical facility is a cylindrical assembly located in the vicinity of the thermal

column of the M.I.T. reactor. The facility and its peripheral equipment and its use as an exponential assembly for stationary experiments have been described in some detail in Ref. (1). A cross-sectional drawing is shown in Fig. 5.1. Aluminum tanks of 60, 48 and 36 inches internal diameter and 72 inches height can be installed. Into these can be suspended, from adjustable aluminum beams, lattices of uranium rods (metal or oxide) clad in aluminum, of varying rod-radius, spacing, U^{235} concentration and over-all composition. In operation, the tank is filled with heavy water to the desired height. Overflow points at 51.25 inches and at 67.25 inches permit the level to be maintained at the top of fuel rods, either 48 inches or 60 inches long, respectively. In experiments conducted at the overflow level, a more uniform moderator temperature is assured by circulation of the heavy water. The heavy water stays all the time in a nitrogen atmosphere to prevent degradation by atmospheric moisture. A glove box arrangement over a 12-inch-diameter plexiglass cover in the top lid makes possible the installation and experimental changes in the tank without atmospheric contamination of the heavy water. The moderator level at any stage can be read off a sight glass indicator outside the concrete shielding surrounding the whole assembly. The temperature of the moderator, as measured by a platinum resistance thermometer at the tank inlet, is continuously recorded. The outside surface (sides and top) of the lattice tank is covered with 0.020-inch-thick cadmium to provide a black boundary for slow neutrons.

Fast neutrons from a side of the core of the M.I.T. reactor pass through removable lead and cadmium shutters and steel "doors" into a horizontal thermal column; the thermal neutrons then enter a graphite-lined cavity or "hohlraum." After reflection through 90° effectively, they enter the flux-shaping graphite pedestal on which the experimental tank stands with an intermediate aluminum honeycomb structure. The thermal neutron flux at this position is of the order of 10^9 $n/cm^2/sec$. Adequate safety systems are provided through automatic scrams, alarms, and an eccentric diagonal control blade. The tank and graphite region are surrounded by concrete shielding blocks. Outside the shielded room are located the heavy water storage (and dump) tank, the moderator and blanket gas piping, and the control panel.

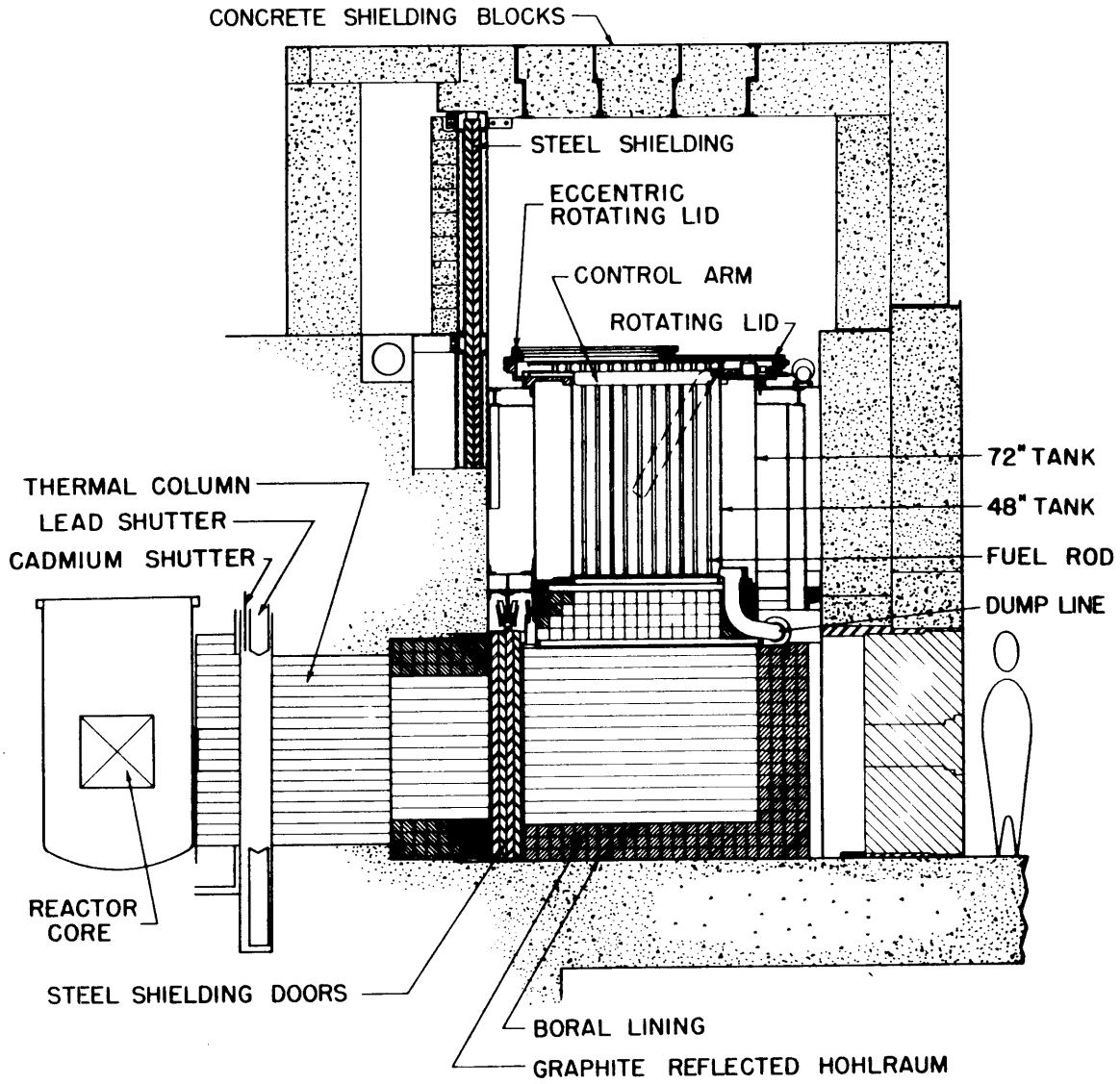

FIG. 5.1 VERTICAL SECTION OF THE SUBCRITICAL ASSEMBLY

5.1.2. Preparation of the Control Rods. The type (shape, size, material composition etc.) of control rod employed in any situation depends upon the purpose and nature of the reactivity that it is to control. In general, among the factors that affect the selection of the control rod material are[4,5] the nuclear properties (the cross-section and its energy dependence, the depletion or "burn-up" rate); physical and mechanical properties (strength, ductility, shock-resistance, vibration and fatique, modulus of elasticity, thermal conductivity); corrosion and wear considerations; resistance to radiation damage; fabricability and metallurgical maneuverability and, finally, cost. The shape and size are to be considered as part of the over-all problem of the particular reactor design.

If – as in the present case – the purpose is research, i.e., to use the control rods for experiments designed to test the methods of measurement of reactivity, the emphasis is on the ability to best interpret the measurements and to provide the type and range of reactivity variation that best serves the purposes and usefulness of the experiment. One of the simplest types, and the one that is most amenable to meaningful interpretation, is a thermally black rod, i.e., one which absorbs all the thermal neutrons incident on it, the reflected current being zero. In this case, the thermal neutron boundary condition is precisely defined and the situation lends itself to a simple theoretical treatment. For a cylindrical assembly, the most appropriate shape of the rods is cylindrical. It would also be desirable to incorporate other features; for example, ease and flexibility in the construction of the rods, which would make it possible to change their response to the epithermal component of the flux.

Metallic cadmium has been one of the most commonly used control rod materials because of its availability, low cost, nuclear stability, good thermal neutron absorption characteristics etc. Especially for low-temperature applications, its low melting point (321°C), and sharp cut-off of neutron absorption (at about 0.4 ev) in the near epithermal energy range make it well-suited. However, its low structural strength makes it necessary to use another stronger metal to support it either by cladding, alloying or mechanical means. Cladding also prevents it from corrosion by the coolant. The absorption cross-section[6] of cadmium for

2200 meters per second neutrons is 2450 barns per atom. Of its several isotopes, Cd^{113} with a cross-section of about 20,000 barns contributes greatest to the absorption; this isotope occurs to the extent of 12.3% in the naturally occurring element.

Considerations such as those above suggested the fabrication of the first set of control rods used in the experiments. These were made by wrapping two layers of 0.020-inch-thick cadmium sheets on Type 6061 aluminum tubes of various diameters. A cross-section of the rods is shown in Fig. 5.2. The aluminum provides the backing, hollow tubular form and structural strength. The thickness of cadmium (i.e., the number of layers of cadmium wrapping) was chosen to ensure complete blackness to thermal neutrons. A convenient criterion for the blackness of a material of microscopic absorption cross-section σ_a is given by Stevens[7] as

$$N\sigma_a t = 2 \tag{5.1}$$

so that the so-called optical thickness is

$$t = \frac{2}{N\sigma_a}$$

Hence, for cadmium, the minimum thickness required for opaqueness (to thermal neutrons) is

$$t = \frac{2 \times 115}{8.6 \times 6.02 \times 10^{23} \times 2210 \times 10^{-24}}$$

$$\approx 0.0192 \text{ cm} = 0.0077 \text{ inch}. \tag{5.2}$$

Thus, the thickness of 0.040 inch provided by the two layers of wrapping is more than adequate for ensuring thermal blackness. The free end of the wrapping was soft-soldered and smoothed so that the rods formed a smooth, clean cylinder. The rods were to be introduced into the heavy water assemblies during runs not exceeding about twelve hours (mostly just one to four hours), and for such short contacts with heavy water, the cadmium does not corrode, provided the rod surface is wiped and dried of heavy water as soon as it is taken out. However, the surface of the rods was covered lengthwise with mylar tape so as to prevent direct contact between cadmium and heavy water.

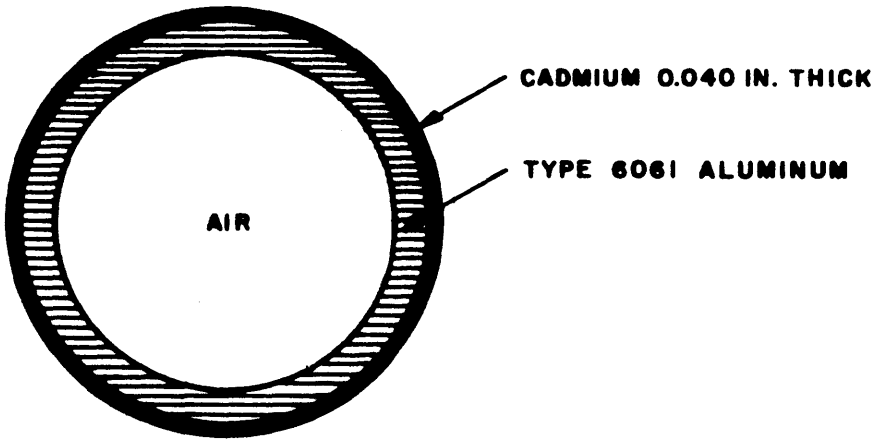

FIG. 5.2 CROSS-SECTIONAL VIEW OF A THERMALLY BLACK CONTROL ROD

A choice existed as to whether the inside of the hollow tubes should be left empty (or filled with a heavy-high z-material) or left to be filled with moderator. In either case, the blackness to thermal neutrons remains unaffected; the difference is in the behavior of the fast flux. In case the tubular control "rod" is empty (or filled with, say, lead), fast neutrons easily pass through the tube and are little affected by the interior of the rod, emerging with the same angular distribution as that with which they entered and without any significant degradation in energy. Analytically, it is equivalent to a solid control rod problem with a net fast neutron current of zero at the surface (flat flux), and the fast neutron extrapolation distance is infinite. If, on the other hand, the rod is filled with moderator, the theoretical analysis of the control rod worth becomes more involved. The moderator material within the control tube effectively serves as a "trap" or sink for fast neutrons; some of the fast neutrons which enter the tube are thermalized and are then stopped by the thermally black control element on the periphery. This results in a substantial increase in the over-all worth of the rod. Such moderator-filled, hollow control rods have been used, for instance, in the MTR[4] (hollow, box-type, rectangular tubes of the absorber material, open at both ends). They can be theoretically treated by the application of diffusion theory to the interior of the rod which constitutes an internal boundary for the fast neutron group.

To provide maximum flexibility in the use of the rods and to simplify the analysis of the experiments, the control rods for these studies were built in such a way as to serve a dual purpose. Each rod was left empty and closed at the bottom end by an aluminum disk which also acts as the supporting guide. At the center of the disk is a 0.250-inch hole that can be closed water-tight by a stopper with a neoprene rubber washer. When the hole is plugged, the hollow inside of the rod is empty. If desired, the stopper can be removed so as to let the moderator (heavy water) from the tank fill the rod. Or, with the bottom end closed, the hollow rod can be filled with any other moderating or control material which is to be investigated. Thus, the same rods can be employed for the composite control rod type experiments suggested in Chapter VIII. Not all such experiments were undertaken in the present work.

When the rods are empty, their placement in the moderator tends to make them float, and it is necessary to provide an arrangement with top and bottom positioners to keep them fixed along the axis against the lateral and upward thrust of the liquid moderator. For experiments in the pure moderator tank (no fuel rods), a cross-shaped aluminum structure with a "cup" at the center was located in the tank as shown in Fig. 5.3, so that the disks attached to the bottom of each rod could sit snugly in this cup. At the top, each rod was fixed with a pin which could fit in a slot made in an aluminum beam spanning the top of the tank.

The positioning of the control rod in the lattice was more problematic as the rod would have to displace several fuel elements. A special plastic adapter shown in Fig. 5.4 was machined for this purpose. This rectangular adapter was installed at the top of the girders from which the fuel elements were hung. Holes and slots, especially milled in the plastic adapter for the lattice with 1.75-inch spacing, provided for the correct placement of the central-region fuel elements. A central circular disk which carried the central fuel rod and the six symmetrically surrounding fuel rods was removed and the control rod could be introduced through this 4-inch-diameter hole. The bottom of the control rods could rest in a "cup" at the base of the lattice while the top of the rods was attached to pins which kept them fixed to the plastic adapter. The removal and insertion of the fuel and control rods was effected through the glove box.

It was also possible to remove just the central fuel element and open a small (1.25-inch-diameter) circular hole around it in the plastic adapter, so that a 1.25-inch O.D. aluminum thimble could be fixed along the central axis of the lattice. This thimble was used to run a small BF_3 detector axially during some of the pulsed neutron runs with the lattice.

5.1.3 The Stationary Flux Mapping Equipment. The stationary flux was measured by means of the integral foil method with the foils located in the moderator region. Gold was chosen as the foil material because of its good activation characteristics and easy availability in highly pure metallic form. The foils were placed in specially milled slots in

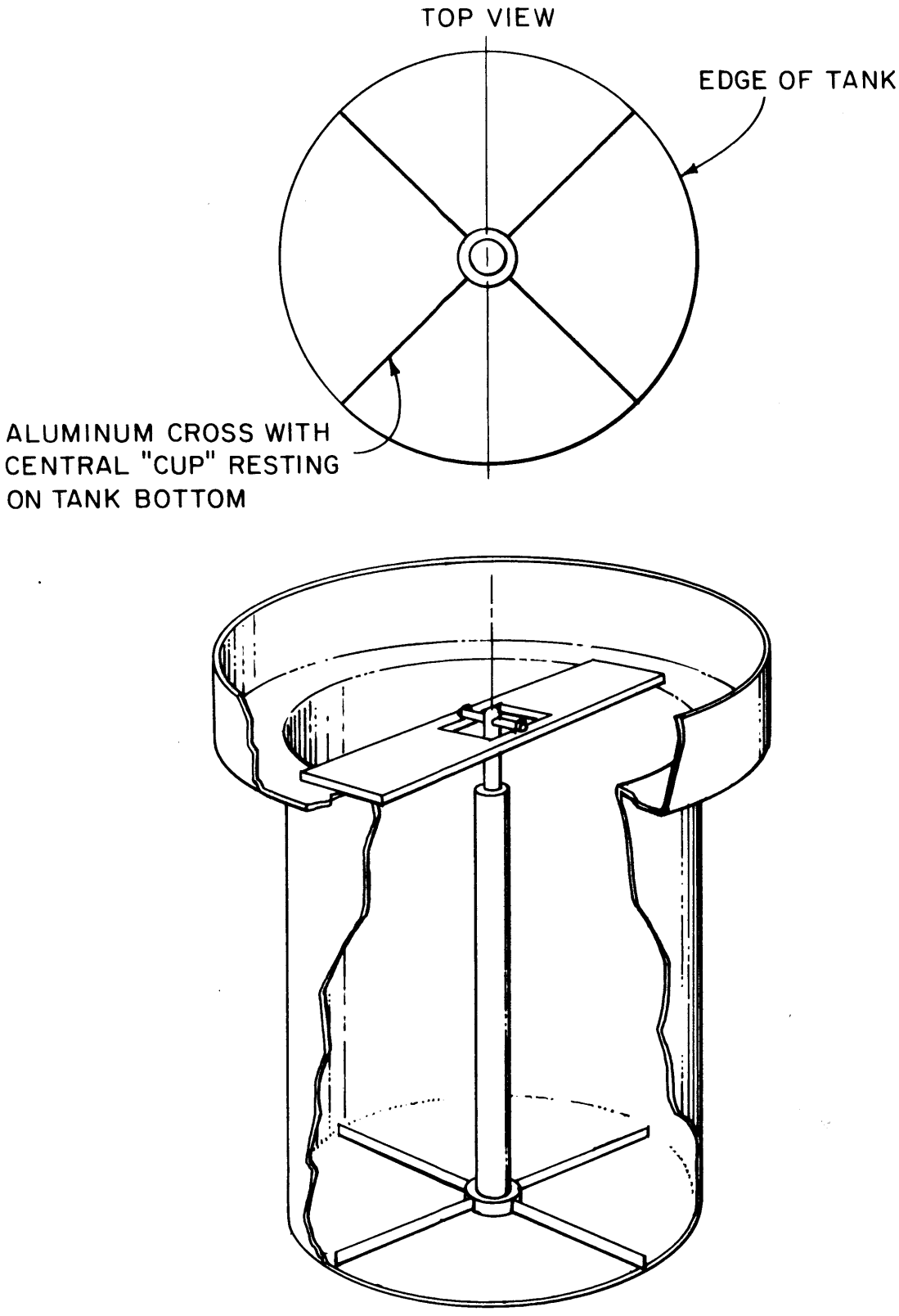

FIG. 5.3 ARRANGEMENT FOR POSITIONING THE CONTROL ROD ALONG THE AXIS IN PURE MODERATOR TANK.

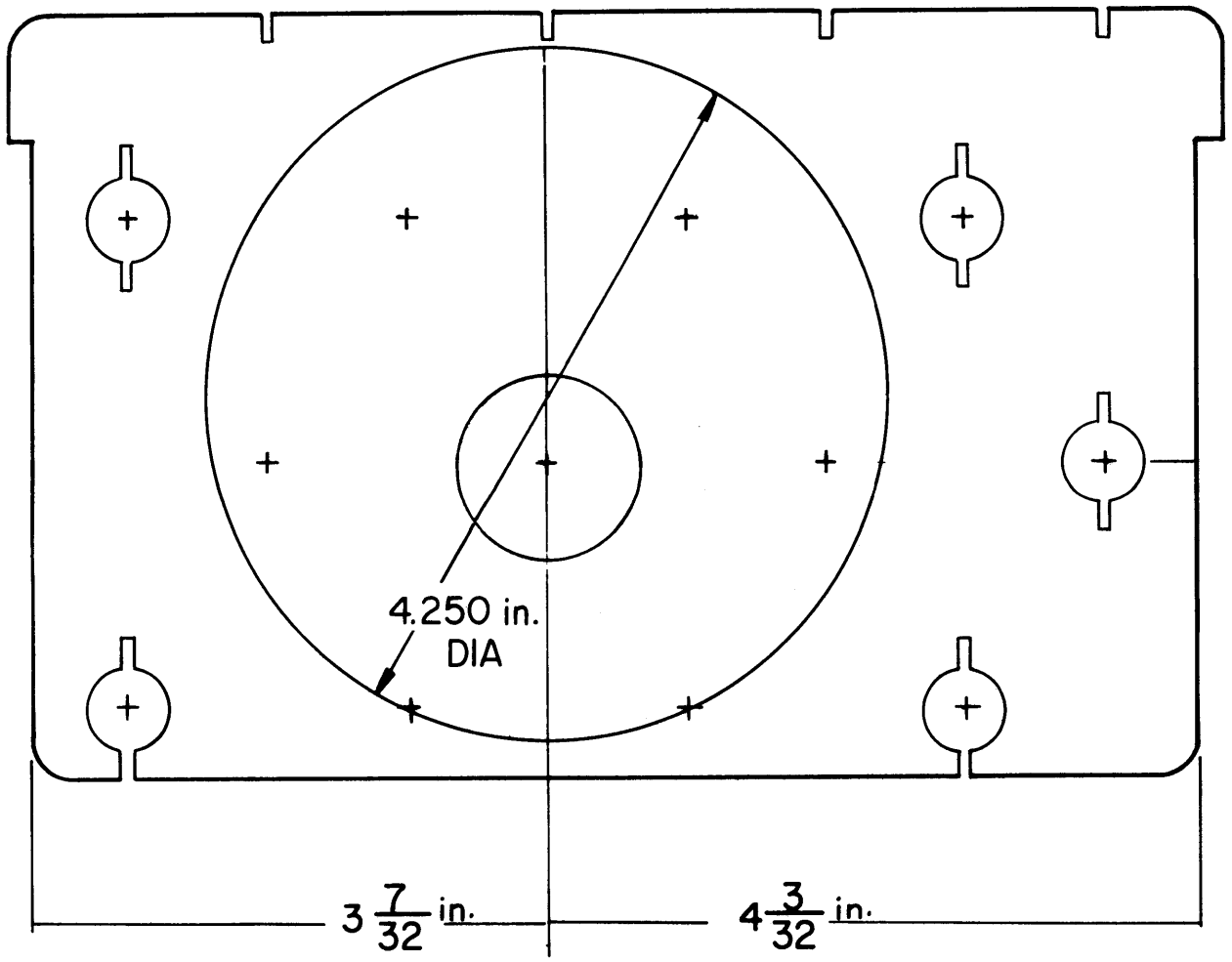

FIG. 5.4 TOP PLASTIC ADAPTER FOR CONTROL ROD AND PULSED NEUTRON RUNS WITH THE LATTICE

aluminum foil holders which could be positioned at the desired region in the assembly in the axial or radial direction. For mapping the epithermal flux, the gold foils were enclosed in cadmium boxes and attached to aluminum foil holders for irradiation.

The data concerning the activation of the detector foils was obtained by counting the induced gamma-ray activity. Beta counting was not used because most of the beta activity detected comes from the foil surface, making it difficult to correct for the weight of the foil. Moreover, even slight imperfections on the foil surface, such as scratches, increase the surface area of the foil and lead to spurious results.

A block diagram of the gamma-counting system is shown in Fig. 5.5. The 1-1/2-inch-diameter, thallium-activated, sodium iodide crystal used in the scintillation counter had an energy resolution of 10 per cent. The detector foils, during counting, are located opposite the face of the crystal housing. The pulses from the photomultiplier – an RCA-6342A – were amplified with a nonoverloading linear amplifier and fed through a differential pulse height selector to a decade scaler whose output was automatically printed on tape. This system was coupled with a Nuclear Chicago automatic sample changer – Model C-110B – to permit the automatic counting of a large number of foils. The resolving time of the electronic equipment was measured by the two-source method to be 0.15 microseconds. The activated gold foils were counted by setting the gamma-counting system to straddle the 411-kev Au^{198} gamma-ray peak with a window width of 60 kev.

The scintillation system was recalibrated each time it was used. Periodic checks for drift were made during the counting of each run; background counts were taken at frequent intervals.

5.2 EQUIPMENT FOR PRELIMINARY PULSED NEUTRON WORK

The initial pulsed neutron work, preparatory to arrangements for setting up the pulsing system with the subcritical facility, was done at a different site where a "target room" was constructed with shielding provided by 19 inches of borated water (5-gallon cans) and 8 inches of dense concrete on the sides and 28 inches of borated water on the roof. A positive ion accelerator had been set up on this site for other studies.

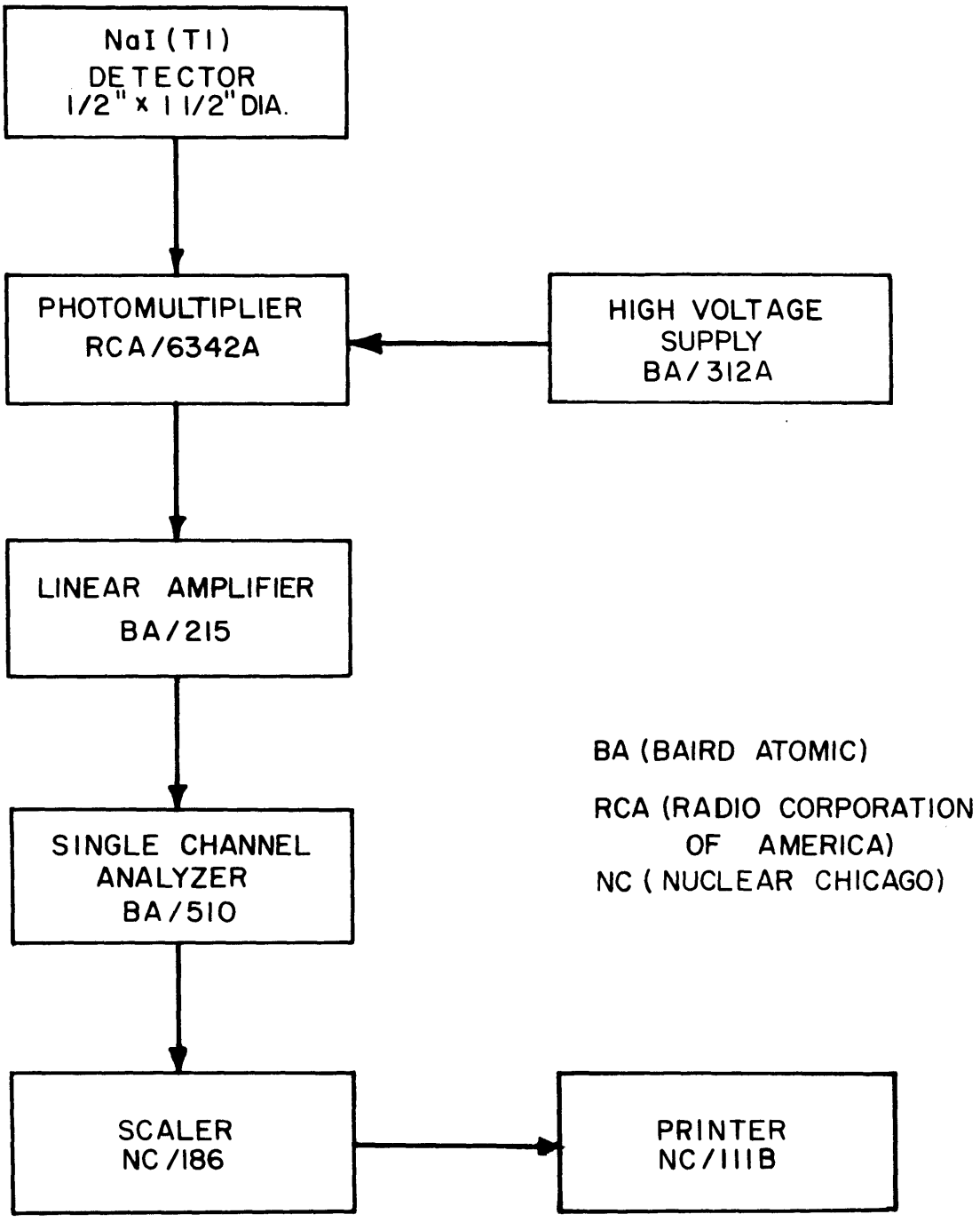

FIG.5.5 BLOCK DIAGRAM OF GAMMA COUNTING SYSTEM

The objective for the use of this equipment was to check out possible instrumentation and to provide guidelines and experience for the main pulsed neutron experiments with the exponential assembly. Some work on heavy water assemblies was also undertaken. This equipment will be described here only briefly; some of the component parts will be described in greater detail in the following sections of this chapter.

The pulsed neutron source was a 150-kev transformer rectifier set of Cockcroft-Walton type built by the Texas Nuclear Corporation and equipped to generate neutrons by the (D,D) and (D,T) reactions; this accelerator has been described in detail in Ref. (8). The pulsing is achieved by a reference signal which triggers a square-wave generator and pulses the deflection voltage. The pulse widths are continuously variable from 1 microsecond to 10^4 microseconds and the repetition rates from 10 pulses per second to the point where pulses begin to overlap. The target of the accelerator was located at the bottom center of the cylindrical test assemblies in most of the experiments. These assemblies were jars of glass or aluminum of diameters varying from 15.5 cm to 43.8 cm, filled with 99.75% heavy water to heights of 17.8 cm to 48.3 cm, thus providing a buckling range of 140 m^{-2} to 855 m^{-2}. The outer surface of the assemblies was covered with 0.020-inch-thick cadmium sheets to provide a slow neutron boundary condition. The heavy water was transferred from the storage vessel to the test assembly in a nitrogen atmosphere to prevent degradation, and the assembly was then closed with plastic, leak-tight covers so that the heavy water remained in a nitrogen atmosphere throughout.

The fast neutrons from the source are thermalized in the assembly and the thermal flux emerging from the assembly is detected by a 5-inch-diameter, Li^6-ZnS plastic fluor mounted on a Dumont 6364 photomultiplier tube. The detector is surrounded on the sides by a 0.020-inch-thick cadmium sheet and is mounted on the axis of the assembly so as to be exposed to a 5-inch circular window cut in the cadmium cover on the top of the assembly. The time analysis of the thermal flux is done by a TMC 256 channel analyzer with a Type 212 pulsed neutron plug-in unit.

The over-all experimental set-up is shown in Fig. 5.6. Figure 5.7 shows a block diagram of the electronic circuit. The primary signal

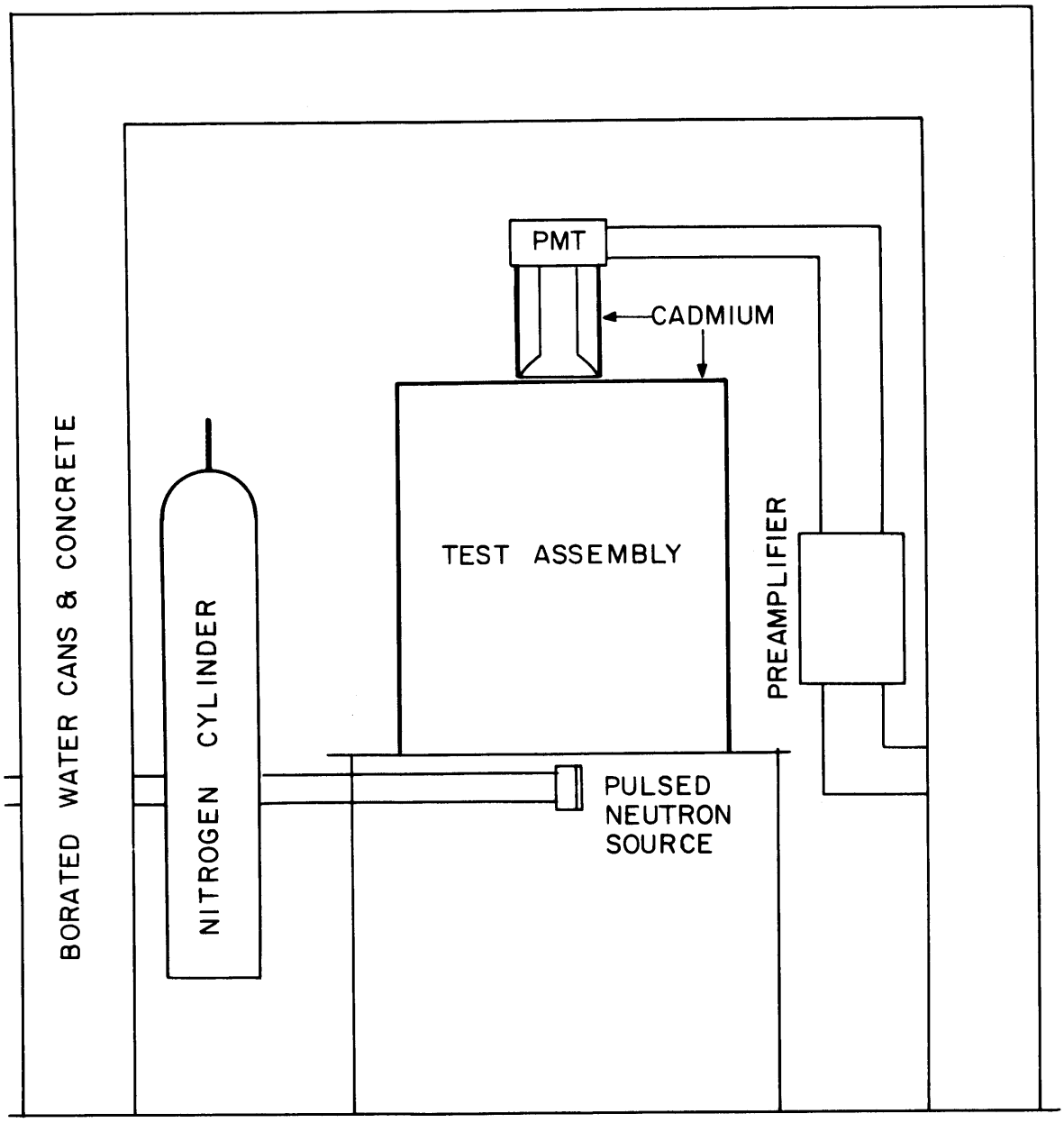

FIG. 5.6 ARRANGEMENT FOR PULSED NEUTRON EXPERIMENTS ON SMALL ASSEMBLIES

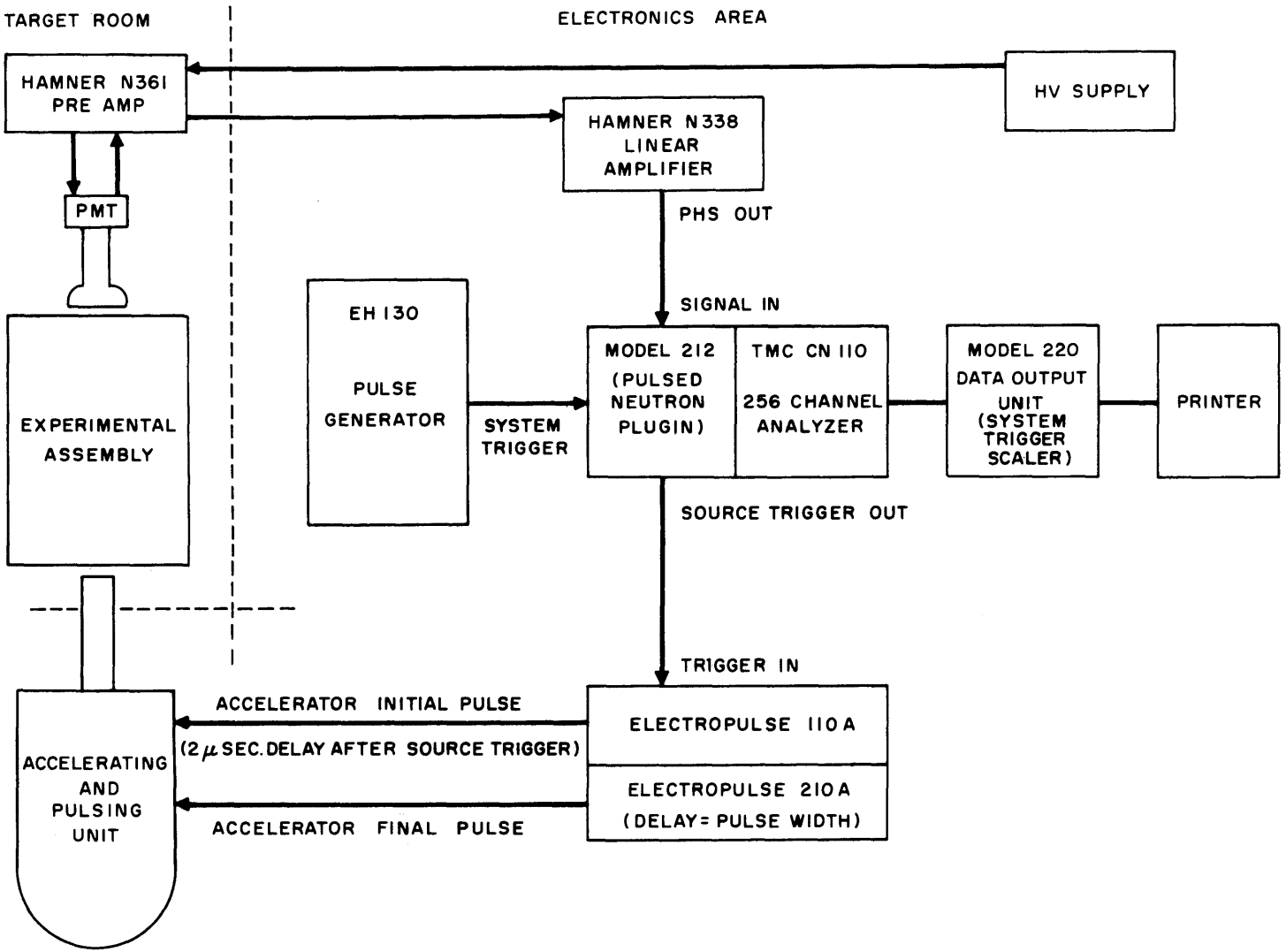

FIG. 5.7 OVERALL CIRCUITRY FOR PULSED NEUTRON EXPERIMENTS WITH TNC ACCELERATOR

from an external pulse generator (EH 130) sets the repetition frequency and triggers the timing cycle of the TMC analyzer, which then accumulates the pre-burst background for a time interval $b\Delta t$ (the channel width is Δt). At the end of this interval, a reference pulse is sent to the accelerator to produce a neutron burst, and after a waiting time of $d\Delta t$ (variable), the time-dependent signal from the detector is received in the successive channels. The background ratio b and the delay multiplier d can be varied in multiples of 2.

5.3 SUBCRITICAL PULSED NEUTRON EQUIPMENT

An important phase of the present program was to bring into operation a complete pulsed neutron system for use with the subcritical facility and to decide upon the type of component parts best suited for this program, taking into consideration the limitations imposed by the proximity of the operating M.I.T. reactor, the immobility of the exponential assembly and the restricted conditions caused by the heavy shielding and other surrounding equipment. It was also necessary to investigate the special problems created by any interaction between the transients caused by pulsing the lattice and the operation of the reactor (which was later found to be nil), the level of neutron and gamma-ray background etc., and to lay down the operating conditions for performing the pulsed neutron runs on the subcritical assembly. The factors affecting the choice of the different components of the pulsed neutron system and the final equipment will be described in some detail in this section.

5.3.1 The Experimental Assembly. The experimental assembly for subcritical pulsed neutron work can be an operating reactor which has been made subcritical by some means[9,10], a critical assembly, an exponential facility or an *ad hoc* subcritical assembly, independently erected exclusively for pulsed neutron work. A desirable requirement is flexibility and the freedom for several alternative locations for the source and the detector. An operating reactor and, to some degree, a critical assembly are always encumbered by heavy shielding, associated channels, safety systems and other extraneous equipment. An exponential assembly fed by the thermal column of a reactor has, in addition, the problems of a

large neutron and gamma-ray background, and it may be possible to use it for pulsed work only during reactor shutdown. An exponential pile with a removable artificial neutron source or an independent subcritical facility provide the best experimental assembly for pulsed neutron work.

The assembly used in these experiments was the exponential facility of the M.I.T. reactor, described in section 5.1.1. For pulsed neutron work, the assembly was isolated from its reactor environment by closing off the steel doors and the lead shutter, blocking it off from the neutron flux from the reactor core. Even then, the neutron background during reactor operation was high enough to cause appreciable pulse pile-up with a medium-sized BF_3 detector. With a very small BF_3 counter (0.5 inch × 4 inches) placed inside the assembly along its axis, the pulsed neutron source did contribute a noticeable exponential decay even during reactor operation, but the background was high enough so that the decay could not be monitored over more than two decades. The M.I.T. reactor operates on a 24-hour weekday basis and it was decided to make the pulsed neutron runs during reactor shutdown, during week ends. It was found that there was no effect of the transients and of pulser operation upon the reactor safety system. The 36-inch-diameter exponential tank was in place at the time of the pulsed neutron runs and its side and top were covered with 0.020-inch-thick cadmium. A circular cadmium plate, 0.020 inch thick and clad in aluminum, was used to cover the bottom face; during each pulsed neutron run, this plate was introduced so as to lie at the bottom of the tank. Thus the whole assembly was surrounded by cadmium to reduce room-return background and to define the slow neutron boundary condition, basic to the definition of the geometrical buckling eigen value. In some experiments, a 1.25-inch-O.D. aluminum thimble was installed on the axis and fixed to a girder or plastic adapter, as discussed in section 5.1.2. A small BF_3 counter could move in it for some of the measurements.

5.3.2. The Pulsed Neutron Source. In pulsed neutron applications, the source is almost always the target of a positive ion accelerator, specifically optimized for one of two nuclear reactions involving the isotopes of hydrogen – the $T(d,n)He^4$ reaction (14-mev neutrons) or the $D(d,n)He^3$

reaction (2.5-mev neutrons); these reactions occur with a fairly low bombardment energy and are prolific in the production of neutrons; the reaction cross-section peaks around 100 kev, permitting the use of reasonably inexpensive low-voltage particle accelerators. Other reactions that have been employed, at high energies, are the $Be^9(d,n)B^{10}$ or $Be^9(\alpha,n)C^{12}$ reactions and the (γ,n) reaction; in the latter case, the photoneutrons are produced by brehmsstrahlung from a betatron or electron linear accelerator striking a heavy metal target (W or U or Pb). The accelerator types in common use are Cockcroft-Walton, Van de Graaf, Linac, or a small sealed tube. An example of a non-accelerator type of pulsed neutron source is the Oak Ridge pulsed reactor core with a chopped thermal neutron beam from another reactor core[11].

Although the pulsed neutron sources of the customary type can be adapted to most of the situations encountered in a wide variety of experimental programs, special features may be desirable or even necessary, depending upon the type of experiments, the level of precision and practical considerations. Thus, in time-of-flight studies, the paramount considerations are neutron intensity, short pulse width and high repetition rates; for fast neutron spectroscopy and the standard type of pulsed neutron experiments on highly enriched uranium systems, very short pulses – of the order of nanoseconds, owing to the short decay times of these systems – and high repetition frequencies are necessary[12]; for pulsed neutron time-dependent studies in the slowing-down and thermalization region, short pulse widths have to be combined with low repetition rates, with duty cycles of the order of 0.01%[8].

Pulsed neutron sources for reactor or subcritical work are comparatively less demanding in these respects. Desirable are high neutron output and small size, since it is usually necessary to pass channels through thick shields under rather congested room conditions. The pulse widths are of the order of a few microseconds; the repetition frequency must be low – as can be seen from Eq. 3.4 – so as to maintain a reasonably good signal-noise (background) ratio. On the other hand, the repetition rate R for applications to reactivity measurements (as in section 3.6.3) must be such that $\alpha > R > \omega$, where ω is the decay constant of the shortest lived precursor. For U^{235}-fueled thermal systems,

$\omega \approx 4.7$ sec^{-1} and it turns out that R must be at least 10. The upper limit is dictated by the degree of subcriticality and other factors as indicated by Eq. 3.4. Since the size of the reactor or the subcritical assembly is relatively large usually and an appreciable background neutron source is always present from previous assembly use (especially photoneutron sources in Be and D_2O systems) and since the repetition rates are to be comparatively low, the neutron output of the source must be high — usually of the order of 10^6 to 10^7 neutrons per burst — if the run times are not to be impracticably large; it should, however, not exceed about 10^{10} n/sec, as this will cause too high counting rates and the corresponding counting losses and multiple pulse pile-up.

Positive ion accelerator neutron sources basically consist of an ion source, an evacuated accelerating section, focusing optics, a pulsing mechanism and a target onto which the ions impinge to generate neutrons. Deuterium gas flows into the ion source where it is ionized in one of several ways; the most common methods are the application of R.F. fields, axial force fields as in the Penning Ion Source (PIG) or magnetic mirrors as in the duo-plasmatron system of ion excitation. The ions are extracted into the accelerating column and, after acceleration, enter the drift tube, which has the target at its other end. The ion source beam operates at a pressure of about a hundred times greater than what is desirable for the long accelerating tube. Consequently, some of the gas is left unionized and leaks into the accelerating chamber along with the useful ions. Hence, if the ions are to travel to the target with a minimum loss of energy by collision, the amount of the unionized gas must be reduced by the use of a vacuum pump.

In recent years, a new category of small ion accelerators[13,14,15,16] (sealed tubes) has been developed which eliminates the need for this differential pressure and permits the realization of a sealed-off neutron source based on the (D,T) reaction. The acceleration is in one stage and, owing to the extremely short accelerating section, the entire tube can be operated at a uniform pressure. These tubes offer considerable saving in complexity and size, are portable, and safe to handle; large ion source apertures and correspondingly large ion currents make it possible to achieve high neutron output rates. Very high rates of output for

microsecond pulse durations are possible and the output is continuously variable. Such small, compact, lightweight, portable tubes encased in appropriate containers are well-suited for use with reactors and subcritical assemblies where mobility and flexibility under rather stringent conditions imposed by shielding etc. are important considerations. Such sealed tubes are made commercially by Elliott Brothers of England; Norelco Phillips of Holland; and Kaman Aircraft Company, Nuclear Division, of Colorado Springs, Colorado, U.S.A.

The availability of a Cockcroft-Walton type machine at the M.I.T. reactor for other pulsed neutron studies prompted a detailed consideration[17] of the feasibility and design of its use with the subcritical facility. Several possible configurations were considered: addition of a long beam tube to the accelerator and its introduction through an opening in the concrete shielding so as to locate the target on the side of the tank; positioning the accelerator on the top of the concrete shielding blocks for vertical operation so as to have the target at the top-center of the tank etc. Apart from the practical difficulties involved in such arrangements, an estimate of the neutron intensity requirements all but ruled out the use of this machine with the subcritical facility. This Texas Nuclear Corporation machine is built with considerable versatility and flexibility in pulse widths, repetition rates etc. but at the cost of mobility, ruggedness of movement and operation and, to some extent, the neutron output.

It was therefore decided to procure a small, compact sealed tube for subcritical pulsed neutron work and to build a system of pulse-forming networks and associated equipment for use in conjunction with the sealed discharge type source tubes that are available. We are indebted to Dr. D. R. Bach of K.A.P.L. for communicating his experience with an Elliott K-tube and for forwarding the circuit diagram for the HV modulator. The final pulse-forming networks were designed and constructed by Mr. D. Gwinn of the MITR Electronics shop staff. Among the sealed discharge tubes commercially available, the K-tube, built by Elliott Brothers of England, was first considered. Finally, however, a Kaman Nuclear tube was brought into active use.

This source is a Type A-810 neutron generator built by Kaman

Nuclear of Colorado. The basic elements of this tube are shown in Fig. 5.8. The ion source, which is of the Penning cold cathode type, produces ions of heavy hydrogen isotopes; these, upon emerging from the source aperture, are accelerated in the direction of the titanium target at the right. The tube is filled with a mixture of deuterium and tritium, providing for the (D,T) reaction. The tritiated titanium target has an effective diameter of one inch and is located one inch from the lower end of the accelerator tube package. The target is so shaped and dimensioned as to secure complete coverage by the ion-beam, permitting optimization of target loading. Since gas clean-up in the discharge would quickly exhaust the supply of deuterium gas originally in the tube, a replenisher of zirconium wire spiraled around a tungsten wire is mounted behind the ion source. Zirconium absorbs hydrogen and releases it when heated. Before the tube is sealed off, the zirconium wire is saturated with deuterium. By varying the voltage across the zirconium filament, it is easy to adjust the pressure inside the tube; the pressure then remains constant for long periods of time. The replenishment process is reversible and therefore lengthens the life and ease of operation of the tube. The ion source, accelerating system, target and the replenisher are all contained in a high strength, hermetically sealed, tubular glass envelope filled with a 50-50 mixture of deuterium and tritium; ceramic annular ring-magnets encircle the left two inches of the tube exterior over the ion source. The whole tube is mounted in an aluminum cylindrical enclosure (11 inches X 5 inches diameter) filled with dried Shell Oil Company Diala-AX insulating oil. The tube contains 5 curies of tritium. The finished tube, its housing and connections are shown in Fig. 5.9.

The target pulse of negative accelerating potential variable between 0 and 120 kv is obtained from a Carad Corporation step-up (1:25) pulse transformer; the shielded, flexible, high-voltage cable (Times Wire and Cable Company, Inc., Jan Type RG-19/U-04145) from the transformer to the source-tube is about 5 feet long. The accelerator assembly and the transformer are located in the shielded lattice room at the top of the exponential assembly, while the entire control unit is placed on the reactor floor about 18 feet below. The control unit supplies pulse voltages for the neutron tube ion source and for the step-up pulse transformer to the

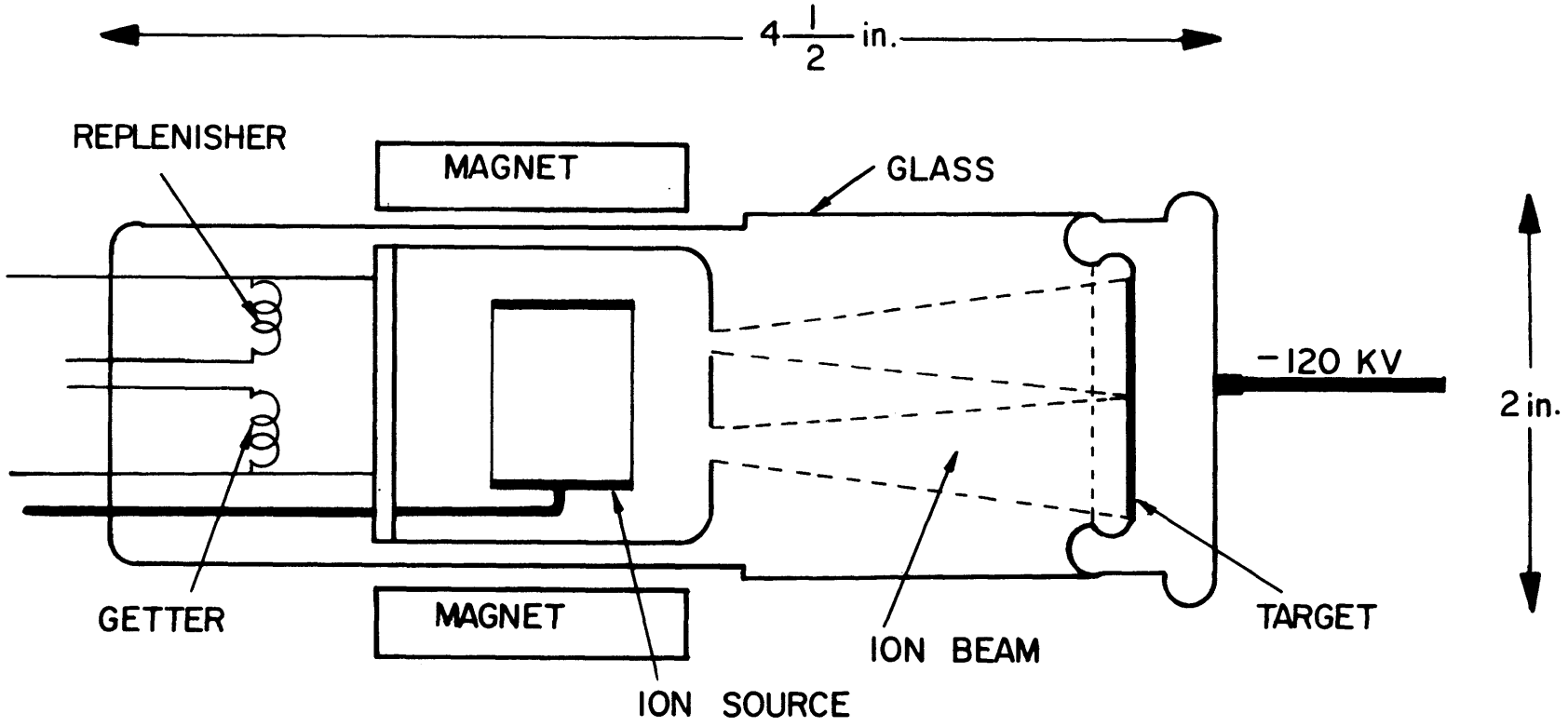

FIG. 5.8 ELEMENTS OF THE SEALED NEUTRON TUBE

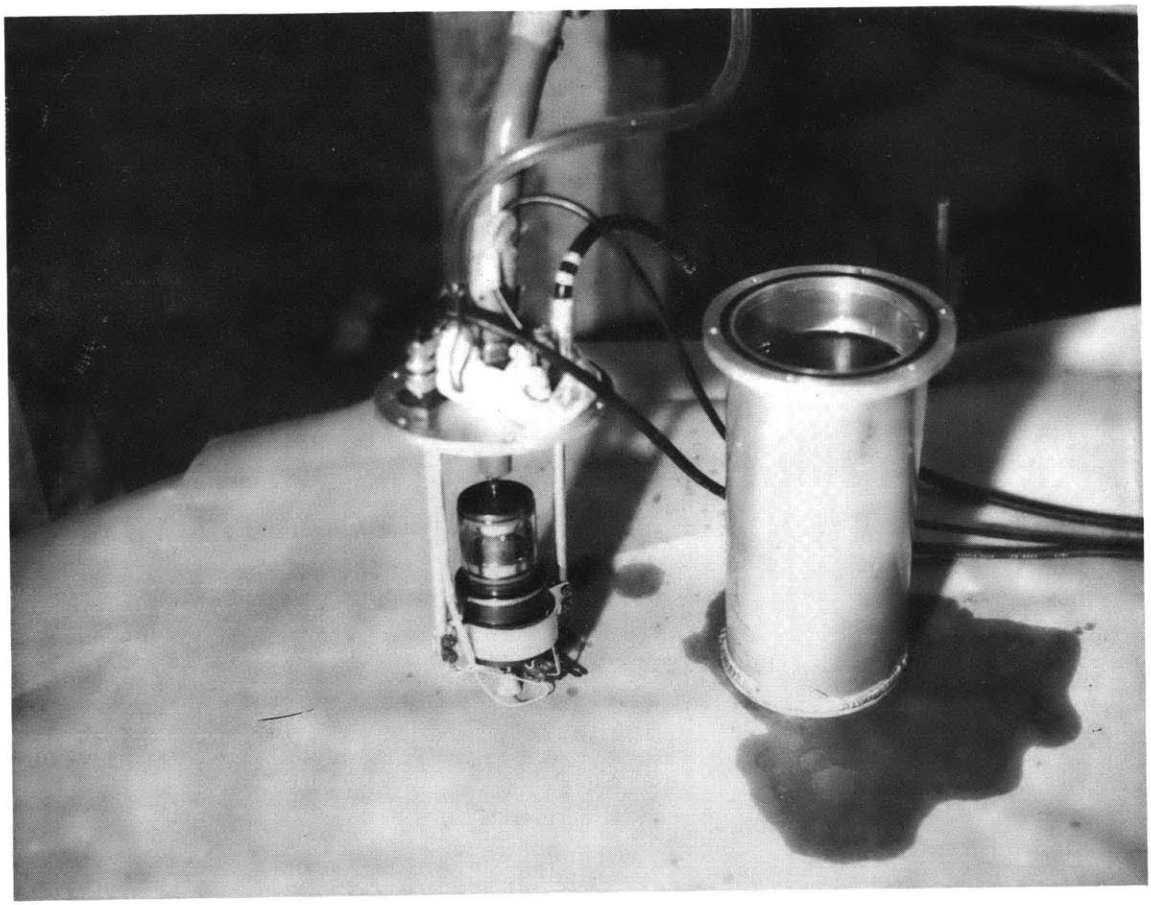

Fig. 5.9 Pulsed Neutron Source, Accelerator Tube

target. The control unit is versatile and can also be used with other types of tubes. It has three independent networks to generate a target pulse, a plasma pulse and a magnetic field pulse (not needed for the Kaman tube); a timer circuit fires the pulse networks at prescribed delays relative to each other. The pulse rate is variable from 1 pps to 10 pps while the pulse width at half amplitude (shape triangular or approximately Gaussian on a time scale) can be made approximately 9, 12 or 15 microseconds. The yield is estimated to be about 10^7 neutrons per burst, having an energy of 14.7 mev.

5.3.3 The Detection System. The thermal neutrons which comprise the asymptotic neutron spectrum after the stabilization of the flux in a pulsed assembly have to be processed through an appropriate detection system before being fed into the time analyzer. Several factors dictate the choice of the detector in a pulsed subcritical assembly. There is appreciable gamma-ray background from fission products and, unless some type of compensating mechanism is employed, the detector itself must be either insensitive to gamma rays or the ionizing radiation on which it is based must result in a large energy release so that the gammas can be discriminated against. The repetition rate has to be kept low but the source intensity is high; the latter may give rise to pulse pile-up effects leading to the spurious decay of multiple pulses. On the other hand, to achieve good statistics in a reasonable time, the over-all efficiency and the thermal neutron sensitivity must be high. A desirable feature which is met, in practice, by most detectors is that the detector scatter very few neutrons back into the experimental assembly. The size of the detector is also sometimes an important consideration. If the detector is to be located inside the assembly – as is usually the case at least for a few runs, to check the detector location dependence of the neutron decay – the detector must be small, compact, flexible and easily movable. If the detector is to be located outside, its shape and size may have to be determined by the conditions needed to suppress spatial harmonics. Another factor is the dead time of the system; the neutron counter must have a time response consistent with the minimum channel widths which are to be used.

If the detector is to be stationed outside the assembly only, a scintillation fluor with a neutron interacting "nuclear host" material imbedded in the crystal in conjunction with a photomultiplier tube provides a fast detection system with a good enough efficiency although discrimination against gamma rays is a problem. The latter can be avoided by the use of a phosphor like ZnS(Ag) (with a Li or uranium compound) which has a large "alpha-beta ratio"[18], provided the pile-up of the gamma pulses may be neglected. Noble gas scintillation counters have a very low dead time and are quite insensitive to gamma radiation. Another possibility is to use loaded plastic or liquid scintillators whenever feasible. Erickson et al.[19] have described the use of a DuMont 6292 photomultiplier with a borated cathode; such neutron detectors have now been made commercially available and have been used by Simmons and King[20] for pulsed neutron experiments on the KAPL FP4 reactor. The α-particles from the $B^{10}(n,\alpha)Li^{7}$ reaction enter the Cs-Sb photocathode layer and produce electron emission directly. This counter has a high neutron sensitivity and an extremely low dead time. Other scintillation detectors that have been used for subcritical pulsed neutron work include a $Li^{6}I(Eu)$ crystal with a CBS-7817 photomultiplier tube[21,22].

However, when the intent is to allow flexibility so that neutron detection can also be done inside the assembly – as in the present case – the large-sized scintillators with phototubes are unsuitable. Perhaps the best compromise is represented by detectors based on the (n,α) reaction or the fission reaction, in each of which the energy release per reaction is quite large. Fission chambers are well suited for high temperature work. The $B^{10}(n,\alpha)$ reaction, because of its high cross-section, simple energy dependence over a wide range, high specific ionization and the large energy of the resultant charged particles, provides a good basis for thermal neutron detection, for example, in the form of boron-trifluoride-filled gaseous detectors. Ordinarily, BF_3 counters are insensitive to gamma radiation, and the thermal neutron sensitivity can be increased by enriching the boron in the B^{10} isotope and increasing the pressure of the filling gas. Their main disadvantage is that they are quite slow. However, the count rates in our assemblies were expected

to be relatively low; this fact, together with the commercial availability of BF_3 proportional counters in a variety of sizes, prompted the decision to use this type of detector in the present studies.

The size, shape, location and configuration of the detector and the nature of its coupling with the experimental assembly are determined by considerations of neutron intensity, harmonics suppression, perturbation effects and practical feasibility. It is desirable to provide some flexibility so as to ensure the constancy of the measured decay constant with respect to the nature and location of the detector. The source was to be located, in most runs, on the axis of the cylindrical assembly, so that the harmonic modes having radial nodal planes through the axis were not excited for reasons of symmetry. It was attempted to manipulate the axial harmonics by using long BF_3 counters and positioning them in such a way as to span a large part of the fundamental mode while at the same time integrating out (annulling) the other harmonics after the manner sketched in Fig. 5.10. Since the source was located on the top-center of the assembly and the bottom was inaccessible because of the presence of the pedestal, shielding etc., only two alternative ways were open for locating the detector: either the inside of the tank, or outside, along the lateral periphery. Several detector arrangements were investigated. The first consisted in stacking longitudinally a bank of eight long (25 inches $\times$ 2 inches) BF_3 counters along the side of the experimental tank with the height and position adjusted in such a way that the unwanted axial harmonics are integrated out, and yet a profitably large portion of the fundamental is spanned (Fig. 5.10). The counters were housed in an aluminum box which was mounted so as to be exposed to an 18-inch $\times$ 20-inch window cut in the cadmium covering of the tank; the outside of the box was covered with cadmium. The counters were individually covered with thin plastic so as to insulate them from the tank-ground; the signal from the individual detectors was summed before being fed into the pre-amplifier. However, such a bank proved to be too sensitive and considerable pulse pile-up could be observed on the oscilloscope. This bank was therefore replaced by a single, long BF_3 tube similarly positioned with respect to harmonics in the tank.

It was desirable to have an alternative detection system for two

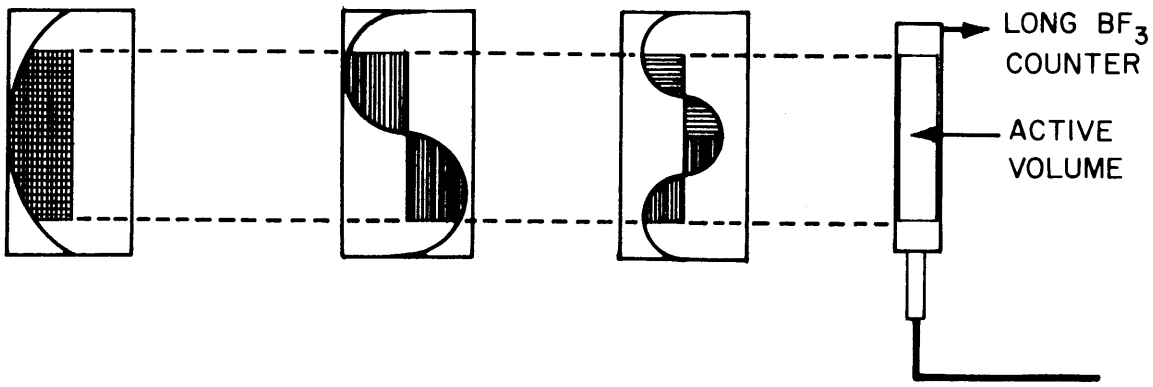

FIG. 5.10 USE OF LONG BF_3 COUNTERS TO SUPPRESS THE UNWANTED AXIAL HARMONICS

reasons. First, two different detection arrangements provide an independent check of the measured decay constant, ensuring that the latter decidedly pertains to the fundamental mode and is uniquely characteristic of the experimental assembly. Second, the above arrangement is unsuitable for those runs in which the level of heavy water – and hence the size of the assembly – is changed, as was necessary in some cases. In another arrangement, a channel was installed on the external side of the tank so that a small BF_3 tube (0.5 inch × 4 inches) could be moved inside it. However, the neutron detection efficiency was found to be inadequate and this arrangement was unsatisfactory for the source intensity available. Finally, a 1-inch-I.D. aluminum thimble was fixed along the axis of the cylindrical assembly and the small BF_3 counter was run inside it. This arrangement proved to be highly satisfactory, giving flexibility, good detection efficiency, harmonics examination etc.; it also made possible the study of introducing such perturbations in the assembly.

Thus, two detection systems were finally provided; these are shown in Fig. 5.11. The long BF_3 counter (N. Wood Model G-20-20, active volume 20 inches × 2 inches diameter, B^{10} enrichment 96%, filling pressure 40 cms Hg) was mounted on the side of the tank so as to be exposed to a narrow slot in the cadmium surrounding the tank and covered on the outer side with cadmium. This detector was used with an RIDL (Model 31-7) pre-amplifier located about three feet from it. The other arrangement employed a small BF_3 tube (N. Wood model, 0.50-inch diameter, 4.0-inch active length, 40 cms Hg filling pressure, B^{10} enrichment 96%) guided by a thin aluminum thimble (1.25-inch O.D.) mounted along the axis of the tank. The BF_3 tube was covered with thin plastic to insulate it from the thimble and tank. A 7-foot-long cable, well shielded with braided wire, passed through an airtight stopper plugged in a hole on the upper side of the tank and connected the detector to a pre-amplifier placed just outside the tank; the pre-amplifier was also insulated from tank-ground by thin plastic. A schematic diagram of this pre-amplifier is included in Fig. 5.12. The amplifier-scaler (RIDL Models 30-19 and 49-30) and the high-voltage supply (RIDL Model 40-9) were located on the reactor floor 18 feet below. The pulses from the detector were monitored on an oscilloscope. The dead time of the detection systems

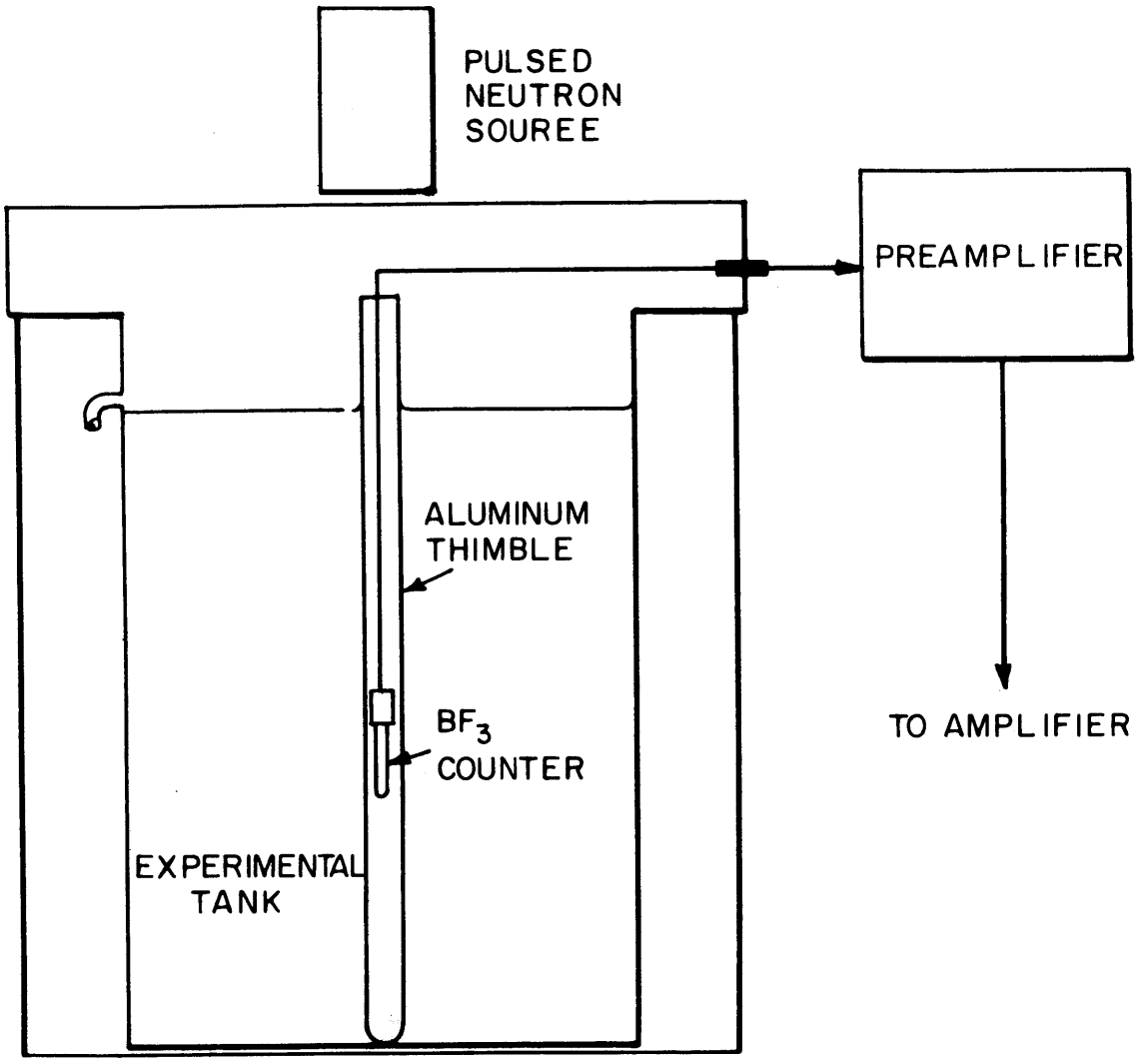

FIG. 5.11a DETECTION SYSTEM USING SMALL BF_2 COUNTER (N. WOOD MODEL, ACTIVE VOLUME 4 INCH X 1/2 INCH 40 CM Hg FILLING PRESSURE) RUNNING IN AN ALUMINUM THIMBLE ALONG AXIS

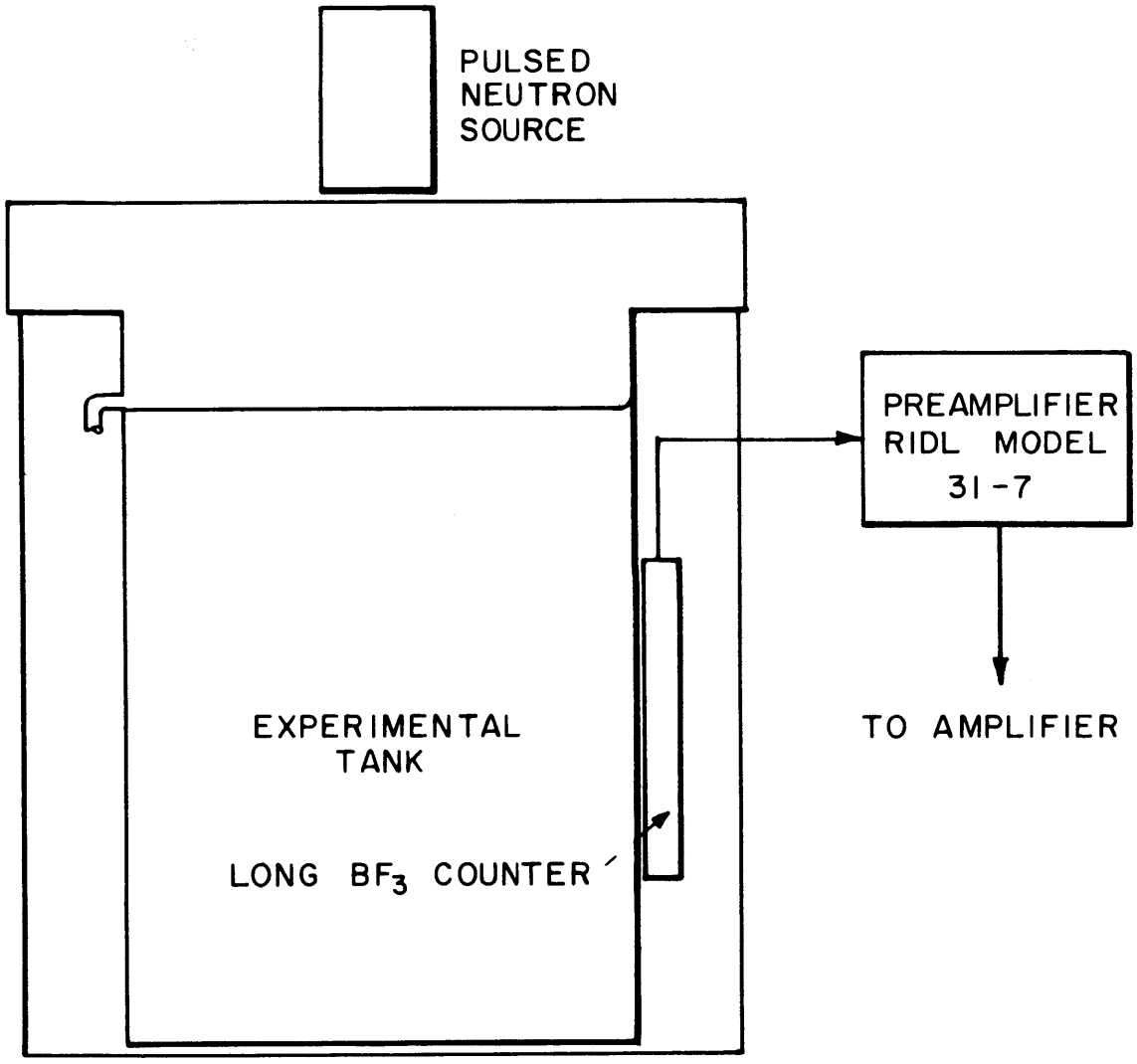

FIG. 5.11b DETECTION SYSTEM USING LONG EXTERNAL BF_3 PROPORTIONAL COUNTER (N. WOOD MODEL, ACTIVE VOLUME 20 INCH X 2 INCH, 40 CM Hg FILLING PRESSURE)

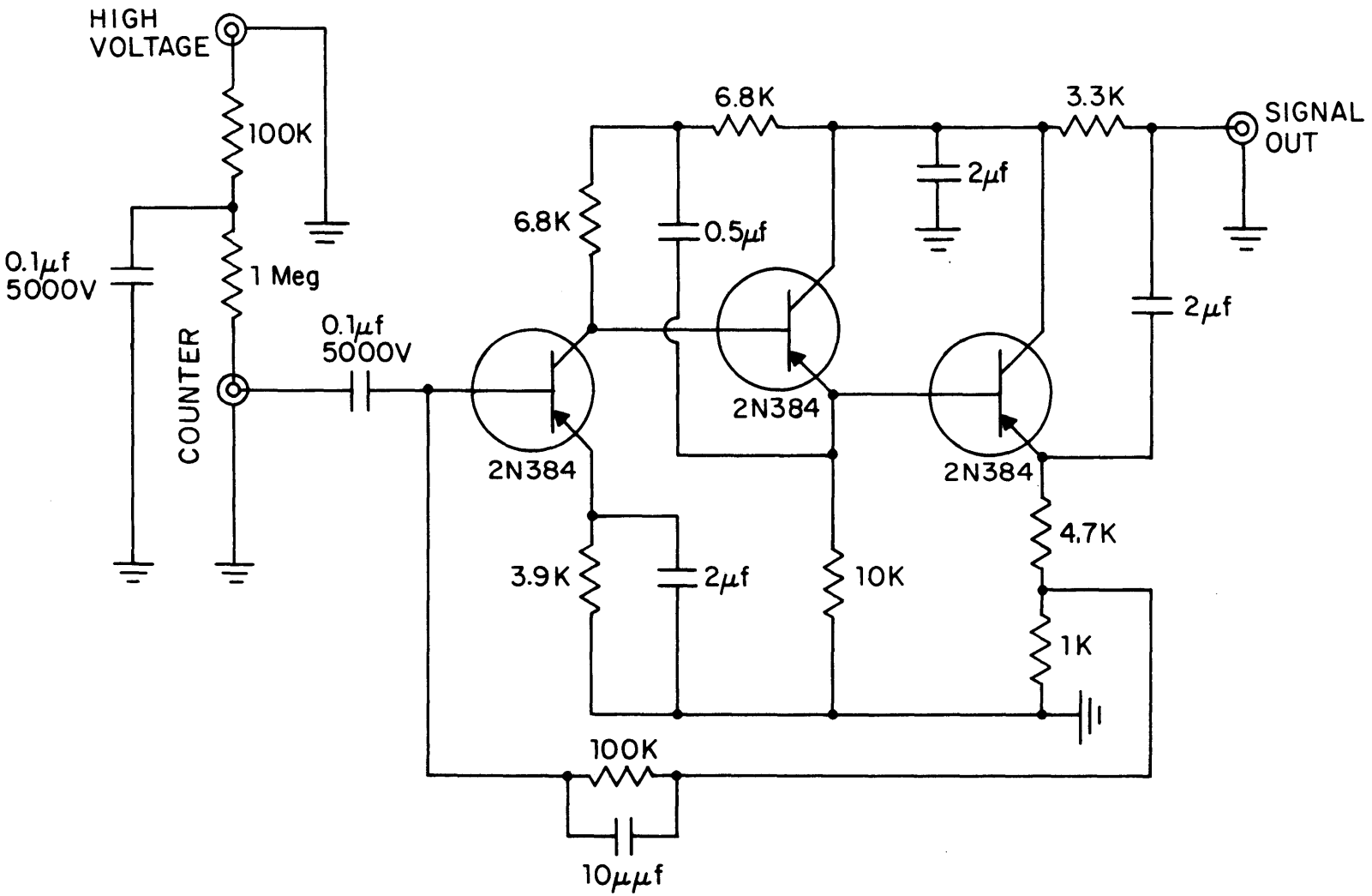

FIG. 5.12 SCHEMATIC OF THE PREAMPLIFIER USED WITH THE SMALL BF_3 COUNTER.
(DESIGNED BY D. GWINN)

was determined to be of the order of two microseconds.

For moderator and simple lattice runs, when the heavy water was at its full height in the tank, both the detection systems could be used and compared. When runs were made with the control rod located along the axis, only the long external detector could be used. For runs where it was necessary to vary the level of heavy water, the small BF_3 tube in the thimble alone was used. The effect of positioning it at different heights along the axis was also studied. However, in actual runs, the small BF_3 counter was located halfway up the level of heavy water.

5.3.4 The Time Analysis System. The basis of time analysis and the principle of operation of a time analyzer are described in detail in Ref (23). Basically, the purpose is to map a time-profile of the decaying flux by recording numbers which are proportional to the neutron density at marked intervals of time. In general, the time analyzer must be of the multichannel type and should have between 40 and 100 channels at least, each variable in width between 10 microseconds and 5 milliseconds. A number of strictly digital analyzers for this type of work have been developed[24-27]. An important requirement for such an analyzer is a reasonably low dead time which should be smaller than 5 microseconds.

The counting rates obtained from the detector-amplifier-discriminator system are often low enough to warrant time analysis by a time-to-height converter in conjunction with a multichannel pulse-height analyzer, although care must be taken to ensure adequate linearity and stability. A special system having high stability and a linearity to within 1% has been recently described by Beckürts[28].

The analyzer used in this work – and one which should be appropriate for general thermal reactor systems – was a fully transistorized TMC-256 channel analyzer including the Model CN-110 digital computer used with a Type 212 pulsed neutron plug-in unit. (These are manufactured by Technical Measurements Corporation, North Haven, Connecticut, U.S.A.) This analyzer consists[22] of a 16-binary scaler for buffer storage of incoming signals, a ferrite-core magnetic memory with a storage capacity of 256 words of 16 binary bits each, and appropriate switching circuitry. "Live" analogue display of the memory contents is

provided via a built-in oscilloscope.

The purpose of the Type 212 plug-in unit is to convert the usual energy scale of the analyzer into a time scale, so that the 256 memory addresses are sequentially sensitized to become time channels with a total count capacity of 1,048,575. The 255 channels (2-256) are analysis channels and are of equal duration Δ, adjustable from 10 to 2560 microseconds in multiples of 2. The first channel accumulates pre-burst background, and its width is independently variable as $2^n\Delta$ with $n = 1, 2, \ldots 8$. The channel width is set by a 100-kc crystal oscillator with a specified accuracy of ± 0.02 per cent from 0°C to 50°C. The time resolution of the analyzer is about 80 nanoseconds for registering detector pulses in buffer storage. This resolving time is specifically that of a pulse-shaping trigger circuit at the entrance of buffer storage. All "read and write" operations between buffer and memory are relegated to a 10-microsecond dead time gap separating the end and the beginning of successive channels.

Data are extracted from the memory via a transmission system and recorded by a Hewett-Packard digital recorder which prints out the counts and channel number on a tape. Continuous live data display on the analyzer oscilloscope conveniently allow observation of the progress of an experiment.

5.3.5 The Over-All Pulsed Neutron Circuitry. The block diagram of the experimental arrangement and the data recording system are shown in Fig. 5.13. The time sequence of the logic operation is as follows. The initiating master-sync signal for the pulsing sequence is generated by an external oscillator (composed of a Tektronix Type 162 Waveform Generator and Type 163 Pulse Generator; the latter shapes the trigger pulse). This system trigger signal is applied to the Type 212 plug-in unit of the analyzer and immediately sensitizes its pre-burst background (first) channel; the width of this background channel is variable independently of the other channels. Upon the closing of the background channel, the analyzer sends out a pulse — the source trigger — which is used to fire the pulsed neutron source. Simultaneously, a variable time delay of duration $2^n\Delta$ (where $n = 1, 2, 3, \ldots 8$; Δ:channel width) is initiated in

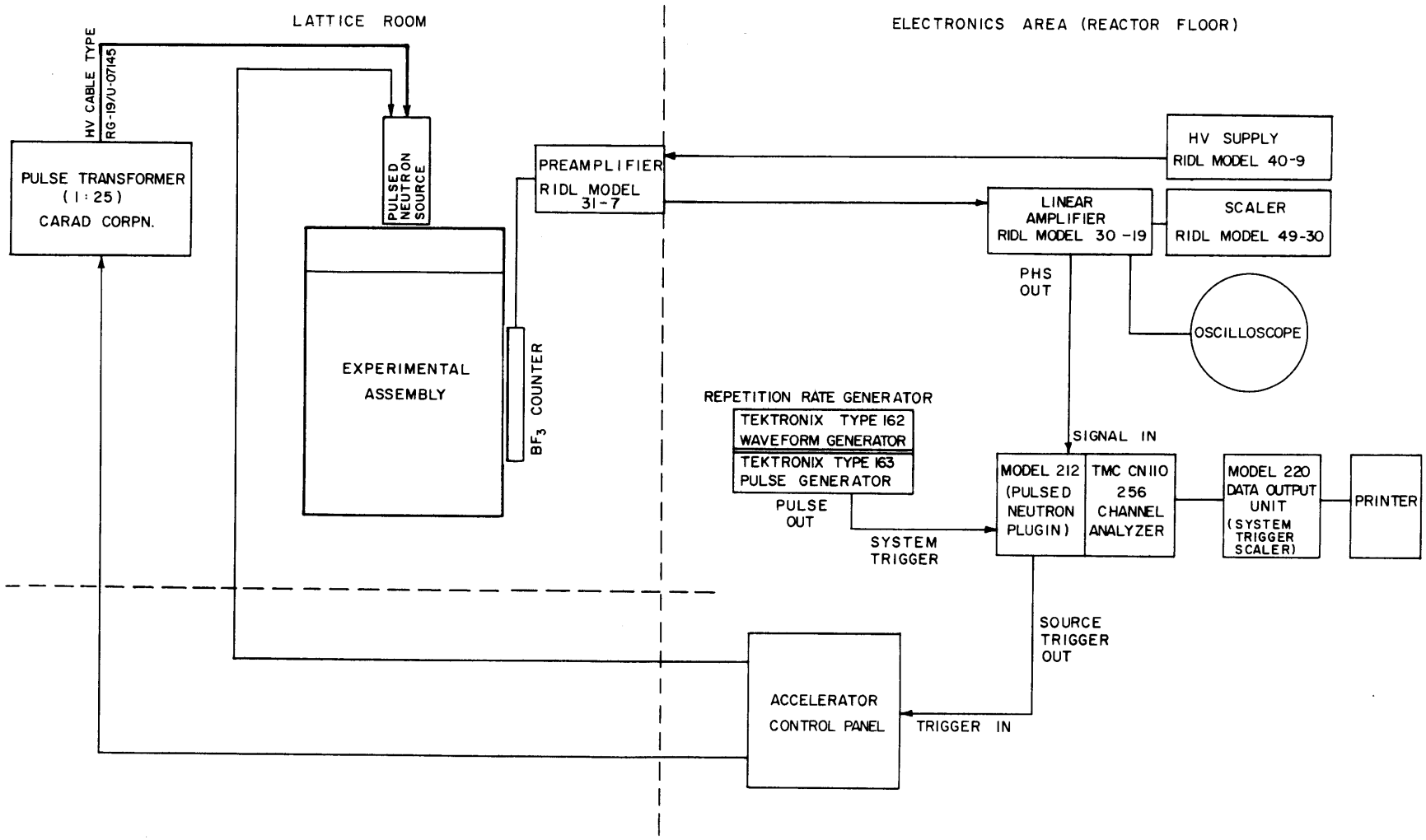

FIG. 5.13 SCHEMATIC OF OVERALL PULSING, DETECTION AND ANALYSIS CIRCUITRY

the time analyzer so that after the neutron source is fired, an appropriate "waiting time" (also variable as $2^n\Delta$) is provided to allow a stable spatial flux distribution to be established. [Actually, there is also a target delay variable continuously from 0 to 100 μsec between the firing of the source and the appearance of the target pulse (and therefore the neutron pulse); thus the net or actual waiting time is reduced by the pre-set target delay.] Thereafter, the remaining channels open in succession and accept counts from the detector. As the last channel in the memory is sensitized, the entire pulsing sequence is ended until another trigger signal is supplied by the repetition rate generator. The analyzer circuit prevents overlapping of sweep time with the repetition period.

The inner mechanism of this sequence is provided in the operational characteristics of the analyzer itself. Upon receipt of the system trigger from the repetition rate generator, a gate is opened to the fast trigger circuit which precedes the 16-binary buffer storage; the subsequent incoming signals from the detector are stored in the buffer, and kept there until the end of the channel, when the gate closes. The accumulated counts are then removed from buffer storage and deposited into ferrite core storage; this process takes 5 μsec which is half the 10-μsec dead time between successive channels. Before the opening of the first channel, the analyzer selects the proper address in ferrite core storage, extracts the counts therein and loads them into the buffer store, which accounts for the other 5 μsec; thereafter, the gate to the trigger circuit opens and any incoming data are added onto that, as long as the channel is open. At the end of the channel, the buffer contents go back into the appropriate address in the ferrite core, the data in the next address are transferred to the buffer and so on.

The cycles are repeated at the pre-set repetition rate defined by the oscillator, and the data from each cycle are accumulated and summed in the analyzer. At the end of the run, the printer prints out the output in the form of a tape giving the channel number and the number of counts in each channel.

A photograph of the control panel and a part of the associated equipment is shown in Fig. 5.14.

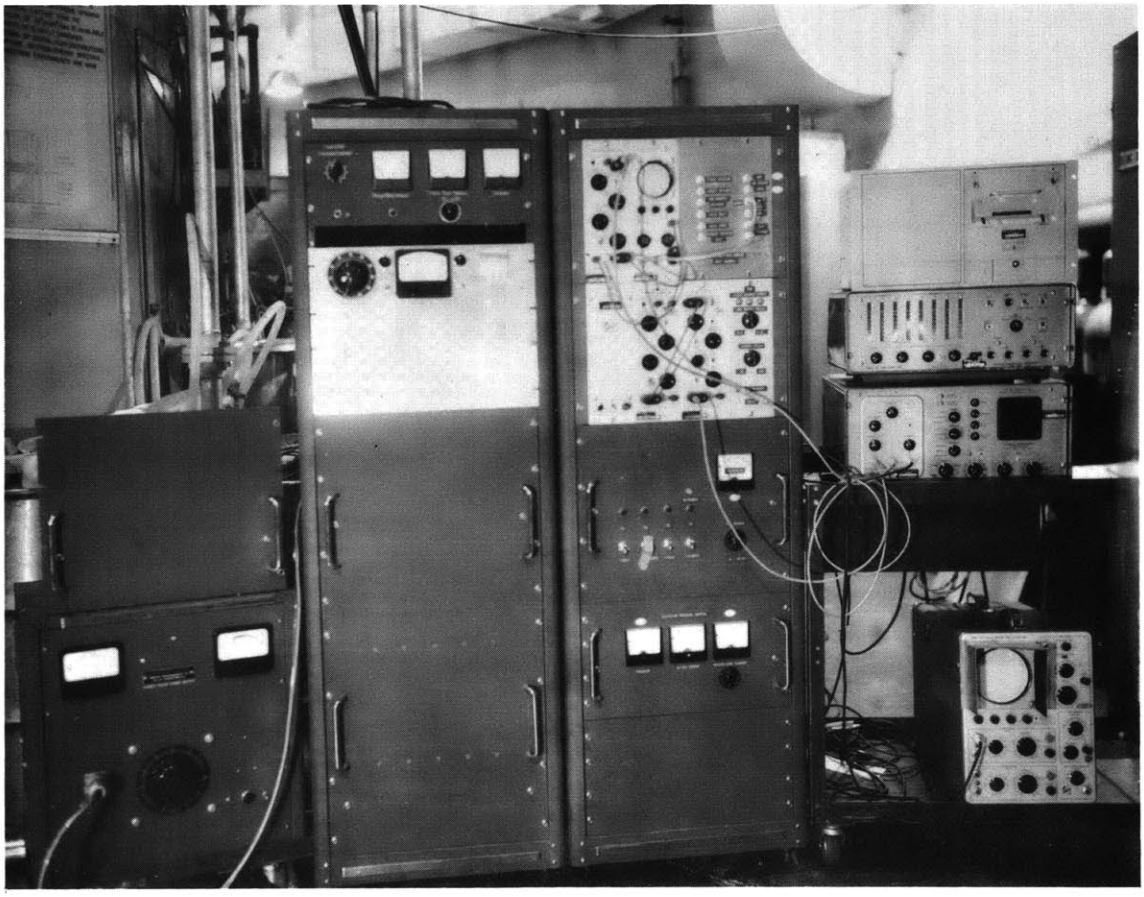

Fig. 5.14 The Control Panel of the Accelerator and the Associated Equipment

References

1. M.I.T. "Heavy Water Lattice Research Project Annual Report," NYO-9658 (September 30, 1961).

2. M.I.T. "Heavy Water Lattice Research Project Annual Report," NYO-10,208 (September 30, 1962).

3. M.I.T. "Heavy Water Lattice Research Project Annual Report," NYO-10,212 (September 30, 1963).

4. W. Kermit Anderson and Theilacker, Neutron Absorber Material for Reactor Control, USAEC, 1962.

5. Survey of the Physics, Metallurgy and Engineering Aspects of Reactor Control Materials, GEAP-3183, June 12, 1959.

6. D. J. Hughes and R. B. Schwartz, BNL-325 (1958).

7. H. E. Stevens, "Nuclear Requirements for Control Materials," Nucl. Sc. and Eng., 4, 373-385 (1958).

8. A. E. Profio, Ph.D. Thesis, Department of Nuclear Engineering, M.I.T. (November, 1962).

9. N. G. Sjöstrand, Arkiv För Fysik, Band 11, nr. 13 (1956).

10. S. Eklund, J. Nucl. Energy, 1, 93 (1954).

11. K. M. Henry, E. B. Johnson, R. Perez-Belles, G. de Saussure and E. G. Silver, Trans. Am. Nucl. Soc., 2, No. 2, 28 (1959).

12. J. Bengston et al., UCRL-5159 (1958).

13. P. O. Hawkins and J. D. L. H. Woods, J.R.N.SS, 15, 6 (November, 1960).

14. P. O. Hawkins and R. W. Sutton, Rev. Sci. Instr. 31, 3 (1960).

15. K. W. Erickson and B. J. Carr, Industrial Research, June, 1963.

16. O. Reifenschweiler, Nucleonics, 18, No. 2, 69 (1960).

17. B. K. Malaviya, Internal Memo, BKM-3, MITR, April, 1962.

18. W. J. Price, Nuclear Radiation Detection, McGraw-Hill Book Company, Inc., New York (1958).

19. G. F. Erickson, S. G. Kaufmann and I. F. Pahis, IRE Trans. on Nucl. Sci. NS-3, No. 3 (1956).

References (concluded)

20. B. E. Simmons and J. S. King, Nucl. Sci. and Eng., 3, 595 (1958).

21. O. C. Kolar and F. A. Kloverstrom, Nucl. Sci. and Eng., 10, 45 (1961).

22. P. Meyer and W. C. Ballowe, GEAP-4019 (1962).

23. W. M. Andrews, UCRL-6083 (1960).

24. G. F. von Dardel, Appl. Sci. Res., B 3, 209 (1953).

25. R. Ramanna, G. S. Mani, P. K. Iyengar, S.B.D. Iyengar and B. V. Joshi, Proc. Int. Conf. on the Peaceful Uses of Atomic Energy, Geneva, Vol. 5, P/872 (1955).

26. F. Glass, ORNL-2480, 22 (1958).

27. E. Gatti, Rev. Sci. Instr., 24, 345 (1953).

28. K. H. Beckürts, Nukleonik, 2, 129 (1960).

Chapter VI

CONTROL ROD THEORY: CALCULATION OF CONTROL ROD WORTH

The theory of control has, as one of its goals, the evaluation of the strength or worth of a control device, e.g., a control rod, under given static conditions. The theory of control rods is especially interesting because in and near control elements, the approximate diffusion theory methods break down and more accurate transport theory methods have to be considered. The complexity of these methods makes it necessary to use "recipes" involving corrections obtained from transport theory to calculate neutron distributions in a chain-reacting system containing control elements. Thus, the control element may be characterized by a local property which is used in a diffusion theory calculation, along with the properties of the rest of the system, to obtain the gross effect of the element on the reactor.[1] This separation is based on the assumption that the local property is independent of the properties of the rest of the system. The local property can take the form of boundary conditions at a boundary which may or may not coincide with the control element surface; an extrapolation distance derived from transport theory may be used here. This representation leads to a boundary value problem for the complete system. Alternatively, the local representation can be simulated by fictitious cross-sections for a part of the system, leading to a multi-region, few-group diffusion calculation. In either case, the local representation can also be used with perturbation theory. In the next section, some of the methods used in control rod theory will be reviewed and evaluated.

6.1 A REVIEW AND CRITIQUE OF METHODS USED IN CONTROL ROD THEORY

As part of this general investigation, a critical review of the literature on the physics of control was undertaken to evaluate the current status of control rod theory. The principal results of reactor control statics are reviewed in several works[2-7] and will not be repeated here. Bibliographical material can be found in Refs. (1,2,7,8).

Most of the methods used in control rod theory to date are based on diffusion theory, either in one-group,[7,10-14] two-group,[7,10,14-19] multigroup[9,20-22] or age-diffusion[23] form. This is so in spite of the fact that the approximations inherent in diffusion theory are particularly poor when applied to control rods which present problems of abrupt changes in cross-sections and diffusion constants and complex shape involving thin regions and sharp corners (in non-cylindrical rods). Many different problems have been treated: single rods (central or off-center) with different control characteristics, partially inserted rods, arrays of rods, control devices with such shapes as thin slabs and crosses, the influence of a reflector, etc.

Within the framework of diffusion theory, various mathematical methods have been used to obtain more accurate solutions in specific cases. These include variational methods,[24,25] perturbation theory,[11,26,27] the Weiner-Hopf technique, infinite series expansions of the flux in two-dimensional geometry,[28] the Fourier transform technique,[11] etc. The boundary condition in the diffusion equation may be treated by expressing the inverse logarithmic spatial derivative of the flux at the control rod surface in terms of the extrapolation distance which can be calculated in ideal cases.[24,29,30] The boundary condition may also be treated by means of variational methods applied to the integral transport equation, with perturbation theory for cylindrical rods of small radii and a Weiner-Hopf analysis for large radii. Another method purporting to improve upon the errors arising from the application of diffusion theory near a black rod, is to use an effective radius in the case of cylindrical rods (or equivalent cylinders for other shapes); the effective radius may be expressed in terms of the extrapolation distance.

Perturbation theory can be applied to the control rod problem[8] in three ways. First, the reactivity effect of a control rod in a reactor can be calculated; the usual theory converges only for weak perturbations, but may be extended to strong perturbations by the method of analytic continuation in the space of perturbations.[31] Second, the boundary perturbation method can be used to compute the effect of an energy-dependent extrapolation distance. Third, this method can be applied to the calculation of the effect on reactivity due to the alteration of the effective boundary by the presence of a partially inserted rod.

An alternative to the boundary value approach is the so-called poison cell method or the use of the principle of equivalence.[32,33] A region of the core containing the control rod is assumed equivalent to a homogeneous multiplying medium of the same volume with a new multiplication factor and a new migration area. The equivalence principle is valid when: 1) there is a large number of rods ("supercells") in a regular lattice; 2) the surrounding medium may be considered homogeneous; 3) the rods are small compared to the region they control; and 4) fast and slow neutrons behave similarly. These are also the conditions for the validity of the cell theory. Although this method by-passes the problem of boundary conditions, it is still based on a diffusion theory solution of the equivalent problem. The division of the calculation into a local calculation to determine short range control element effects and a full reactor calculation is made by defining a local control element cell. The cell calculation can be made in great detail to determine fictitious cross-sections to use for a second calculation which represents the cell as a homogeneous region. A variety of methods may be used for the cell region; for example, two-dimensional, one-group, Monte Carlo program TUT[34] has been developed for some problems at the Bettis Atomic Power Division of Westinghouse.

Since a control rod or a group of control rods in a heterogeneous reactor produces a "defect" in an otherwise perfect lattice, any method of estimating control rod effectiveness in which the reactor is homogenized will be somewhat inaccurate.[6] Feinberg[35] has pointed out that the heterogeneous sink method may be applied to the problem of control rods. The neutron flux at any point is regarded as a superposition of the effects

of the fuel element sources and control rod sinks. Such a superposition is representable by a lattice sum, which can be easily evaluated for a regular lattice. For a reactor with regularly placed control rods, the lattice sum can be treated numerically. In general, however, the calculations are tedious, and, for practical work, the methods in which the reactor is homogenized are more tractable.

The shortcomings of most of these methods stem mainly from the approximations inherent in the diffusion theory. The methods involving the use of the logarithmic derivative, the effective rod radius and the principle of equivalent poison in a cell, all suffer from the diffusion theory approximations. The more sophisticated mathematical techniques, mentioned earlier, usually result in errors which are consistently smaller than the basic error involved in the use of the diffusion theory approximation. Despite the basic inadequacies of diffusion theory, it has been widely used because of its simplicity and wide applicability. An example of a machine calculation scheme involving a combination of transport and diffusion theory is to be found in Ref. (36).

There are several methods which might be tried to improve on diffusion theory. For example, a transport theory solution in a purely absorbing rod might be combined with a P_3-solution in the core region through appropriate boundary conditions. An iterative solution of the integral transport equation could be attempted by using the Liouville method.[8,37,39] The use of spatial moments, with an accompanying moment inversion technique,[39] has not been applied to control rod problems. Comparisons of theoretical methods for control rod solutions have generally been concerned with different formulations of the diffusion theory equations[15,16] rather than with the estimation of the accuracy of a method with respect to a rigorous solution.

The effectiveness of a control rod in a reactor is determined by factors which are conveniently subdivided into two groups.[3] The first contains effects of the shape and material of the rod itself and the region immediately surrounding it. The second contains the effects of additional control rods, if any, and of reactor size, shape and constitution. Corresponding to this general grouping, the calculation of control rod effectiveness proceeds in two steps. The first is devoted to a determination of an

effective rod radius or extrapolation distance to describe the effect of an individual rod on the neutron flux in its vicinity. Then the diffusion equation can be solved for a particular reactor and rod arrangement. The buckling B^2 of the system is determined as usual from the requirement that the secular determinant must vanish. Once the buckling is known, it is possible to find the infinite multiplication factor, k_o, which would restore the reactor to criticality with the rod inserted. This yields the change in reactivity, δk, produced by the insertion of the rod. An example of this general method is the treatment by Murray and Niestlie[16] of single rods with different boundary conditions.

6.2 TWO-GROUP TREATMENT OF A CENTRAL CONTROL ROD WITH THE EXTRAPOLATION LENGTH BOUNDARY CONDITION

A central control rod may be treated[7] under two-group theory by applying the boundary condition for thermal neutrons in terms of an effective radius at which the flux vanishes. However, for rods of small radius, the extrapolated surface lies outside the rod and, according to the usual definition ($R' = R_o - d$), the effective radius is negative. This complicates the calculation of the rod worth from the two-group expression. In this section, the central control rod will be treated by a similar method involving boundary conditions for the thermal group neutrons as defined by an extrapolation distance. The fast flux will be assumed to be flat at the surface of the rod.

Consider a cylindrical, bare, homogeneous reactor of extrapolated radius R and height H which has a thermally black control rod of actual physical radius a, along the full length of its axis. As usual, the r and z variables are separable in the solution to the Helmholtz equation and the radial parts of both the slow and fast neutron flux are given as the solutions of the equation:

$$\nabla^2\theta(r) + \alpha^2\theta(r) = 0 \ , \tag{6.1}$$

where α^2 is either root of the two-group characteristic equation:[7]

$$\mu^2 = \frac{1}{2}\left[-\left(\frac{1}{\tau}+\frac{1}{L^2}\right) + \left\{\left(\frac{1}{\tau}+\frac{1}{L^2}\right)^2 + \frac{4(k_o-1)}{\tau L^2}\right\}^{1/2}\right],$$

$$-\nu^2 = \frac{1}{2}\left[-\left(\frac{1}{\tau}+\frac{1}{L^2}\right) - \left\{\left(\frac{1}{\tau}+\frac{1}{L^2}\right)^2 + \frac{4(k_o-1)}{\tau L^2}\right\}^{1/2}\right]; \qquad (6.2a,b)$$

both μ^2 and ν^2 are positive if $k_o > 1$. The solutions to Eq. 6.1 corresponding to these two values of a^2 are:

$$Z_1(r) = J_o(\mu r) + AY_o(\mu r) ,$$

$$Z_2(r) = CJ_o(\nu r) + K_o(\nu r) , \qquad (6.3a,b)$$

and the radial parts of both the fast and the slow flux are linear combinations of these two solutions.

The fluxes vanish at the extrapolated outer boundary so that:

$$Z_1(r) = J_o(\mu r) - \frac{J_o(\mu R)}{Y_o(\mu R)} Y_o(\mu r) ,$$

and (6.4a,b)

$$Z_2(r) = K_o(\nu r) - \frac{K_o(\nu R)}{I_o(\nu R)} I_o(\nu r) .$$

If we write:

$$\mu = \mu_o + \Delta\mu , \qquad (6.5)$$

where μ_o is the value of μ in the unperturbed reactor, it can be shown[7] that

$$Z_1(r) \approx J_o(\mu r) + 1.22 \frac{\Delta\mu^2}{\mu_o^2} Y_o(\mu r) ,$$

$$Z_2(r) \approx K_o(\nu r) . \qquad (6.6a,b)$$

The fast flux is given by:

$$\phi(r) = Z_1(r) + AZ_2(r) ,$$

and, if the fast flux is assumed to be flat at the rod surface, we have:

$$\frac{d\phi}{dr} = 0, \quad \text{at } r = a \, . \tag{6.8}$$

If we apply this condition to Eq. 6.7, and use the results:

$$\text{for } \mu a \ll 1, \quad J_1(\mu a) \to 0 \, ,$$

$$Y_o(\mu a) \to -\frac{2}{\pi}\left(0.116 + \ell n \frac{1}{\mu a}\right) , \tag{6.9}$$

$$K_o(\mu a) \to \left(0.116 + \ell n \frac{1}{\nu a}\right) ,$$

we get:

$$A = -1.22 \frac{\Delta\mu^2}{\mu_o^2} \cdot \frac{2}{\pi} \, . \tag{6.10}$$

We are chiefly interested in the thermal flux; the radial part of this is given by

$$\psi(r) = S_1 Z_1(r) + A S_2 Z_2(r) \, , \tag{6.11}$$

where S_1 and S_2 are the usual coupling coefficients, given by:

$$S_1 = \frac{D_1}{\tau D_2}\left(\frac{1}{L^2} + \mu^2\right)^{-1} ,$$

and (6.12a,b)

$$S_2 = \frac{D_1}{\tau D_2}\left(\frac{1}{L^2} - \nu^2\right)^{-1} ,$$

so that

$$\frac{S_2}{S_1} = \frac{\frac{1}{L^2} + \mu^2}{\frac{1}{L^2} - \nu^2} \, . \tag{6.13}$$

Using Eqs. 6.6 and 6.10, we get from Eq. 6.11:

$$\psi(r) = S_2\left[J_o(\mu r) + 1.22 \frac{\Delta\mu^2}{\mu_o^2}\left\{Y_o(\mu r) + \frac{S_2}{S_1} \cdot \frac{2}{\pi} K_o(\nu r)\right\}\right] \, . \tag{6.14}$$

Now, we apply the boundary condition for the thermal flux in terms of the extrapolation length d, into the rod:

$$d = \left.\frac{\psi(r)}{\psi'(r)}\right|_{r=a} , \tag{6.15}$$

where $\psi'(r)$ denotes derivative with respect to r. Substituting for $\psi(r)$ from Eq. 6.14 in Eq. 6.15 and simplifying, we get:

$$1.22\frac{\Delta\mu^2}{\mu_o^2} = -\frac{J_o(\mu a) + d\mu J_1(\mu a)}{\left[Y_o(\mu a) + d\mu Y_1(\mu a) + \frac{2}{\pi}\cdot\frac{S_2}{S_1}(K_o(\nu a) + d\nu K_1(\nu a))\right]} . \tag{6.16}$$

Now, for $\mu a \ll 1$, $J_o(\mu a) \to 1$ and $J_1(\mu a) \to 0$. Hence, we finally have:

$$\frac{\Delta\mu^2}{\mu_o^2} = -0.820\left[Y_o(\mu a) + d\mu Y_1(\mu a) + \frac{2}{\pi}\frac{S_2}{S_1}(K_o(\nu a) + d\nu K_1(\nu a))\right]^{-1} . \tag{6.17}$$

This expression gives the fractional change in the radial buckling caused by the rod, explicitly in terms of the extrapolation length d. The excess multiplication Δk controlled by the rod can be obtained from the relation:

$$\frac{\Delta\mu^2}{\mu_o^2} = \frac{\Delta k}{\mu_o^2(L^2+\tau)} . \tag{6.18}$$

Eq. 6.17 will be used for comparison with the results of pulsed neutron and steady-state experiments with a central cadmium rod in a multiplying assembly.

References

1. Vallecitos Atomic Laboratory Report, GEAP-3183 (1959).
2. L. J. Templin (Coördinator), ANL-5800 (2nd Ed.), 1963.
3. T. Auerbach, BNL Internal Memo.
4. H. Soodak (Ed.), Reactor Handbook, Vol. III, Part A (2nd Ed.), Interscience Publishers, New York (1962).
5. K. Sato, M.S. Thesis, Nuclear Eng. Dept., M.I.T. (1961).
6. A. M. Weinberg and E. P. Wigner, The Physical Theory of Neutron Chain Reactors, The University of Chicago Press, Chicago (1958).
7. S. Glasstone and M. C. Edlund, The Elements of Nuclear Reactor Theory, D. Van Nostrand Company, Inc., New York (1952).
8. D. Schiff, Internal Report, Raytheon Manufacturing Company (unpublished).
9. TID-7532 (Pt. I) Reactor Control Meeting Held in Los Angeles, March 6-8, 1957.
10. R. Scalettar and L. W. Nordheim, MDDC-42 (1946).
11. A. D. Gelanin, Proc. Int. Conf. on the Peaceful Uses of Atomic Energy, P/668 (1956).
12. H. Hurwitz, Jr. and G. M. Roe, J. Nuclear Energy, 2, 85 (1956).
13. F. L. Fillmore, NAA-SR-1567 (1956).
14. F. T. Adler, AECL-253 (1956).
15. H. L. Garabedian, AECD-3666 (1950).
16. R. L. Murray and J. W. Niestie, Nucleonics 13, No. 2, 18 (1955).
17. J. Codd and C. A. Rennie, AERE-R/R-818 (1952).
18. R. Avery, Nuclear Sci. and Eng. 3, 504 (1958).
19. R. L. Murray, W. T. Price and S. H. Binken, Nuclear Sci. and Eng. 8, 254 (1960).
20. E. L. Wachspress, KAPL-1318 (1955).

21. B. Wolfe, J. Nuclear En. 7, 71 (1958).

22. B. Wolfe, J. Nuclear En. 8, 63 (1958).

23. H. Uberall, Nuclear Sci. and Eng. 7, 228 (1959).

24. S. A. Kushneriuk and C. McKay, CRT-566 (1954).

25. E. P. Gyftopoulous and L. de Sobrino, Nuclear Sci. and Eng. 6, 135 (1959).

26. B. Wolfe and D. L. Fischer, Nuclear Sci. and Eng. 4, 785 (1958).

27. B. Wolfe and D. L. Fisher, Nuclear Sci. and Eng. 5, 5 (1959).

28. W. Thompson, AD-65678 (1955).

29. B. Davison and S. A. Kushneriuk, MT-214 (1946).

30. W. P. Seidel, B. Davison and S. A. Kushneriuk, MT-207 (1946).

31. P. M. Morse and H. Feshbach, Methods of Theoretical Physics, McGraw-Hill Book Company, Inc., New York (1953).

32. P. F. Gast, Proc. Int. Conf. on the Peaceful Uses of Atomic Energy, Geneva, P/612 (1956).

33. L. Friedman, WAPD-SFR-Ph-124 (1955).

34. J. Spanier et al., WAPD-TM-125 (1959).

35. S. M. Feinberg, Proc. Int. Conf. On the Peaceful Uses of Atomic Energy, Vol. 5, 484 (1955).

36. G. H. Kear and M. H. Ruderman, GEAP-3937 (1962).

37. R. Courant and B. Hilbert, Methods of Mathematical Physics, Vol. I, Interscience, New York (1943).

38. H. Resnikoff and D. Schiff, WAPD-TN-505 (1954).

39. J. S. Langer and R. S. Varga, WAPD-TN-516 (1955).

Chapter VII

RESULTS AND DISCUSSION

The theoretical treatment of a pulsed neutron multiplying system, undertaken in Chapter II, was explored in the following chapter with a view to seeking relations that might lend themselves to experimental analysis and interpretation, and a number of possible experimental studies suggested themselves. Chapter IV explored a similar goal with respect to the exponential experiments with control rods. A description of the experimental equipment demanded by the suggested experiments was the subject of Chapter V. It is the purpose of the present chapter to incorporate this material in the actual measurements and analyses. This chapter will, therefore, be devoted to an attempt to describe the experimental conditions and procedures, to investigate the effect of special experimental variables, to check the internal consistency of the data and to obtain qualitative and quantitative results. The results will be analyzed, interpreted and discussed; wherever possible, they will be compared and correlated.

7.1 PULSED NEUTRON EXPERIMENTS ON NON-MULTIPLYING MEDIA IN THE EXPONENTIAL TANK: GENERAL PROCEDURES IN PULSED NEUTRON EXPERIMENTS

The first set of experiments with the new accelerator and pulsed neutron instrumentation was undertaken with only heavy water in the tank of the exponential facility. The 36-inch-diameter, aluminum tank was in place at the time, and the sides and top were covered with 0.020-inch-thick cadmium; an aluminum-clad circular plate of cadmium of the same thickness covered the bottom of the tank during the use of the facility for pulsed neutron work. Heavy water, in a nitrogen atmosphere, could be pumped up from a storage tank to any desired height up to 52 inches, and the level could be read on an external sight-glass indicator,

correct to within 0.20 cm. The temperature of the heavy water was recorded continuously by means of a platinum resistance thermometer. The pulsed neutron runs were made with the M.I.T. reactor shut down - during weekends and periods of reactor maintenance - so that the neutron and gamma-ray backgrounds were minimal. The first few experiments were devoted to establishing a systematic procedure for the determination of the characteristic decay constant of the fundamental thermal flux mode and to an examination of the effects of some of the experimental variables on the measured decay constant. These experiments and their analysis will be described in the next section.

7.1.1 Study of the Diffusion Characteristics of Heavy Water at Room Temperature

It was thought desirable to improve our knowledge of the diffusion parameters of heavy water; there have been relatively few pulsed neutron die-away experiments on heavy water, and these have been restricted to small assemblies,[1,2,3] in the buckling range $B^2 = 140\ m^{-2}$ to $1200\ m^{-2}$, having linear dimensions smaller than ten times the transport mean-free path. In these cases, the extrapolation distance may be as large as 15 per cent of a linear dimension with the result that there may be significant systematic errors if the extrapolation distance deviates from the value $0.71\ \lambda_{tr}$. Moreover, the absorption cross-section of heavy water is so small that it can only be measured, with such pulsed neutron experiments, in very large assemblies, corresponding to the buckling range in which the higher order terms in the λ vs. B^2 relationship may be neglected.

The availability of a relatively large quantity of heavy water and of the pulsed neutron system associated with the exponential facility made it possible to conduct such experiments. A knowledge of the diffusion parameters of heavy water is needed in the determination of the geometrical buckling of the moderator assembly with the control rods and in the evaluation of the prompt neutron lifetime as discussed in Section 3.5. These diffusion parameters are so sensitive to the isotopic and chemical purity that they should be determined for the particular sample of heavy water used in a sequence of experiments.

Before proceeding with the actual runs, attention was devoted to establishing criteria for the selection of the asymptotic decay constant characteristic of the experimental assembly. The measured decay constant was checked for reproducibility, variation with "waiting time" and detector position (which affect the quality and content of the higher harmonics), channel width (which enters in the dead-time correction), repetition rate (which affects the delayed neutron and background correction), discriminator setting (which reveals if there is any significant pulse pile-up) and, finally, the perturbation introduced by the thimble and detector when these are placed inside the assembly.

The raw data from the analyzer in any die-away experiment consist of the total number of counts in successive channels. Each set of data is treated by an IBM-7090 code, EXPO, which has been written as part of this program, to facilitate the reduction of the data from pulsed neutron experiments (Appendix 2). This code fits the corrected experimental counts vs. time data to a single exponential plus a constant background, i.e., to an expression of the form:

$$n = A\, e^{-\lambda t} + B \,, \tag{7.1}$$

and computes, by means of a weighted, least-squares iterative technique, the values of the parameters λ, A and B, together with their associated uncertainties. As shown in the listings of the code, the counting loss for each channel (Ith) is calculated as:

$$\text{Corrn}(I) = \frac{(\text{Tdead})(Q(I))}{(\text{Pulsno})(\text{Width})} \,, \tag{7.2}$$

where Q(I) is the experimental number of counts in Ith channel, Tdead is the dead time, Pulsno is the total number of bursts (trigger pulses) and Width is the channel width. The corrected number of counts is then given by:

$$P(I) = \frac{Q(I)}{1 - \text{Corrn}(I)} \,. \tag{7.3}$$

The code also sets the time at the middle of each channel:

$$T(I) = (\text{Chdel}) \times (\text{Width}) - \text{Tdel} + (\text{Spac}) \times (I - 0.5) \,, \tag{7.4}$$

where Chdel is the delay multiplier, Tdel is the "target delay" (see Chapter V, Section 5.3.5), and Spac(= Width+Gap) is the total spacing between channel ends. The weights are based on the Poisson statistical errors in the numbers of counts and are given by:

$$WT(I) = \frac{1}{[P(I)]^{1/2}} . \tag{7.5}$$

The code then fits P(I) against T(I) in a three-parameter fit of the form of Eq. 7.1 and computes the decay constant λ and the background correction B together with their standard errors. In analyzing the data, the code has provisions to drop the initial channels one by one and to calculate the decay constant for fewer channels each time, thus effectively varying the "waiting time" between the injection of the burst and the start of the data analysis along the decay curve. The effect on the decay constant of dropping the points from the other end can also be studied with the code.

In all the runs, the delay multiplier on the time-analyzer was set at its minimum value, d=×2, and the target delay at its maximum value, 100 μsec (Section 5.3.5), so that almost the entire decay curve was obtained. Thus, for example, with a channel width of 80 μsec and the maximum target delay 100 μsec, only the first 60 μsec (= 80×2 − 100) of the decay curve were left out. On the basis of an over-all dead time of 2 μsec, the count-loss corrections amounted to a maximum of less than 1.0 per cent.

The source was always positioned at the top lid of the tank on the central axis; this location prevents the excitation of higher azimuthal flux modes. It would have been desirable to place the source in other positions with respect to the assembly and to investigate the effect, if any, on the measured decay constant. However, with the fixed exponential assembly tank, other positions for the source were either inaccessible or impractical. Typical decay curves obtained by plotting the background-subtracted number of experimental counts (corrected for counting losses) against time are shown in Fig. 7.1 for two different detectors located differently. The lower curve was obtained by the use of the small BF_3 counter running in a thimble along the axis and located at half the total heavy water height. The effect on the decay, of varying the counter

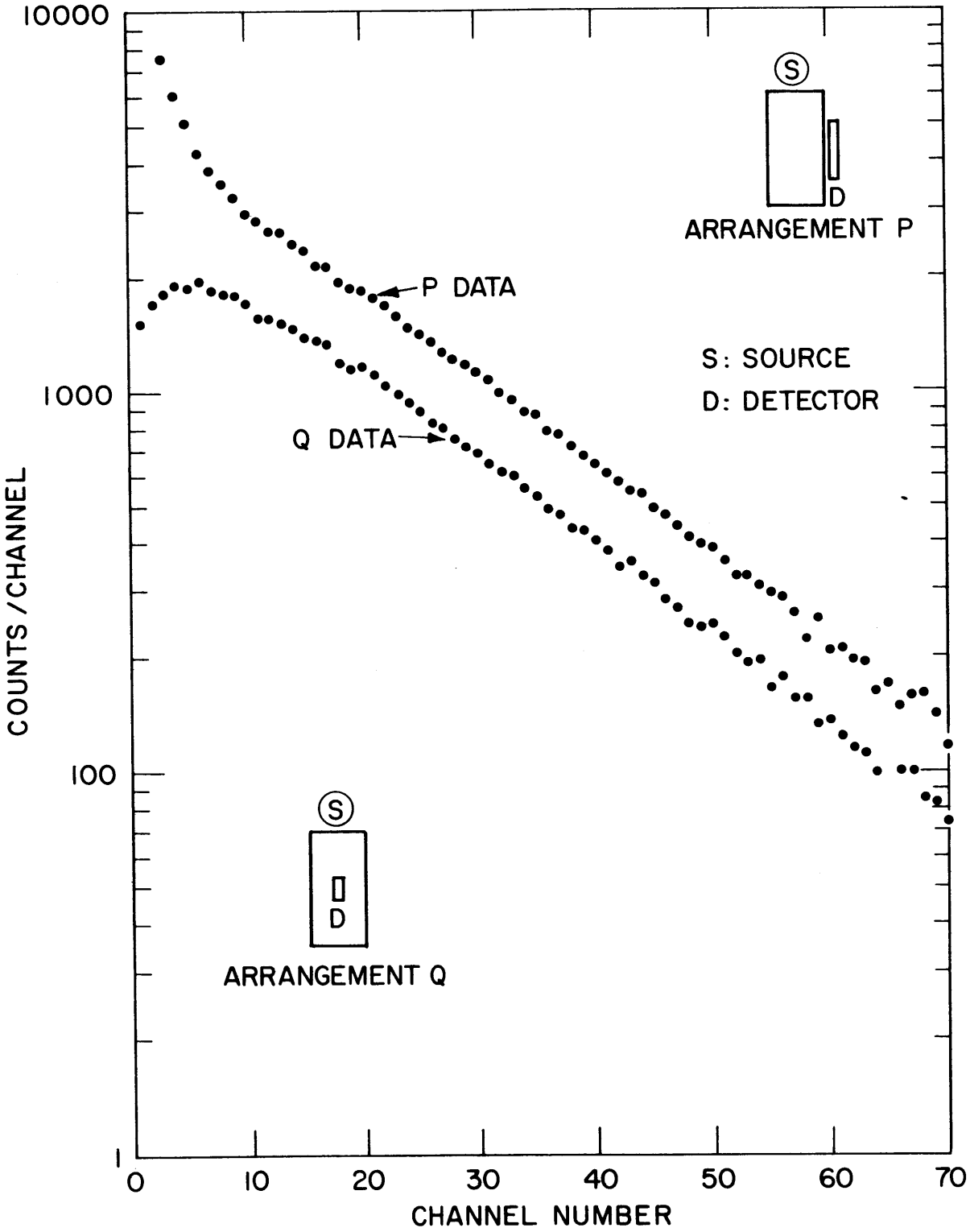

FIG. 7.1 THERMAL NEUTRON DECAY CURVES IN A PURE MODERATOR $[D_2O]$ ASSEMBLY WITH DIFFERENT DETECTION SYSTEMS.

position axially, was also investigated and found to be significant; this point will be discussed more fully in a later section on experiments with the lattice. The upper curve in Fig. 7.1 is based on the other detection arrangement (Fig. 5.11b) with the long BF_3 counter located on a side of the tank and external to it.

It is evident from the figure that the initial profiles of the two curves are markedly different, as is to be expected from the different harmonic effects. However, as soon as the higher space and energy modes have decayed and the flux has stabilized, each curve assumes a single exponential behavior and the two curves have the same slope, characteristic of the decay of the fundamental mode. With the reactor shut down, the background with these moderator assemblies was almost negligible with the discriminator setting chosen, and it was possible to monitor the decay of the fundamental mode over about two decades.

The variation of the decay constant with the waiting time, as obtained from the computer code, is shown in Fig. 7.2 for each of the two above detector configurations. As the waiting time is increased, so as to exclude more of the initial time interval during which the harmonics are important, the changes in the resultant decay constant become progressively smaller; finally, each curve levels off, showing little fluctuations in the decay constant, and the two curves merge to give a single, unique value for the decay constant which corresponds to the persisting mode. The first point at which the decay constant assumes its constant value gives the waiting time required for the particular assembly; this point corresponds, on the decay curve, to the point at which a single exponential behavior begins. These considerations establish the criteria which permit the selection of a unique value for the asymptotic decay constant that is independent of the judgment of the experimenter.

The uncertainties shown for the decay constant are the statistical errors arising from the least-squares fitting. The errors in the final value of the decay constant were always less than 1 per cent. The reproducibility (based on three repeat runs) was found to be within the experimental uncertainties. The dependence of the decay constant on other experimental variables was also investigated. No significant effects were observed when the analyzer channel width (changed to 40 μsec, 80 μsec,

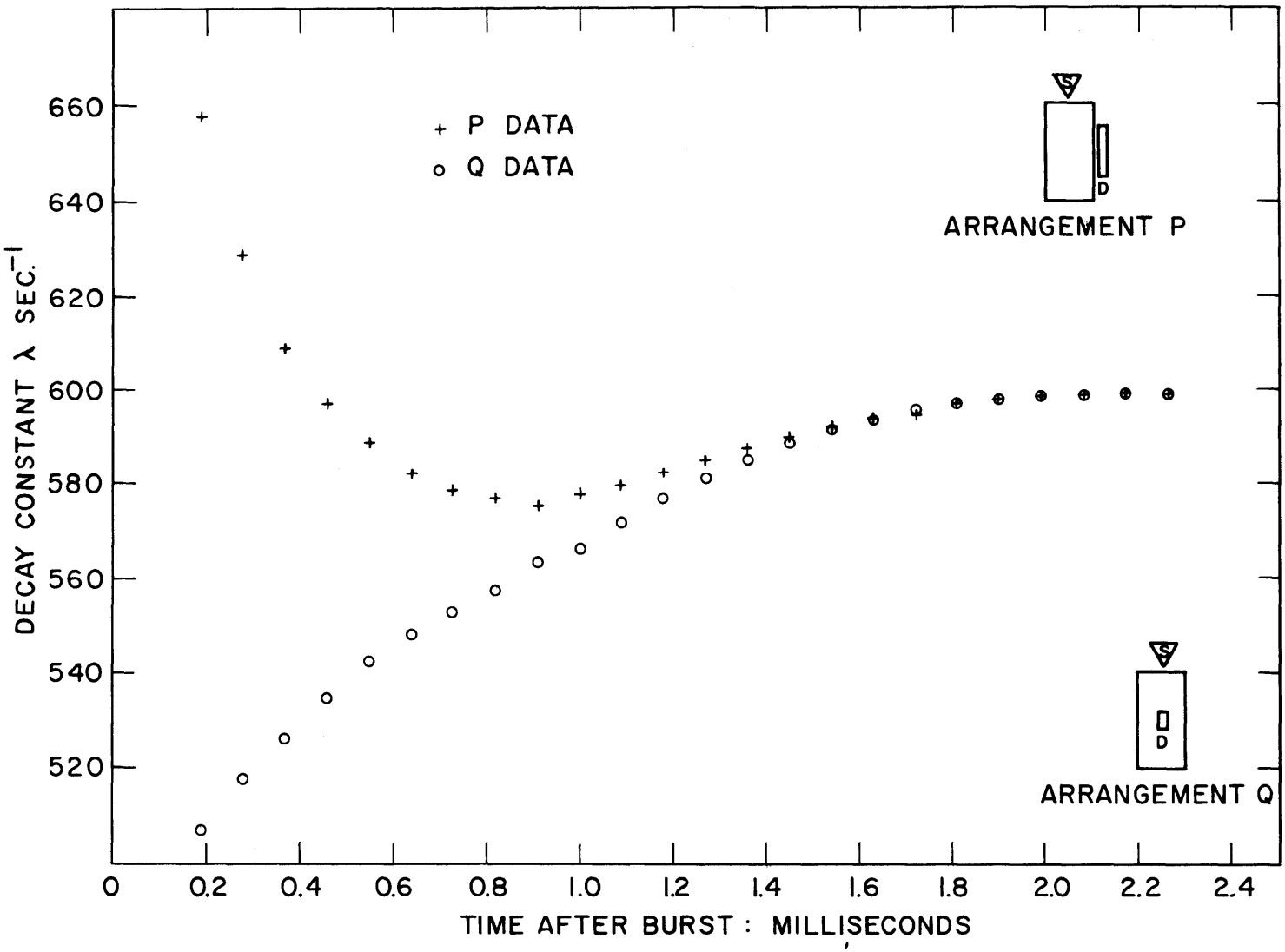

FIG. 7.2 THE VARIATION OF DECAY CONSTANT WITH "WAITING TIME" IN A PURE MODERATOR $[D_2O]$ ASSEMBLY WITH DIFFERENT DETECTORS

160 μsec), the repetition rate (10 and 5 pulses per second) or the discriminator setting (at three different readings on the dial) were varied. The perturbation introduced by placing the thimble and small BF_3 counter inside the experimental assembly was studied by using the long, external BF_3 detector and measuring the decay constant with and without the central thimble and/or the small BF_3 counter along the axis of the assembly. The resulting correction was found to be very small.

After the completion of these preliminary studies of the factors determining the final decay constant, the formal measurements were made of the diffusion parameters of heavy water at room temperature. These consisted of obtaining the fundamental mode decay constants for moderator assemblies of varying dimensions. The size of the assembly (in the 36-inch-diameter tank) was varied by changing the moderator height; since the level had to be varied, the external BF_3 counter was not suitable and, in all these runs, the small BF_3 detector tube running along the central thimble was used, its position in each case being fixed at half the moderator height. At least ten different heights were investigated varying from 55.7 cm to 132.7 cm. The waiting time was found to vary from about 1 msec to about 2.2 msec from the smallest to the largest sizes, respectively.

The final measured values of the decay constant λ together with the standard errors $\delta\lambda$, corresponding to the various sizes of the moderator assemblies and the computed values of the geometrical buckling are shown in Table 7.1. The geometrical buckling was calculated in each case from the inner tank radius R = 45.72 cms and the indicated heavy water height H according to the relation:

$$B^2 = \left(\frac{2.405}{H + d}\right)^2 + \left(\frac{\pi}{H + 2d}\right)^2 . \qquad (7.6)$$

The extrapolation distance d was assumed to be given by:

$$d = 0.710\,\lambda_{tr} ; \qquad \lambda_{tr} = \frac{3D}{\bar{v}} , \qquad (7.7a,b)$$

where the value of D was derived from the experimental data as will be discussed below.

TABLE 7.1

Measured Decay Constant λ as a Function of Geometrical Buckling B^2 for 99.60% Heavy Water at 21°C

Height of D_2O H, cm	Geometrical Buckling B^2, m^{-2}	Decay Constant λ, sec^{-1}
132.7	30.10	598.9 ± 5.2
123.2	31.87	649.2 ± 5.5
112.5	33.07	675.5 ± 5.1
102.4	34.54	700.6 ± 6.1
91.5	36.70	738.4 ± 6.7
81.1	39.56	795.4 ± 7.0
71.5	43.34	867.3 ± 7.0
65.7	46.42	926.4 ± 8.1
59.8	50.46	1004.0 ± 9.5
55.7	54.11	1073.3 ± 9.9

The λ vs. B^2 data from Table 7.1 are plotted in Fig. 7.3. The variation is almost linear except at higher buckling values where the effect of higher order terms in B^2, especially the diffusion cooling term, becomes noticeable. The upper six points are plotted separately in Fig. 7.3a, showing more clearly the effect of diffusion cooling in small assemblies.

Two IBM-7090 computer codes have been prepared to facilitate the reduction of (λ, B^2) data for the extraction of the diffusion parameters (Appendix 2). One of these, the DEECEE code, performs a two-parameter, weighted, least-squares fit of the form:

$$\lambda = \lambda_o + DB^2 - CB^4 \ , \tag{7.8}$$

by means of an iterative procedure to calculate D and C together with their standard errors. The code takes the actual physical dimensions of the assemblies as input data and a calculated value of λ_o as an input parameter and computes the geometrical bucklings from an assumed initial value of D in Eq. 7.7b. A fit of these buckling values against λ then yields D and C; the new value of D is then used to compute the value of the buckling again from Eqs. 7.6 and 7.7 and a new fit is made. The process is repeated until self-consistent values are obtained. The value of the average velocity characteristic of a Maxwellian spectrum, is taken in the code to be:

$$\bar{v} = \frac{2}{\sqrt{\pi}} \times 2.2 \times 10^5 \left(\frac{T}{293}\right)^{1/2} \text{ cm/sec} \ , \tag{7.9}$$

where T is the absolute temperature, in degrees Kelvin, of the moderator.

The second code, DIFFN, makes a three-parameter fit of the form of Eq. 7.8 in a similar manner and computes from the data the values of all three parameters $\lambda_o (= \overline{v\Sigma}_a)$, D and C along with the associated errors. This code is useful in the analysis of the (λ, B^2) data, if the latter cover a wide enough buckling range and if they pertain to a moderator for which the diffusion parameters are large enough so that the allowable uncertainties warrant a three-parameter analysis.

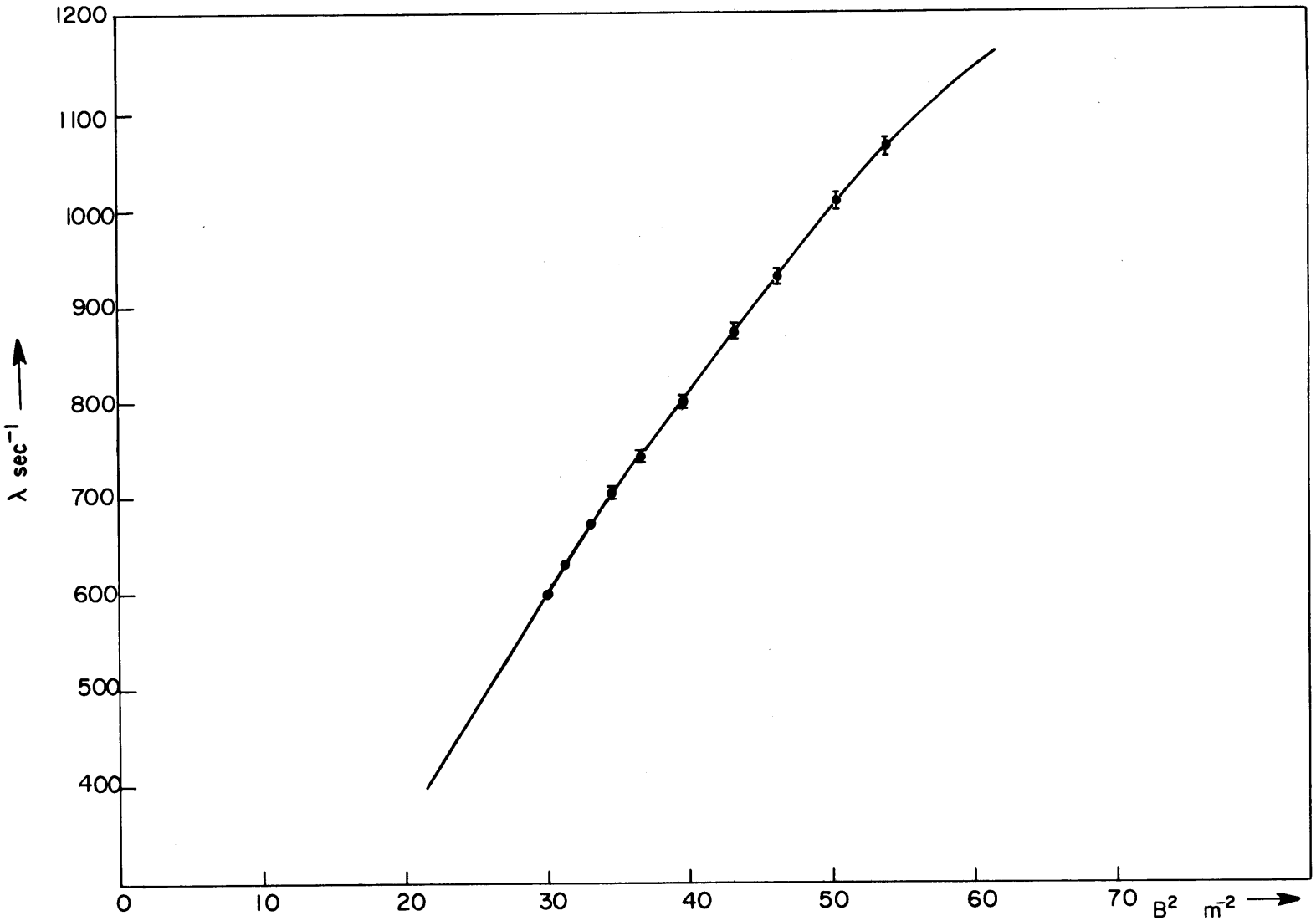

FIG. 7.3 MEASURED DECAY CONSTANT λ FOR PURE MODERATOR $[D_2O]$ AS A FUNCTION OF GEOMETRICAL BUCKLING B^2

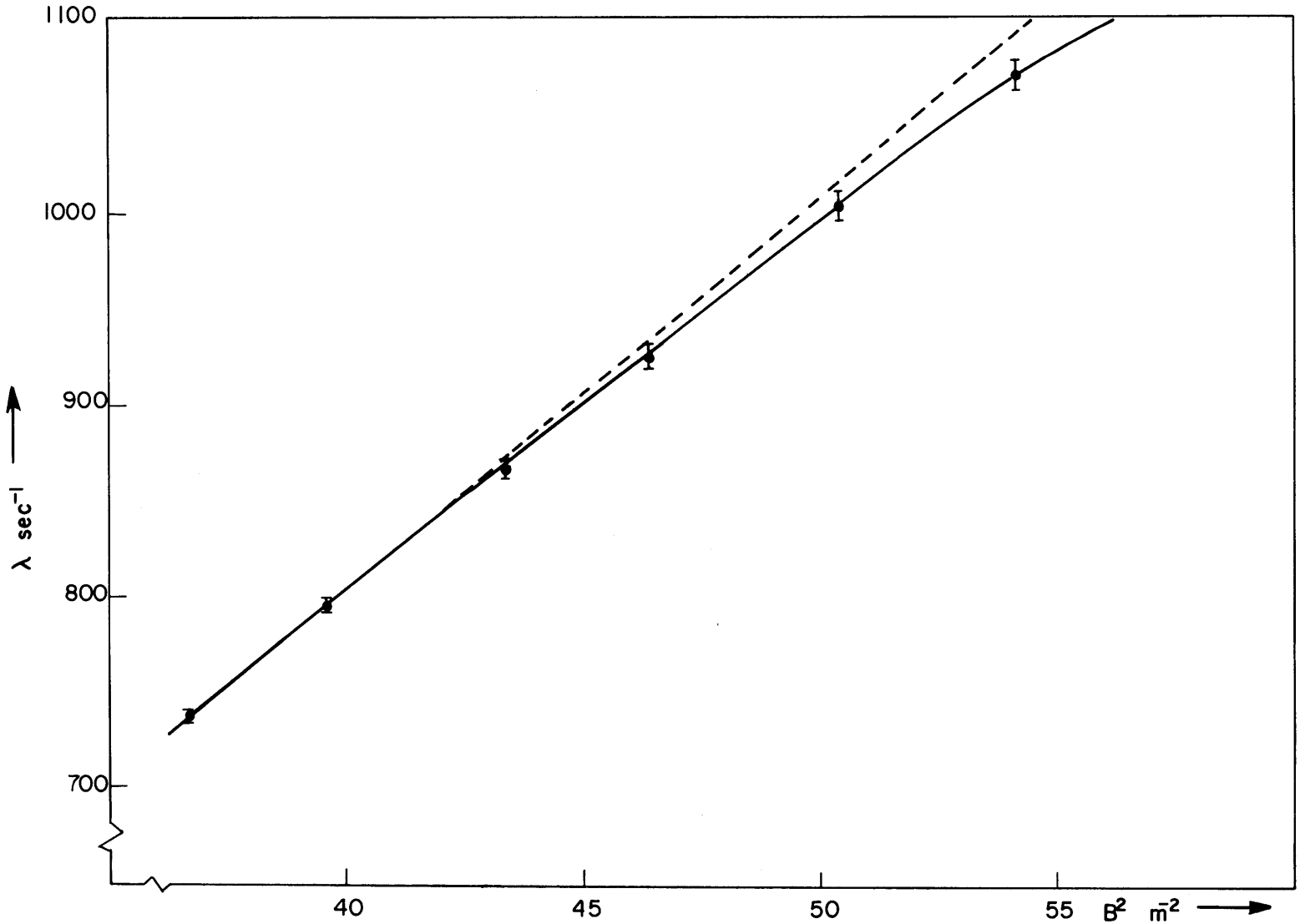

FIG. 3a MEASURED DECAY CONSTANT λ AS A FUNCTION OF B^2 FOR PURE MODERATOR [D_2O] IN THE LARGE BUCKLING RANGE

7.1.1.1 Determination of the Diffusion Parameters of Heavy Water

Finally, to obtain the values of $\overline{v\Sigma}_a$, D and C from the experimental data, first the upper six points corresponding to the high buckling range (Fig. 7.3a) were treated to a weighted, least-squares fit of the form of Eq. 7.8 by using the DEECEE code. The value of the infinite medium decay constant λ_o was computed for 99.60 mole per cent heavy water (sample analyzed at the Savannah River Laboratory) according to the relation:

$$\lambda_o = 2.2 \times 10^5 \, N_{D_2O}\left[p\sigma_{D_2O}+(1-p)\sigma_{H_2O}\right]. \tag{7.10}$$

Here, N_{D_2O} is the number of heavy-water molecules per cm^3; σ_{D_2O} and σ_{H_2O} are, respectively, the 2.2×10^5 cm/sec microscopic absorption cross-section of heavy and light water and p is the heavy-water concentration. The value of λ_o as calculated above represents a Maxwellian-averaged value. The values of the 2.2×10^5 cm/sec absorption cross-sections used were: σ_{D_2O} = .0012 barn and σ_{H_2O} = 0.66 barn (Ref. 4). For 99.60 mole per cent D_2O, this yields a value of λ_o = 26.6 sec^{-1}. With this value of λ_o, the least-squares fit of the (λ, B^2) data yields the following values for D and C:

$$vD = (1.961 \pm 0.020) \times 10^5 \ cm^2 \ sec^{-1}, \tag{7.11a,b}$$

$$C = (4.87 \pm 0.31) \times 10^5 \ cm^4 \ sec^{-1}.$$

The temperature of the heavy water was 20° C.

The complete set of (λ, B^2) data in Table 7.1 was then analyzed. An analysis by means of the DIFFN code showed that the buckling values did not represent a wide enough range to permit a three-parameter fit. A two-parameter fit of the form:

$$\lambda = \overline{v\Sigma}_a + vDB^2 - CB^4, \tag{7.12}$$

with the value of C obtained above in Eq. 7.11b, was therefore attempted, yielding the values:

$$\overline{v\Sigma}_a = (27.0 \pm 5.0)\ \text{sec}^{-1}\ ,$$
$$vD = (1.967 \pm 0.023) \times 10^5\ \text{cm}^2\ \text{sec}^{-1}\ . \qquad (7.13a,b)$$

The values of vD in Eqs. 7.11a and 7.13b are consistent within the limits of the uncertainties. Hence, the final values of the thermal neutron diffusion parameters of 99.60 mole per cent heavy water at 20° C for the buckling range investigated (30-55 m^{-2}), are:

$$\overline{v\Sigma}_a = (27.0 \pm 5.0)\ \text{sec}^{-1}\ ,$$
$$vD = (1.967 \pm 0.023) \times 10^5\ \text{cm}^2\ \text{sec}^{-1}\ , \qquad (7.14a,b,c)$$
$$C = (4.87 \pm 0.31) \times 10^5\ \text{cm}^4\ \text{sec}^{-1}\ .$$

These values are compared in Table 7.2 with the values obtained by other investigators in the literature. While the present work was in progress, Meister and Kussmaul[5] reported the results of their pulsed neutron die-away experiments for the measurements of the thermal neutron diffusion parameters of 99.82 mole per cent heavy water at 22° C, based on a wide buckling range (13 m^{-2} to 470 m^{-2}). Their results are also included in Table 7.2. The values of vD and C from the present work are in good agreement with those of Meister and Kussmaul. The somewhat lower value of vD is due to the difference in the concentration of heavy water. Although the value of $\overline{v\Sigma}_a = (27.0 \pm 5.0)\ \text{sec}^{-1}$ is consistent with the value $\lambda_o = 26.6\ \text{sec}^{-1}$ calculated from nuclear cross-sections for 99.60 per cent D_2O, it is not very significant because of its large uncertainty.

7.2 PULSED NEUTRON EXPERIMENTS IN MODERATOR WITH CONTROL RODS

The values of the diffusion parameters obtained in the last section were used to evaluate the geometrical buckling of cylindrical moderator assemblies modified by placing individual absorbing rods along the central axis. In these experiments, the 36-inch-diameter tank was used, filled with heavy water to a height of 132.5 cm; an overflow vent on the side of the tank allowed the level of heavy water to be maintained constant during the run. In all the runs, the long, external BF_3 counter was used for the detection of thermal neutrons. The rods were fixed at the top and bottom so as to be located exactly along the vertical axis of the assembly.

TABLE 7.2

Comparison of the Thermal Neutron Diffusion Parameters of Heavy Water

	Brown and Hennely[6] (Steady State)	Ganguly and Waltner[3]	Meister and Kussmaul[5]	Present Work
Buckling Range, m^{-2}	-	630 - 1000	13 - 470	30 - 55
Temperature, °C	20	20	22	21
Mole % D_2O	99.30	99.88	99.82	99.60
$\lambda_o = \overline{v\Sigma_a}$ sec^{-1}	-	-	19.0 ± 2.5	27.0 ± 5.0
$D_o = vD \times 10^{-5}$ cm^2 sec^{-1}	(2.051 ± 0.025)*	2.08 ± 0.05	2.000 ± 0.009	1.967 ± 0.023
$C \times 10^{-5}$ cm^4 sec^{-1}	-	3.72 ± 0.50	5.25 ± 0.25	4.87 ± 0.31

*From the value of $D\left(=\frac{D_o}{\bar{v}}\right) = (0.827 \pm 0.010)$ cm, using $\bar{v} = \frac{2}{\sqrt{\pi}} \times 2.2 \times 10^5$ cm sec^{-1}.

The thermal neutron decay curves of the assembly with and without a typical rod (7.94 cm diameter) along the axis are shown in Fig. 7.4. A significant change in the decay constant is evident. Altogether, seven different rod sizes were investigated. The results are summarized in Table 7.3. The values of the geometrical buckling B^2 are found by solving Eq. 7.8 as a quadratic in B^2, with the values of the parameters determined experimentally in the last section. Figure 7.5 shows a graph of the change in buckling produced by the rod as a function of its diameter, and compares the results with a theoretical curve. The latter is obtained on the basis of one-group theory with values of the extrapolation distance for the thermal flux in the rods obtained from measurements in exponential experiments[7] (Section 7.6.1.1). The agreement is fair, although one-group theory somewhat overestimates the effectiveness of the rod in changing the buckling.

The results listed in Table 7.3 will be used later in the evaluation of the thermal neutron lifetimes for the different configurations and the values of β/ℓ.

7.3 PULSED NEUTRON EXPERIMENTS WITH THE LATTICE FOR THE DETERMINATION OF ITS REACTOR PARAMETERS

The first multiplying system to be fully investigated with the methods developed in Section 3.5 was a lattice of slightly enriched uranium fuel rods moderated by heavy water. The U^{235} concentration was 1.03 per cent and the 0.25-inch-diameter fuel rods clad in aluminum of thickness 0.028 inch were arranged in a triangular lattice with a spacing of 1.75 inches. The actual fuel length was 48 inches, so that in the lattice there was a bottom reflector of 2.5 inches, including aluminum end plugs, adapter and the grid plate. The entire lattice was placed in a tank of inner diameter 36 inches. This tank was also used in the moderator experiments described in the two preceding sections and the over-all experimental arrangement and detection systems used were the same. When the small BF_3 counter was used along the axis in the assembly, the central thimble replaced the single central fuel element and was surrounded by six fuel rods as shown in Fig. 7.6. The change could be made with the

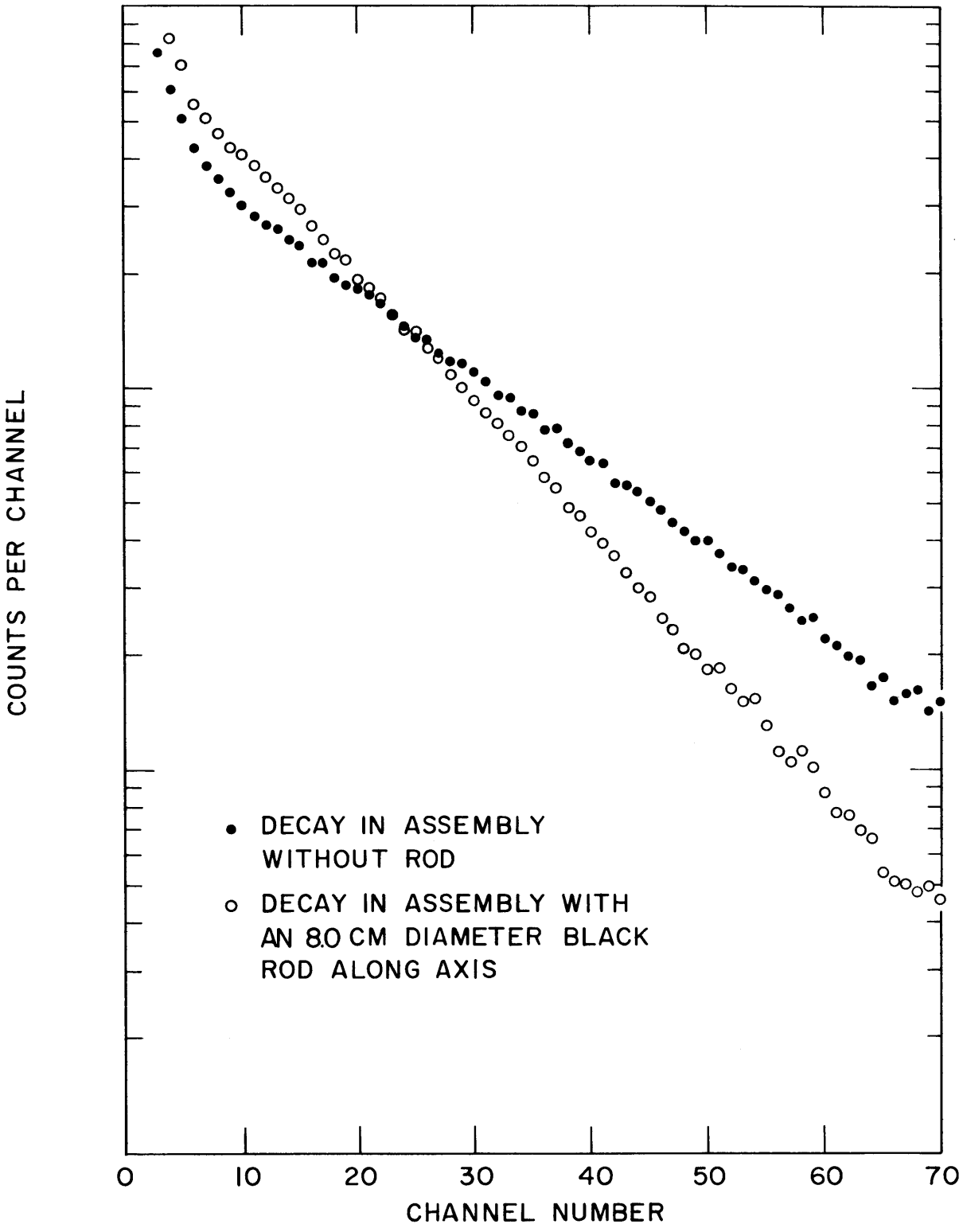

FIG. 7.4 THERMAL NEUTROR DECAY CURVES IN PURE MODERATOR [D_2O] ASSEMBLY (36 INCH DIAM TAN), WITH AND WITHOUT A THERMALLY BLACK ROD ALONG AXIS.

TABLE 7.3

Measured Decay Constant of a Cylindrical Pure Moderator Assembly with Thermally Black Rods of Different Radii Along the Axis

Rod Radius cm	Decay Constant λ, sec^{-1}	Geometrical Buckling B^2, m^{-2}	Change of Buckling ΔB^2, m^{-2}	Fractional Change of Buckling $\frac{\Delta a^2}{a_o^2}$, $\times 10^{-2}$
None	594.1 ± 4.0	29.02 ± 0.22	–	–
0.635	670.3 ± 4.3	33.12 ± 0.24	4.10 ± 0.32	16.11 ± 1.2
1.295	728.5 ± 4.2	35.97 ± 0.24	6.95 ± 0.32	27.12 ± 1.2
1.714	757.3 ± 5.1	37.49 ± 0.25	8.47 ± 0.33	33.05 ± 1.3
2.209	789.8 ± 5.4	39.22 ± 0.26	10.20 ± 0.34	39.80 ± 1.3
2.667	813.7 ± 6.0	40.58 ± 0.26	11.56 ± 0.34	45.10 ± 1.3
3.327	848.1 ± 6.4	42.37 ± 0.27	13.35 ± 0.35	52.08 ± 1.4
3.969	875.5 ± 6.4	43.83 ± 0.28	14.81 ± 0.36	57.78 ± 1.4

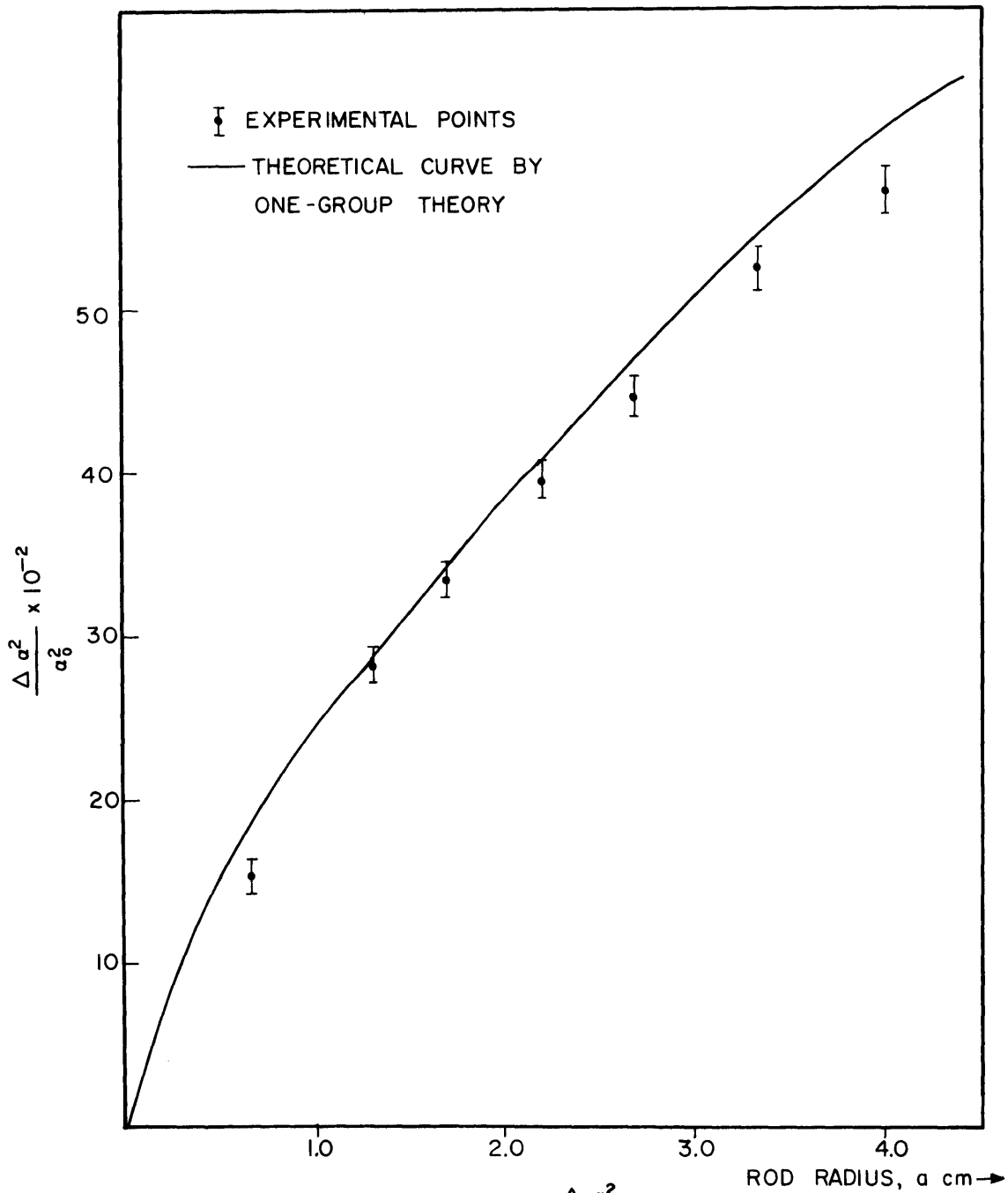

FIG. 7.5 FRACTIONAL BUCKLING CHANGE $\frac{\Delta a^2}{a_0^2}$ CAUSED BY THERMALLY BLACK RODS IN PURE MODERATOR $[D_2O]$ ASSEMBLY, BY THE PULSED NEUTRON METHOD

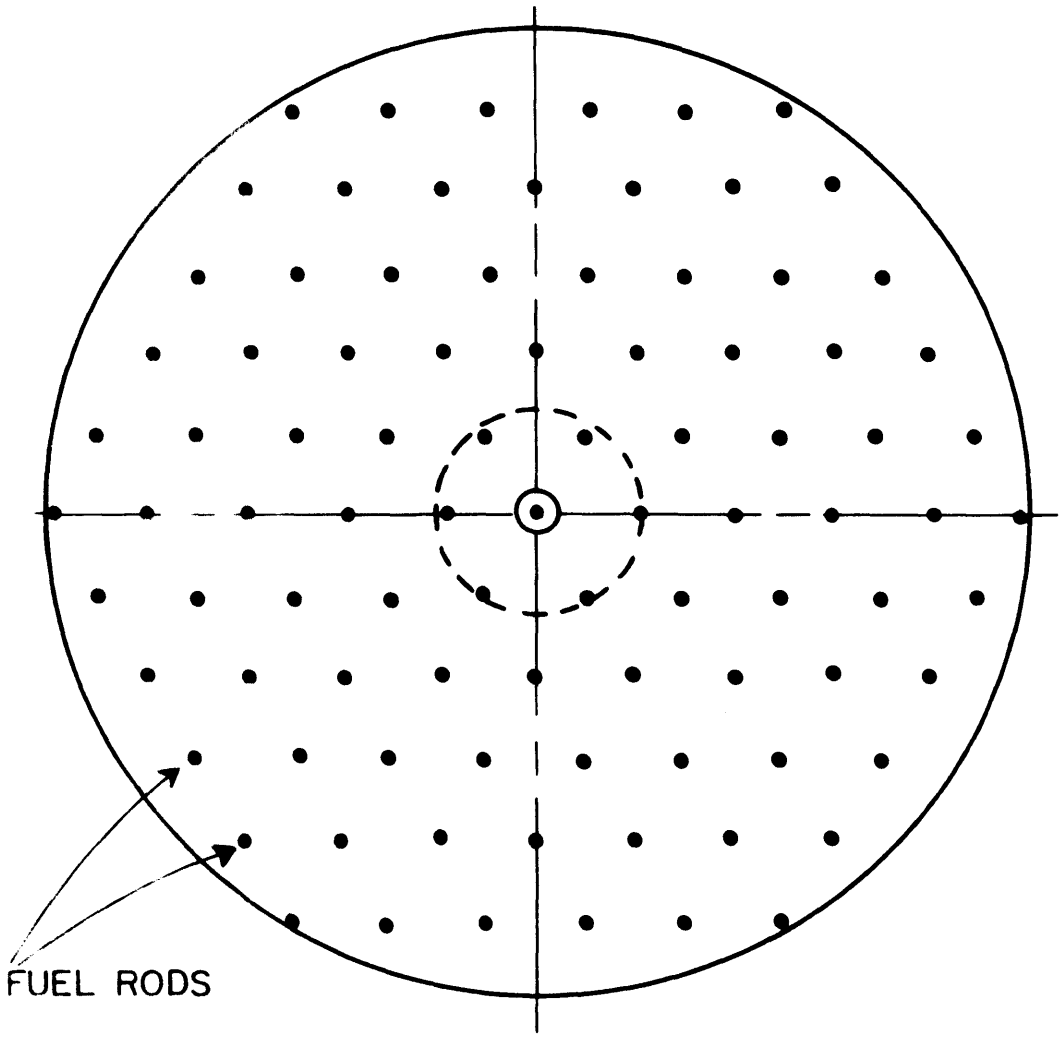

FIG 7.6 CONFIGURATION OF FUEL RODS IN THE LATTICE
SMALL CENTRAL HOLE IS FOR AXIAL THIMBLE
LARGE CIRCLE REPRESENTS REGION OF CONTROL ROD INSERTION.

aid of a hole in the top plastic adapter especially fabricated for this purpose and for control rod experiments. The circular cadmium plate clad in aluminum was allowed to rest in and cover the bottom of the tank so that the whole assembly was surrounded on the outside surface, including the top, with 0.020-inch-thick cadmium.

The effect on the measured decay constant, of the detector location and waiting time was investigated first. Figure 7.7 shows the thermal neutron decay curves (corrected for count losses and background) obtained with the long external detector and with the small detector placed axially at half the moderator height inside the assembly. As in the case of the moderator runs, although the initial slopes are markedly different, each gives the same asymptotic decay constant after the initial flux stabilization region is excluded from the analysis. This result is shown in Fig. 7.8 in which the decay constant for each run is shown as a function of the waiting time. The decay constant approaches the constant value from different directions, and the delay time is about the same in the two cases.

The variation of the decay constant with the axial position (height) of the small BF_3 detector is more interesting and instructive. From physical intuition and symmetry considerations, it would appear that the most natural location for the detector is at half the moderator or assembly height. This expectation is borne out since only in this case does the decay constant approach a constant value with a reasonable waiting time, and this constant value is the same as that obtained with the long external detector.

The effect of placing the small BF_3 counter at several heights along the axis was also studied. Thermal flux decay curves in three typical cases, with the detector at the midway point, and 7 inches above and below it, are shown in Fig. 7.9. It is seen that in the latter two cases, a very long time is needed for the flux to show a persisting single-exponential behavior; by this time, the fundamental mode has decayed to such an extent that the remaining portion of the curve is statistically unreliable. In the upper position, the proximity of the fast source interferes with the quick establishment of a fundamental mode. The above observation is strengthened by considering the variation of decay constant with waiting time in the three cases, as shown in Fig. 7.10. While the decay constant for the central

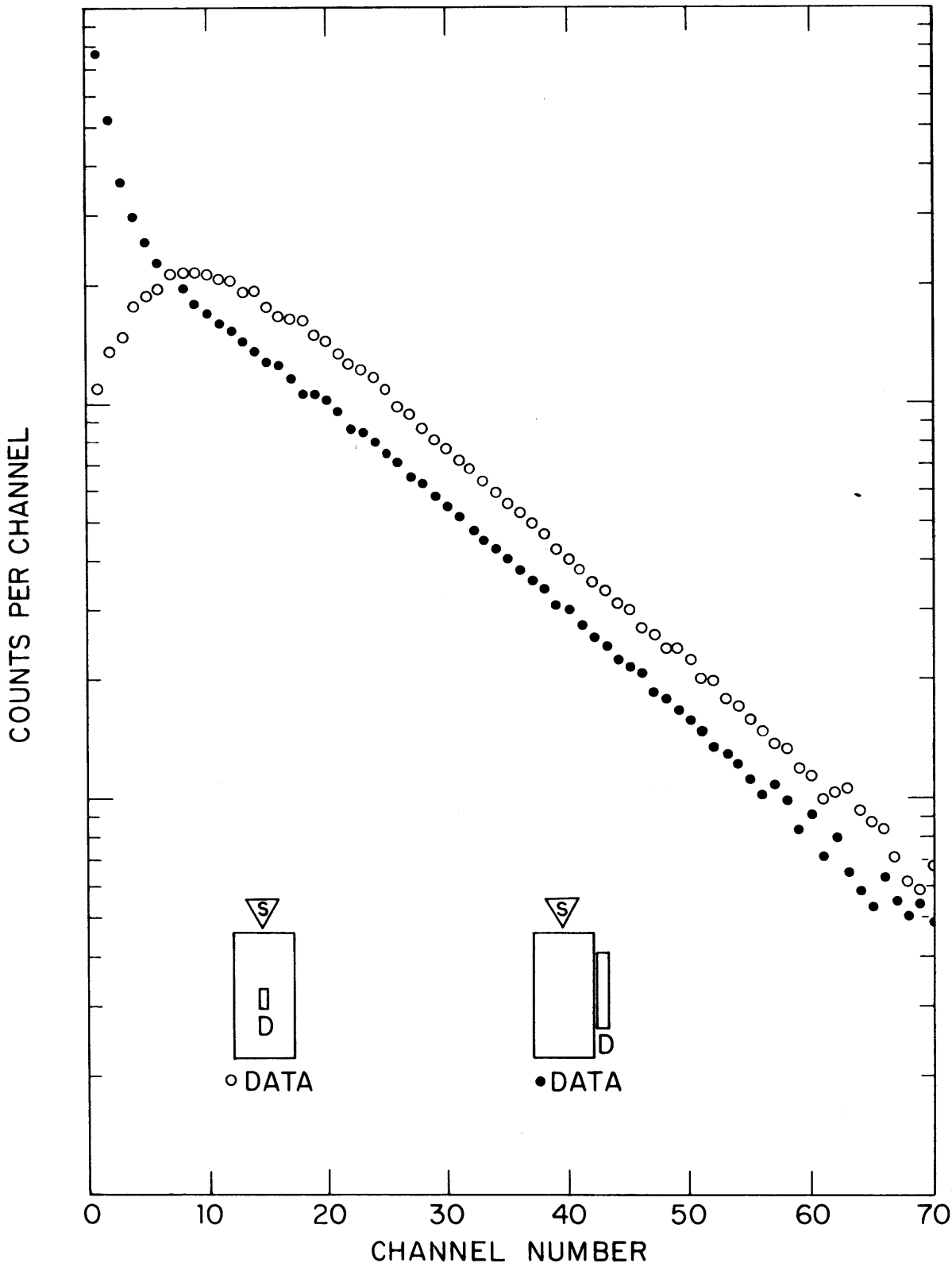

FIG. 7.7 THERMAL NEUTRON DECAY CURVES IN THE MULTIPLYING ASSEMBLY WITH DIFFERENT DETECTION SYSTEMS.

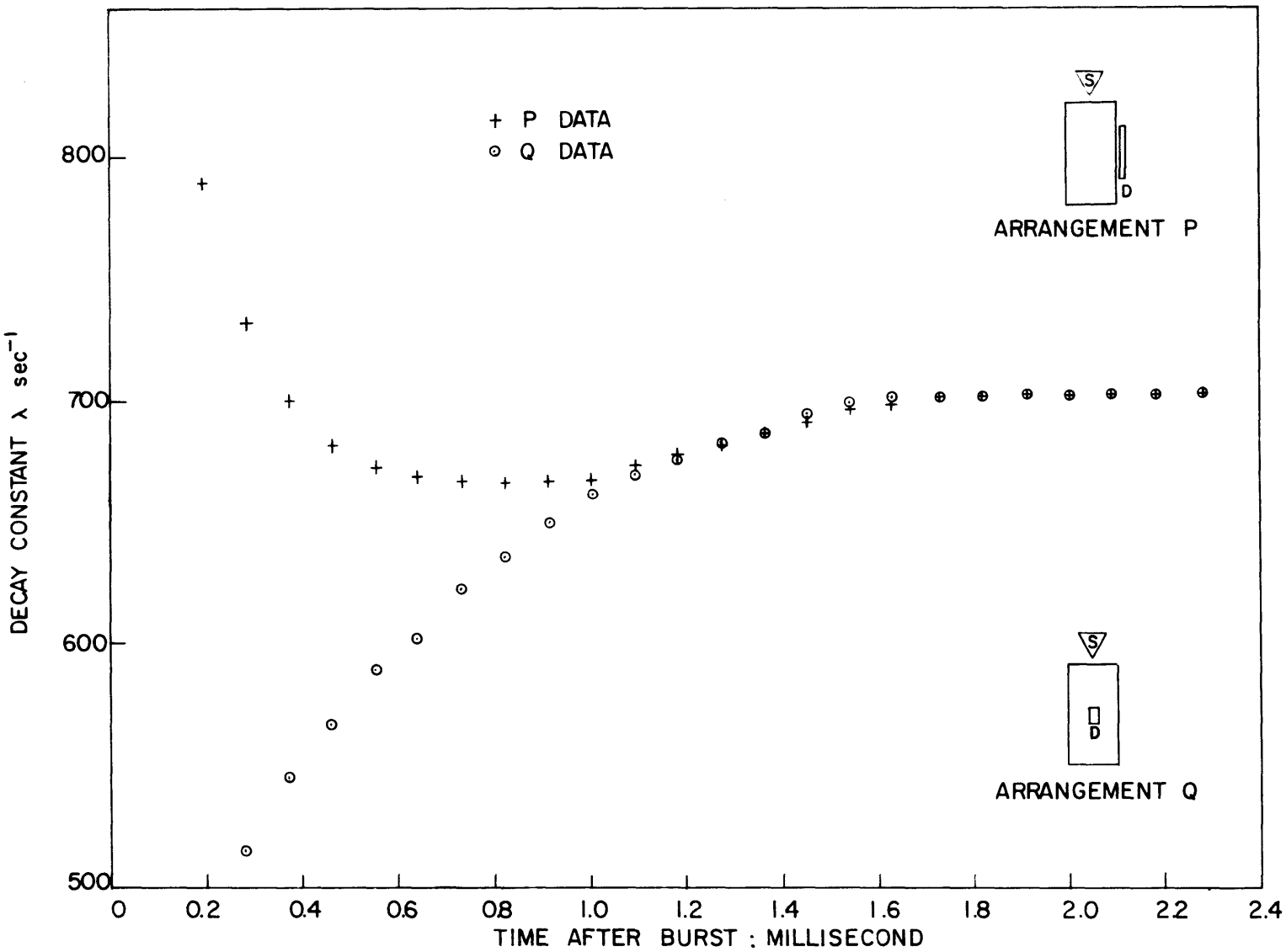

FIG 7.8 VARIATION OF THE MEASURED DECAY CONSTANT WITH 'WAITING TIME' IN THE MULTIPLYING ASSEMBLY, WITH DIFFERENT DETECTORS.

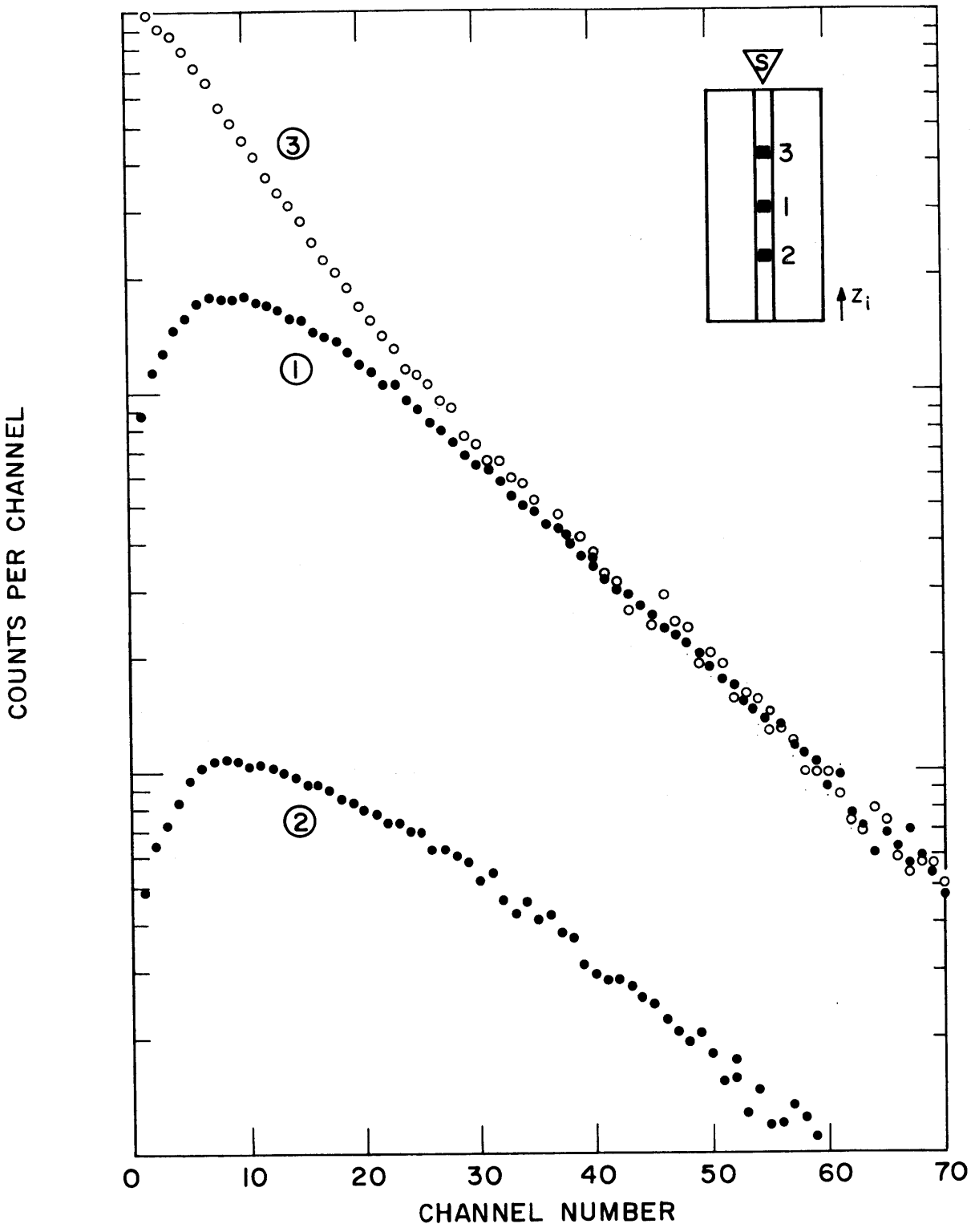

FIG. 7.9 THERMAL NEUTRON DECAY CURVES IN MULTIPLYING ASSEMBLY WITH DIFFERENT DETECTOR LOCATIONS ALONG CENTRAL AXIS.

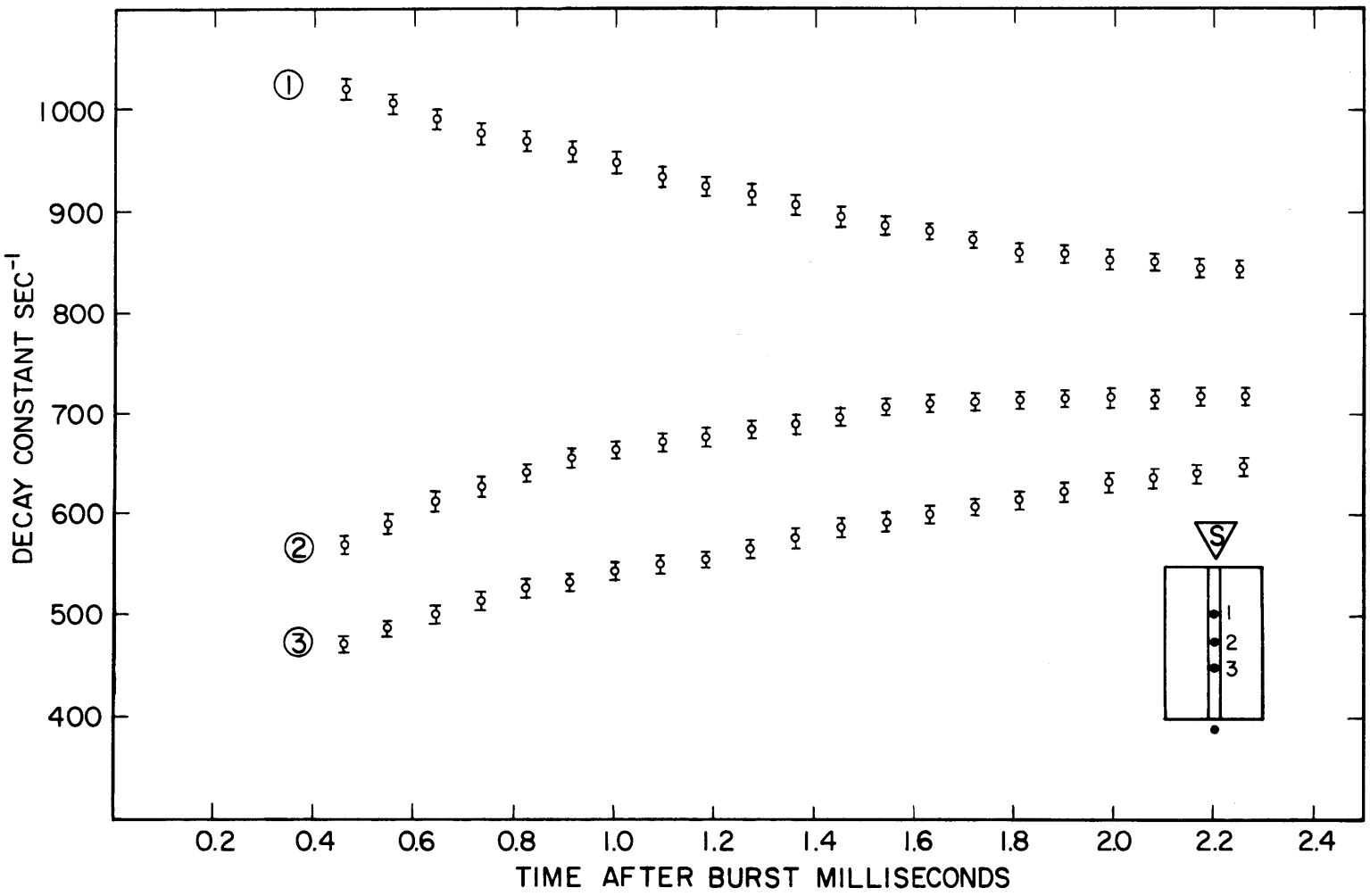

FIG. 7.10 THE VARIATION OF THE PROMPT NEUTRON DECAY CONSTANT WITH " WAITING TIME" IN MULTIPLYING ASSEMBLY FOR DIFFERENT DETECTOR LOCATIONS ALONG THE CENTRAL AXIS.

position assumes a constant value at about 2.2 msec, in the other two cases it continues to vary slowly and seems to tend to the constant value of the middle curve.

As an independent study, the effect of harmonics was further investigated by mapping the axial flux at different stages of the stabilization of the flux in the assembly. By moving the small BF_3 counter successively to five different positions along the axis and measuring the prompt neutron flux decay in each case, the axial flux distribution $\phi(z_i,t)$ was obtained at different times. An attempt was made to normalize these runs by keeping the total number of bursts the same and maintaining the absolute source strength constant. However, no special means were provided to ensure normalization; a separate monitor detector can be used for this purpose. The axial flux distribution at different times after the burst is shown in Fig. 7.11 which brings out several interesting features. Just after the injection of the fast neutron burst from the source (at t = 105 μs), we have a highly skew flux distribution which peaks near the top of the tank, i.e., near the location of the source. The peak gradually moves toward the center of the tank and the distribution approaches a symmetrical normal mode. This phenomenon begins at about the value t = 2.3 msec and confirms the earlier independent observation of a waiting time of about 2.2 msec at the full heavy water height.

The effect of the perturbation introduced by the thimble, the detector, etc. was also examined. The heavy water was kept at the full height of 130.5 cm, and the external long BF_3 counter was used. The decay constant was measured with and without the thimble and/or the small BF_3 counter and with and without the central fuel element in place along the axis. The effect of removing the central thimble is to change the measured decay constant by as much as 1.5 per cent. The small BF_3 counter or the central fuel element by themselves do not produce any significant effect on the decay constant. The correction due to the introduction of the thimble is small and will be considered later in the discussion on sources of errors.

The delayed neutron decay was studied by locating the small BF_3 detector at half the core height and running at a repetition rate of one pulse per second with a channel width of 1280 μsec. The pulsed source was in operation for some time before this run was started. Since the assembly

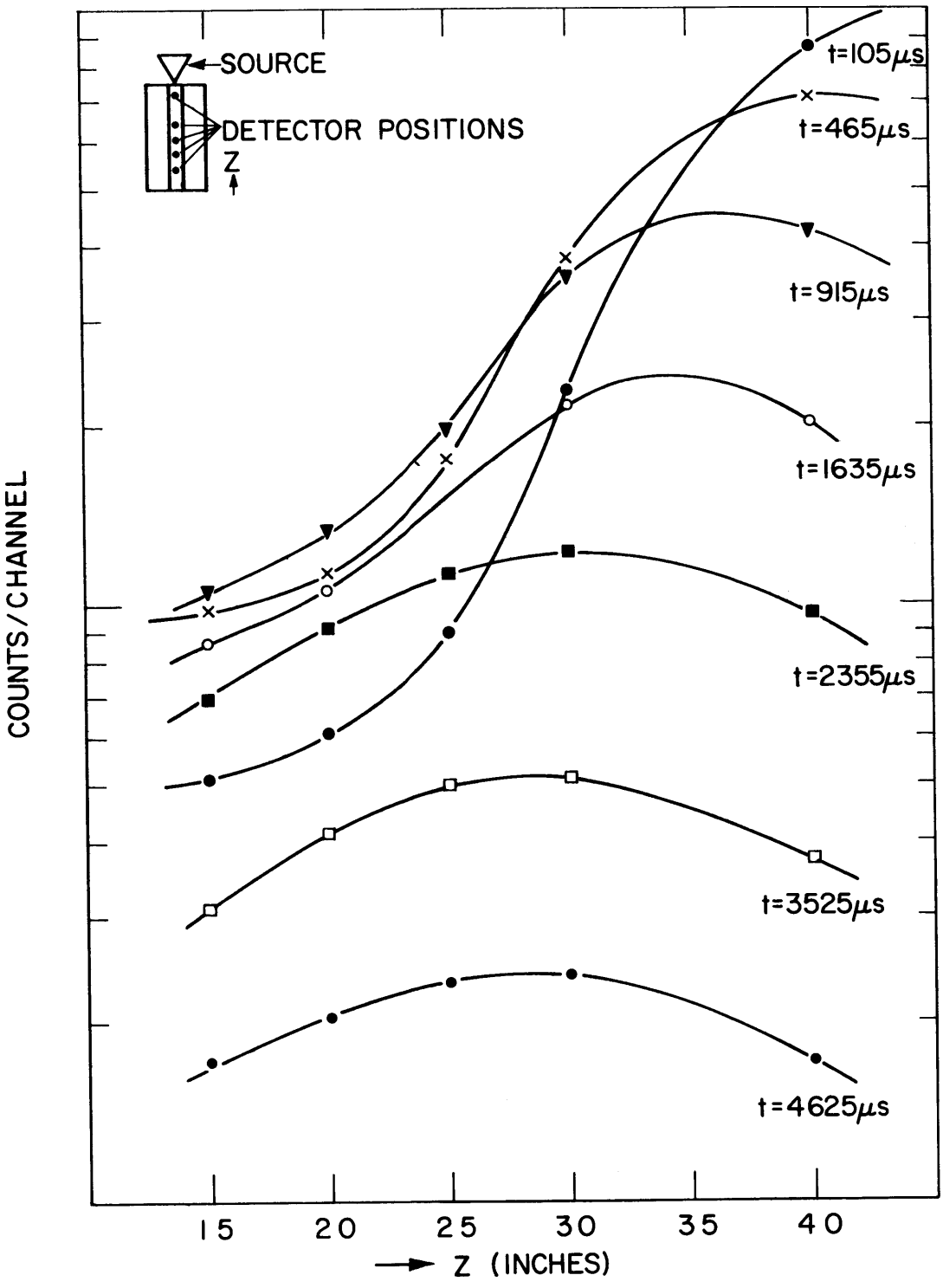

FIG.7.11 SPATIAL THERMAL FLUX DISTRIBUTION IN AXIAL DIRECTION $\phi(z,t)$ AT DIFFERENT TIMES t AFTER BURST IN THE MULTIPLYING ASSEMBLY

was far subcritical, the statistics of the delayed neutron tail were very poor and no distinct delayed neutron contribution from the assembly was noticeable. The over-all variation in the delayed neutron tail was less than 3 per cent within a 100-msec timing cycle and could be considered as a constant background to be subtracted from the observed counts. The background intensity can be determined from the pre-burst background, i.e., the first, channel (Section 5.3.4) of the time analyzer, and the corrected prompt neutron flux $\phi(t)$ can be determined. The background intensity can also be obtained from the code EXPO (Appendix 2) which reduces the experimental data or by averaging the counts in the end channels of the decay curve.

After these auxilliary studies, the main runs were made and the prompt neutron decay constant λ was measured as a function of the geometrical buckling, B^2, corresponding to different heights of the moderator in the assembly. In every case, the small BF_3 counter was located at half the moderator height and the asymptotic decay constant determined by the methods described above. In all, eleven different points were obtained for the (λ, B^2) data. The results are shown in Table 7.4 and the λ vs. B^2 curve is plotted in Fig. 7.12.

The points are found to lie approximately on a straight line, especially in the lower buckling range, thus supporting qualitatively the conclusion drawn from the theoretical study (Section 3.5). In Fig. 7.13, the (λ vs. B^2) curves for the pure moderator assembly and the subcritical lattice system are shown on the same graph. This figure brings out the mutually counteracting effects of additional absorption and multiplication due to the introduction of the lattice in the pure moderator tank.

7.3.1 Evaluation of the Lattice Parameters

In this section, we follow the methods outlined in Section 3.5 and utilize the data obtained so far, from the pulsed neutron runs on pure moderator and lattice assemblies, to obtain quantitative information about the lattice. For this analysis, we need the values of the effective delayed neutron fraction $\bar{\beta}$ and the neutron age to thermal τ for the lattice; the calculation of these quantities for the lattice is shown in detail in Appendix 3. The parameter $\bar{\beta}$ is calculated by taking into account, also, the delayed

TABLE 7.4

Measured Prompt Neutron Decay Constant as a Function of Buckling for the Lattice of 0.25-Inch-Diameter, 1.03% U^{235} Uranium Rods with a Triangular Spacing of 1.75 Inches

Moderator Height H cm	Buckling B^2 m^{-2}	Prompt Decay Constant λ sec^{-1}
130.2	31.26	713.6 ± 6.5
122.0	31.95	741.5 ± 6.4
110.7	33.31	787.3 ± 7.0
101.5	34.50	826.2 ± 7.2
90.7	36.89	902.5 ± 8.1
80.5	39.78	1001.0 ± 8.9
75.4	41.71	1052.2 ± 8.7
70.6	43.81	1126.1 ± 10.0
65.8	46.48	1199.5 ± 11.1
60.8	49.78	1294.5 ± 11.8
55.6	54.22	1427.0 ± 13.1

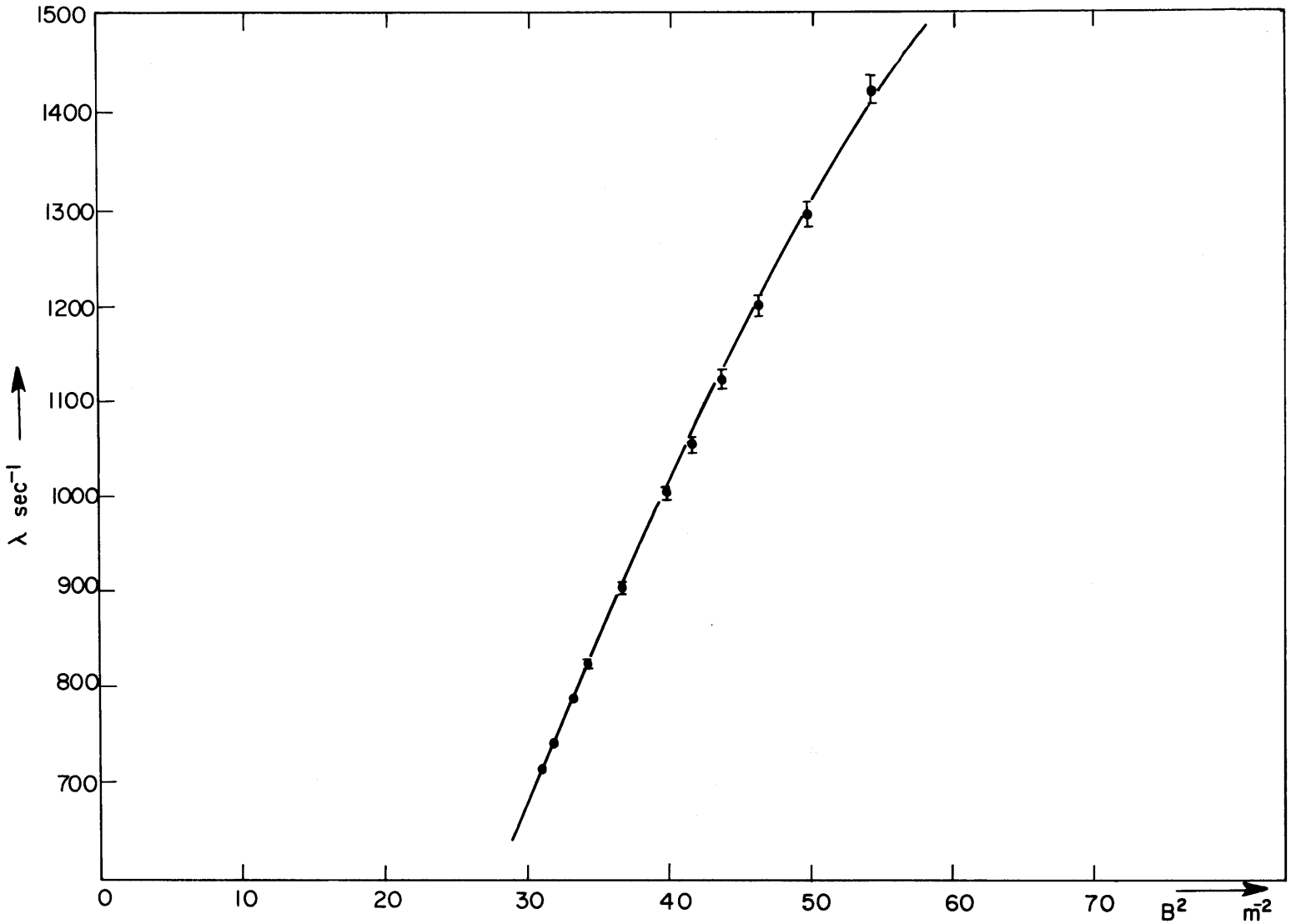

FIG. 7.12 PROMPT NEUTRON DECAY CONSTANT λ AS A FUNCTION OF BUCKLING B^2, FOR THE LATTICE OF 0.25-INCH DIAM, 1.03 % U^{235} RODS IN HEAVY WATER WITH A TRIANGULAR SPACING OF 1.75 INCHES

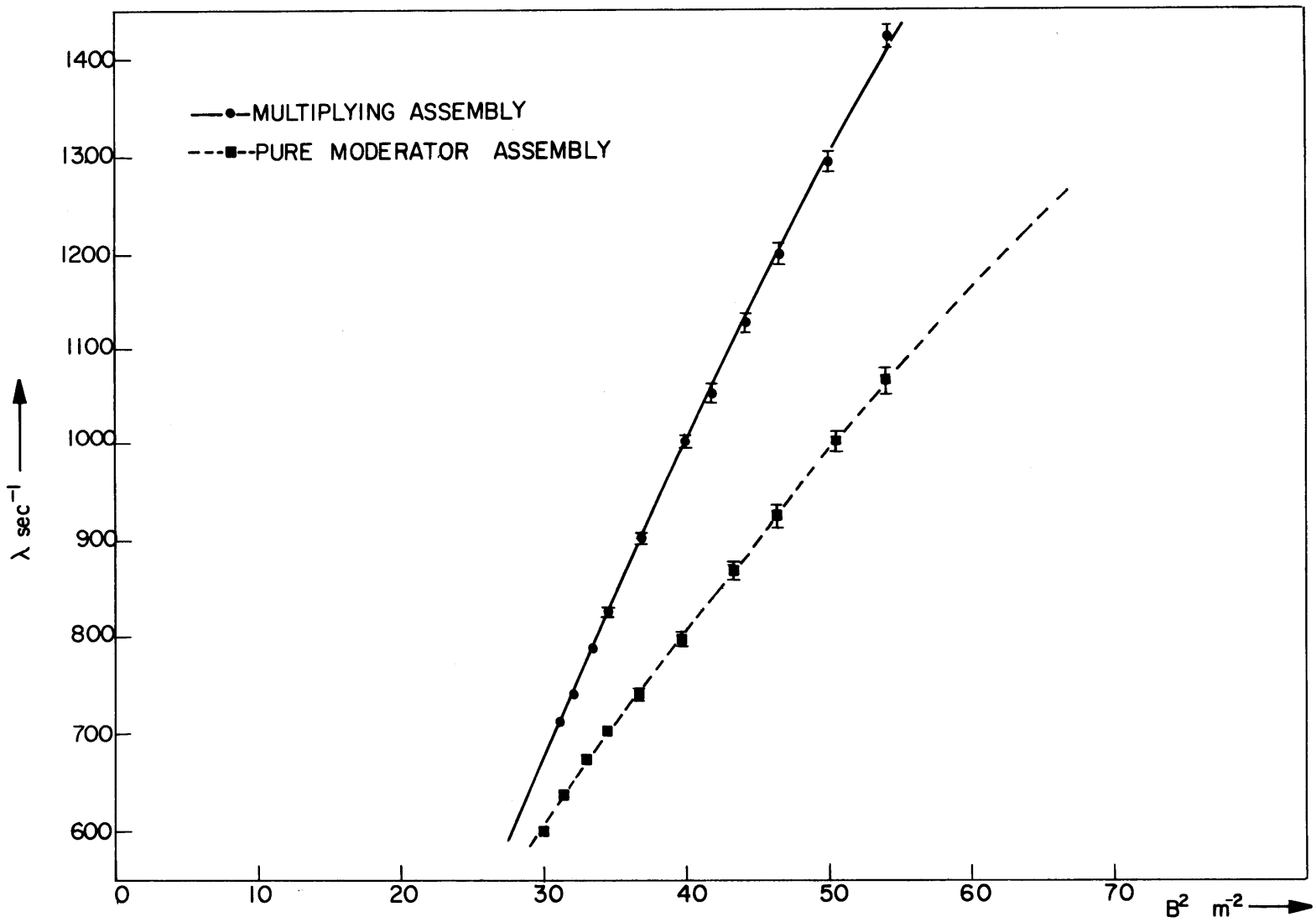

FIG. 7.13 VARIATION OF THE MEASURED DECAY CONSTANT λ WITH GEOMETRICAL BUCKLING B^2 FOR A MULTIPLYING AND A NON-MULTIPLYING ASSEMBLY.

photoneutrons in heavy water; and τ is corrected for light-water contamination, inelastic scattering and the reduced moderator volume. We have the following values:

$$\bar{\beta} = 0.00783$$
$$\tau = 120.0 \pm 3 \qquad (7.12a,b)$$

We transcribe the data obtained earlier from moderator runs:

$$\overline{v\Sigma_a}^{mod} = (27.0 \pm 5.0)\ sec^{-1}$$
$$\overline{vD} = (1.967 \pm 0.023) \times 10^5\ cm^2/sec \qquad (7.13a,b)$$

Finally, if the λ vs. B^2 data from runs on the subcritical assembly (Fig. 7.12) are fitted to an expression of the form:

$$\lambda = -m + nB^2 - qB^4\ , \qquad (7.14)$$

we get:

$$m = \overline{v\Sigma_a}\left((1-\bar{\beta})k_o - 1\right) = (467.2 \pm 23.7)\ sec^{-1}\ ,$$
$$n = \overline{vD} + \overline{v\Sigma_a}(1-\bar{\beta})k_o\tau = (4.203 \pm 0.048) \times 10^5\ cm^2\ sec^{-1}\ ,$$
$$q = \frac{1}{2}\overline{v\Sigma_a}(1-\bar{\beta})k_o\tau^2 = (13.2 \pm 2.5) \times 10^6\ cm^4\ sec^{-1}\ . \qquad (7.14a,b,c)$$

In the range of values of the buckling covered by the data, a typical value of $B^2\tau$ is 0.4, and it is necessary to include the term in B^4 in the approximation $e^{-B^2\tau} \approx 1 - B^2\tau + \frac{1}{2}B^4\tau^2$, so that Eq. 3.17 for the decay constant reduces to Eq. 7.14. The λ vs. B^2 points are very well represented by the fitted curve with the values of Eqs. 7.14a,b,c and Eq. 7.14 is adequate.

From Eqs. 7.14a and 7.14b, we get for the total absorption cross section in the lattice:

$$\overline{v\Sigma_a} = \frac{n - \overline{vD}}{\tau} - m\ , \qquad (7.15)$$

and, using the values given above, we get:

$$\overline{v\Sigma_a} = (1396.1 \pm 65.5)\ sec^{-1}\ . \qquad (7.16)$$

From Eqs. 7.13a and 7.16, we obtain the macroscopic absorption cross section for the fuel as:

$$\overline{v\Sigma}_a^{fuel} = \overline{v\Sigma}_a - \overline{v\Sigma}_a^{mod} = (1369.1 \pm 65.7)\ sec^{-1} .$$

We also have, from Eqs. 7.14a and 7.14b, the expression for the prompt infinite multiplication factor:

$$(1-\bar{\beta})k_o = \frac{n - \overline{vD}}{(n-\overline{vD}) - m\tau} , \tag{7.18}$$

which can be written as:

$$\frac{1}{(1-\bar{\beta})k_o} = 1 - \frac{m\tau}{(n-\overline{vD})} . \tag{7.19}$$

Putting in the values of the constants m, n, $\overline{vD}$ and τ, we get:

$$(1-\bar{\beta})k_o = 1.335 \pm 0.026 , \tag{7.20}$$

from which, by using Eq. 7.12a, we get:

$$k_o = 1.345 \pm 0.026 . \tag{7.21}$$

The diffusion area in the moderator (99.60 mole per cent heavy water) is given by:

$$L_m^2 = \frac{\overline{vD}}{\overline{v\Sigma}_a^m} = (7280 \pm 138)\ cm^2 . \tag{7.22}$$

As discussed in Section 3.5, we assume that since the fuel concentration is low, $D \approx D^{mod}$. Then the diffusion area in the lattice is given by:

$$L^2 = \frac{\overline{vD}}{\overline{v\Sigma}_a} = (140.9 \pm 6.9)\ cm^2 . \tag{7.23}$$

The moderator thermal utilization, f_m, is given as:

$$f_m = \frac{L^2}{L_m^2} = 0.0193 \pm 0.0037 , \tag{7.24}$$

so that,

$$f_U + f_{A\ell} = 1 - f_m = 0.9807 \pm 0.0037 , \tag{7.25}$$

where $f_{A\ell}$ represents the neutron absorption by the cladding.

If we use the value of the "thermal utilization" for the cladding given by the THERMOS code,

$$f_{A\ell} = 0.015 \ , \tag{7.25a}$$

then Eq. 7.25 yields the thermal utilization for the lattice:

$$f = 1 - f_{A\ell} - f_m = 0.9657 \pm 0.0037 \ .$$

Actually, it can be shown[8] that Eq. 7.24 contains six other terms which are negligible provided $N_m \gg N_U$; i.e., if the fuel concentration is low. In the present case, $V_M/V_U = 52.4$ and the combined contribution of these terms amounts to about one per cent in f_m.

Now, the basic equation for the decay constant of the subcritical system is:

$$\lambda = \overline{v\Sigma}_a + \overline{vD}B^2 - \overline{v\Sigma}_a(1-\bar{\beta})k_o \, e^{-B^2\tau} \ . \tag{7.26}$$

For the subcritical assembly with full heavy water height, we have from Table 7.4,

$$\lambda = (713.6 \pm 6.5) \ \text{sec}^{-1} \quad \text{and} \quad B^2 = 31.26 \times 10^{-4} \ \text{cm}^{-2} \ . \tag{7.27}$$

Using these values and those of $\overline{vD}$ and $\overline{v\Sigma}_a$ from Eqs. 7.13a, 7.16, in Eq. 7.26, we get:

$$(1-\bar{\beta})k_o \, e^{-B^2\tau} = 0.929 \pm 0.064 \ . \tag{7.28}$$

We also have from the value of L^2 in Eq. 7.23 the thermal non-leakage factor,

$$\frac{1}{1 + L^2B^2} = 0.694 \pm 0.011 \ . \tag{7.29}$$

Hence, from the last two equations, we get the prompt multiplication factor (effective):

$$(1-\bar{\beta}) \, \frac{k_o \, e^{-B^2\tau}}{1 + L^2B^2} = 0.645 \pm 0.046 \ , \tag{7.30}$$

whence,

$$k = \frac{k_o \, e^{-B^2\tau}}{1 + L^2B^2} = 0.650 \pm 0.046 \ . \qquad (7.31)$$

Furthermore, the prompt neutron lifetime is:

$$\ell = \frac{1}{\overline{v\Sigma_a} + \overline{vD}B^2} = (497.3 \pm 16.4)\,\mu\text{sec} \ . \qquad (7.32)$$

The prompt-critical buckling B^2_{pc}, corresponding to $\lambda = 0$, is given by solving Eq. 7.14 as a quadratic in B^2, with the values of m, n and q from Eqs. 7.14a,b,c:

$$B^2_{pc} = (1152 \pm 53)\ \mu B \ . \qquad (7.33)$$

Finally, the material buckling for the subcritical assembly may be obtained from the two-group equation:

$$B^2_m = \frac{1}{2\tau L^2}\left[-(\tau+L^2) + \left\{(\tau+L^2)^2 + 4(k_o-1)\tau L^2\right\}^{1/2}\right]; \qquad (7.34)$$

with the values, obtained earlier:

$$\tau = (120 \pm 3)\ \text{cm}^2 \ , \qquad L^2 = (140.89 \pm 6.7)\ \text{cm}^2 \ ,$$

$$k_o = 1.3451 \pm 0.025 \ ,$$

we get:

$$B^2_m = (1250 \pm 72)\mu B \ .$$

We can also use the age-theory transcendental equation instead of Eq. 7.34 to evaluate the material buckling B^2_m.

Finally, the last of Eqs. 7.14 can be used to obtain a rough value for the neutron age in the lattice. If we put in the values of $v\Sigma_a$, $(1-\bar{\beta})k_o$, etc. from above, in Eq. 7.14, we get:

$$\tau = 118 \pm 20 \ .$$

The uncertainty is large but this does show that the value, $\tau = 120 \pm 3$, that has been used is reasonable.

These results will be discussed and evaluated in a later section.

7.4 PULSED NEUTRON EXPERIMENTS ON PERTURBED MULTIPLYING SYSTEMS

The next set of experiments, following the analysis outlined in Section 3.7, involved the measurement of the prompt decay constant of the subcritical assembly, perturbed by the full insertion of a single control rod along the axis. The same lattice was used as for the measurements described in Section 7.2. However, to make room for a control rod along the axis, the seven central fuel elements were removed and a 4.0-inch-diameter circular hole was opened in the special plastic adapter (Fig. 7.6). The fabrication of the control rods and the arrangement for positioning them along the axis rigidly, are described in Section 5.1.2. The control rods in all these experiments were hollow and empty, being closed at the bottom. The heavy-water level was maintained constant at the overflow line (132.5 cm). The detection system with the long, external BF_3 counter fixed longitudinally on the side of the tank (Section 5.3.3, Fig. 5.11b) was used throughout these runs. The pulsed neutron source was placed on the top lid of the tank along the axis and the assembly was surrounded on all sides by 0.020-inch-thick cadmium. At the end of each run, the time analyzer was allowed to sweep for about 10 minutes after the source was shut off so as to ensure the conditions for a quasi-equilibrium (Section 3.6.3); these same runs could then be used for the application of the $k\beta/\ell$ method (ibidem). The repetition rate was 10 pulses per second and the time analyzer channel width was 80 μsec. The delay multiplier of the time analyzer was set at X2 and the target delay (Section 5.3.5) at its maximum value, 100 μsec, so that all but the first 60 μsec of the decay curve could be mapped.

Cadmium control rods of seven different sizes were used and the decay constant was measured in each case. The results are shown in Table 7.5. The change in decay constant $\Delta\lambda$, with respect to the unperturbed lattice (without the seven central fuel elements), is related to the change in buckling caused by the rods, according to the relation (Section 3.7):

$$\Delta B^2 = \frac{\Delta\lambda}{vD + v\Sigma_a(1-\bar{\beta})k_o\tau\, e^{-B^2\tau}} \qquad (7.35)$$

TABLE 7.5

Measured Prompt Neutron Decay Constant and the Change in Buckling Due to Cadmium Rods of Different Radii Along the Axis; Lattice of 0.25-Inch Diameter, 1.03% U^{235} Uranium Rods in Heavy Water, with a Triangular Spacing of 1.75 Inches

Rod Radius cm	Prompt Decay Constant λ, sec^{-1}	Change in Decay Constant $\Delta\lambda$, sec^{-1}	Change in Buckling $\Delta B^2 = \Delta a^2 (10^{-4}\ cm^{-2})$	Fractional Buckling Change $\frac{\Delta a^2}{a^2} \times 10^{-2}$
None	689.9 ± 4.0	-	-	-
0.635	771.1 ± 5.1	81.2 ± 6.4	2.300 ± 0.18	8.97 ± 0.7
1.295	846.5 ± 5.4	156.6 ± 6.72	4.436 ± 0.19	17.30 ± 0.7
1.714	879.7 ± 6.1	189.8 ± 7.3	5.387 ± 0.21	21.02 ± 0.8
2.209	935.0 ± 7.0	245.1 ± 8.0	6.943 ± 0.23	27.09 ± 0.9
2.667	963.9 ± 7.7	274.0 ± 8.7	7.762 ± 0.24	30.28 ± 0.9
3.327	997.5 ± 8.2	307.6 ± 9.1	8.714 ± 0.26	34.00 ± 1.0
3.969	1029.9 ± 9.0	340.0 ± 9.8	9.632 ± 0.28	37.58 ± 1.1

The values of the parameters occurring in Eq. 7.35 have been obtained earlier – either through measurement or calculation. The buckling B^2 refers to the unperturbed lattice. Since the height of the core is maintained constant in all the runs, ΔB^2 is also the change in the radial buckling caused by the rod:

$$\Delta B^2 = \Delta a^2 \ . \tag{7.36}$$

The last column in Table 7.5 shows the value of the fractional change in radial buckling $\Delta a^2/a_o^2$, caused by the rods of different sizes. In Fig. 7.14, $\Delta a^2/a_o^2$ is plotted against the rod radius. These results will later be compared with the results of steady-state experiments and two-group calculations.

The value of the geometrical buckling with the control rod in the assembly from Table 7.3, and the value of the prompt neutron decay constant from Table 7.5, may be used to evaluate the prompt neutron lifetime ℓ, the parameter $\bar{\beta}/\ell$ and the negative reactivity of the assembly with the rod in place. The results are shown in Table 7.6. The value of the parameter $\bar{\beta}/\ell$ is seen to vary from 15.6 sec^{-1} to 17.6 sec^{-1} over the range of reactivity studied. The negative reactivity, or the degree of subcriticality of the lattice in any configuration, is calculated from the prompt neutron lifetime and the measured decay constant by the relation (Section 3.7.1):

$$\rho = \frac{\lambda - \frac{\bar{\beta}}{\ell}}{\frac{1}{\ell} - \lambda} . \tag{7.37}$$

The values of ρ for the lattice in the unperturbed state and with the control rods of different sizes individually inserted, are shown in the next to last column of Table 7.6. Finally, the last column of this Table 7.6 shows the reactivity worth, $\Delta\rho$, of the rods as measured by the change of subcriticality caused by the rod in the unperturbed assembly. The values of $\Delta\rho$ are plotted in Fig. 7.15 as a function of the control rod radius. The points lie on a smooth curve of the general shape expected from theoretical considerations.

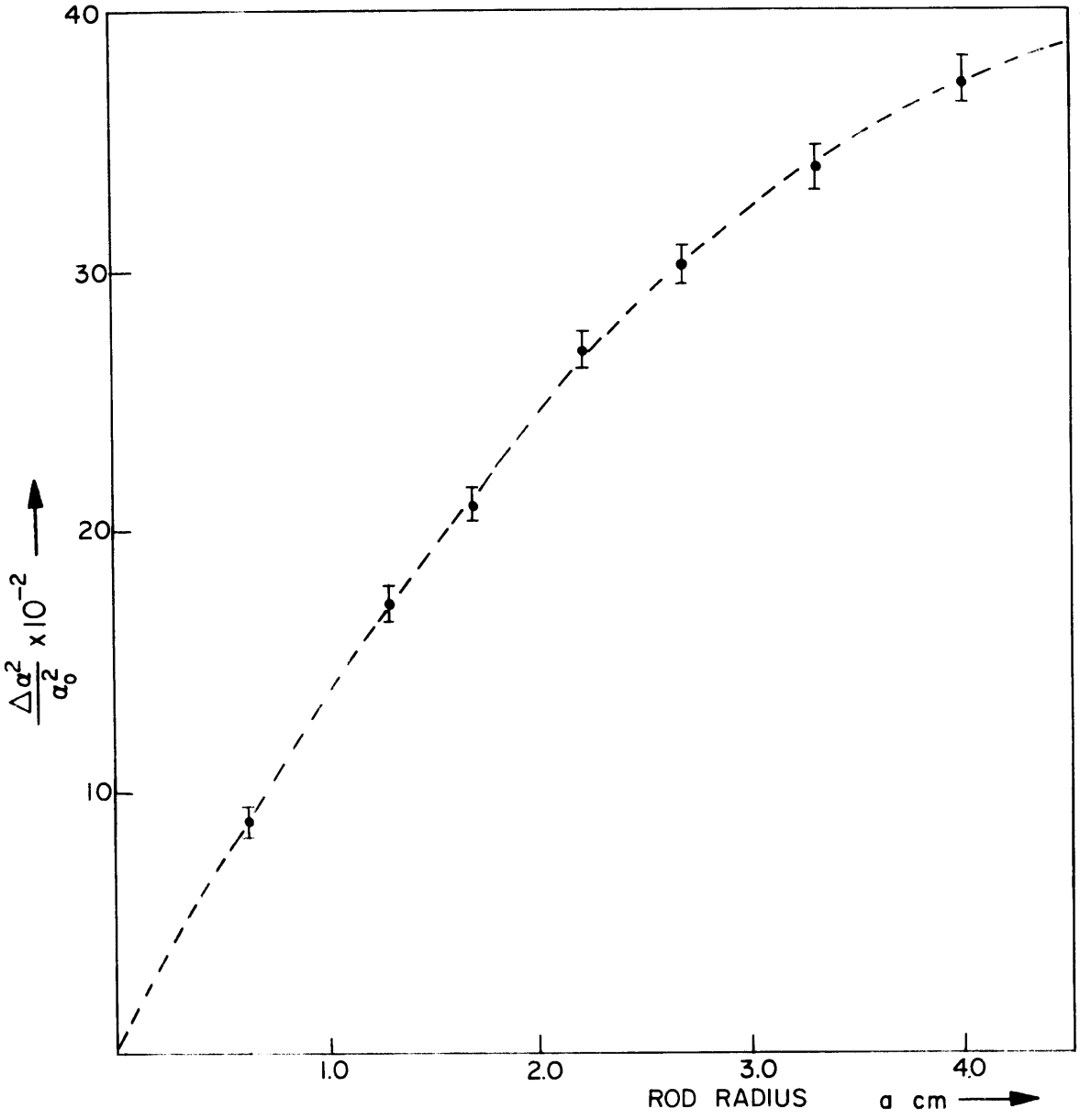

FIG. 7.14 FRACTIONAL BUCKLING CHANGE PRODUCED BY CADMIUM RODS IN THE MULTIPLYING ASSEMBLY, BY PULSED NEUTRON METHOD.

TABLE 7.6

Prompt Neutron Lifetime and Reactivity for the Perturbed Lattices, Measured by the Pulsed Neutron Method

Rod Radius (a :cm)	Geometrical Buckling (B^2:m^{-2})	Prompt Neutron Lifetime (ℓ:μsec)	Inverse Lifetime Parameter $\frac{\beta}{\ell}$, sec^{-1}	Prompt Decay Constant (λ:sec^{-1})	Negative Reactivity $\left(\rho = \frac{\lambda - \frac{\beta}{\ell}}{\frac{1}{\ell} - \lambda}\right)$	Rod Worth $\Delta\rho$
None	29.02 ± 0.22	502.7 ± 16.3	15.58 ± 0.50	689.9 ± 4.1	0.519 ± 0.02	–
0.635	33.12 ± 0.24	490.3 ± 15.9	15.97 ± 0.51	771.1 ± 5.2	0.595 ± 0.03	0.076 ± 0.007
1.295	35.97 ± 0.24	475.0 ± 15.4	16.48 ± 0.53	846.5 ± 5.4	0.659 ± 0.03	0.140 ± 0.008
1.714	37.49 ± 0.25	469.4 ± 15.2	16.68 ± 0.54	879.7 ± 6.1	0.690 ± 0.04	0.171 ± 0.009
2.209	39.22 ± 0.26	463.3 ± 15.0	16.90 ± 0.55	935.0 ± 7.0	0.750 ± 0.04	0.231 ± 0.009
2.667	40.58 ± 0.26	458.2 ± 14.6	17.08 ± 0.55	963.9 ± 7.7	0.777 ± 0.04	0.258 ± 0.009
3.327	42.37 ± 0.27	451.1 ± 14.5	17.35 ± 0.56	997.5 ± 8.5	0.804 ± 0.04	0.285 ± 0.010
3.969	43.83 ± 0.28	445.9 ± 14.4	17.56 ± 0.57	1029.9 ± 9.0	0.835 ± 0.04	0.316 ± 0.010

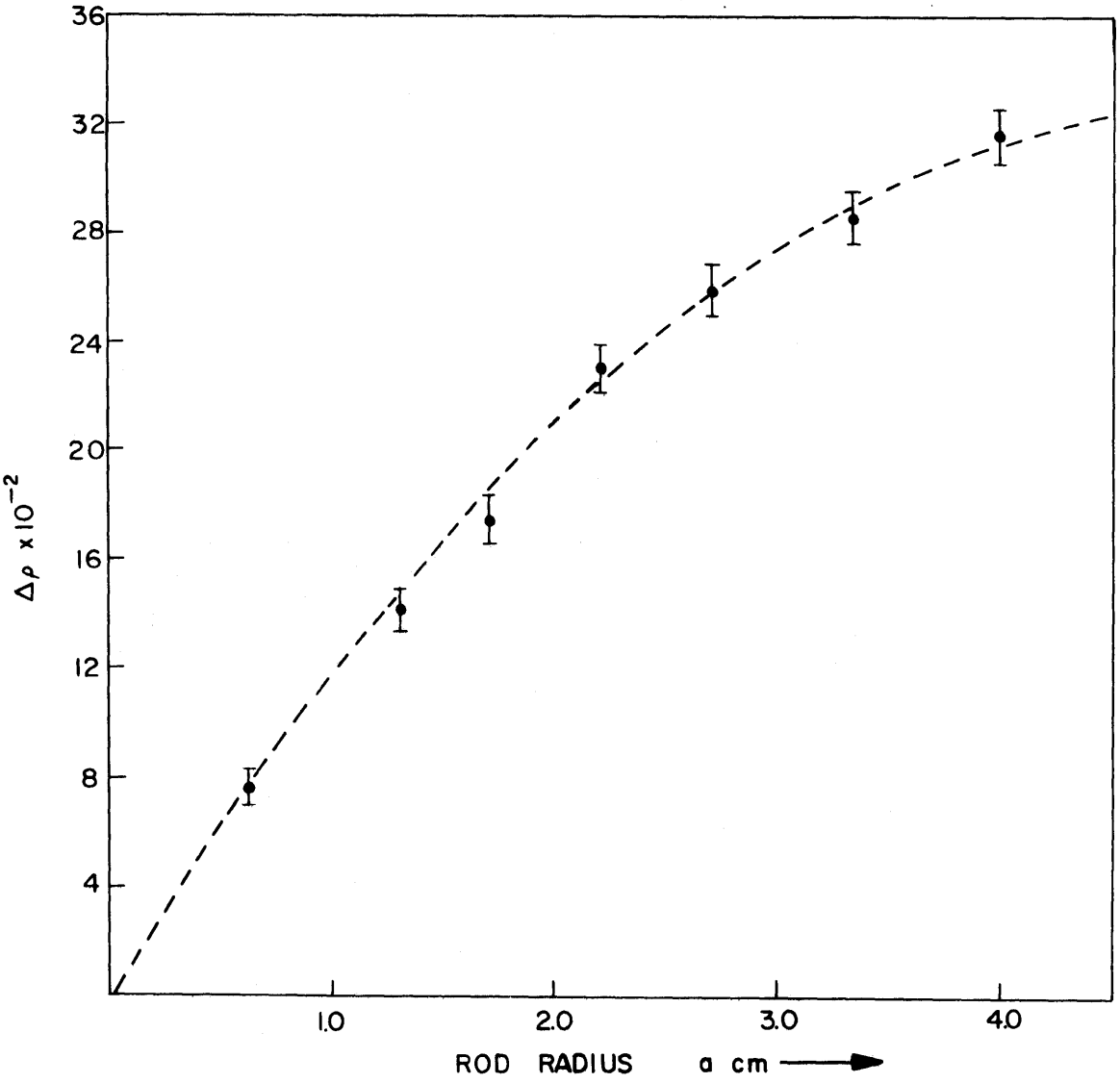

FIG. 7.15 REACTIVITY WORTH $\Delta\rho$ OF CENTRAL CADMIUM RODS AS A FUNCTION OF RADIUS a , MEASURED IN THE SUBCRITICAL ASSEMBLY BY PULSED NEUTRON METHOD.

7.5 PULSED NEUTRON EXPERIMENTS ON SMALL ASSEMBLIES OF PURE MODERATOR

In the early stages of the pulsed neutron work of the present investigation, a Cockcroft-Walton type accelerator was used in several die-away experiments involving different assembly configurations and detection systems based on varying means of suppressing the harmonics, to extract the fundamental mode decay. The purpose of these experiments was primarily to test the over-all pulsing, detection and analyzing circuitry and to gain experience in the selection of appropriate experimental pulsing parameters, preparatory to setting up the main pulsed neutron system in conjunction with the exponential facility. However, a few experiments were done on small assemblies of moderator - especially heavy water - to study their thermal neutron diffusion characteristics. It was originally intended to compare the results from these runs on heavy water to those from die-away runs with the large exponential tank and compare the diffusion parameters based on different buckling ranges. However, the heavy water sample had an uncertain history in various experiments with a resulting uncertainty in its purity. Hence, although it was useful for our early experiments, a valid comparison of the results obtained could not be made with those obtained in the later experiments in the exponential tank.

The equipment used for these experiments has been described in Section 5.2 (Fig. 5.6). The test assemblies were cylindrical jars of glass or aluminum, with diameters varying from 15.5 cm to 43.8 cm, filled with heavy water to heights of 17.8 cm to 48.3 cm, thus providing a buckling range of 140 m^{-2} to 855 m^{-2}. The outer surface of each assembly was covered with 0.020-inch-thick cadmium sheets. The heavy water was transferred from the storage vessel to the test assembly in a nitrogen atmosphere to prevent degradation and the assembly was subsequently closed with plastic, leak-tight covers so that the heavy water remained in a nitrogen atmosphere throughout. The pulsed neutron source was a 150-KV Cockcroft-Walton type accelerator equipped to generate neutrons by the (D,D) reaction. The pulse widths used varied from 5 μsec to 12 μsec and the repetition rate from 500 pulses per sec to about 670 pulses per sec. The fast neutrons from the source were allowed to thermalize and

the asymptotic thermal flux emerging from the assembly was detected by a 5-inch, Li^6-ZnS plastic fluor mounted on a Dumont 6364 phototube. The detector was surrounded on the sides by a 0.020-inch cadmium sheet and was mounted on the axis of the assembly so as to be exposed to a 5-inch-diameter circular window cut in the cadmium cover on the top of the assembly. The target was located on the axis of the assembly at the bottom. Thus, the harmonic modes having radial nodal planes through the axis were not excited for reasons of symmetry. The complete electronic circuit is shown in Fig. 5.7.

The analysis of the data was done in a manner similar to that described in Section 7.1; the EXPO code was used to extract the fundamental mode decay constant from the experimental data. With the source-detector configuration described above, the variation of the decay constant with waiting time was also studied. An example of this variation for a typical assembly is shown in Fig. 7.16; it is seen that as the fundamental mode is approached, the decay constant assumes a constant, unique value. The uncertainties in the final value of the decay constant were between 1 and 2 per cent as given by the fitting procedure. The reproducibility in repeated runs was within these uncertainties. The waiting time varied from about 150 μsec for the smallest to about 200 μsec for the largest assemblies.

The final values of the decay constant λ and the corresponding geometrical buckling B^2 are shown in Table 7.7. The buckling was calculated according to the prescription of Eqs. 7.6 and 7.7. The curve of λ vs. B^2 is shown in Fig. 7.17. The effect of diffusion cooling is evident at larger values of the bucklings. Finally, the data from Table 7.7 were fitted to an expression of the form of Eq. 7.8 by a least-squares iterative procedure, with the code DEECEE described earlier. A value of λ_o = 26.6 sec^{-1}, based on a calculation for an assumed concentration of 99.60 mole per cent D_2O, was used. The experimental points are well represented by the least-squares-fitted curve, thus suggesting that the role of a higher B^6-term in the λ vs. B^2 relationship (7.8) is, at most, very small. The values of the two parameters from the least-square fit are:

$$vD = (1.790 \pm 0.016) \times 10^5 \text{ cm}^2/\text{sec} ,$$
$$C = (3.581 \pm 0.360) \times 10^5 \text{ cm}^2/\text{sec} . \qquad (7.38a,b)$$

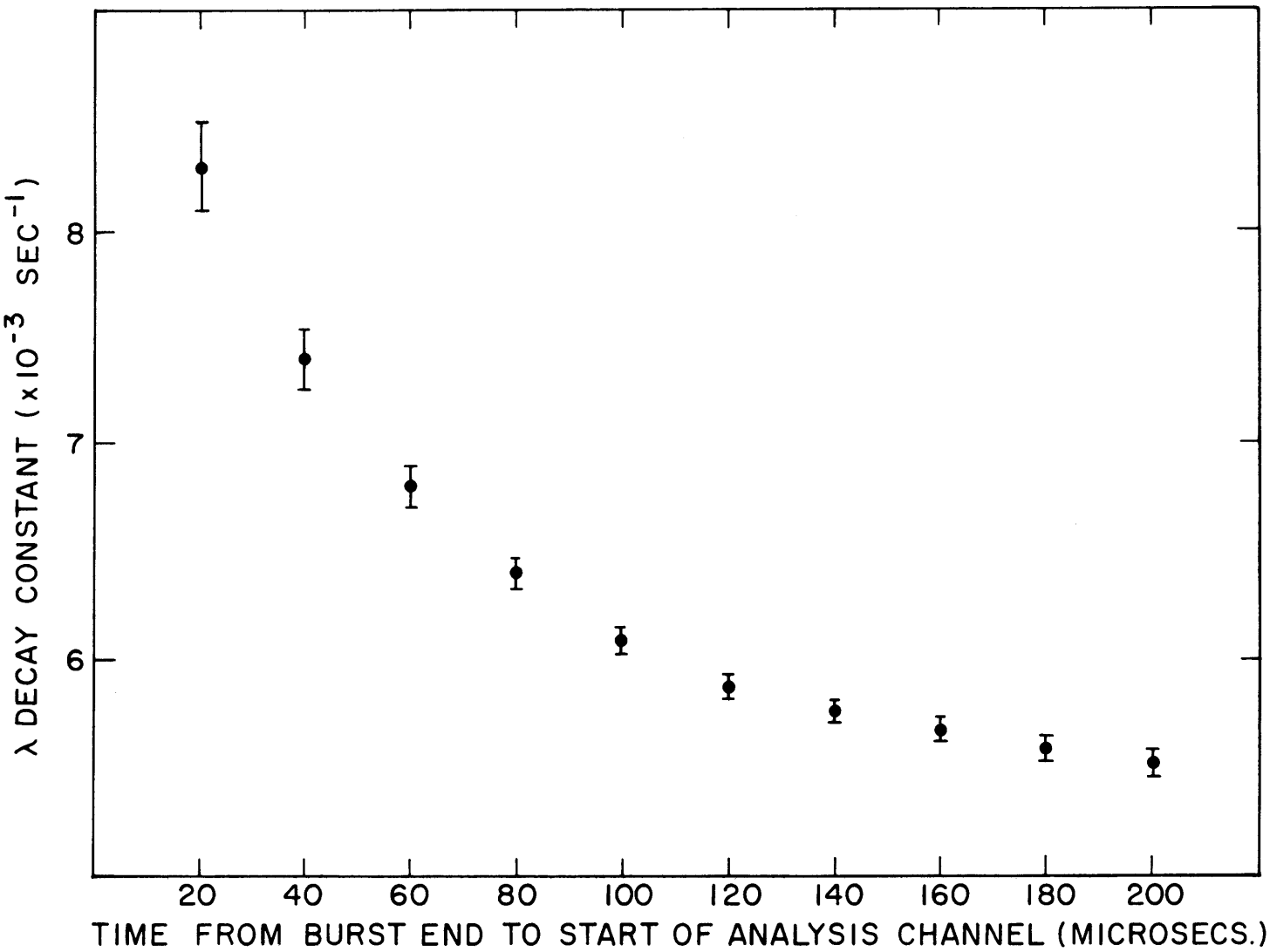

FIG. 7.16 VARIATION OF DECAY CONSTANT WITH "WAITING TIME"

TABLE 7.7

Measured Decay Constant as a Function of Buckling
for Small Cylindrical Assemblies of Heavy Water

Radius R, cm	Height H, cm	Buckling B^2, m^{-2}	Measured Decay Constant λ, sec^{-1}
21.907	48.260	140	2448.5 ± 31.5
19.367	40.640	180	3154.4 ± 42.7
12.224	40.640	347	5812.7 ± 55.3
10.160	22.860	549	9045.8 ± 112.8
10.160	17.780	625	10117.5 ± 184.3
7.779	17.780	854	12520.9 ± 301.9

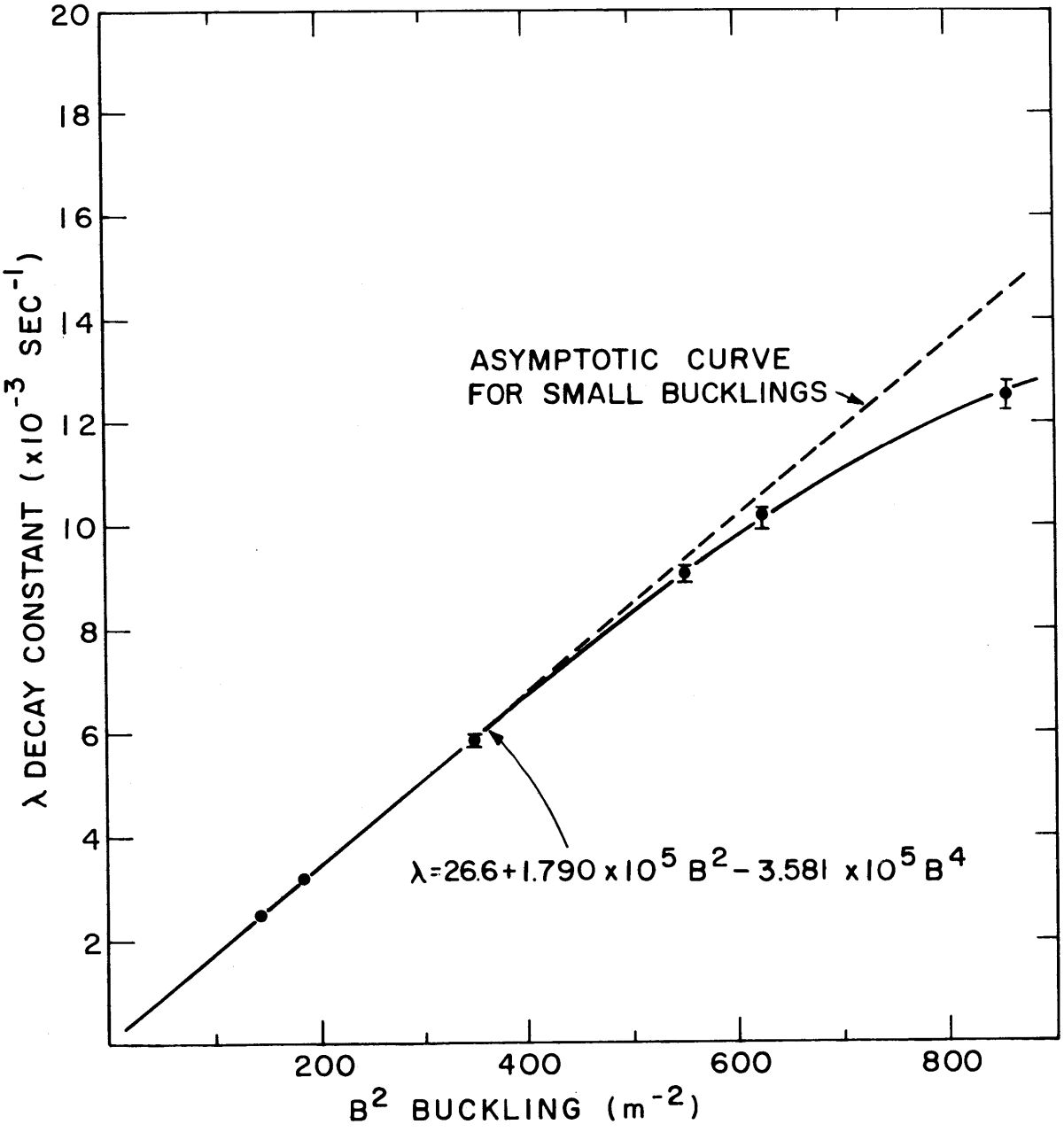

FIG. 7.17 DECAY CONSTANT VS. BUCKLING

The temperature of the heavy water was 21°C. The value of C is in agreement with that of Ganguly and Waltner[3] (Table 7.2) based on measurements in a comparable buckling range. The value of vD is decidedly lower than expected. However, the validity of any quantitative comparison of these values is somewhat doubtful in view of the uncertainty in the purity of the heavy water sample used in these runs.

7.6 STEADY-STATE EXPONENTIAL EXPERIMENTS WITH CONTROL RODS

In this section, the analysis developed in Chapter IV will be applied to obtain information about control rods in exponential experiments. The subcritical facility was used as an exponential assembly with the thermal column of the MITR as the neutron source. Experiments were done with the exponential tank filled with heavy water alone, and with the lattice.

7.6.1 Moderator Experiments

7.6.1.1 Measurement of the Extrapolation Distance For Black Cylinders. The extrapolation length of a thermally black cylindrical rod was determined by relating it to the change in axial buckling produced by the rod in an assembly of pure moderator irradiated by a stationary thermal neutron source. The measurements were made for black rods of different diameters. In a bare cylindrical assembly of moderator of extrapolated radius R, with a black cylindrical rod placed along its axis, the radial flux is given under one-group diffusion theory as:

$$\phi(r) = A\left[J_o(\alpha r) - \frac{J_o(\alpha R)}{Y_o(\alpha R)} Y_o(\alpha r)\right] . \qquad (7.39)$$

When this expression is inserted in the equation defining the extrapolation distance d, the result is:

$$d = \left.\frac{\phi(r)}{\phi'(r)}\right|_{r=a} = \frac{1}{\alpha} \frac{Y_o(\alpha R)J_o(\alpha a) - Y_o(\alpha a)J_o(\alpha R)}{Y_1(\alpha a)J_o(\alpha R) - Y_o(\alpha R)J_o(\alpha a)} . \qquad (7.40)$$

Thus, if α is known, Eq. 7.40 gives d for a rod of radius a. The parameter α can be determined by measuring the axial buckling of the moderator

assembly with (γ) and without (γ_o) the rod along its axis and observing that the material buckling is not changed by the introduction of the additional boundary. Then:

$$B_m^2 = a^2 - \gamma^2 = a_o^2 - \gamma_o^2 ,$$

$$a^2 = a_o^2 + \Delta\gamma^2 . \qquad (7.41a,b)$$

The measurements were made in the 48-inch-diameter tank in the M.I.T. exponential facility. The tank was filled with heavy water (99.70 mole per cent, temperature 20° C) up to a height of 52 inches and fed at the bottom with neutrons from the thermal column of the MITR. The axial buckling was measured in each run by activating 0.25-inch-diameter, 0.010-inch-thick gold foils attached to aluminum foil holders, and mapping the axial flux. After irradiation, the foils were gamma-counted by setting the counting system (Section 5.1.3, Fig. 5.5) to straddle the 411-kev Au^{198} gamma-ray peak with a window width of 60 kev.

Figure 7.18 shows the axial flux distribution in the moderator tank without the rod (continuous curve) and with a typical (2.10-inch-diameter) cadmium rod along the axis (dashed curve). The measured flux is adequately represented by a single exponential in both measurements and the change in the slope produced by the rod can be measured with satisfactory precision. The axial buckling was calculated from the axial flux with the help of an IBM-7090 code AXFIT. The errors given by the least-squares fit are of the order of 0.25 per cent.

The results are listed in Table 7.8. The corresponding values of the radial buckling calculated from Eq. 7.41b and the values of d computed from Eq. 7.40 are also given. The value of the extrapolated core radius R is obtained by augmenting the actual physical radius by the extrapolation distance for a "plane" boundary:

$$R = R_o + 0.71045 \times \lambda_{tr}(D_2O) , \qquad (7.42)$$

with

$$\lambda_{tr}(D_2O) = 2.5 \text{ cms.}^{(9)} \qquad (7.42a)$$

The errors in d are due to uncertainties in γ and amount to about 2 per cent. The values of d (cm) are plotted as a function of the radius of the

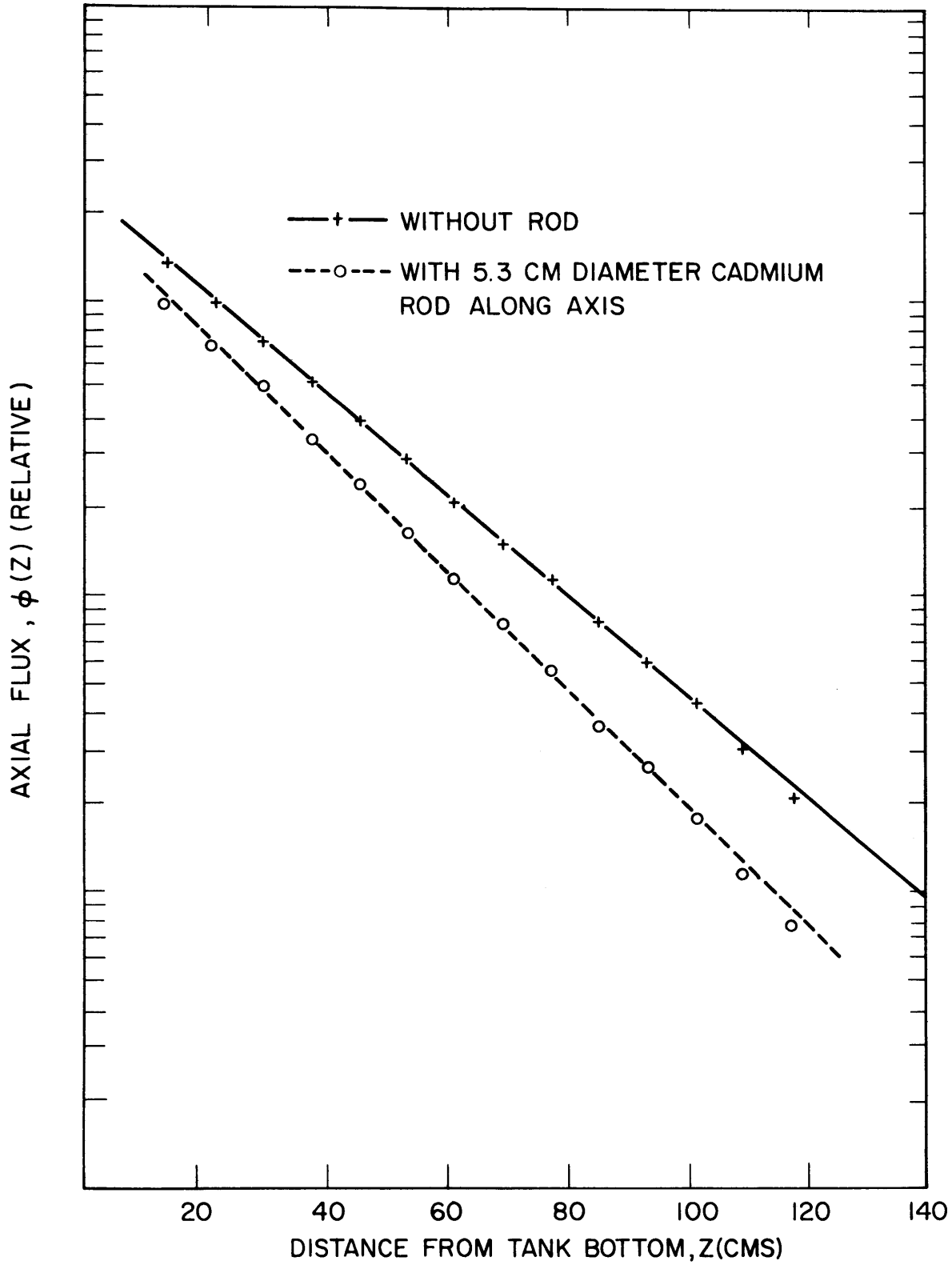

FIG. 7.18 AXIAL FLUX DISTRIBUTION IN TANK OF PURE MODERATOR

TABLE 7.8

Measured Extrapolation Distance of Thermally Black Rods

Rod Radius cm	Axial Buckling γ^2 10^{-6} cm^{-2}	Radial Buckling Parameter, α 10^{-3} cm^{-1}	Buckling Change $\Delta\alpha^2 = \Delta\gamma^2$ 10^{-6} cm^{-2}	Extrapolation Distance, d cm
0.635	1732 ± 4	41.43	238	2.82 ± .08
1.295	1882 ± 4	43.20	388	2.62 ± .07
1.714	1968 ± 3	44.19	474	2.44 ± .06
2.209	2055 ± 4	45.16	561	2.29 ± .05
2.667	2128 ± 5	45.96	634	2.20 ± .05
3.327	2225 ± 5	47.01	731	2.11 ± .05
3.969	2315 ± 5	47.96	821	2.02 ± .05

Axial buckling of moderator assembly without rod: $\gamma_o^2 = 0.001494 \pm .0000038$

black cylinder in Fig. 7.19.

Figure 7.20 shows the variation of $\Delta a^2/a_o^2$ with rod radius. For small values of the radius, the variation is approximately linear as is to be expected on simple theoretical grounds, as will now be shown. The radial flux distribution in the tank without the rod is:

$$\phi_o(r) = A_o J_o(a_o r) . \tag{7.43}$$

If an absorber is introduced along the axis of the assembly, the asymptotic part of the radial flux may be written as:

$$\phi(r) = A[J_o(ar) + CY_o(ar)] , \tag{7.44}$$

where

$$C = - \frac{J_o(aR)}{Y_o(aR)} . \tag{7.45}$$

For small values of the rod radius, we can write:

$$a = a_o + \Delta a . \tag{7.46}$$

After some simplification, we obtain:

$$\frac{\Delta a^2}{a_o^2} = 2C \frac{Y_o(a_o R)}{a_o R J_1(a_o R)}$$

$$= 2C \frac{0.510}{2.405 \times 0.519} = 0.817\ C . \tag{7.47}$$

On the other hand, the strength of the perturbation, C, is proportional to the strength of the (negative) source represented by the absorber, i.e.,

$$C \sim (2\pi a)\ \Sigma_a \phi_o(a) . \tag{7.48}$$

From Eqs. 7.47 and 7.48, it follows that

$$\frac{\Delta a^2}{a_o^2} \propto a . \tag{7.49}$$

Thus, for small values of the rod radius, the fractional buckling change, in a pure moderator assembly, should vary linearly with the rod radius.

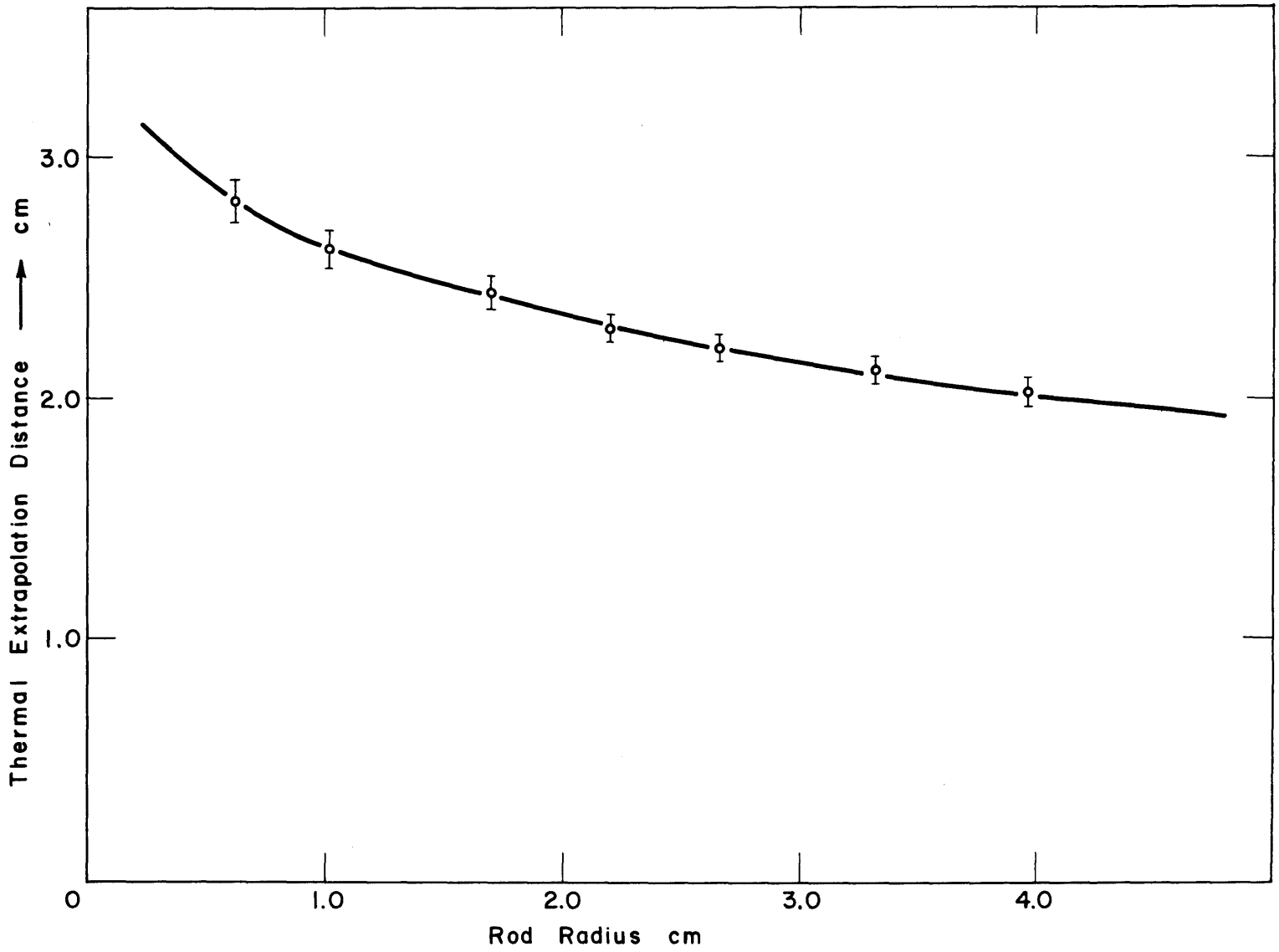

Fig.7.19 Measured Extrapolation Distance of Thermally Black Cylinders as a Function of Radius

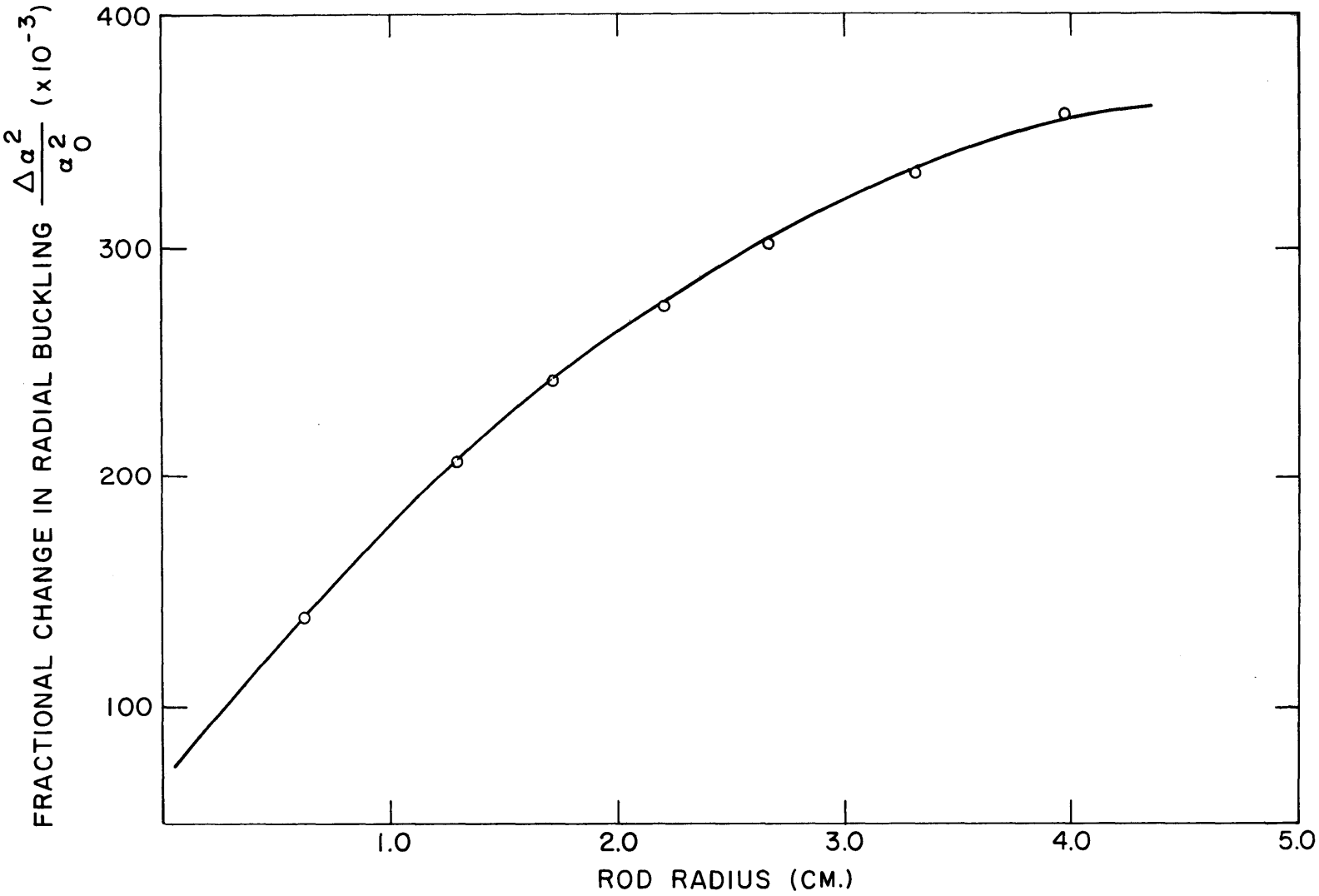

FIG. 7.20 FRACTIONAL CHANGE OF RADIAL BUCKLING OF A PURE MODERATOR TANK, PRODUCED BY CD. RODS OF DIFFERENT RADII

The extrapolation distance can also be obtained from pulsed neutron experiments (Section 7.2) which yield the change in buckling $\Delta B^2 (= \Delta\alpha^2)$ due to the rod. The results of the two methods agree within experimental uncertainties.

7.6.1.2 Mapping of the Radial Flux with the Control Rod in a Moderator Assembly. The validity of the above method depends on the accuracy with which the parameter α can be determined from Eq. 7.41b. To check this condition, the experimental radial flux was plotted for each of two typical rod sizes and was compared with that given by Eq. 7.39 with the value of α calculated from Eq. 7.41b. The agreement was good, as is evident from Fig. 7.21.

7.6.2 Exponential Experiments with Control Rods in Multiplying Assemblies

7.6.2.1 Measurements Based on Axial Flux Distributions. In this section, the analysis presented in Chapter IV will be further applied to measure the change in buckling caused by the rod in an exponential subcritical assembly. These experimental runs were done in the 36-inch-diameter, exponential tank, with 0.25-inch-diameter uranium rods containing 1.03 per cent U^{235}, arranged in a triangular lattice with a spacing of 1.75 inch. The seven central fuel elements were removed to make room for the control rod (Fig. 7.6). The latter was introduced through a top plastic adapter and positioned along the axis of the assembly in the manner described in Section 7.3. An axial foil folder of aluminum could be fixed in an off-center position in the moderator region between fuel rods. Gold foils, 0.010 inch thick and 1/8 inch in diameter, were attached to the foil holder. The lattice was irradiated with thermal neutrons from the thermal column of the MITR. After irradiation, the foils were gamma-counted as described in Section 5.1.3. The experimental counts were corrected for dead time, long-term drift, background, foil weights, decay during counting, etc., and the final axial distribution was obtained for the unperturbed lattice and for the lattice with each of seven different size rods individually placed along the axis. An example of the axial distribution is shown in Fig. 7.22. In a large enough region, the harmonic content is negligible and the data are fitted well by a single exponential. The change in the slope of the curve, caused by the placement of the rod, is seen to be significant.

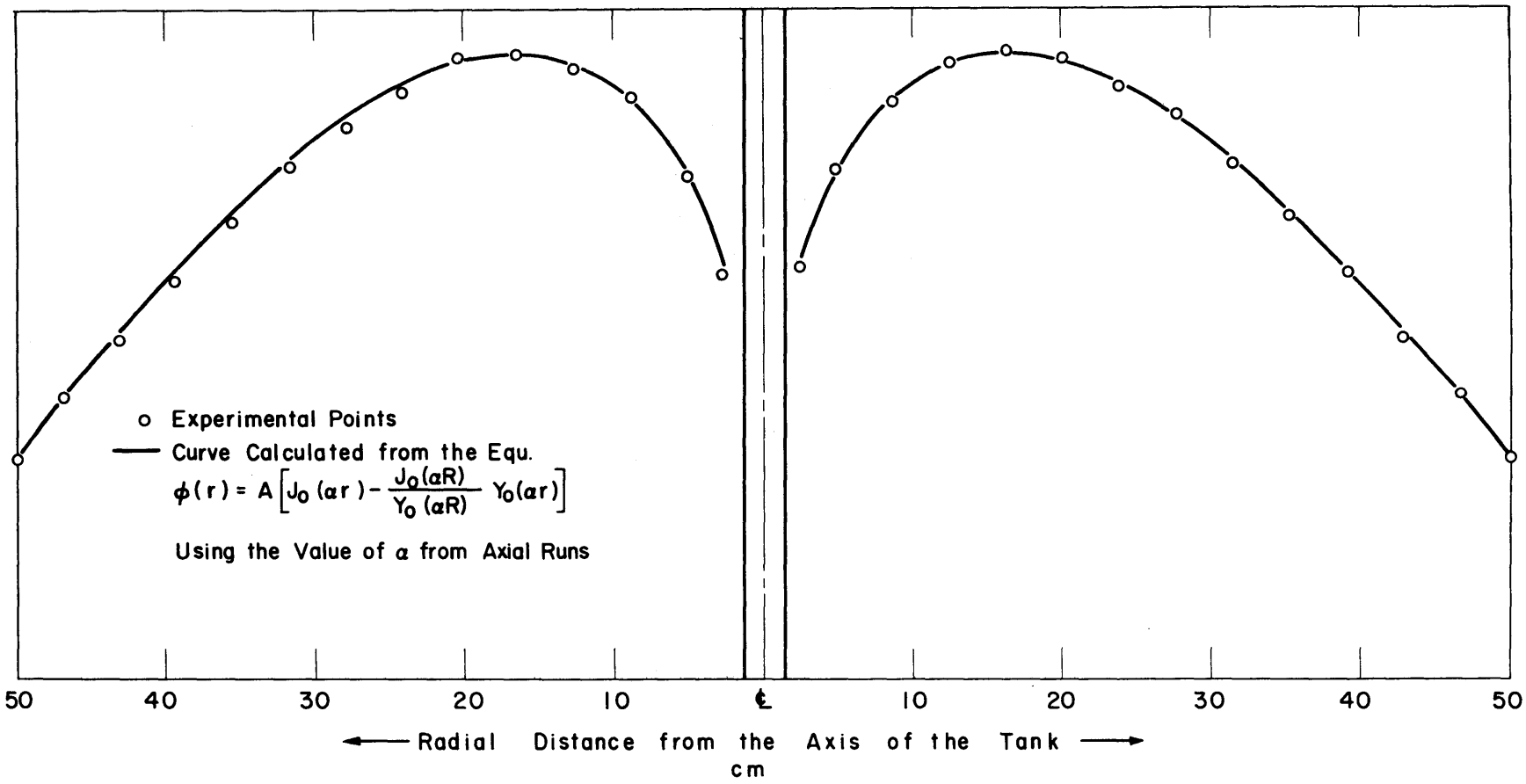

Fig. 7.21 Radial Run With 2.60 Cm. O.D. Cd Rod Placed Axially in Tank of Pure Moderator

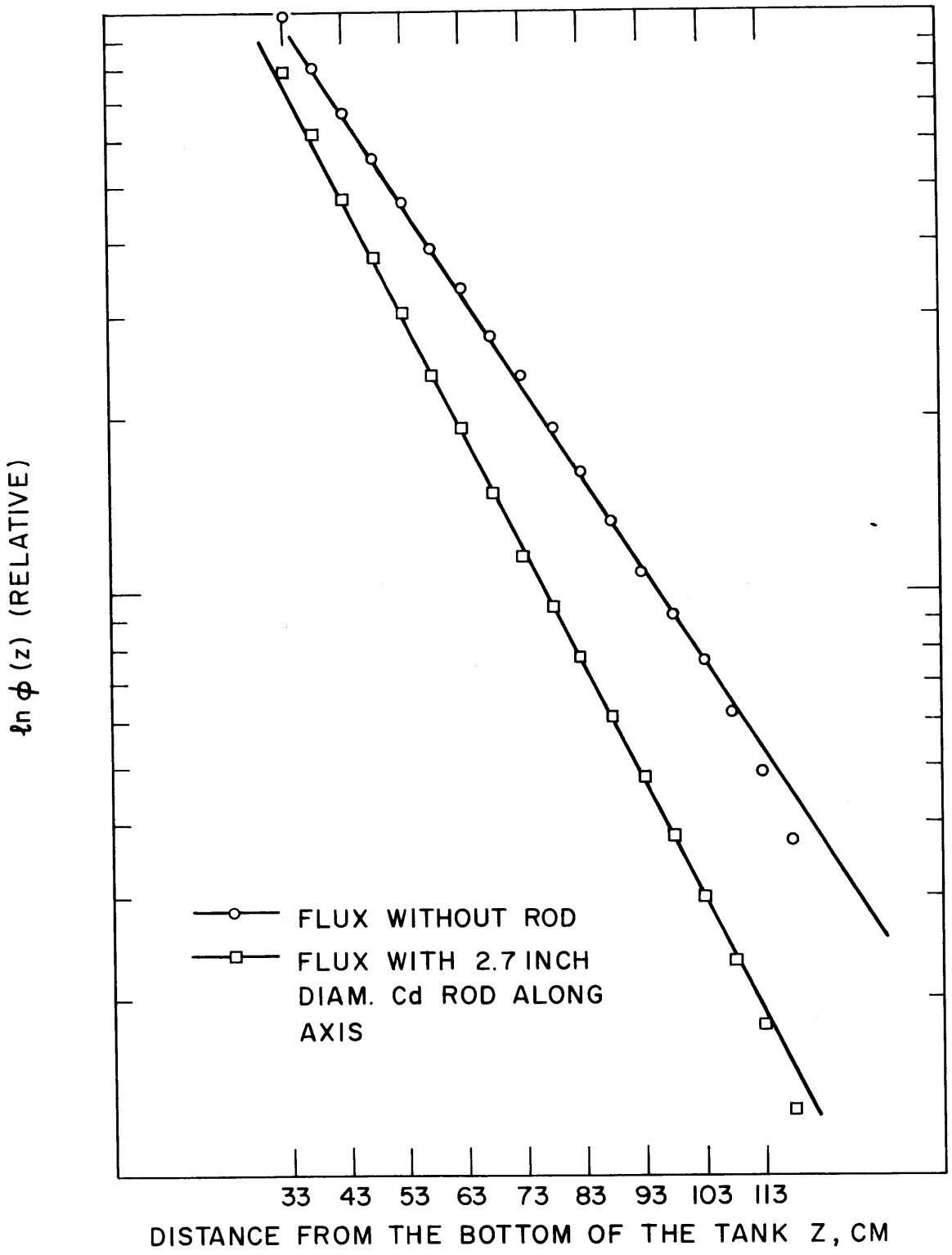

FIG. 7.22 AXIAL FLUX DISTRIBUTION IN THE EXPONENTIAL ASSEMBLY WITH AND WITHOUT A CONTROL ROD.

The value of the fundamental axial buckling γ^2 was calculated in each case by fitting the axial flux distribution $\phi(z)$ to the function $A \sinh \gamma(h-z)$, by means of a least-squares fit. This is done by an IBM-7090 computer code AXFIT. Thus, the experiments give directly the change in axial buckling produced by a control rod. The conversion of result to the equivalent change in radial buckling is based on the theory discussed in Section 4.2. The results are given in Table 7.9. The unperturbed lattice refers to the lattice without a control rod and without the seven central fuel rods. The fractional change in radial buckling caused by the rod, as measured in this steady-state exponential experiment, is compared in Table 7.10 with the results of pulsed neutron experiments. The results of the two methods agree within the experimental uncertainties, although these uncertainties are somewhat larger in the steady-state case.

7.6.2.2 Examination of the Flux Spectrum: Radial Runs. As discussed in Section 4.3, a necessary condition for the results of exponential experiments such as those above, to be analyzed in terms of the properties of the lattice by simple theory, is that the neutron spectrum, which is perturbed near the rod, should recover its asymptotic value within the bounds of the assembly. To examine this condition, radial flux distributions were measured in the unperturbed and perturbed assemblies with bare and cadmium-covered gold foils. The 0.010-inch-thick, 1/8-inch-diameter, gold foils were attached to a horizontal aluminum foil holder placed along a chord of the tank so as just to graze the control rod in the perturbed assembly. This configuration and the setting of the foils with respect to the fuel rods and the control rod are shown in Fig. 7.23. Cadmium boxes providing a cadmium sheath 0.020 inch thick were used to obtain the activation above the cadmium cut-off energy. The foil holder was placed sufficiently far from the bottom (neutron source) so that the measured flux distribution was representative of the lattice spectrum; in previous exponential runs, it was found that at 60 cm and 108 cm above the bottom of the tank, good fits to a $J_o(\alpha r)$ were obtained.

Figure 7.24 shows the radial flux distribution, with bare gold foils, in the assembly with and without the largest (8.0 cm diameter) control

TABLE 7.9

Buckling Change Produced by Axial Cadmium Rods of Different Radii in the Multiplying Assembly, Measured in Exponential Experiments

Rod Radius (cm)	Axial Buckling ($\gamma^2 : m^{-2}$)	Change of Buckling ($\Delta a^2 = \Delta\gamma^2 : m^{-2}$)	Fractional Buckling Change $\frac{\Delta a^2}{a_o^2}$
None	12.148 ± 0.18	-	-
0.635	14.340 ± 0.21	2.192 ± 0.28	0.092 ± 0.012
1.295	16.188 ± 0.23	4.040 ± 0.29	0.170 ± 0.012
1.714	17.068 ± 0.25	4.920 ± 0.31	0.207 ± 0.013
2.209	18.513 ± 0.26	6.365 ± 0.32	0.268 ± 0.013
2.667	19.468 ± 0.28	7.320 ± 0.33	0.308 ± 0.014
3.327	20.365 ± 0.29	8.217 ± 0.33	0.346 ± 0.014
3.969	20.912 ± 0.29	8.764 ± 0.34	0.369 ± 0.014

TABLE 7.10

Comparison of the Fractional Buckling Change Caused by Axial Cadmium Rods of Different Radii in the Lattice, by Pulsed Neutron and Steady-State Experiments

Rod Radius (cm)	Steady-State Experiment $\frac{\Delta a^2}{a_o^2}$	Pulsed Neutron Experiment $\frac{\Delta a^2}{a_o^2}$
0.635	0.092 ± 0.012	0.089 ± 0.007
1.295	0.170 ± 0.012	0.173 ± 0.007
1.714	0.207 ± 0.013	0.210 ± 0.008
2.209	0.268 ± 0.013	0.271 ± 0.009
2.667	0.308 ± 0.014	0.303 ± 0.009
3.327	0.346 ± 0.014	0.340 ± 0.010
3.969	0.369 ± 0.014	0.376 ± 0.010

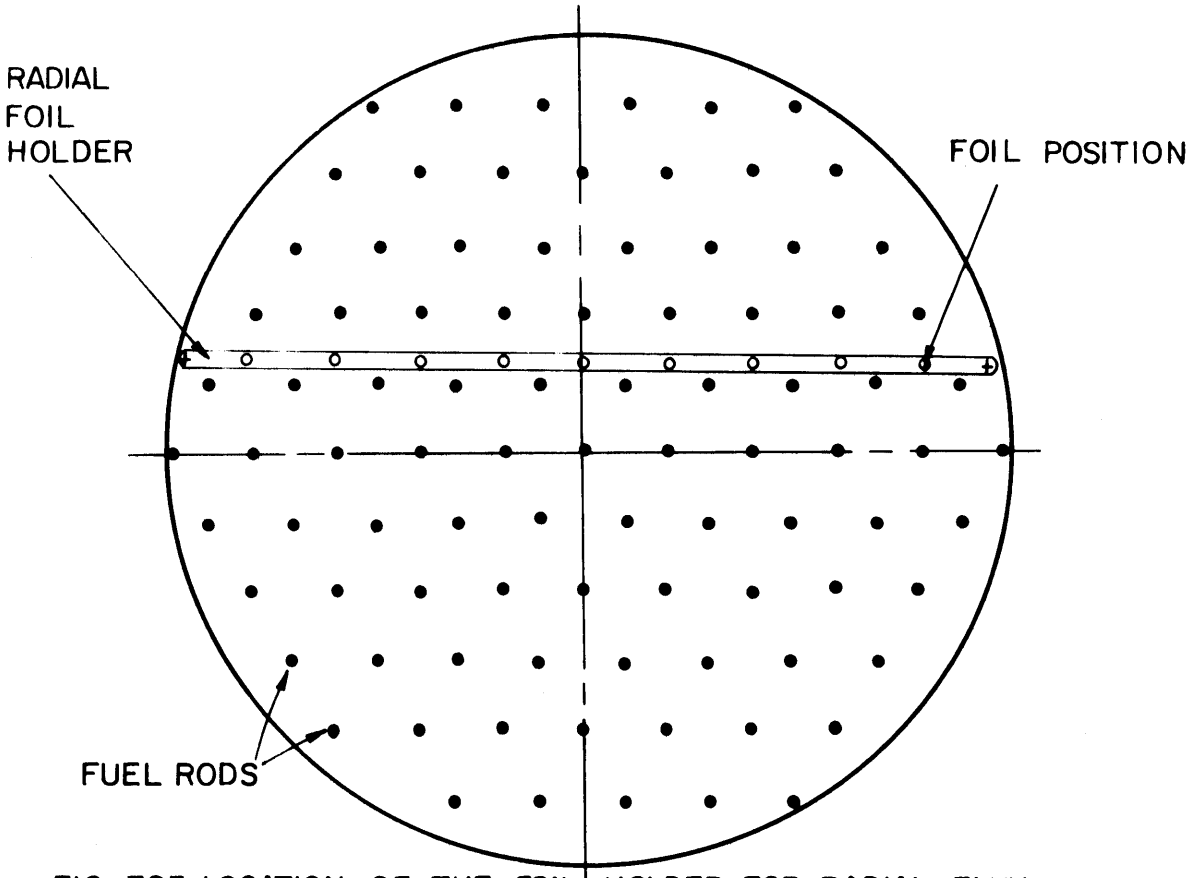

FIG. 7.23 LOCATION OF THE FOIL HOLDER FOR RADIAL FLUX MAPPING IN THE EXPONENTIAL ASSEMBLY

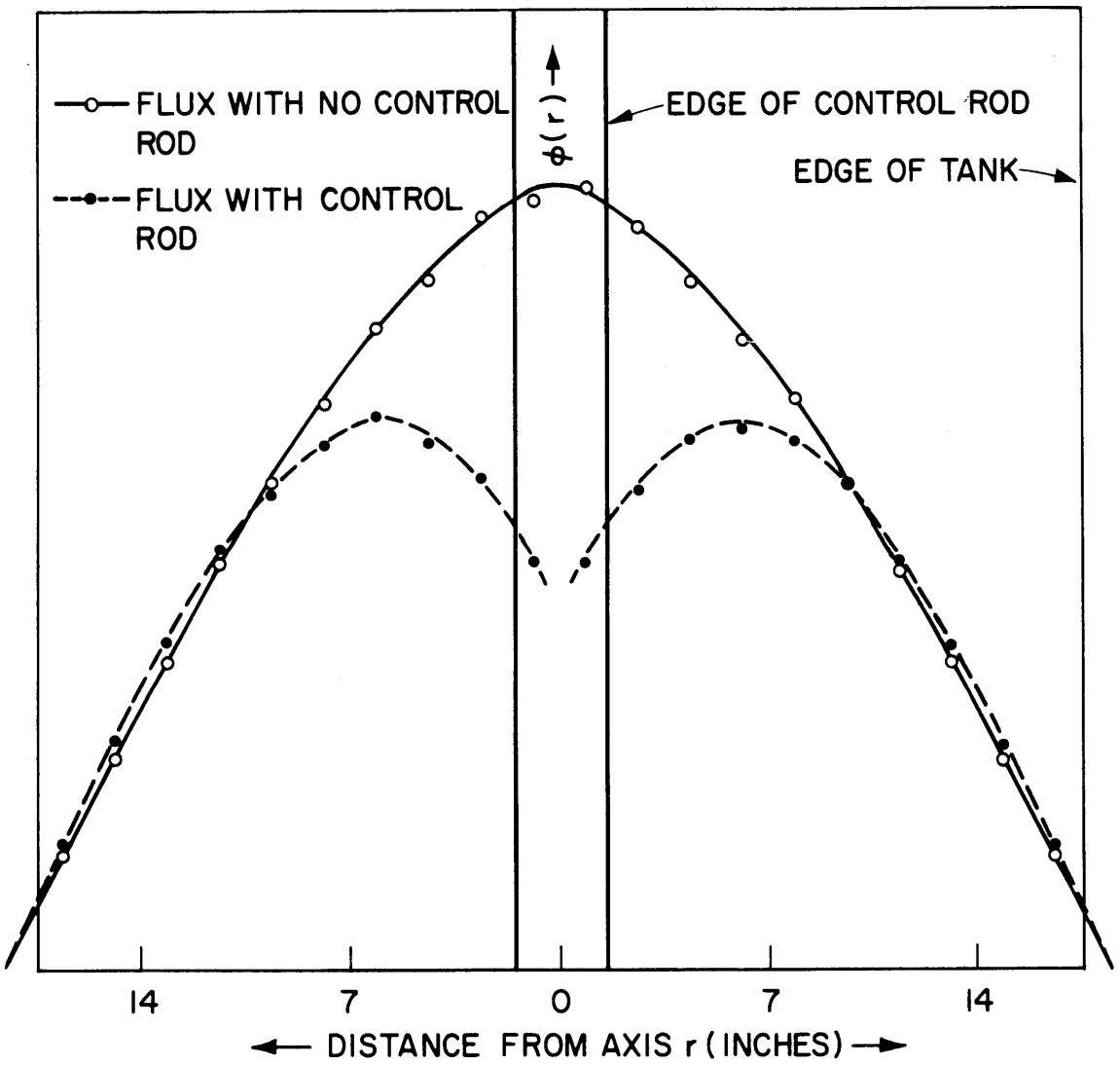

FIG. 7.24 RADIAL FLUX DISTRIBUTION (WITH BARE GOLD FOILS) IN THE EXPONENTIAL ASSEMBLY WITH AND WITHOUT A CONTROL ROD.

rod along the axis. The distribution with cadmium-covered gold foils is shown in Fig. 7.25. The effect of the rod on the flux distribution and the difference between the subcadmium and epicadmium flux distributions are both evident from these two figures. The slight bulging of the flux caused by the rod at the outer edge of the tank is also observed, as predicted by theory.

To examine more clearly the influence of the rod on the cadmium ratio, the gold-cadmium ratio was calculated, from the measured flux, at every point in the assembly with and without the rod. In Fig. 7.26, the cadmium ratio is plotted as a function of the radial distance from the axis. The hardening of the spectrum, as indicated by the decrease in the cadmium ratio, near the rod is well illustrated; however, the cadmium ratio returns to its unperturbed value at about 7 inches from the axis in this 18-inch-radius tank. Thus, the main condition for the validity of the results, viz., the recovery of the unperturbed spectrum (at least as indicated by the gold-cadmium ratio) within the bounds of the assembly, is well satisfied. The small rise in the cadmium ratio in the unperturbed case near the axis is due to the moderator region left by the removal of the seven central fuel rods. There is also seen in both the perturbed and unperturbed cases a significant hardening of the flux near the outer edge of the tank, illustrating the variation of leakage with neutron energy, as discussed in Section 4.4.

7.7 DISCUSSION OF THE RESULTS

The preliminary investigation of the conditions governing the thermal neutron decay curves in non-multiplying and multiplying assemblies has provided criteria for the determination of the fundamental mode decay from the experimental data. Figure 7.11 shows the approach to a normal axial mode after the injection of the burst. For assembly sizes corresponding to a buckling of about 30 m^{-2}, waiting times of the order of 2.2 msec are adequate for flux stabilization. Under suitable conditions, the measured decay constant of the fundamental mode is independent of the size and location of the detector. For a detector along the central axis, the best position is at half the

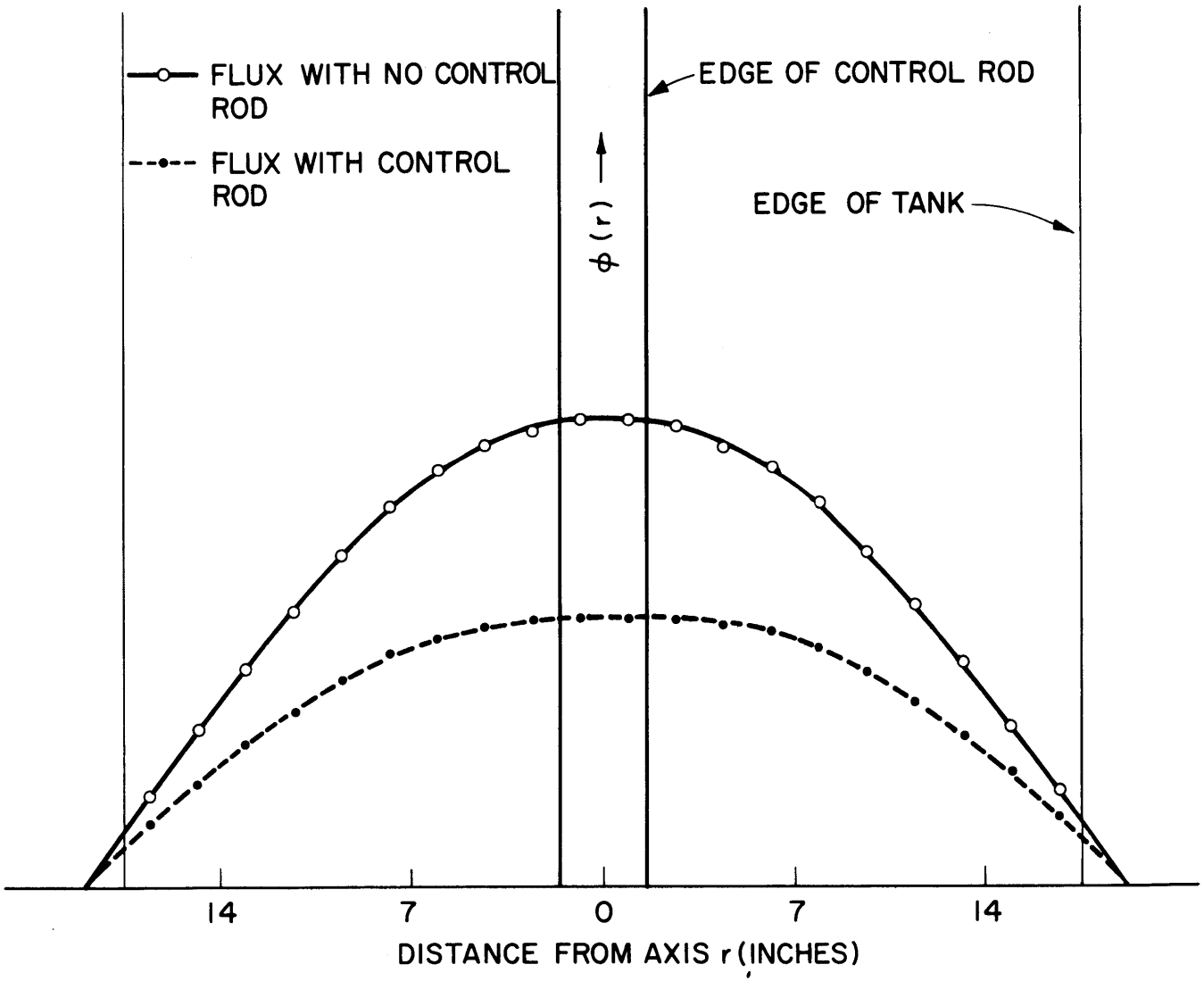

FIG. 7.25 RADIAL FLUX DISTRIBUTION (WITH CD-COVERED GOLD FOILS) IN THE EXPONENTIAL ASSEMBLY WITH AND WITHOUT A CONTROL ROD

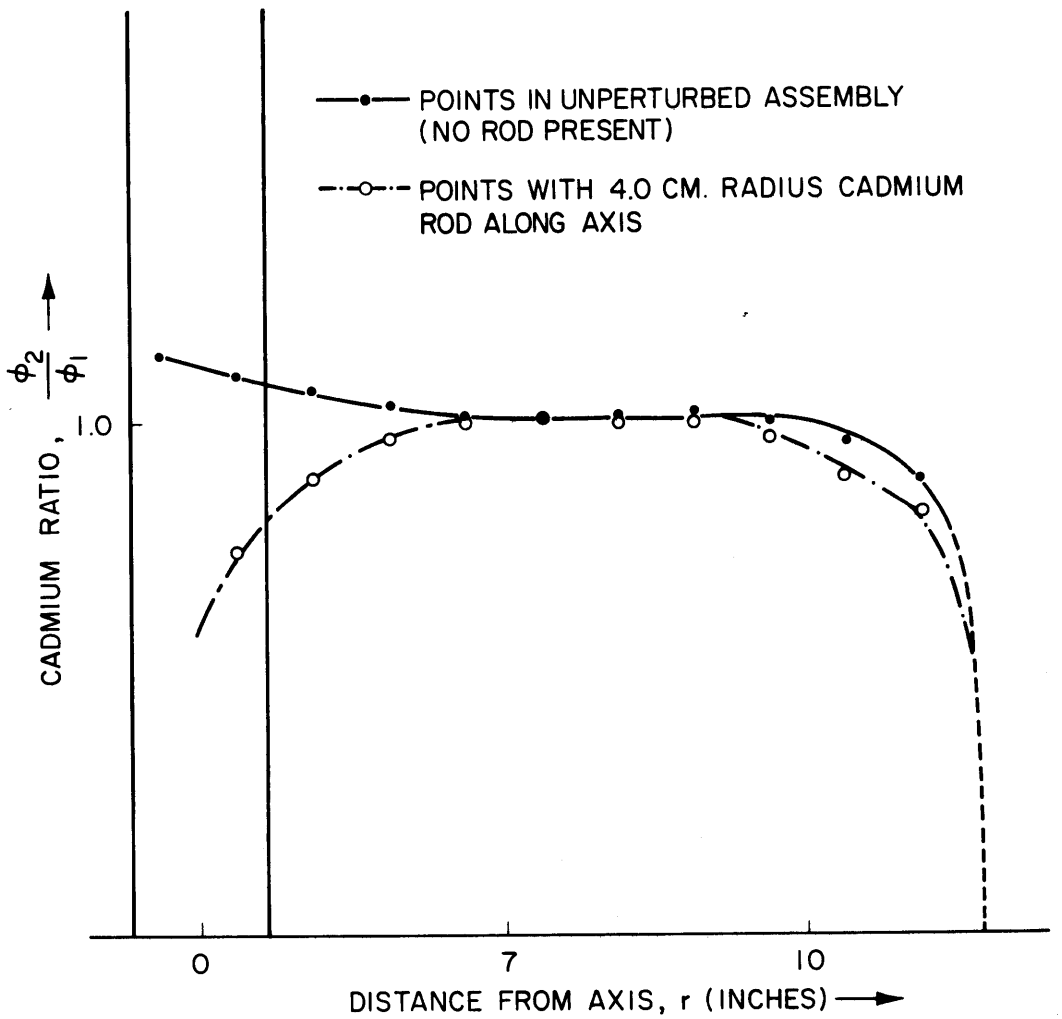

FIG. 7.26 VARIATION OF THE GOLD CADMIUM-RATIO $\frac{\phi_2}{\phi_1}$ ALONG A RADIUS OF THE EXPONENTIAL ASSEMBLY WITH AND WITHOUT A THERMALLY BLACK ROD ALONG AXIS.

core height; in this position the measured decay constant agrees with that based on a detection system with an external, long counter located so as to suppress some of the axial harmonics. The measured decay constant is also independent of the other, pulsing parameters, e.g., the repetition rate, channel width, discriminator setting, etc., over a wide range of these variables. The dead time corrections amount to less than one per cent. For the lattice investigated, a pulse repetition rate of 10 gives a delayed neutron tail that is practically flat.

The pulsed neutron die-away experiments on pure moderator in the 36-inch-diameter tank have yielded the values of the diffusion parameters for 99.60 mole per cent heavy water at room temperature (21° C). The values of vD and C are in good agreement with those of Meister and Kussmaul[5] based on measurements over a wider buckling range. The somewhat smaller value of vD in the present work is thought to be due to the larger concentration of H_2O in the sample of moderator used. The data for the larger bucklings are analyzed separately in a two-parameter fit to give vD and C, while the entire buckling range is used to obtain the parameters $\overline{v\Sigma}_a$ and vD. The values of vD from the two analyses are found to be in agreement, as is to be expected if consistent results are to be obtained. The value of $\overline{v\Sigma}_a$ (27.0 ± 5.0) is consistent with the value computed, from the cross sections, for 99.60 mole per cent D_2O. However, the uncertainty in the measured value of $\overline{v\Sigma}_a$ is large, owing to the inadequate buckling range covered by the data which makes the extrapolation of the λ vs. B^2 curve to zero buckling uncertain. The errors can be reduced by using larger assemblies and more intense sources. If the configuration of source and detector is to be the same as in these experiments, a Fourier analysis of the experimental decay curve for large assemblies should further reduce the uncertainty in the fundamental mode decay constant. The errors shown are the standard deviations.

The values of the diffusion parameters for pure moderator obtained above are used in Section 7.2 to determine the geometrical buckling of a bare, cylindrical moderator assembly which is perturbed by the introduction of a single, full-length, absorbing rod along the axis. Cadmium rods of seven different sizes have been used. The introduction of the rod causes a significant change in the decay constant λ. The bucklings (B^2)

are obtained by solving the basic equation relating λ and B^2 and using the experimentally determined values of the parameters occurring in this equation. Figure 7.5 shows the change in buckling caused by rods of varying radii. The results are compared with the theoretical curve given by one-group theory; the experimental data and the theoretical curve agree to within a few per cent.

The λ vs. B^2 curve for a multiplying system has been obtained by varying the moderator height for the lattice of 0.25-inch-diameter, 1.03% U^{235} metal rods with a triangular spacing of 1.75 inches. When these data are fitted to an expression of the form, $\lambda = -m + nB^2 - qB^4$, the polynomial coefficients yield the values of $\overline{v\Sigma}_a$ and k_o, if the value of vD from moderator runs and calculated values of $\bar{\beta}$ and τ are used. The values of several other lattice parameters are derived from the quantities measured in the pulsed neutron runs on moderator and multiplying systems. The values of these parameters are listed in Table 7.11 and compared, wherever possible, with the values obtained from other sources - either the THERMOS code[17,18] or steady-state experiments on the subcritical lattice.

The value of k_o is compared with the value of 1.345 ± 0.03 obtained from the four-factor formula, with the value of η obtained from the THERMOS code (corrected for the epithermal effect by the GAM code), f from THERMOS, and p and ϵ from quantities related to these parameters, measured in steady-state exponential experiments by D'Ardenne and Bliss.[10] The value of the material buckling B_m^2 is also compared with the result of steady-state exponential experiments.[11] As seen from Table 7.11, the values of lattice parameters, obtained by the pulsed neutron method, agree within the experimental uncertainties with the value from other sources, wherever these are available. The uncertainties in k_o in the present work, which are about 2 per cent, are larger than those usually obtained in k_o measurements by other methods. For example, Meister[12] reports errors of about one per cent in k_o from exponential experiments on heavy water lattices. Experiments with heavy water lattices in PLATR and PCTR have yielded k_o with stated errors of less than one per cent.[13] Brooks et al.[14] have measured k_o with uncertainties of less than half a per cent in PLATR experiments with uranium carbide lattices in heavy

TABLE 7.11

Comparison of the Values of Lattice Parameters Obtained by the Pulsed Neutron Method with Those Obtained by Other Methods; Lattice with 0.25-Inch-Diameter, 1.03% U^{235} Metal Rods in a Triangular Spacing of 1.75 Inches

Parameter	Value Obtained by the Pulsed Neutron Method	Value Obtained by Other Source	Name of Source
k_o	1.345 ± 0.026	1.35 ± 0.03	THERMOS and SSEE*
L^2 cm^2	140.9 ± 6.9	134.7	THERMOS
f_m	0.0193 ± 0.0037	0.016	THERMOS
$f_{A\ell}$	-	0.015	THERMOS
f_U	0.9657 ± 0.0037	0.9673	THERMOS
ℓ μsec	497.3 ± 16.4	-	
$\overline{v\Sigma_a}$ sec^{-1}	1396.1 ± 65.5	-	
k	0.650 ± 0.046	-	
B^2_{pc} cm^{-2}	1152 ± 53	-	
B^2_m cm^{-2}	1250 ± 72	1235 ± 25	SSEE

*SSEE stands for Steady-State Exponential Experiments

water. Donahue et al.[15,16] have measured the infinite multiplication factor of a wide range of natural uranium, graphite lattices in the PCTR, with a standard deviation of a few tenths of a per cent.

However, the results - summarized in Table 7.11 - of these die-away experiments on the subcritical assembly have demonstrated the application of the pulsed neutron technique for the measurement of several parameters of interest of the lattice. Of particular significance among these are the infinite multiplication factor k_o and the diffusion area L^2 of the lattice, because these two parameters are especially difficult to measure in simple experiments. Measurements with the PCTR[15] or PLATR[14,16] involve elaborate and expensive equipment. The uncertainties in k_o by the pulsed neutron method can be reduced, as will be discussed below and it is expected that they can be brought down to about one per cent.

An important question bearing on the application of this technique concerns the range of bucklings needed to be covered and the size of the multiplying assembly that is adequate for the investigation of the lattice parameters by the pulsed neutron method. The size of the assembly and the buckling range affect the degree of precision in the final values of the derived parameters and the type of analysis to be used in the reduction of data. In the present measurements, the assembly was far subcritical (about 65 dollars) and the analysis based on the approximation,

$$e^{-B^2\tau} \simeq 1 - B^2\tau + \frac{1}{2} B^2\tau^4 ,$$

represented the experimental data well. However, uncertainties in the final values of the lattice parameters (L^2, k_o) still amount to a few per cent, and it should be advantageous to use a larger assembly, e.g., one with a 4-foot-diameter tank. Small assemblies are unsuitable for several reasons. At very large bucklings, the effect of diffusion cooling becomes increasingly significant. This effect is not fully understood for multiplying systems and, supposing that the diffusion cooling coefficient for the multiplying system is the same as for pure moderator, the effect is significant at sufficiently large values of the geometrical buckling. The diffusion cooling effect in the thermal spectrum is caused by the preferential leakage of faster neutrons and results in a decrease of the average

diffusion constant vD, as it is known from a pure moderator. In a multiplying medium, diffusion cooling may also have some effect on other parameters, such as ℓ and k_o in addition to vD. Although no detailed information, on neutron spectra for small assemblies, is available, it is expected that for very high bucklings the neutron spectrum changes and approaches the moderator spectrum, since multiplication and absorption processes are overcome by thermal neutron leakage. It is well to limit the measurements to the range of bucklings for which the diffusion cooling effect can be ignored. Moreover, as noted in Chapter II, for small multiplying assemblies the simple interpretation of buckling breaks down and the escape probabilities depend not only on the dimensions (geometrical buckling) but also on shape. Further, in small assemblies in which the fuel concentration is low $\left(\frac{V_M}{V_U} \gg 1\right)$, the multiplicative contribution to the thermal neutron decay rate becomes less important and the decay constant is relatively insensitive to the parameters characterizing multiplication. It is expected, from general considerations, that assemblies between 10 and 30 dollars subcritical for any system should provide results with good accuracy; but this possibility should be investigated further experimentally.

The results of the evaluation of the prompt neutron lifetime ℓ and the absolute negative reactivity ρ for the perturbed lattices is shown in Table 7.6. The parameter $\bar{\beta}/\ell$ is found to vary from 15.6 to 17.6 over the range of reactivity studied. The uncertainties in ρ amount to about 5 per cent. The last column of Table 7.6 gives the reactivity worth of the control rods as defined in terms of the difference $\Delta\rho$ from the degree of subcriticality of the unperturbed lattice. The variation of $\Delta\rho$ with rod radius is shown in Fig. 7.15 and the general shape is as predicted by theory. The errors in $\Delta\rho$ are due to uncertainties in the measured decay constant.

The results of the reactivity effect of control rod in terms of the fractional buckling change $\Delta a^2/a_o^2$ caused by the rod in the lattice, are shown in Tables 7.5 and 7.9. This quantity has been obtained both in pulsed neutron and steady-state experiments. The results of the two methods are compared in Table 7.10 and Fig. 7.27; the two agree within the experimental uncertainties, although the uncertainties are somewhat larger in the steady-state experiments. Figure 7.27 also shows the

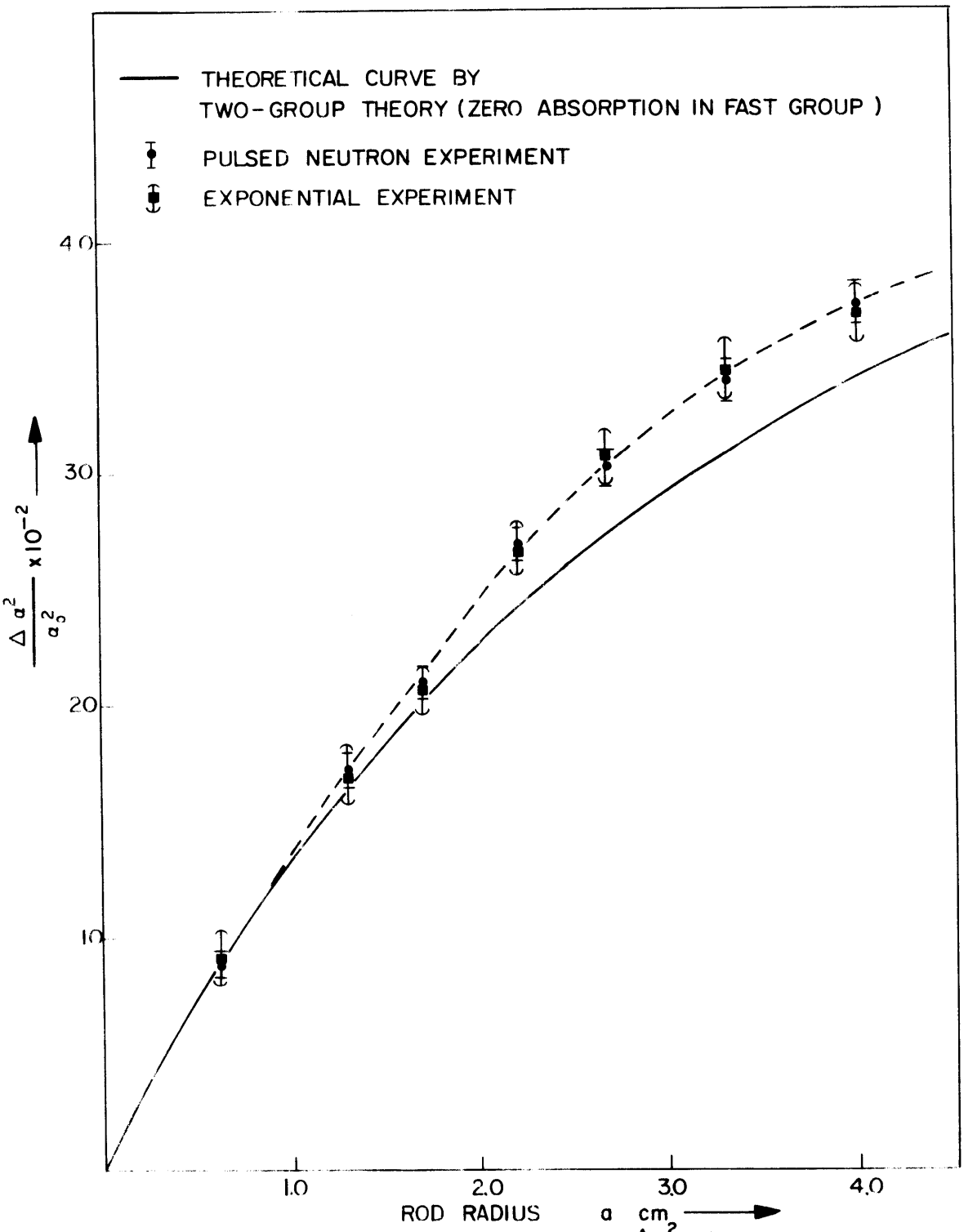

FIG 7.27 FRACTIONAL CHANGE IN BUCKLING $\frac{\Delta a^2}{a_0^2}$ PRODUCED BY CADMIUM RODS OF DIFFERENT RADII a , IN THE SUBCRITICAL ASSEMBLY

curve for $\Delta a^2/a_o^2$ as given by a two-group theory expression:

$$\frac{\Delta a^2}{a_o^2} = -0.820\left[Y_o(\mu a) + d\mu Y_1(\mu a) + \frac{2}{\pi}\frac{S_2}{S_1}(K_o(\nu a) + d\nu K(\nu a))\right]^{-1},$$

derived in Chapter VI, based on flat boundary conditions for the fast neutron group. The experimental points agree with the theoretical curve for small values of the rod radius; for large rods, the theory underestimates the worth of the rod by a few per cent; this is believed to be due to the neglect of fast absorption in the two-group treatment.

One of the necessary conditions for the validity of the exponential experiments, as discussed in Section 4.4, is that the spectrum in the assembly which is perturbed by the introduction of the rod, should be regained within the assembly. This condition is investigated in Section 7.6.2.2 by determining the cadmium ratio along a radius of the exponential assembly with and without the largest control rod. As seen from Fig. 7.26, the spectrum, as indicated by the cadmium ratio, regains its unperturbed value well within the bounds of the lattice.

Some of the ways in which the results obtained in this chapter can be improved and the techniques extended, will be suggested in the next chapter.

References

1. B. K. Malaviya and A. E. Profio, Trans. Am. Nucl. Soc. 6 (1), 58 (1963).

2. A. F. Waltner and F. R. Westfall, Trans. Am. Nucl. Soc. 5 (2), 386 (1962).

3. N. K. Ganguly and A. W. Waltner, Trans. Am. Nucl. Soc. 4 (2), 282 (1961).

4. A. M. Weinberg and E. P. Wigner, The Physical Theory of Neutron Chain Reactors, The University of Chicago Press, Chicago (1958).

5. Private communication to A. E. Profio from J. L. Shapiro.

6. H. D. Brown and E. J. Hennelly, Proc. of the Brookhaven Conf. on Neutron Thermalization, Vol. III, BNL-719 (C-32), 879 (1962).

7. B. K. Malaviya, T. J. Thompson and I. Kaplan, Trans. Am. Nucl. Soc. 6 (2), 240 (1963).

8. I. Kaplan, Private communication.

9. L. J. Templin (Coördinator), Reactor Physics Constants, (2nd Ed.), ANL-5800 (1961).

10. W. H. D'Ardenne, Private communication.

11. F. Clikeman, Private communication.

12. von H. Meister, Nukleonik, Band 3, Heft 6, 236 (1961).

13. J. L. Crandall, DP-833 (1963).

14. W. L. Brooks, M. R. Fleishman, G. G. Foster and R. D. Schamberger, NDA-2131-40 (1961).

15. D. J. Donahue, D. D. Lanning, R. A. Bennett and R. E. Heineman, Nuclear Sci. and Eng. 4, 297 (1958).

16. P. Anthony, S. Davis, R. Schamberger and J. Hutton, NDA-2131-25 (1961).

17. H. C. Honeck, Ph.D. Thesis, Nuclear Eng. Dept., M.I.T. (1959).

18. H. C. Honeck, BNL-5826 (1961).

Chapter VIII

SUMMARY, CONCLUSIONS AND RECOMMENDATIONS

This chapter summarizes the present work and the conclusions that can be drawn from it. Some ways are suggested in which the precision of the results can be improved and the techniques extended; recommendations are made for future investigations along the lines initiated in this work.

8.1 SUMMARY AND CONCLUSIONS

The theoretical work in this study has been concerned mainly with the determination of certain properties of neutron transport media bombarded by pulses of fast neutrons. A pure moderator has been treated by a generalized time-dependent age theory, and expressions have been derived for the slowing-down and thermal die-away rates. Multiplying systems have been treated according to several theoretical models to study the space- and time-dependent thermal flux in pulsed assemblies and to derive expressions for the prompt neutron decay constant in different situations. It has been found that the asymptotic prompt neutron decay constant can be related in several ways to parameters characterizing the multiplying system and quantitative information about reactor systems can be obtained in this way.

The theoretical analysis of an exponential assembly with a control rod has shown the possibility of making steady-state measurements of control rod effectiveness in subcritical assemblies for simple control rod configurations. The conditions under which the information obtained from exponential experiments with control rods can be analyzed in terms of simple theory and related to critical system studies have also been considered.

The experimental program has proceeded along two lines - pulsed neutron and steady-state studies. The conditions affecting the measurement

of the fundamental mode decay constant in pulsed assemblies have been investigated, as have the effects of several experimental variables, types and location of detector, etc. Computer codes have been written to facilitate data reduction in pulsed neutron experiments. Experiments in a 36-inch-diameter tank have yielded values of the diffusion parameters of 99.60 mole per cent heavy water at room temperature. The values of vD based on different ranges of values of the buckling are found to be consistent. The relatively large uncertainty in the value of $v\Sigma_a$ has indicated the need for future experiments on larger assemblies of heavy water. The values of the diffusion parameters have been used to evaluate the geometrical buckling of a cylindrical moderator assembly modified by placing a single absorbing rod along the axis. The changes in buckling due to rods of different radii agree with calculations based on one-group theory.

A significant aspect of the present work has been the use of the pulsed neutron technique to obtain information about the lattice parameters of subcritical systems. This has been accomplished by means of thermal die-away experiments on subcritical assemblies of varying core height, combined with the use of theoretical relations between λ and B^2 to analyze the experimental data. By combining the results of these experiments with those on pure moderator assemblies and using calculated values of $\bar{\beta}$ and τ, the values of a number of lattice parameters, e.g., k_o, L^2, L_m^2, f_m, k, B_m^2, etc., can be obtained. The results for the parameters k_o and L^2 are of special interest because these quantities are difficult to measure in simple experiments. The values of these parameters by the pulsed neutron method are found to be in agreement, within the experimental uncertainties, with the results of exponential experiments and THERMOS calculations, wherever such comparisons are possible. However, the uncertainties in the values of these parameters obtained in the present experiments (which were made on assemblies far below critical) are somewhat larger than those obtained by other methods. The advantages of the pulsed neutron method make it worthwhile to extend the technique to larger systems to reduce the uncertainties, and to try to improve the methods used in the present study.

Pulsed neutron measurements of the prompt neutron decay constant

in perturbed lattices can yield the prompt neutron lifetime and the absolute negative reactivity when combined with the lattice parameters determined as described above. This procedure makes use of the explicit relation between the prompt neutron decay constant λ and reactivity ρ. The uncertainties in ρ, which amount to less than 5 per cent, arise mainly from the error in ℓ; the latter can also be reduced by improving the precision of the lattice parameters.

The effect of a control rod on the reactivity of a lattice has been obtained by relating the change in prompt neutron decay constant due to the insertion of the rod to the change in buckling caused by the rod and expressing the effect in terms of the fractional change in radial buckling. This effect has also been measured in exponential (steady-state) experiments by foil activation techniques and the results of the two methods agree within the experimental uncertainties. The latter are somewhat larger in the steady-state case. A comparison of these results with those of a two-group theoretical treatment, with no allowance for fast absorption, shows that this theory somewhat underestimates the effectiveness of the rod, especially for large rod sizes.

In exponential experiments, radial and axial flux plots were made in the assembly with and without a control rod. The radial flux in the moderator with a central control rod is given well by a one-group theory using the value of the radial buckling derived from axial runs. A measurement of the cadmium ratio along a radial direction of the lattice with and without an axial control rod showed that the perturbation in the neutron spectrum (at least, as indicated by the cadmium ratio) due to the insertion of the rod, does not extend over the whole range of the assembly. This property ensures a necessary condition for the validity of the control rod experiments in exponential assemblies.

8.2 RECOMMENDATIONS FOR FURTHER WORK

The present investigation began the pulsed neutron portion of the work of the M.I.T. Lattice Project and demonstrated the utility of this technique in the measurement of reactor parameters (including reactivity) and control rod worths in the subcritical assembly. Consequently, a large part of the effort was devoted to setting up the apparatus and "establishing

the technique." The latter constituted the main goal of the investigation, rather than the application of the method to different lattices for the purpose of compiling data. The measurements reported here can be applied to other lattices and to other types and configurations of control rods. In addition, effort should be directed toward improving the precision of the results and to extending the method to the determination, if possible, of additional properties of multiplying systems. Some suggestions along these lines will be made in the following sections.

8.2.1 Experiments on Moderator Assemblies

New experiments on moderator assemblies should be directed toward improving the precision in the values of the diffusion parameters and a more detailed examination of the effects of experimental variables on the measured decay constant of the fundamental mode, especially in larger assemblies. The first step should be die-away experiments in the 4-foot-diameter tank, which will allow a wider range of values of the geometrical buckling. Other types and configurations of the detector can also be examined, e.g., a large BF_3 counter, movable in an external tube on a side of the tank. When the detector is placed in a thimble along the axis, a modal analysis method[1] can be used for very low bucklings. According to this method, the neutron flux decay $\phi(z_i,t)$ is measured at (N-1) equidistant axial detector positions, $z_i = \frac{H}{N} i$ [H:effective height, $i = 1,2,\ldots(N-1)$] and then the Fourier coefficents of the axial flux distribution are obtained from the relations:

$$\phi(z_i,t) = \sum_{k=1}^{\infty} A_k(t) \sin \frac{k\pi}{H} z \ ,$$

$$A_k(t) = A_{ko}\, e^{-\lambda_k t} \ ,$$

$$A_k^*(t) = \frac{2}{\pi} \sum_{i=1}^{N-1} \phi(z_i,t) \sin \frac{ik}{N} \pi \ .$$

By plotting $A_k^*(t)$ against t, we can determine the decay constants λ_k of the k^{th} spatial mode. The parameter λ_1, for instance, can be used to evaluate

the thermalization time constant. Time-space distributions can also be obtained by using an external detector to count capture gamma rays from a small absorber moved about in the moderator.[2]

The study of the effect of the location of the source on the decay constant should be instructive. With a localized source and a localized detector, it may be possible to investigate the reciprocity condition experimentally.

An interesting experiment would be to apply the pulsed neutron technique to the measurement of the neutron age in heavy water. Two methods have been used for measuring the age of neutrons from a pulsed neutron source in a medium. One of these has been described by Ramanna et al.[3] who have determined the age in water by using the relation between the initial thermal neutron density and a geometrical factor characterizing the moderator. The other method has been described by Frank[4] and used by Dlouhy[5] to measure the neutron age in graphite. This method makes use of the slowing-down kernel in the medium to obtain an expression for the age $\tau(t)$ in terms of the thermal neutron density at different positions in the medium at a certain time t.

The availability of mixtures of H_2O and D_2O at different D_2O concentrations would permit pulsed neutron measurements of the diffusion characteristics of the mixture as function of the concentration of D_2O. Apart from its intrinsic interest, the results may be of interest in the future development of spectral-shift reactors.

The sensitivity of the diffusion parameters of heavy water to isotopic and chemical purity can be utilized as a routine check on the sample of heavy water. The parameter vD should be sensitive to hydrogen (H) concentration, while $v\Sigma_a$ depends on both hydrogen and other absorption. Relatively small assemblies of the moderator are needed to measure vD. With an appropriate set-up, a standard procedure can be established to keep a regular check on the sample of heavy water, used, for instance, in lattice experiments.

The pulsed neutron method may also be applied to the study of heterogeneous absorption and the measurement of buckling for complex geometrical shapes; such effects may be introduced by the presence of voids, or by the introduction of absorbing rods. The latter studies may include the

effects of partially inserted or diagonal rods. Such studies might be used to evaluate the results of perturbation theory and other theoretical methods for solving the wave equation in a region of complex shape.

8.2.2 Pulsed Neutron Experiments on Subcritical Assemblies

A great deal of work can be done with pulsed neutron experiments on subcritical assemblies, extending and improving upon the measurements reported in this investigation. It would be desirable to have a separate, independent subcritical facility exclusively for pulsed neutron work. This possibility is suggested to increase the efficiency of scheduling and experimenting at the M.I.T. Lattice Project. Availability of spare exponential tanks, large quantities of heavy water and several sets of fuel rods and other lattice equipment should make it relatively easy to set up a second subcritical facility, independent of the reactor. This would simplify and improve the experiments and broaden the type of measurements that can be undertaken with ease. Congestion by shielding and channels would be avoided as would interference or background from the proximity of the reactor. Greater flexibility and a wider choice in the locations of the source and detection system would be possible. The same type of lattice can subsequently be used in the exponential experiments so that the possibility of comparison of the pulsed neutron and steady-state experiments will not be lost. A separate lattice for pulsed neutron experiments would also make possible a more detailed and diversified investigation of the experimental variables affecting the determination of the fundamental mode decay constant. The pulsed neutron experiments in the exponential facility are now limited to week ends and periods of reactor shutdown; this limitation would also be removed.

An interesting study could be based on a measurement of the spatial - vertical and radial - flux distributions in the pulsed subcritical assembly. One possible method is the gamma-ray scanning of the fuel elements with an appropriate discriminator base line setting. The flux profile along the vertical axis can be obtained by scanning the central fuel element after pulsing. The radial flux distribution can be obtained by making a scan along a horizontal plane at the location of the highest activity. The radial distribution in a pulsed assembly from theoretical considerations is a J_o

function, and a fitting of the experimental flux profile can yield a "dynamic radial buckling" which can be compared with the radial buckling from steady-state distributions; information about the difference in spectra and the extrapolation distance in the two cases might also be obtained. The form of the axial flux distribution can be studied with different locations of the source and with different thicknesses of reflectors.

The application of the λ vs. B^2 experiments on a lattice to the measurement of its reactor parameters should be explored further by using larger assemblies and covering a wider range of values of the buckling. As noted in the last chapter, such measurements should reduce the uncertainties in the values of the parameters. In larger assemblies, the errors involved in the calculation of the bucklings are also smaller. Other methods of analyzing the (λ, B^2) data than the one used in this work should also be tried. For example, by fitting the (λ, B^2) points to an expression of the form, $\lambda = a + bB^2 + ce^{-B^2\tau}$, in a three-parameter fit (with a calculated value of τ), it may be possible to determine vD for the lattice. A fit to the two-group expression (Chapter II) instead of the age theory relation could also be attempted.

Another possibility is to use the values of the lattice parameters and group constants - either calculated or from steady-state exponential experiments - and to compare the measured values of the prompt decay constant with the value calculated on the basis of different theoretical models, treated in Chapter II. Such a procedure for lattices with different values of V_M/V_U, different U^{235} concentration, and varied lattice spacing will give information about the sensitivity of the calculation of the prompt decay constant to the theoretical model. The prompt neutron decay constant computed from multigroup codes can also be compared with measured values. The contribution of delayed neutrons should be examined. The effect of the dependence of the lattice parameters on the buckling, arising from such factors as a possible anisotropy introduced by heterogeneities in the lattice, significant reflector thickness, the diffusion cooling effect, etc. should also be investigated. The assumption, $D \approx D^m$, can be examined by correcting the diffusion constant due to "voids" of uranium in a lattice.

8.2.3 Reactivity and Related Studies

The techniques developed in this work should be applied to the study of a variety of control rods under different conditions and compared with the results of calculation based on specific theoretical models. The effect of partially inserted rods, diagonal and off-center rods, and of multiple rods to study the shadowing effect, should also be investigated. Moderator-filled control rods or "flux traps," B_4C rods, and composite and discrete layer types of rods should be studied. An example of the last type is a control rod with a core of boron surrounded by a layer of cadmium. The boron would provide epithermal absorption and the cadmium absorption in the thermal range would reduce the amount of helium generated in the boron, thereby increasing the useful rod life. The convenience of the pulsed neutron method would make it easy to investigate control rods of various absorber materials, e.g., different rare earths, or combinations of these elements. The other types of control rods mentioned above may provide better means of studying the fast neutron boundary conditions on the rod surface; the fast neutron extrapolation distance can be measured in exponential experiments as discussed in Chapter IV.

Some of the other methods of measuring reactivity (Chapter I) should also be studied and compared in the region of their common validity. The rod drop, source-jerk, and new statistical methods (noise analysis, pseudo source modulation, etc.) should be especially useful in this regard. The recently proposed $k\beta/\ell$ method (Section 3.6.3) should be studied further. The preliminary investigation of this method in this work (Appendix IV) seems to indicate that it is not applicable to systems as far below critical as those used here. The main reason seems to be the small contribution of the delayed neutrons to the decay curve, on the complete analysis of which, the method is based. Thus, a larger system closer to criticality would be advantageous. Once the validity of several methods in yielding results on reactivity in agreement is established, this agreement could be used to obtain the values of other parameters, e.g., the effective delayed neutron fraction $\bar{\beta}$ for a lattice.

There is a great need for a set of systematic measurements of control rod worths in critical assemblies, for, in the final analysis, it is the critical assembly which provides the "true" value of the rod worth against

which any theoretical value or the results of measurements by other methods should be compared. The lack of such experiments is a serious obstacle to the correlation of theory and experiment in control rod studies. If the data on the measured rod worths in critical assemblies are available, then the various methods with the same type of rod and an exponential or subcritical assembly of the same constitution would provide a valuable basis for the needed quantitative correlation.

It is suggested that the role of the prompt neutron decay constant as an independent parameter, characterizing a multiplying system, be examined more closely. It is becoming increasingly apparent that the reactivity is an unsuitable parameter in several ways; its interpretation in situations involving large changes in the multiplication characteristics of the system, and the distinction between static and dynamic reactivity are far from clear. Moreover, reactivity is not directly measurable; the operationally meaningful quantity is the reactor period. For these and other reasons, it is to be expected that reactivity might be replaced by other parameters; a serious contender for this role is the prompt neutron decay constant. As an example of a practical situation, the usual criticality studies based on inverse multiplication experiment can be replaced by pulsed neutron studies of the prompt neutron decay constant.

Along with the experimental programs of the measurement of control rod worths, new methods in the area of control rod theory should also be investigated. Analytical and machine calculation methods based on the more accurate transport theory and combinations of transport theory with multidimensional diffusion theory are especially needed. Some of the possible approaches are suggested in Chapter VI. Also desirable would be a theoretical method that seeks to relate the effect of control rods in terms of the change, not in reactivity, but in the prompt neutron decay constant, so as to make possible a more direct and valid comparison between theory and experiment.

It is expected that a continuation of the efforts initiated in this investigation would further extend the techniques, improve the results, and lead to a better over-all understanding of the physics of subcritical lattices, in line with the basic goal of any study in the field of reactor physics.

References

1. H. Meister, To be published in J. Nuclear Energy.

2. A. E. Profio, Ph.D. Thesis, Nucl. Eng. Dept., M.I.T. (1962).

3. R. Ramanna et al., Proc. of the Int. Conf. on the Peaceful Uses of Atomic Energy, Geneva, Vol. 5, p. 24 (1955).

4. I. M. Frank, Ibid., p. 3 (1955).

5. Z. Dlouhy, Reactor Sci. and Techn., 16, 311 (1962).

Appendix 1

NOMENCLATURE

a	Radius of control rod (cm)
B	Background from the decay curve
B^2	Geometrical buckling (cm^{-2})
B_m^2	Material buckling (cm^{-2})
B_{pc}^2	Prompt critical buckling (cm^{-2})
C	Diffusion cooling coefficient ($cm^4\ sec^{-1}$)
C_i	Concentration of precursors from which the i^{th} group of delayed neutrons arise (cm^{-3})
d	Extrapolation distance (cm)
D	Diffusion coefficient ($cm^2\ sec^{-1}$)
$d\tau$	Element of volume (cm^3)
E	Energy (ev)
f	Thermal utilization
f_m	Moderator "thermal utilization"
$f(E)$	Normalized fission spectrum
$\bar{f}(s)$	Laplace Transform of f(t)
$F(B^2)$	Fast non-leakage probability
$g_e(\vec{\Omega}';u';\Omega,u)$	Relative probability of a neutron being left with velocity parameters $(\vec{\Omega},u)$ as a result of an elastic collision before which its velocity parameters were $(\Omega';u')$
$g_f(u)$	Relative probability that a fission neutron is born with letharge u

H	Operator in Eq. 1.2; also height (cm)
$H(\tau)$	Heaviside function
I	Operator in Eq. 1.2
J	Operator in Eq. 1.4
J_o	Bessel function of first kind of order zero
K	Operator in Eq. 1.2
k	Effective multiplication factor or criticality factor
k_o	Infinite multiplication factor (k_∞)
k_p	Prompt neutron multiplication factor
K_Q	Modified Bessel function of second kind of order zero
k_q	Thermal criticality factor
k_r	Resonance criticality factor
ℓ	Prompt neutron lifetime (sec)
ℓ_o	Infinite medium neutron lifetime (sec)
L^2	Diffusion area (cm^2)
M	Adjoint of the neutron density N
M^2	Migration area (cm^2)
$N(\vec{r},\Omega,u,t)$	The number of neutrons whose position vectors lie in the volume element $d\vec{r}$ about $\vec{r}$, whose velocities lie in the solid angle $d\vec{\Omega}$ about $\vec{\Omega}$ and whose lethargies are between u and $u + du$, all measured at time t
p	Resonance escape probability
P	Probability that a neutron generated in a uranium slug will undergo a collision before leaving the slug
q	Slowing-down density with absorption (cm^{-3})
$q(\lvert\vec{r}-\vec{r}'\rvert,t-t')$	Probability per unit volume, per unit time that a neutron born at $(\vec{r}',t')$ will become thermalized at $(\vec{r},t)$

$Q(I)$	Experimental number of counts in I^{th} channel
Q_{sj}	Number of neutrons per cm^3 per second scattered into group j from all higher energy groups
$\vec{r}$	Position vector
R	Radius of cylindrical assembly (cm)
s	Laplace Transform variable
S	External source
\$	Reactivity in dollars
S_1, S_2	Coupling coefficients
t	Time variable (sec)
T	Slowing-down time (sec)
T(I)	Time corresponding to the I^{th} channel of time analyzer
u	Lethargy
v	Velocity (cm sec^{-1})
V	Volume (cm^3)
WT	Weights in least-squares fitting
Y_o	Modified Bessel function of first kind
Z	Radial flux

Greek Symbols

α^2	Radial buckling (cm^{-2})
β_i	Delayed neutron fraction for the i^{th} group
$\bar{\beta}$	Effective delayed neutron fraction
γ^2	Axial buckling (cm^{-2})
δ	Ratio of U^{235} fast fissions to U^{235} thermal fissions
$\delta(\vec{r}-\vec{r}_o)$	Direct delta function
δ_{ij}	Kronecker delta

ϵ	Fast fission factor
η	Number of neutrons released per thermal absorption in fuel
$\theta(r)$	Radial flux
λ	Decay constant of the fundamental mode of the thermal flux in a pulsed assembly (sec^{-1})
Λ	Neutron generation time
λ_t	Transport mean-free path (cm)
μ^2,ν^2	Buckling from two-group criticality equation (cm^{-2})
ν	Average number of fast neutrons released per slow neutron fission
ν_c	Parameter in Eq. 1.6
ξ	Average logarithmic energy decrement per collision
ρ	Reactivity
Σ	Macroscopic cross-section (cm^{-1})
Σ_{ij}	Macroscopic inelastic removal cross-section from group j (cm^{-1})
Σ_{ej}	Macroscopic elastic removal cross-section from group j (cm^{-1})
Σ_{aj}	Total removal cross-section from group j (cm^{-1})
τ	Neutron age (cm^2)
$\phi(\vec{r},\vec{\Omega},u,t)$	Vector neutron flux
ϕ	Neutron flux
$\bar{\phi}$	Laplace transform of ϕ
$\bar{\bar{\phi}}$	Finite Hankel transform of $\bar{\phi}$
$\bar{\bar{\bar{\phi}}}$	Finite sine transform of $\bar{\bar{\phi}}$
$\chi(o,u,t)$	Slowing-down density without absorption
$\chi(\vec{r},t)$	Fission source distribution

ω	Decay constant of the delayed neutron precursor (sec^{-1})
$\vec{\Omega}$	A unit vector in the direction of motion of the neutron
Ω	Geometrical factor (Fig. 2.1)

Subscripts and Superscripts

a	Absorption
Aℓ	Refers to cladding region
e	Elastic scattering
fuel	Fuel region
i	Inelastic scattering
j	j^{th}-energy group
ℓ	Leakage
m, mod	Moderator region
s	Scattering
t	Total
1	Fast group (as in ϕ_1)
2	Thermal group (as in ϕ_2)

Appendix II

COMPUTER CODES

The availability of an IBM-7090 computer made possible a rapid, complete and efficient analysis of the experimental data. Several computer codes were developed in the course of this investigation for the reduction of data in different phases of this work. The description and Fortran listings of some of these programs are included in this appendix.

A2.1 THE EXPO CODE

In any pulsed neutron experiment of the die-away type, the raw experimental data consist of a series of counts taken over equally spaced time intervals. Superimposed on the decay is a background which is almost constant in time, if the room return following a pulse has died away. One is interested in the decay rate of the fundamental or normal mode which persists after the higher modes have decayed away; each mode decays in an exponential manner. Thus, the problem is to isolate the portion of the decay data which is in the fundamental mode and to analyze it for a single exponential plus a constant background, i.e., for the functional form,

$$n(t) = a + b\, e^{-\lambda t} .$$

The basic quantity of interest is the decay constant λ of this mode.

If sufficient time has not been allowed before the opening of the first analysis channel, the first few channels will contain harmonics resulting in a departure from a single exponential decay. The isolation of the fundamental mode will involve excluding these initial channels from the analysis. It is also instructive to study the effect of excluding the end-channels. Hence, whatever method is adopted for the reduction of data, should have provision for dropping successively points from both ends so as to select the "best" time interval for analysis. It will be seen that the choice of the point at which the analysis is started is of

considerable importance, while the decay constant is relatively insensitive to the choice of the point at which the analysis is terminated.

The best approach to the reduction of data appears to be a weighted, least-squares fitting of the counts (y_i) versus time (t_i) data to an expression of the form,

$$y_i = A + B\, e^{-Ct_i}, \tag{A2.1}$$

so that the parameters A, B, C are determined from the condition that the sum of the weighted squares of residuals,

$$\sum_{i=N}^{M} W_i \left[y_i - \left(A + B e^{-Ct_i} \right) \right]^2, \tag{A2.2}$$

is to be a minimum. (M-N) is the total number of data points used in the analysis and W_i is the statistical weight of the y_i data point.

A2.1.1 Theoretical Basis of the Code

The IBM-7090 code EXPO fits a set of up to 300 points to the curve (A2.1) by the least-squares technique and computes the parameters A, B, C together with the associated standard deviations of the estimates of A, B, C, due to uncertainties in the measured data.

The code minimizes the expression (A2.2) by means of an iterative scheme. We can express the functional form of the "true" counts at each time-point, as

$$f_i(A,B,C) \equiv y_i = A + B\, e^{-Ct_i}$$

$$= (A_o + a) + (B_o + b)\, e^{-(C_o + c)t_i},$$

where a, b, c are small increments on A_o, B_o, C_o, the initial estimates of A, B, C; a rough estimate of A_o, B_o, C_o can be obtained from a plot of the data. The least-squares technique may be applied directly only to parameters in a linear relationship. In order to apply it to (A2.1), we must linearalize the function f_i by expanding it in a Taylor series about the point (A_o, B_o, C_o):

$$f_i(A,B,C) = F_i(A_o,B_o,C_o) + \left(\frac{\partial f_i}{\partial A}\right)_o a + \left(\frac{\partial f_i}{\partial B}\right)_o b + \left(\frac{\partial f_i}{\partial C}\right)_o c + \ldots , \tag{A2.3}$$

where each partial derivative is evaluated at the initial point (A_o,B_o,C_o) and

$$a = A - A_o , \qquad b = B - B_o , \qquad c = C - C_o .$$

If we define

$$\left(\frac{\partial f_i}{\partial A}\right)_o = \mu_i , \qquad \left(\frac{\partial f_i}{\partial B}\right)_o = \nu_i , \qquad \left(\frac{\partial f_i}{\partial C}\right)_o = \omega_i , \tag{A2.4}$$

then

$$\begin{aligned} \mu_i &= 1 , \\ \nu_i &= e^{-C_o t_i} , \\ \omega_i &= -B_o t_i e^{-C_o t_i} . \end{aligned} \tag{A2.5}$$

As Eq. A2.3 is linear in a, b, c, the method of weighted least-squares fit may be used to minimize Eq. A2.2 which now takes the form,

$$\sum_i W_i \left[y_i - A_o - B_o e^{-C_o t_i} - a - b e^{-C_o t_i} + c B_o t_i e^{-C_o t_i} \right]^2 . \tag{A2.6}$$

The resulting solutions for a, b, c are then the corrections which are applied to the initial guesses, A_o,B_o,C_o, to obtain the next set of estimates. The process is then repeated until some pre-set convergence criteria are satisfied. The final results do not depend on the initial guesses; i.e., the method gives a unique set of values, independent of the first estimates. The number of iterations necessary to arrive at the final answer depends on the initial estimates as well as the convergence criteria.

The deviations of the experimental points y_i from the fitted curve f_i are given by:

$$d_i = y_i - f_i(A_o,B_o,C_o) - a\mu_i - b\nu_i - c\omega_i ,$$

$$d_i = \phi_i - a\mu_i - b\nu_i - c\omega_i , \qquad \text{(A2.7)}$$

where

$$\phi_i = y_i - f_i(A_o,B_o,C_o) .$$

The simplest form of the least-squares principle now requires that the quantity,

$$\delta^2 = \sum_{i=N}^{M} W_i d_i^2 , \qquad \text{(A2.8)}$$

be minimized with respect to the parameters A, B, C so that the normal equations determining a, b, c, are:

$$0 = \frac{\partial}{\partial A} \delta^2 = \sum_i W_i(\phi_i - a\mu_i - b\nu_i - C\omega_i)\mu_i ,$$

$$0 = \frac{\partial}{\partial B} \delta^2 = \sum_i W_i(\phi_i - a\mu_i - b\nu_i - C\omega_i)\nu_i , \qquad \text{(A2.9)}$$

$$0 = \frac{\partial}{\partial C} \delta^2 = \sum_i W_i(\phi_i - a\mu_i - b\nu_i - C\omega_i)\omega_i .$$

If we set

$$F_i = W_i \phi_i , \quad U_i = W_i \mu_i , \quad V_i = W_i \nu_i , \quad W_i = W_i \omega_i ,$$

and follow the convention that a repeated index implies summation, i.e.,

$$(U_i V_i) = \sum_i U_i V_i ,$$

then the normal equations become:

$$a(U_iU_i) + b(U_iV_i) + c(U_iW_i) = (F_iU_i) ,$$

$$a(U_iV_i) + b(V_iV_i) + c(V_iW_i) = (F_iV_i) , \qquad \text{(A2.10)}$$

$$a(U_iW_i) + b(V_iW_i) + c(W_iW_i) = (F_iW_i) .$$

These linear equations can be solved for a, b, c so as to yield:

$$a = \frac{\begin{vmatrix} (F_iU_i) & (U_iV_i) & (U_iW_i) \\ (F_iV_i) & (V_iV_i) & (V_iW_i) \\ (F_iW_i) & (V_iW_i) & (W_iW_i) \end{vmatrix}}{D}, \qquad \text{(A2.11)}$$

$$b = \frac{\begin{vmatrix} (U_iU_i) & (F_iU_i) & (U_iW_i) \\ (U_iV_i) & (F_iV_i) & (V_iW_i) \\ (U_iW_i) & (F_iW_i) & (W_iW_i) \end{vmatrix}}{D}, \qquad \text{(A2.12)}$$

$$c = \frac{\begin{vmatrix} (U_iU_i) & (U_iV_i) & (F_iU_i) \\ (U_iV_i) & (V_iV_i) & (F_iV_i) \\ (U_iW_i) & (V_iW_i) & (F_iW_i) \end{vmatrix}}{D}, \qquad \text{(A2.13)}$$

with

$$D = \begin{vmatrix} (U_iU_i) & (U_iV_i) & (U_iW_i) \\ (U_iV_i) & (V_iV_i) & (V_iW_i) \\ (U_iW_i) & (V_iW_i) & (W_iW_i) \end{vmatrix}. \qquad \text{(A2.14)}$$

In terms of the minors of the determinant D,

$$
\begin{aligned}
D_{11} &= (V_i V_i)(W_i W_i) - (V_i W_i)^2 , \\
D_{12} &= (V_i W_i)(U_i W_i) - (U_i V_i)(W_i W_i) , \\
D_{13} &= (U_i V_i)(V_i W_i) - (U_i W_i)(V_i V_i) , \\
D_{22} &= (U_i U_i)(W_i W_i) - (U_i W_i)^2 , \\
D_{23} &= (U_i V_i)(U_i W_i) - (U_i W_i)(V_i W_i) , \\
D_{33} &= (U_i U_i)(V_i V_i) - (U_i V_i)^2 .
\end{aligned}
\qquad \text{(A2.15)}
$$

a, b, c are given as:

$$
\begin{aligned}
a &= \frac{(F_i U_i)D_{11} + (F_i V_i)D_{12} + (F_i W_i)D_{13}}{D} , \\
b &= \frac{(F_i U_i)D_{12} + (F_i V_i)D_{22} + (F_i W_i)D_{23}}{D} , \\
c &= \frac{(F_i U_i)D_{13} + (F_i V_i)D_{23} + (F_i W_i)D_{33}}{D} ,
\end{aligned}
\qquad \text{(A2.16)}
$$

with

$$
D = (U_i U_i)D_{11} + (U_i V_i)D_{12} + (U_i W_i)D_{13} . \qquad \text{(A2.17)}
$$

Now a, b, c are the first-order corrections to the initial guesses A_o, B_o, C_o. The new estimates are

$$
A_1 = A_o + a , \qquad B_1 = B_o + b , \qquad C_1 = C_o + c .
$$

As the method is based upon retaining only the first-order terms in the Taylor expansion (A2.3), it is necessary to repeat the calculation, starting with A_1, B_1, C_1 as the initial guesses. The process is to be repeated until adequate convergence is reached, as defined by ϵ_1, ϵ_2, ϵ_3:

$$
\frac{A_n - A_{n-1}}{A_n} < \epsilon_1 , \qquad \frac{B_n - B_{n-1}}{B_n} < \epsilon_2 , \qquad \frac{C_n - C_{n-1}}{C_n} < \epsilon_3
\qquad \text{(A2.18)}
$$

where ϵ_1, ϵ_2, ϵ_3 are arbitrarily small quantities which may be specified in the code input.

It is also desirable to determine the standard deviations and probable errors of A, B, C. For this, we must carry out the above analysis with $(a+\delta a)$, $(b+\delta b)$, $(c+\delta c)$ substituted for a, b, c. Then the estimates of error in A, B, C due to uncertainties in y_i are:

$$\Delta A = \frac{D_{11}}{D}, \quad \Delta B = \frac{D_{22}}{D}, \quad \Delta C = \frac{D_{33}}{D}. \tag{A2.19}$$

The standard deviations of the estimates of A, B, C are given by:

$$\sigma_A = \Delta A \sqrt{\frac{\delta^2}{M-3}}, \quad \sigma_B = \Delta B \sqrt{\frac{\delta^2}{M-3}}, \quad \sigma_C = \Delta C \sqrt{\frac{\delta^2}{M-3}}. \tag{A2.20}$$

A2.1.2 Description of the Code

The EXPO code adapts the above analysis in a main program and translates it into the FORTRAN language in the form of instructions punched out on cards. The successive steps in the logic are displayed in the flow chart outlined in Fig. A2.1. The detailed operation of the code can be best understood with the aid of this block diagram and the complete FORTRAN listings which are included at the end of this section.

As discussed in Section 7.1.1, the code corrects the experimental number of counts in each channel for counting losses:

$$P(I) = \frac{Q(I)}{1 - CORRN(I)}, \tag{A2.21}$$

and determines the time corresponding to each channel:

$$T(I) = (CHDEL) \times (WIDTH) - TDEL + (SPAC) \times (I-0.5). \tag{A2.22}$$

The weighting of the points is based on the Poisson statistical errors in the number of counts:

$$WT(I) = \frac{1}{[P(I)]^{1/2}}. \tag{A2.23}$$

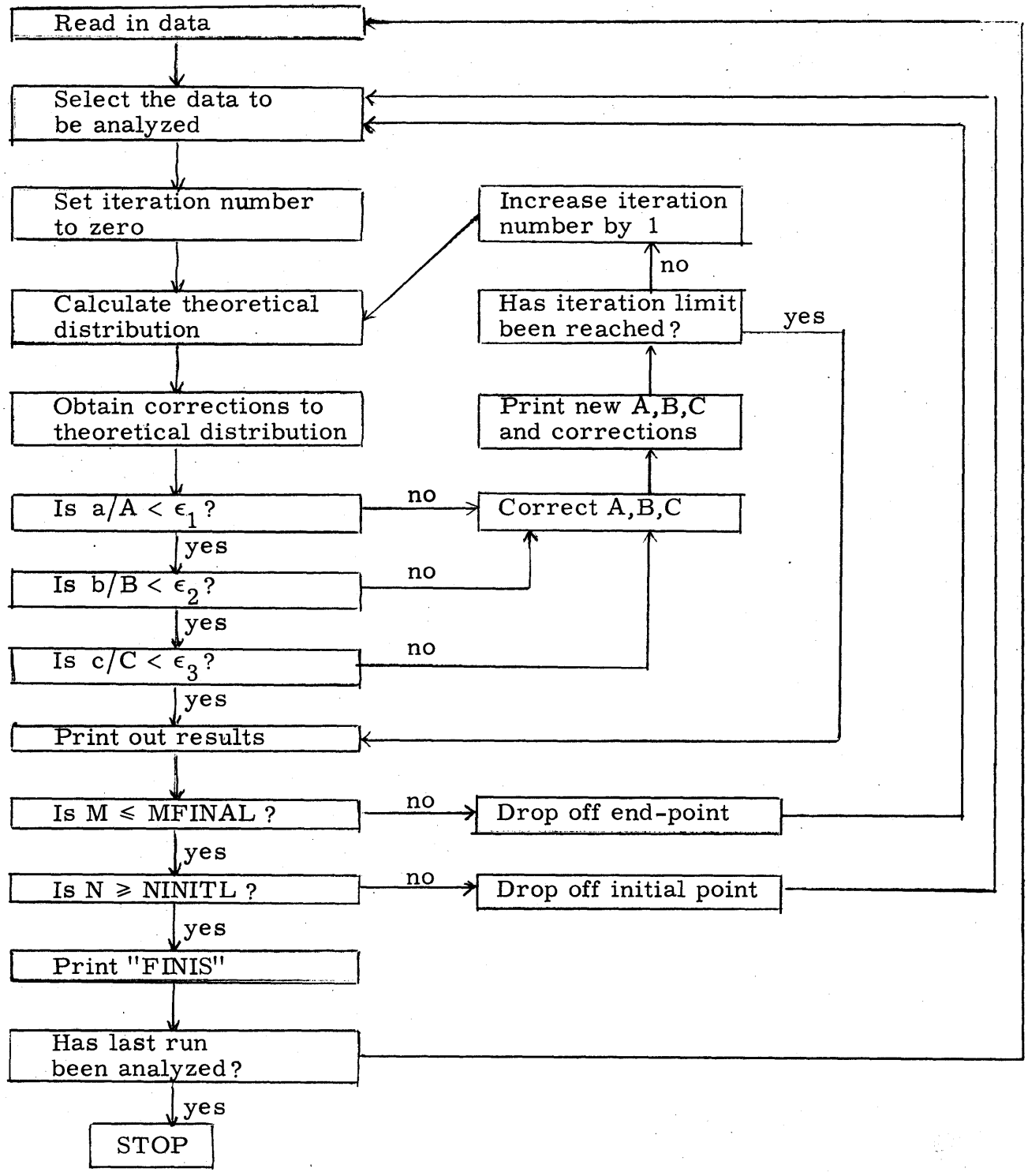

Fig. A2.1 Flow Chart for the EXPO Code

The code then fits P(I) against T(I) in a three-parameter fit of the form of Eq. A2.1 and computes the decay constant C and the background correction B, together with their standard deviations. In analyzing the data, the code has provisions to drop the initial channels one by one and to calculate the decay constants for fewer channels each time. The effect of dropping points from the other end can also be studied. At any stage, if the convergence criteria are satisfied or the iteration limit is reached, the quantities of interest are printed out.

A2.1.3 Vocabulary of the EXPO Code

Symbol in Code	Definition of Symbol	Designation in Section A2.1.1
NORUN	Run number	
LASTRN	Last run of a series	
MFINAL	Last point included in analysis	M
NINITL	First point included in analysis	N
MN1	Number of points used	
ITS	Number of iterations to be used	
ITSFNL	Limit of iterations	
AZERO, BZERO CZERO	First guesses for A, B, C	A_o, B_o, C_o
EPS1, EPS2, EPS3	Convergence criteria	$\epsilon_1, \epsilon_2, \epsilon_3$
XTRA, XTRB XTRC	Multiples of a, b, c used as correction factors to A, B, C	
DELTM, DELTAB, DELTAC		a, b, c
WIDTH	Channel width	
T(I)	Time points	t_i
Q(I)	Experimental no. of counts at t_i	y_i
WT(I)	Weighting factor	w_i
SUMUU		$\Sigma U_i U_i = (U_i U_i)$

Symbol in Code	Definition of Symbol	Designation in Section A2.1.1
SSQRES		δ^2
FIT(I)	Theoretical no. of counts at t_i	$A + Be^{-Ct_i}$
DIFFR(I)	Deviation of Exp. from Theor. no. of counts at t_i	
U(I), V(I), W(I)		U_i, V_i, W_i
DELA, DELB, DELC	Probable errors in A, B, C	
EXP. FLUX	Experimental no. of counts at t_i	
FIT FLUX	Theoretical no. of counts at t_i	
TAU	Neutron lifetime	1/C
TDEAD	Dead time	
PULSNO	Total number of bursts	
P(I)	Corrected no. of counts	
CHDEL	Delay multiplier	
TDEL	Target delay	
SPAC	Total spacing between channel-ends	

LISTINGS FOR CODE EXPO

```
*      LIST 8
*      LABEL
C      BIMAL K. MALAVIYA *  PULSED NEUTRON DATA REDUCTION
C      THIS PROGRAM CALCULATES THE PARAMETERS A,B,C FROM THE LEAST
C      SQUARES FIT TO  N=A+B(EXP(-CT))
CEXPO
       DIMENSION Q(300),P(300),F(300),T(300),U(300),V(300),W(300),WT(300)
      1,FIT(300),DIFFR(300),HYEXPO(300),CORR(300),CORRN(300)
     1 FORMAT (1H1,4X,45H B.K.MALAVIYA * PULSED NEUTRON DATA REDUCTION)
       WRITE OUTPUT TAPE 2,1
       CALL CLOCK(2)
     2 FORMAT (1X,6I3)
     5 FORMAT (1X,F7.0,F9.0,F12.7,3F8.6)
     3 FORMAT (1X,7F9.0)
     7 FORMAT (12HORUN NUMBER I4)
     8 FORMAT (1X,2F7.1,2F6.1)
     9 FORMAT (1X,2E12.4)
    10 FORMAT (1X,3F5.2)
     4 READ INPUT TAPE 4,2,M,N,NORUN,LASTRN,NINITL,MFINAL
       READ INPUT TAPE 4,2,ITSFNL
       READ INPUT TAPE 4,10,XTRA,XTRB,XTRC
       READ INPUT TAPE 4,3,(Q(I),I=1,M)
       WRITE OUTPUT TAPE 2,7,NORUN
       READ INPUT TAPE 4,5,AZERO,BZERO,CZERO,EPS1,EPS2,EPS3
       READ INPUT TAPE 4,8,WIDTH,GAP,CHDEL,TADEL
       READ INPUT TAPE 4,9,PULSNO,TDEAD
       SPAC=WIDTH+GAP
       DO 27 I=N,M
    22 CORRN(I)=(Q(I)*TDEAD)/(PULSNO*WIDTH)
       IF(CORRN(I)-.001)25,25,23
    23 P(I)=Q(I)/(1.-CORRN(I))
       GO TO 26
    25 P(I)=Q(I)
    26 T(I)=(CHDEL*WIDTH-TADEL)+SPAC*(FLOATF(I)-.5)
       PA=1.0/P(I)
       WT(I)=SQRTF(PA)
    27 CONTINUE
    28 A=AZERO
       B=BZERO
       C=CZERO
    29 ITS=0
   291 DO 30 I=N,M
       BETA=-C*T(I)
    30 HYEXPO(I)=EXPF(BETA)
       SUMUU=0.0
       SUMUV=0.0
       SUMUW=0.0
       SUMVV=0.0
       SUMVW=0.0
       SUMWW=0.0
       SUMFU=0.0
       SUMFV=0.0
       SUMFW=0.0
       SSQRES=0.0
```

```
      DO 35 I=N,M
      U(I)=WT(I)
      V(I)=HYEXPO(I)*WT(I)
      W(I)=-B*(T(I))*HYEXPO(I)*WT(I)
      FIT(I)=A+B*HYEXPO(I)
      DIFFR(I)=P(I)-FIT(I)
      F(I)=(P(I)-FIT(I))*WT(I)
      SUMUU=SUMUU+U(I)**2
      SUMUV=SUMUV+U(I)*V(I)
      SUMUW=SUMUW+U(I)*W(I)
      SUMVV=SUMVV+V(I)**2
      SUMVW=SUMVW+V(I)*W(I)
      SUMWW=SUMWW+W(I)**2
      SUMFU=SUMFU+F(I)*U(I)
      SUMFV=SUMFV+F(I)*V(I)
      SUMFW=SUMFW+F(I)*W(I)
      SSQRES=SSQRES+F(I)**2
   35 CONTINUE
      D11=SUMVV*SUMWW-SUMVW**2
      D22=SUMUU*SUMWW-SUMUW**2
      D33=SUMUU*SUMVV-SUMUV**2
      D12=SUMVW*SUMUW-SUMUV*SUMWW
      D13=SUMUV*SUMVW-SUMUW*SUMVV
      D23=SUMUV*SUMUW-SUMVW*SUMUU
      DOM=SUMUU*D11+SUMUV*D12+SUMUW*D13
      DELTAA=(SUMFU*D11+SUMFV*D12+SUMFW*D13)/DOM
      DELTAB=(SUMFU*D12+SUMFV*D22+SUMFW*D23)/DOM
      DELTAC=(SUMFU*D13+SUMFV*D23+SUMFW*D33)/DOM
      IF (ABSF(DELTAA)/A-EPS1)36,36,39
   36 IF (ABSF(DELTAB)/B-EPS2)37,37,39
   37 IF (ABSF(DELTAC)/C-EPS3)40,40,39
   39 A=A+XTRA*DELTAA
      B=B+XTRB*DELTAB
      C=C+XTRC*DELTAC
  369 FORMAT (1H0,6E12.4)
      WRITE OUTPUT TAPE 2,369,(A,B,C,DELTAA,DELTAB,DELTAC)
      IF(ITS-ITSFNL)391,392,392
  391 ITS=ITS+1
      GO TO 291
  393 FORMAT(30H0TERMINATED ON ITERATION LIMIT)
  392 WRITE OUTPUT TAPE 2,393
   40 EM=M
      ZIP=SQRTF(SSQRES/(EM-3.0))*0.6745
      DELA=SQRTF(D11/DOM)*ZIP
      DELB=SQRTF(D22/DOM)*ZIP
      DELC=SQRTF(D33/DOM)*ZIP
      TAU=1.0/C
      MN1=M-N+1
      DO 500 I=N,M
  500 CORR(I)=P(I)-A
   70 FORMAT (I3,21H ITERATIONS WERE USED)
   41 FORMAT (F7.0,F9.0,3X,F12.3,3X,F12.3,3X,F12.3)
   46 FORMAT (60H0  TIME     EXP. FLUX     FIT FLUX        DIFFR         CORR
     1 FLUX)
   42 FORMAT (1H0,2X,18HDECAY CONSTANT(C)=F12.7,1X,12HINVMICROSEC.,3X,5H
     1DELC=F10.4)
   48 FORMAT (1H0,2X,2HA=F7.0,2X,2HB=F9.0,4X,5HDELA=E10.4,2X,5HDELB=E10.
     14)
   47 FORMAT (1H0,2X,4HTAU=F9.3,1X,9HMICROSEC.)
   71 FORMAT (21H EPSILONS USED=FOR A,F8.6,7H FOR B,F8.6,7H FOR C,F8.6)
  721 FORMAT (I4,17H POINTS WERE USED)
```

```
      WRITE OUTPUT TAPE 2,46
   43 WRITE OUTPUT TAPE 2,41,(T(I),P(I),FIT(I),DIFFR(I),CORR(I),I=N,M)
   44 WRITE OUTPUT TAPE 2,42,(C,DELC)
      WRITE OUTPUT TAPE 2,48,(A,B,DELA,DELB)
      WRITE OUTPUT TAPE 2,47,(TAU)
      WRITE OUTPUT TAPE 2,70,(ITS)
      WRITE OUTPUT TAPE 2,721,(MN1)
      WRITE OUTPUT TAPE 2,71,(EPS1,EPS2,EPS3)
      IF (N-NINITL)401,402,402
  401 N=N+1
      GO TO 29
  402 IF (M-MFINAL)404,404,403
  403 M=M-1
      GO TO 29
  404 CONTINUE
  405 FORMAT (10HOF I N I S)
      WRITE OUTPUT TAPE 2,405
   45 IF (LASTRN-NORUN)52,52,50
   50 GO TO 4
   52 CALL EXIT
      END
```

A2.2 THE DIFFN CODE

In certain applications of the die-away pulsed neutron technique for the study of the diffusion characteristics of a pure moderator, the experimental data consist of a set of values of the asymptotic decay constant λ_i, corresponding to different values of the buckling B_i^2. A fit is then to be made to an expression of the form:

$$\lambda_i = A + DB_i^2 - CB_i^4 , \tag{A2.24}$$

to extract the values of the diffusion parameters A, D and C.

An IBM-7090 code DIFFN was developed for this purpose. This code fits a set of up to 50 λ vs. B^2 points to an expression of the form of Eq. A2.24 and determines the parameters A, D and C, together with the associated errors, by using a weighted, least-squares technique in an iterative scheme. The weighting of the points is done according to the relation:

$$W_i = \frac{1}{\Delta\lambda_i} , \tag{A2.25}$$

where $\Delta\lambda_i$ is the uncertainty in λ_i (given by the EXPO code). The theoretical basis of this code is similar to that of EXPO, described in Section A2.1.1.

The buckling is calculated from the input dimensions of the cylindrical assembly, according to the relation:

$$B_i^2 = \left(\frac{2.405}{R_i+d}\right)^2 + \left(\frac{\pi}{H_i+2d}\right)^2 , \tag{A2.26}$$

where

$$d = 0.710\ \lambda_t ,$$

$$\lambda_t = \frac{3D}{\bar{v}} ,$$

$$\bar{v} = \frac{2}{\sqrt{\pi}} \times 2.2 \times 10^5 .$$

The code starts with an initial value of D specified in the input and calculates the geometrical bucklings B_i^2 which are then used with λ_i in the

fitting process, so as to yield values of A, D and C. The bucklings B_i^2 are recalculated using the new value of D, and a new fitting is made. The process is repeated until self-consistent values are obtained.

LISTINGS FOR CODE DIFFN

```
*      LIST 8
*      LABEL
C      BIMAL K. MALAVIYA *  PULSED NEUTRON DATA REDUCTION
C      THIS PROGRAM CALCULATES THE PARAMETERS A,D,C FROM THE LEAST
C      SQUARES FIT TO  Y=A+D*X-C*(X**2) , WHERE
C      X=(2.405/(R+E))**2 + (3.14159/(H+2*E))**2  AND
C      E=0.710446*T , T=3*D/V , V=2*220000/SQRTF(PAI) , PAI=3.14159
CDIFFN
       DIMENSION Y(50),B(50),F(50),U(50),V(50),W(50),WT(50),FIT(50),DIFFR
      1(50),R(50),Z(50)
     1 FORMAT (1H1,2X,51H B.K.MALAVIYA * CALCULATION OF DIFFUSION PARAMET
      1ERS)
       WRITE OUTPUT TAPE 2,1
       CALL CLOCK(2)
     2 FORMAT (1X,7I3)
     5 FORMAT (1X,3E10.4,3F8.6)
     3 FORMAT (1X,2F7.3)
     7 FORMAT (12HORUN NUMBER I4)
     8 FORMAT (1X,7F10.2)
    10 FORMAT (1X,4F5.2)
     4 READ INPUT TAPE 4,2,M,N,NORUN,LASTRN,NINITL,MFINAL
       READ INPUT TAPE 4,2,ITSFNL
       READ INPUT TAPE 4,10,XTRA,XTRD,XTRC
       READ INPUT TAPE 4,8,(Y(I),I=N,M)
       READ INPUT TAPE 4,8,(S(I),I=N,M)
       WRITE OUTPUT TAPE 2,7,NORUN
       READ INPUT TAPE 4,5,AZERO,DZERO,CZERO,EPS1,EPS2,EPS3
       READ INPUT TAPE 4,3,((R(I),Z(I)),I=N,M)
       DO 27 I=N,M
       WT(I)=1.0/S(I)
    27 CONTINUE
    28 A=AZERO
       D=DZERO
       C=CZERO
    29 ITS=0
       PAI=3.14159
       VEE=2.0*220000.0/SQRTF(PAI)
       TRAM=3.0*D/VEE
       E=0.710446*TRAM
   291 DO 26 I=N,M
    26 B(I)=(2.405/(R(I)+E))**2+(3.14159/(Z(I)+2.0*E))**2
    30 SUMUU=0.0
       SUMUV=0.0
       SUMUW=0.0
       SUMVV=0.0
       SUMVW=0.0
       SUMWW=0.0
       SUMFU=0.0
       SUMFV=0.0
       SUMFW=0.0
       SSQRES=0.0
       DO 35 I=N,M
       U(I)=WT(I)
       V(I)=B(I)*WT(I)
```

```
      W(I)=-(B(I)**2)*WT(I)
      FIT(I)=A+D*B(I)-C*(B(I)**2)
      DIFFR(I)=Y(I)-FIT(I)
      F(I)=(Y(I)-FIT(I))*WT(I)
      SUMUU=SUMUU+U(I)**2
      SUMUV=SUMUV+U(I)*V(I)
      SUMUW=SUMUW+U(I)*W(I)
      SUMVV=SUMVV+V(I)**2
      SUMVW=SUMVW+V(I)*W(I)
      SUMWW=SUMWW+W(I)**2
      SUMFU=SUMFU+F(I)*U(I)
      SUMFV=SUMFV+F(I)*V(I)
      SUMFW=SUMFW+F(I)*W(I)
      SSQRES=SSQRES+F(I)**2
   35 CONTINUE
      D11=SUMVV*SUMWW-SUMVW**2
      D22=SUMUU*SUMWW-SUMUW**2
      D33=SUMUU*SUMVV-SUMUV**2
      D12=SUMVW*SUMUW-SUMUV*SUMWW
      D13=SUMUV*SUMVW-SUMUW*SUMVV
      D23=SUMUV*SUMUW-SUMVW*SUMUU
      DOM=SUMUU*D11+SUMUV*D12+SUMUW*D13
      DELTAA=(SUMFU*D11+SUMFV*D12+SUMFW*D13)/DOM
      DELTAD=(SUMFU*D12+SUMFV*D22+SUMFW*D23)/DOM
      DELTAC=(SUMFU*D13+SUMFV*D23+SUMFW*D33)/DOM
      IF (ABSF(DELTAA)/A-EPS1)36,36,39
   36 IF (ABSF(DELTAD)/D-EPS2)37,37,39
   37 IF (ABSF(DELTAC)/C-EPS3)40,40,39
   39 A=A+XTRA*DELTAA
      D=D+XTRD*DELTAD
      C=C+XTRC*DELTAC
  369 FORMAT(6E12.4)
      WRITE OUTPUT TAPE 2,369,(A,D,C,DELTAA,DELTAD,DELTAC)
      IF(ITS-ITSFNL)391,392,392
  391 ITS=ITS+1
      GO TO 291
  393 FORMAT(30H0TERMINATED ON ITERATION LIMIT)
  392 WRITE OUTPUT TAPE 2,393
   40 EM=M
      ZIP=SQRTF(SSQRES/(EM-3.0))*0.6745
      DELA=SQRTF(D11/DOM)*ZIP
      DELD=SQRTF(D22/DOM)*ZIP
      DELB=SQRTF(D22/DOM)*ZIP
      SIGMA=A/VEE
      D0=D/VEE
      MN1=M-N+1
   70 FORMAT (I3,21H ITERATIONS WERE USED)
   41 FORMAT (E10.4,3X,E10.4,4X,E10.4,2X,E10.4)
   42 FORMAT (1H0,2X,2HA=E10.4,4X,2HD=E10.4,4X,2HC=E10.4)
   46 FORMAT (48H0  BUCKLING    EXP DECONS    FIT DECONS    DIFFR)
   47 FORMAT (2X,5HDELA=E10.4,2X,5HDELD=E10.4,2X,5HDELC=E10.4)
   48 FORMAT (2X,6HSIGMA=E10.4,10X,3HD0=E7.4)
   71 FORMAT (21H EPSILONS USED=FOR A,F8.6,7H FOR D,F8.6,7H FOR C,F8.6)
  721 FORMAT (I3,17H POINTS WERE USED)
      WRITE OUTPUT TAPE 2,46
   43 WRITE OUTPUT TAPE 2,41,(B(I),Y(I),FIT(I),DIFFR(I),I=N,M)
   44 WRITE OUTPUT TAPE 2,42,(A,D,C)
      WRITE OUTPUT TAPE 2,47,(DELA,DELD,DELC)
      WRITE OUTPUT TAPE 2,48,(SIGMA,D0)
      WRITE OUTPUT TAPE 2,70,(ITS)
      WRITE OUTPUT TAPE 2,721,(MN1)
```

```
      WRITE OUTPUT TAPE 2,71,(EPS1,EPS2,EPS3)
      IF (N-NINITL)401,402,402
  401 N=N+1
      GO TO 29
  402 IF (M-MFINAL)404,404,403
  403 M=M-1
      GO TO 29
  404 CONTINUE
  405 FORMAT (10H0F I N I S)
      WRITE OUTPUT TAPE 2,405
   45 IF (LASTRN-NORUN)52,52,50
   50 GO TO 4
   52 CALL EXIT
      END
```

A2.3 THE DEECEE CODE

In certain applications, it is necessary to attempt a two-parameter, rather than a three-parameter, fit to the λ vs. B^2 data. A fit is made to the expression:

$$\lambda_i = \lambda_o + DB_i^2 - CB_i^4 \qquad \text{(A2.27)}$$

where λ_o is fixed (input parameter) and the fitting procedure yields the values of the two parameters D and C.

An IBM-7090 code DEECEE was developed for this analysis. This code fits a set of up to 50 λ vs. B^2 points to an expression of the form of Eq. A2.27 and determines the values of the parameters D and C, together with their standard deviations, by an iterative, least-squares method. The operation of this code is similar to that of DIFFN and is easily understood from its Fortran listings which are included here.

A2.4 OTHER CODES

Other major computer programs that have been written in the course of this work include the following:

The code RWORTH calculates the control rod worth according to the relation (Section 6.2),

$$\frac{\Delta a^2}{a_o^2} = -0.820\ \left[Y_o(\mu a) + d\mu Y_1(\mu a) + \frac{2}{\pi}\frac{S_2}{S_1}\left(K_o(\nu a) + d\nu K_1(\nu a)\right)\right]^{-1} . \qquad \text{(A2.28)}$$

The code PEACE calculates the extrapolation distance d from the relation (Section 4.1),

$$d = \frac{1}{a}\,\frac{Y_o(aR)\,J_o(aa) - Y_o(aa)\,J_o(aR)}{Y_1(aa)\,J_o(aR) - Y_o(aR)\,J_1(aa)} . \qquad \text{(A2.29)}$$

The code ASOKA calculates the relative radial flux distribution $\phi(r)$ according to the relation (Section 4.1),

$$\phi(r) = A\,J_o(ar) - \frac{J_o(aR)}{Y_o(aR)}\,Y_o(ar) . \qquad \text{(A2.29a)}$$

References

1. F. B. Hildebrand, Introduction to Numerical Analysis, McGraw-Hill Book Company, Inc., New York (1956).

2. M. Merriman, A Text Book on the Method of Least Squares, John Wiley, New York (1892).

3. E. Whittaker and G. Robinson, The Calculus of Observations, Blackie and Son, London (1958).

4. B. L. Anderson and T. J. Lawton, WAPD-TM-26 (1956).

5. J. Jedruch, YAEC-86 (1958).

LISTINGS FOR CODE DEECEE

```
*      LIST 8
*      LABEL
C      BIMAL K. MALAVIYA *  PULSED NEUTRON DATA REDUCTION
C      THIS PROGRAM CALCULATES THE PARAMETERS D AND C FROM THE LEAST
C      SQUARES FIT TO  Y = Y0 + D*X - C*(X**2) , WHERE
C      X=(2.405/(R+E))**2 + (3.14159/(H+2*E))**2  AND
C      E=0.710446*T , T=3*D/V , V=2*220000/SQRTF(PAI) , PAI=3.14159
C      Y0 CAN BE GIVEN ANY VALUE IN THE INPUT DATA
CDFECEF
       DIMENSION Y(50),B(50),F(50),V(50),W(50),WT(50),FIT(50),DIFFR(50),
      1R(50),Z(50),S(50)
     1 FORMAT (1H1,2X,51H B.K.MALAVIYA * CALCULATION OF DIFFUSION PARAMET
      1ERS)
       WRITE OUTPUT TAPE 2,1
       CALL CLOCK(2)
     2 FORMAT (1X,7I3)
     5 FORMAT (1X,2E10.4,2F8.6)
     3 FORMAT (1X,2F7.3)
     7 FORMAT (12HORUN NUMBER I4)
     8 FORMAT (1X,7F10.2)
     9 FORMAT (1X,F7.3)
    10 FORMAT (1X,4F5.2)
     4 READ INPUT TAPE 4,2,M,N,NORUN,LASTRN,NINITL,MFINAL
       READ INPUT TAPE 4,2,ITSFNL
       READ INPUT TAPE 4,10,XTRD,XTRC
       READ INPUT TAPE 4,8,(Y(I),I=N,M)
       READ INPUT TAPE 4,8,(S(I),I=N,M)
       READ INPUT TAPE 4,9,Y0
       WRITE OUTPUT TAPE 2,7,NORUN
       READ INPUT TAPE 4,5,DZERO,CZERO,EPS2,EPS3
       READ INPUT TAPE 4,3,((R(I),Z(I)),I=N,M)
       DO 27 I=N,M
       WT(I)=1.0/S(I)
    27 CONTINUE
    28 D=DZERO
       C=CZERO
    29 ITS=0
       PAI=3.14159
       VEE=2.0*220000.0/SQRTF(PAI)
       TRAM=3.0*D/VEE
       E=0.710446*TRAM
   291 DO 26 I=N,M
    26 B(I)=(2.405/(R(I)+E))**2+(3.14159/(Z(I)+2.0*E))**2
    30 SUMVV=0.0
       SUMVW=0.0
       SUMWW=0.0
       SUMFV=0.0
       SUMFW=0.0
       SSQRES=0.0
       DO 35 I=N,M
       V(I)=B(I)*WT(I)
       W(I)=-(B(I)**2)*WT(I)
       FIT(I)=Y0+D*B(I)-C*(B(I)**2)
       DIFFR(I)=Y(I)-FIT(I)
```

```
      F(I)=(Y(I)-FIT(I))*WT(I)
      SUMVV=SUMVV+V(I)**2
      SUMVW=SUMVW+V(I)*W(I)
      SUMWW=SUMWW+W(I)**2
      SUMFV=SUMFV+F(I)*V(I)
      SUMFW=SUMFW+F(I)*W(I)
      SSQRES=SSQRES+F(I)**2
   35 CONTINUE
      DOM=SUMVV*SUMWW-SUMVW**2
      DELTAD=(SUMFV*SUMWW-SUMFW*SUMVW)/DOM
      DELTAC=(SUMFW*SUMVV-SUMFV*SUMVW)/DOM
      IF (ABSF(DELTAD)/D-EPS2)37,37,39
   37 IF (ABSF(DELTAC)/C-EPS3)40,40,39
   39 D=D+XTRD*DELTAD
      C=C+XTRC*DELTAC
  369 FORMAT(6E12.4)
      WRITE OUTPUT TAPE 2,369,(D,C,DELTAD,DELTAC)
      IF(ITS-ITSFNL)391,392,392
  391 ITS=ITS+1
      GO TO 291
  393 FORMAT(30H0TERMINATED ON ITERATION LIMIT)
  392 WRITE OUTPUT TAPE 2,393
   40 EM=M
      ZIP=SQRTF(SSQRES/(EM-2.0))*0.6745
      DELD=SQRTF(SUMWW/DOM)*ZIP
      DELC=SQRTF(SUMVV/DOM)*ZIP
      D0=D/VEE
      MN1=M-N+1
   70 FORMAT (I3,21H ITERATIONS WERE USED)
   41 FORMAT (E10.4,3X,E10.4,4X,E10.4,2X,E10.4)
   46 FORMAT (48H0  BUCKLING     EXP DECONS     FIT DECONS     DIFFR)
   42 FORMAT (1H0,2X,2HD=E10.4,7X,2HC=E10.4)
   48 FORMAT (1H0,2X,5HDELD=E10.4,4X,5HDELC=E10.4)
   71 FORMAT (21H EPSILONS USED FOR D,F8.6,7H FOR C,F8.6)
   75 FORMAT (4H0Y0=F5.2,13X,3HD0=F7.4)
  721 FORMAT (I3,17H POINTS WERE USED)
      WRITE OUTPUT TAPE 2,46
   43 WRITE OUTPUT TAPE 2,41,(B(I),Y(I),FIT(I),DIFFR(I),I=N,M)
   44 WRITE OUTPUT TAPE 2,42,(D,C)
      WRITE OUTPUT TAPE 2,48,(DELD,DELC)
      WRITE OUTPUT TAPE 2,75,(Y0,D0)
      WRITE OUTPUT TAPE 2,70,(ITS)
      WRITE OUTPUT TAPE 2,721,(MN1)
      WRITE OUTPUT TAPE 2,71,(EPS2,EPS3)
      IF (N-NINITL)401,402,402
  401 N=N+1
      GO TO 29
  402 IF (M-MFINAL)404,404,403
  403 M=M-1
      GO TO 29
  404 CONTINUE
  405 FORMAT (10H0F I N I S)
      WRITE OUTPUT TAPE 2,405
   45 IF (LASTRN-NORUN)52,52,50
   50 GO TO 4
   52 CALL EXIT
      END
```

Appendix III

CALCULATION OF THE NEUTRON AGE AND EFFECTIVE DELAYED NEUTRON FRACTION FOR THE LATTICE

As discussed in Section 3.5, the interpretation of the pulsed neutron (λ, B^2) data for a subcritical assembly involves a knowledge of the neutron age τ to thermal and the effective delayed neutron fraction $\bar{\beta}$ for the lattice. This appendix discusses the methods of evaluating these parameters.

A3.1 CALCULATION OF THE NEUTRON AGE IN A LATTICE

The experimentally measured quantity in the measurement of the slowing-down area is the neutron age in a pure moderator - usually from fission energies to indium resonance (1.44 ev). For heavy water, a measurement[1] of (109 ± 3) cm^2 as the age to 1.44 ev is taken as the basis for calculation. For age to lower energies, we can use the relation[4]

$$\Delta\tau = 4.94\, \ell n\, (1.44/E)\ . \qquad \text{(A3.1)}$$

The age to thermal of 99.75 mole per cent D_2O at 20° C is found to be[2] (125 ± 3) cm^2. For other D_2O concentrations or temperatures, corrections can be applied to obtain the value of τ. The age increases as the inverse square of the D_2O density:

$$\tau_T = \tau_{20} \left(\frac{\rho_{20}}{\rho_T}\right)^2 , \qquad \text{(A3.2)}$$

and the correction due to a change "δc" in the H_2O concentration is given by[3]:

$$\Delta\tau = -6\tau\delta c\ . \qquad \text{(A3.3)}$$

In calculating the age in a multiplying heterogeneous assembly, it is necessary to consider the effect of the non-moderator constituents on the age. In general, the presence of fuel and structural materials tends to increase the age. The inelastic scattering in uranium, on the other

hand, can be quite effective in decreasing the age by moderating the neutrons out of the fission energy spectrum. Several empirical formulae are available for taking account of these effects.[4,5]

A neutron generated in a uranium slug has a certain probability of undergoing an inelastic collision with a uranium atom. If we denote by τ_o the age for a neutron which has not made an inelastic collision and by τ_1 the age for a neutron which has done so, then a mean value of the age is given by[3]

$$\tau = \tau_o \left(1 - \frac{\sigma_i}{\sigma_i + \sigma_e} P\right) + \tau_1 \frac{\sigma_i}{\sigma_i + \sigma_e} P ,$$

$$= \tau_o \left(1 - \left(1 - \frac{\tau_1}{\tau_o}\right) \frac{\sigma_i}{\sigma_i + \sigma_e} P\right) , \qquad \text{(A3.4)}$$

where σ_i and σ_e are the inelastic and elastic cross-sections, respectively, in uranium; P is the probability that a neutron generated in a uranium slug will undergo a collision before leaving the slug. For heavy water,[3] $\tau_1/\tau_o = 0.7$. Tables of P can be found in Ref. (6).

Finally, a correction is made due to "voids" in the moderator since the elastic scattering in materials other than D_2O of volume V_1 does not result in energy loss. This yields the relation

$$\tau = \tau_o \left(1 - \left(1 - \frac{\tau_1}{\tau_o}\right) \frac{\sigma_i}{\sigma_i + \sigma_e} P\right) \left(1 + \frac{V_o}{V_1}\right)^2 , \qquad \text{(A3.5)}$$

where V_o is the volume of non-D_2O constituents.

For a lattice of 0.25-inch-diameter, 1.03% U^{235} uranium rods in heavy water with a triangular spacing of 1.75 inches, using the values of the constants from Refs.(5) and (3), Eq. A3.5 yields

$$\tau = (120 \pm 3) \text{ cm}^2 .$$

A3.2 EVALUATION OF THE EFFECTIVE DELAYED NEUTRON FRACTION

The effective delayed neutron fraction $\bar{\beta}$ is a parameter of major interest in reactor kinetics. It is the basis of the dollar unit of reactivity and its knowledge is essential for the analysis and interpretation

of reactivity measurement. Physically, it is given by

$$\bar{\beta} = \frac{\text{Effective production rate of precursor}}{\text{Precursor rate}}$$

Thus, $\bar{\beta}$ is an index of the margin of reactor control available (larger $\bar{\beta}$, greater is the margin of control) and is related to safety considerations.

The "effective" delayed neutron fraction $\bar{\beta}$, for an actual chain-reacting system, differs from the delayed neutron fraction of any fissioning species for several reasons. The delayed neutrons are emitted with an energy spectrum lower (average energy 240-450 kev) than that of fission neutrons (average energy about 2 mev). In a finite assembly, therefore, the delayed neutrons are less likely to leak out than the fission neutrons, and it is necessary to assign greater importance or "worth" to delayed neutrons. According to Hurwitz,[2] the ratio $\bar{\beta}_i/\beta_i$ is just the probability of a delayed neutron to produce fission divided by the probability of a prompt neutron to cause fission. For a simple reactor, this probability is given by the ratio of the non-leakage probabilities of the respective types of neutrons. Thus, for a bare reactor, according to age theory,

$$\frac{\bar{\beta}_i}{\beta_i} = \frac{e^{-B^2\tau^i}}{e^{-B^2\tau^f}},$$

where the superscripts f and i refer to fission and i^{th} delayed group neutrons. The amount by which $\bar{\beta}$ is increased depends on the nature of the moderator and the buckling of the reactor. Gwinn[7] has considered the magnitude of this increase for several systems. For a large heavy water assembly, this effect is small.

Another correction is due to fast fission in U^{238}. Hellens[2] has suggested an expression of the form:

$$\bar{\beta}_i = \frac{P_i}{P_o}\left[\frac{\beta_i^{25}}{\epsilon^{28}} + \frac{\nu^{28}}{\nu^{25}}\beta^{28}\,\frac{\delta}{\epsilon^{28}}\right],$$

where P_i and P_o are the non-leakage probabilities of the i^{th} delayed neutron group and for fission neutrons, respectively; δ is the ratio of U^{28} fast fissions to U^{25} thermal fissions and other symbols have their

usual meaning. The magnitude of this correction is usually to increase β by the fast fission factor ϵ.

The computation of $\bar{\beta}$ for a system containing a mixture of isotopes is based on perturbation methods[8] and is usually carried out by multi-group diffusion or transport theory codes. Thus, for a uranium-fueled system, an average value of β is

$$\bar{\beta} = F_{25}\beta_{25} + F_{28}\beta_{28} ,$$

where F_{25} is the fraction of all neutrons which come from U^{235} fission and F_{28} is the corresponding quantity for U^{235} fission. Kear and Rudermann[9] have calculated F_{25} and F_{28} using three group fluxes averaged over the fuel-bearing region supplied in the PDQ output together with the homogenized values of $\nu\Sigma_f$ for each group. Combining these with values[5]

$$\beta_{25} = 0.0064 \pm 0.0003 ,$$

$$\beta_{28} = 0.0157 \pm 0.0012 ,$$

they have obtained a value of 0.00652 for $\bar{\beta}$, for slightly enriched (1.3% U^{25}) uranium heavy water system.

In systems moderated by heavy water[10] (and also beryllium or its compounds), there is another important contributory source of "delayed" neutrons - the photoneutrons produced in the moderator by the gamma activity from fission products. In kinetics calculations, photo-neutrons can be considered simply as additional groups of delayed neutrons having decay constants λ_j and group fractions β_j. Due allowance must be made for build-up factors for each group $(1 - e^{-\lambda_j t})$ where t is the effective irradiation time, and for relative photoneutron effectiveness.

The yield of photoneutrons for U^{235} fission products has been measured in heavy water by Bernstein et al.[10]. The decay constants and yields for the principal groups of delayed[5] and photoneutrons[10] are summarized in the following table.

Delayed Neutrons			Photoneutrons		
i	λ_i sec^{-1}	$\beta_i \times 10^4$	i	λ_i sec^{-1}	$\beta_i \times 10^4$
1	0.0124	2.25	7	0.277	1.980
2	0.0305	15.50	8	1.69×10^{-2}	0.622
3	0.111	14.32	9	4.8×10^{-3}	0.213
4	0.301	29.57	10	1.5×10^{-3}	0.105
5	1.13	9.88	11	4.28×10^{-4}	0.063
6	3.00	3.52	12	1.17×10^{-4}	0.071
			13	4.38×10^{-5}	0.010
			14	3.64×10^{-6}	0.003

From this table,

$$\beta = \sum_{i=1}^{14} \beta_i = 0.00781 \ .$$

Williams[12,12a] has reported a value of 0.00783 for the total effective delayed neutron fraction in a D_2O-moderated reactor.

The effective delayed neutron fraction $\bar{\beta}$ has also been measured experimentally by several investigators[13-16]. The experimental methods are reviewed in Ref. (15). From a combination of the reactivity measurement of a heavy water reactor by two methods, Küchle[16] has derived a value for the effective delayed neutron fraction,

$$\bar{\beta} = (0.783 \pm 0.018) \times 10^{-2} \ .$$

References

1. J. W. Wade, Nuclear Sci. and Eng. 4, 12 (1958)

2. H. Etherington (Ed.), Nuclear Engineering Handbook, McGraw-Hill Book Company, Inc., New York (1958).

3. A. D. Gelanin, Thermal Reactor Theory, Pergamon Press, New York (1960).

4. J. A. Thie, Heavy Water Exponential Experiments Using ThO_2 and UO_2, Pergamon Press, New York (1961).

5. L. J. Templin, Reactor Physics Constants, 2nd Ed., ANL-5800 (1963).

6. K. M. Case, F. de Hoffmann and G. Placzek, Introduction to the Theory of Neutron Diffusion, Vol. I, U.S. Government Printing, Washington (1953).

7. R. Gwinn, ORNL-2081, 84 (1956).

8. L. N. Ussachoff, Proc. Int. Conf. on the Peaceful Uses of Atomic Energy, Geneva, Vol. 5, P/656, p. 503 (1955).

9. G. H. Kear and M. H. Rudermann, GEAP-3937 (1962).

10. C. E. Cohn, Nuclear Sci. and Eng. 6, 284 (1959).

11. S. Bernstein et al., Phys. Rev. 71, 573 (1947).

12. H. T. Williams, ORNL, CF-51-12-122.

12a. P. Meyer and W. C. Ballowe, GEAP-4019 (1962).

13. T. F. Ruane et al., Trans. Am. Nuclear Soc. 1, No. 2, 142 (1958).

14. J. D. Kengton, R. Perez-Belles and G. De Saussure, Nuclear Sci. and Eng. 12, 505 (1962).

15. T. F. Ruane, Nucleonics 20, No. 10, 94 (1962).

16. M. Küchle, Symposium on Exponential and Critical Experiments, Amsterdam, P/SM-42/6 (Sept. 1963).

Appendix IV

APPLICATION OF THE $k\beta/\ell$ METHOD

The recently proposed "$k\beta/\ell$" method for the measurement of the reactivity of an assembly has been described in Section 3.6.3. The method is based on the fact that the equilibrium neutron density $N(\vec{r},t)$ in a pulsed subcritical system is composed of a prompt neutron contribution N_p and a delayed neutron part N_d which are, under certain conditions, related by the equation:

$$\int_0^\infty N_p \exp\left[\left(\frac{k\beta}{\ell}\right) t\right] dt - \int_0^\infty N_p \, dt = \frac{Nd}{R} \quad , \tag{A4.1}$$

where R is the repetition rate of the source. Hence, knowing the prompt neutron distribution $N_p(t)$ from the experimental curve, the above integral relationship determines $k\beta/\ell$, since N_d is known from the experiment. Once $k\beta/\ell$ is known, the reactivity can be obtained from the relation:

$$\$ = \frac{\lambda - (k\beta/\ell)}{(k\beta/\ell)} \quad . \tag{A4.2}$$

In general, the restriction on the pulse repetition rate is such that $\omega \ll R \ll \lambda$, where ω is the decay constant of the shortest lived precursor.

This method was applied to the lattice studied in this investigation, with and without a control rod. These runs are described in Section 7.4. A repetition rate of 10 per second was used. The channel width was 80 μsec; the delay multiplier was set at $\times 2$ and the target delay was 100 μsec. The time analyzer was allowed to sweep for about 10 minutes after shutting off the source, to ensure the conditions for a quasi-equilibrium.[1]

However, the results of the application of this method are inconclusive and this preliminary study seems to indicate that the method is not applicable to assemblies as far below critical as the ones used here. In the application of this method, a precise knowledge of the delay tail is

crucial. If the assemblies are too far subcritical, the delayed neutron contribution may be so insignificant as to make an accurate determination of N_d in Eq. A4.1 difficult. Another reason might be that the repetition rate of 10 per sec, used in these runs, is too low, even though it satisfies the condition mentioned earlier. The KAMAN pulsed neutron tube is limited to a repetition frequency of about 10; it may be possible[2] to run it at 12 pulses per second. It would be desirable to explore further the applicability of this useful method in the range of far subcriticality and the investigation is expected to be continued.

The analysis of the data in this method is based on the extraction of the value of $k\beta/\ell$ from the integral relationship, Eq. A4.1. An IBM-7090 computer code was brought into operation for this purpose. It is included here for future investigators. I am indebted to Dr. P. Meyer of the Vallecitos Atomic Laboratory, California, for useful discussions of this method and for his having communicated the original version of the code EDPUNS.

The code is based on the following procedure:

Let N(i) be the corrected counts and calculate

$$N(i-1) = N_m(i)\left[1 - \frac{\tau N_m(i) - 1}{\Delta t P}\right], \quad i = 2,3,\ldots, I+1.$$

Let t(i) be the time corresponding to N(i). This is given by

$$t(i-1) = m_d \Delta t - t_d + (i-1)\rho + (i-3/2)\Delta t, \quad i = 2, 3, \ldots, I+1 .$$

Let

$$n_{p_i} = N(i) - n_t$$

and calculate

$$(1) \qquad I_1 = \int_0^{t(I)} n_p(I)\, d\tau + \frac{N[t(I)]}{a \cdot 10^{-6}}$$

where the integrand can exclude the points $(0_i - 1)$. Calculate

$$(2) \qquad I_2 = \int_0^{t(I)} n_{p_i} e^{(10^{-6} p\tau)}\, d\tau + \frac{N[t(I)]\, e^{(10^{-6} p t(I))}}{10^{-6} \cdot (a-p)}$$

where the above integrand is subjected to the same restrictions as in (1). Calculate

$$(3) \qquad p_{corr} = p\, n_d \quad 10^{-6} R(I_2 - I_1) \quad .$$

If $|p_{corr} - p| \leq \epsilon$, then proceed to the next step. If not, return to (2) and recalculate (2), using p_{corr}. Calculate

$$(4) \qquad \$ = (a - p_{corr})\ p_{corr}$$

and stop. Print the input and the iterates on p. Also print \$.

The operation of the code and the input instructions are best understood from the Fortran listings, which are included in this appendix.

References

1. E. Garelis, Trans. Am. Nucl. Soc., Vol. 6, No. 2, p. 289 (1963).

2. P. Meyer, Private communication.

LISTINGS FOR CODE EDPUNS

```
*     LIST 8
*     LABEL
C   *            PULSED NEUTRON SOURCE
CEDPUL
      EQUIVALENCE                ( SS(10), ND        ), ( SS(20), A1        )
     1, ( SS( 1), INT       ), ( SS(11), ALPHA     ), ( SS(21), AREAX     )
     2, ( SS( 2), NOCH      ), ( SS(12), P         ), ( SS(22), VALUE1    )
     3, ( SS( 3), PCAP      ), ( SS(13), E         ), ( SS(23), KLANK     )
     4, ( SS( 4), TAU       ), ( SS(14), PINE      ), ( SS(24), KOUNT     )
     5, ( SS( 5), DT        ), ( SS(15), ALDER     ), ( SS(25), LL        )
     6, ( SS( 6), R         ), ( SS(16), BIRCH     ), ( SS(26), AREAZ     )
     7, ( SS( 7), DM        ), ( SS(17), TERM1     ), ( SS(27), EXPCT     )
     8, ( SS( 8), TD        ), ( SS(18), AREA1     ), ( SS(28), CEDAR, C  )
     9, ( SS( 9), RHO       ), ( SS(19), A2        ), ( SS(29), TERM2     )
      EQUIVALENCE               ( SS(30), AREA2     ), (SS(31), VALUE2     )
     1, ( SS(  41), XN(1)   ), ( SS( 941), TN(1)   ), ( SS(1251), PC(1)   )
     2, ( SS( 341), YN(1)   ), ( SS(1241), MO(1)   ), ( SS(1351), HOL(1)  )
     3, ( SS( 641), ZN(1)   ), ( SS(1246), MC(1)   ), ( SS(1361),BOSH(1)  )
      COMMON  SS
      DIMENSION XN(300), YN(300),  ZN(300),  TN(300),  MO(5),  MC(5)
      DIMENSION PC(100), HOL(10),  BOSH(100), SS(1500)
C     THE ARRAY IJKLMN IS INTENDED TO BE USED AS A PATCHING AREA
      DIMENSION   IJKLMN(50)
      CALL CLOCK(2)
C   GLOSSARY OF PROGRAMMING SYMBOLS
C           INPUT
C   TAU     CHANNEL RESOLVING TIME, MICROSECONDS
C   DT      CHANNEL WIDTH, MICROSECONDS
C   PCAP    TOTAL NUMBER OF BURSTS
C   INT     CHANNEL NUMBER FOR INTEGRATION LIMIT
C   R       PULSE RATE, PULSES PER SECOND
C   DM      DELAY MULTIPLIER
C   TD      TIME DELAY FROM CLOSING TO SOURCE BURST, MICRO SECONDS
C   RHO     CHANNEL GAP, MICROSECONDS
C   DN      AVERAGE DELAYED BACKGROUND
C   CN      AVERAGE DELAYED BACKGROUND FOR CALCULATING P
C   ALPHA   PROMPT MODE DECAY CONSTANT, RECIPROCAL SECONDS
C   P       INITIAL APPROXIMATION OF (KB/L), RECIPROCAL SECONDS
C   E       ERROR CRITERION ON P
C   MO(5)   CHANNEL NUMBERS OF COUNTS TO BE OMITTED
C   HOL(10)   COMMENT ON THE FIRST LINE OF INPUT
C   XN(300)   RAW COUNTS PER CHANNEL
C
C           COMPUTED
C   YN(300)   TIME AND BACKGROUND CORRECTED COUNTS
C   ZN(300)   EXPONENTIALL CORRECTED COUNTS
C   TN(300)   TIMES CORRESPONDING TO YN AND ZN
C   PC(100)   P ITERATES
C   BOSH(100)    DELTA ITERATES
C   VALUE1    VALUE OF EQUATION 1 ( I1 )
C   VALUE2    VALUE OF EQUATION 2 ( I2 )
C   DOLLAR    VALUE OF EQUATION 4 ($)
C   CENTS     VALUE OF (APLHA-P)/R
C
```

```
C
C    GLOSSARY OF SUBROUTINES
C
C    PATCH     INTERPOLATES OMITTED VALUES
C
C    SIM       INTEGRATES USING SIMPSONS RULE
C
C    CASE      READS CASE CARD BEARING ACCOUNTING INFORMATION
C
C    ERRSYS    RECOVERY POINT FOR A SYSTEMS INPUT ERROR,
C              EG, A LETTER OF THE ALPHABET IN AN INTEGER FIELD
C
C    COMCC     EVALUATES EQUATION 2 (I2) USING THE CURRENT VALUE FOR P
C
C
C    *      IX       =  NO OF ERRORS
C    *      ITAPB    =  SYMBOLIC OUTPUT TAPE
C    *      ITAPA    =  SYMBOLIC INPUT TAPE
       ITAPB=4
       ITAPOT=2
       LL = 50
       GO TO 4
     1 WRITE OUTPUT TAPE ITAPOT, 1001
  1001 FORMAT( 46H0 PROBLEM WAS HALTED BECAUSE OF AN INPUT ERROR  )
     5 FORMAT (12HORUN NUMBER I4)
  1005 FORMAT (1X,2I3)
  1050 FORMAT (2X,I5,I5,10A6)
  1052 FORMAT (2X,5E12.4)
  1054 FORMAT (2X,2E12.4,5I5)
  1058 FORMAT (1X,7F9.0)
     4 READ INPUT TAPE 4,1005,NORUN,LASTRN
       READ INPUT TAPE 4,1050,INT,NOCH,(HOL(I),I=1,10)
       READ INPUT TAPE 4,1052,PCAP,TAU,DT,R,DM
       READ INPUT TAPE 4,1052,TD,RHO,CN,DN,ALPHA
       READ INPUT TAPE 4,1054,P,E,(MO(J),J=1,5)
       WRITE OUTPUT TAPE 2,5,NORUN
       WRITE OUTPUT TAPE ITAPOT, 1003, (HOL(I),I=1,10), INT, NOCH,
      1 PCAP, TAU, DT,R,DM, TD, RHO, CN, DN, ALPHA, P,E, (MO(J),J=1,5)
  1003 FORMAT(  1H0, 20X, 26HPULSED NEUTRON SOURCE DATA / 1H0, 10A6/
     121H0 INTEGRATION LIMIT =,10X,I5 / 22H0 NUMBER OF CHANNELS =,9X,I5
     2 /20H0 NUMBER OF BURSTS =, 11X, E17.9 / 18H0 RESOLVING TIME =, 13X
     3,E17.9 / 17H0 CHANNEL WIDTH =, 14X, E17.9 / 14H0 PULSE RATE =, 17X
     4,E17.9 /20H0 DELAY MULTIPLIER =, 11X, E17.9/14H0 DELAY TIME =, 17X
     5,E17.9 /15H0 CHANNEL GAP =, 16X, E17.9 / 25H0 DELAYED BACKGROUND(1
     6) =, 9X, E17.9 / 25H0 DELAYED BACKGROUND(2) = ,9X, E17.9
     7             /31H0 PROMPT MODE DECAY CONSTANT = , E17.9 /19H0 P APP
     8ROXIMATION =, 12X, E17.9 /19H0 ERROR CRITERION =, 12X, E17.9 /
     918H0 OMITTED POINTS =, 13X, 5I5    )
       NOCH = INT + 1
       IF( P - ALPHA ) 3, 1, 1
     3 IF(NOCH-257) 2,1,1
C    *      READ CHANNEL COUNTS
     2 READ INPUT TAPE 4,1058,(XN(I),I=1,NOCH)
C    *      TEST INPUT VALUES
       IF( DT * PCAP ) 1, 1, 6
     6 IF( ALPHA ) 1, 1, 7
     7 IF( E ) 1, 1, 8
     8 IF( INT ) 1, 1, 9
     9 IF( INT - NOCH ) 10, 1, 1
```

```
   10 DO 12 I = 1, 5
      IF( MO(I) ) 1, 12, 11
   11 CONTINUE
      IF( MO(I) - INT ) 12, 12, 1
   12 CONTINUE
C   *     COMPUTE CORRECTED COUNTS, TIMES, ETC.
      PINE = TAU / DT / PCAP
      ALDER= ( DM + 0.5 ) * DT + RHO - TD
      BIRCH= RHO + DT
      IF(BIRCH) 1, 1, 13
   13 CONTINUE
      DO 14 I = 1, INT
      YN(I) = XN(I+1) / ( 1.0 - PINE * XN(I+1) )  - DN
      TN(I) = ALDER
      ALDER = ALDER + BIRCH
   14 CONTINUE
C   *     INTERPOLATE VALUES FOR OMITTED POINTS
      CALL PATCH( MO, YN, INT )
C   *     COMPUTE LAST TERM OF EQUATION (1)
      TERM1 = YN(INT) * 1000000.0 / ALPHA
C   *     COMPUTE INTEGRAL OF EQUATION (1)
      AREA1 = SIM( YN, 1, INT, BIRCH )
      A2 = ( YN(1)/TN(1) - YN(2)/TN(2) ) / ( TN(1) - TN(2) )
      A1 =  YN(1)/TN(1) - A2 * TN(1)
CC
CC * * * * * * * * * * * * * * * * * * * * * * * * * * * * * * * * * * * * *
CC
      IF( A1 ) 98, 97, 97
   97 IF( A2 ) 99, 99, 98
   98 A2 = 0.0
      A1 = YN(1) / TN(1)
   99 CONTINUE
CC
CC * * * * * * * * * * * * * * * * * * * * * * * * * * * * * * * * * * * * *
CC
      AREAX = ( 0.5*A1 + A2/3.0*TN(1) ) * TN(1) * TN(1)
C   *     COMPUTE VALUE OF EQUATION (1)
      VALUE1 = AREA1 + TERM1 + AREAX
      CALL COMCC
      RII1 = R*(VALUE2-VALUE1)/1000000.0
      PC(1) = P
      BOSH(1) = CN - RII1
      PC(2) = P*CN / RII1
      IF( PC(2) - ALPHA ) 16, 15, 15
   15 PC(2) = ( ALPHA + PC(1) ) / 2.0
   16 P = PC(2)
      CALL COMCC
      RII2 = R*(VALUE2-VALUE1)/1000000.0
      BOSH(2) = CN - RII2
      PC(3) = (PC(1)*BOSH(2)-PC(2)*BOSH(1))/(BOSH(2)-BOSH(1))
      IF( PC(3) - ALPHA ) 18, 17, 17
   17 PC(3) = ( ALPHA + PC(2) ) / 2.0
   18 P = PC(3)
      CALL COMCC
      BOSH(3) = CN - R*(VALUE2-VALUE1)/1000000.0
       J = 3
C
C  A B C   A*B   B*C
C  + + +    +     +      NO  - BOTH +
```

```
C  + + -    +      -    YES
C  + - +    -      -    YES
C  + - -    -      +    YES
C  - + +    -      +    YES
C  - + -    -      -    YES
C  - - +    +      -    YES
C  - - -    +      +     NO  - BOTH +
   19 IF( BOSH(J) * BOSH(J-1) ) 121, 119, 119
  119 IF( BOSH(J-1) * BOSH(J-2) ) 121, 120, 120
  120 PC(J+1) = (PC(J-1)*BOSH(J)-PC(J)*BOSH(J-1))/(BOSH(J)-BOSH(J-1))
      GO TO 122
  121 CONTINUE
      PC(J+1) = ( BOSH(J)*(PC(J-2)*BOSH(J-1)-PC(J-1)*BOSH(J-2))
     1            / (BOSH(J-1)-BOSH(J-2))
     2          - BOSH(J-1)*(PC(J-2)*BOSH(J)-PC(J)*BOSH(J-2))
     3            / (BOSH(J)-BOSH(J-2)) ) / (BOSH(J)-BOSH(J-1))
  122 CONTINUE
      IF( PC(J+1) - ALPHA ) 21, 20, 20
   20 PC(J+1) = ( PC(J) + ALPHA ) / 2.0
   21 IF( ABSF( PC(J+1) - PC(J) ) - E ) 33, 22, 22
   22 J = J + 1
      IF(J-LL) 23, 23, 34
   23 P = PC(J)
      CALL COMCC
      BOSH(J) = CN - R*(VALUE2-VALUE1) / 1000000.0
      GO TO 19
   33 J = J + 1
   34 KLANK = J - 1
      P = PC(J)
      DOLLAR = ( ALPHA - P ) / P
      CENTS = ( ALPHA - P ) * 1000000.0 / R
C   *     EDIT COMPUTED VALUES
      WRITE OUTPUT TAPE ITAPOT, 1035, P, DOLLAR, CENTS, (PC(I),I=1,J)
 1035 FORMAT(5H0 P =,E20.9,5X,8HDOLLAR =,E20.9,5X,13H(ALPHA-P)/R =,
     1 E20.9 / 1H0, 13X, 10HP ITERATES /// 10( 1X, 5E20.9 / )  )
      WRITE OUTPUT TAPE ITAPOT, 1075, ( BOSH(I), I = 1, KLANK )
 1075 FORMAT( 15H0  DELTA VALUES /// 10( 1X, 5E20.9 / )  )
      WRITE OUTPUT TAPE ITAPOT, 1111, AREAX, AREA1, TERM1, AREAZ, AREA2
     1, TERM2,  A1, A2
 1111 FORMAT( 11H0EQUATION 1,11X,7HTERM1 =,E20.9,10H   TERM2 =,E20.9,
     1 10H   TERM3 =,E20.9 /
     2         11H0EQUATION 2,11X,7HTERM1 =,E20.9,10H   TERM2 =,E20.9,
     3 10H   TERM3 =,E20.9 /
     4 9H0PARABOLA,16X,4HA1 =,E20.9,6X,4HA2 =,E20.9 /
     5 1H0,20X,4HTIME,13X,9HRAW COUNT,9X,15HCORRECTED COUNT,6X,
     614HEXP-CORR COUNT / 1H   )
      DO 222 I = 1, INT
      JJJ = I+1
      WRITE OUTPUT TAPE ITAPOT, 2222, TN(I), XN(JJJ),YN(I),ZN(I)
 2222 FORMAT(1H ,10X, 4E20.9)
  222 CONTINUE
  405 FORMAT (10H0F I N I S )
      WRITE OUTPUT TAPE 2,405
   45 IF (LASTRN-NORUN)52,52,50
   50 GO TO 4
   52 CALL EXIT
      END
      SUBROUTINE PATCH ( MO, YN, INT )
      DIMENSION MO(5), YN(300)
```

```
      DIMENSION ISAVE(6)
C     *     PARABOLIC INTERPOLATION OF VALUES TO BE REPLACED IN AN ARRAY
C     *   MO      AN ARRAY OF INDEX NUMBERS REPRESENTING THE SPECIFIC
C     *                   ELEMENTS TO BE REPLACED
C     *   YN      AN ARRAY OF VALUES TO BE PATCHED BY PARABOLIC INTERP.
C     *   INT     THE NUMBER OF ELEMENTS WITHIN YN TO BE CONSIDERED IN THE
C     *                   PATCHING INTERPOLATION.
C     *   FIRST, SET THE NUMBER OF POINTS TO BE USED IN THE INTERPOLATION
      MAX = 3
C     *   FIND THE HALF-WAY POINT
      N = INT / 2
C     *   EXAMINE IN TURN EACH OF THE FIVE POINTS FOR OMISSION
      DO 100 NN = 1, 5
C     *   IF THE INDICATED OMISSION IS ZERO, SKIP IT.
      IF( MO(NN) ) 100, 100, 5
    5 NEXT = MO(NN)
C     *   INITIALIZE TO ZERO THE NUMBER OF POINTS SELECTED
      KOUNT = 0
C     *   INITIALIZE TO ZERO THE NUMBER OF STEPS TO THE LEFT AND TO THE
C     *           RIGHT OF THE OMITTED POINT
      JL = 0
      JR = 0
C     *   NOW TEST TO SEE IF THE OMITTED POINT IS IN THE LEFT OR RIGHT
C     *           SIDE OF THE DATA
      IF( NEXT - N )  15, 10, 10
C     *
C     *   PREPARE TO CHECK POINTS TO THE LEFT OF THE OMITTED POINT
   10 JL = JL + 1
      INDEX = NEXT - JL
C     *   QUESTION - HAS THIS POINT EXCEEDED THE LIMITS OF THE DATA
C     *                   IF SO, ADD A POINT TO THE RIGHT INSTEAD
      IF(INDEX) 15, 15, 11
C     *   QUESTION - IS THE POINT BEING CHECKED IN THE LIST OF
C     *                   OMITTED POINTS.   IF SO, CHECK THE NEXT ONE.
   11 DO 12 I = 1, 5
      IF( MO(I) - INDEX )12, 10, 12
   12 CONTINUE
C     *   COUNT, SAVE, AND TEST FOR COMPLETION
      KOUNT = KOUNT + 1
      ISAVE(KOUNT) = INDEX
      IF(KOUNT-MAX) 15, 30, 30
C     *
C     *   PREPARE TO CHECK POINTS TO THE RIGHT OF THE OMITTED POINT
   15 JR = JR + 1
      INDEX = NEXT + JR
C     *   QUESTION - HAS THIS POINT EXCEEDED THE LIMITS OF THE DATA
C     *                   IF SO, ADD A POINT TO THE LEFT INSTEAD
      IF( INDEX - INT ) 16, 16, 10
C     *   QUESTION - IS THE POINT BEING CHECKED IN THE LIST OF
C     *                   OMITTED POINTS.  IF SO, CHECK THE NEXT ONE.
   16 DO 17 I = 1, 5
      IF(MO(I) - INDEX) 17, 15, 17
   17 CONTINUE
C     *   COUNT, SAVE, AND TEST FOR COMPLETION
      KOUNT = KOUNT + 1
      ISAVE(KOUNT) = INDEX
      IF(KOUNT-MAX) 10, 30, 30
C     *
C     *   NOW OBTAIN THE VALUES TO BE USED IN DETERMINING THE COEFFICIENTS
```

```
C    *          OF THE PARABOLA
C    *
C    *     NOTE -  THIS VERSION PROVIDES AN EXACT FIT THROUGH 3 POINTS
   30 X1 = FLOATF( ISAVE(1) )
      X2 = FLOATF( ISAVE(2) )
      X3 = FLOATF( ISAVE(3) )
      I  = ISAVE(1)
      Y1 = YN(I)
      I  = ISAVE(2)
      Y2 = YN(I)
      I  = ISAVE(3)
      Y3 = YN(I)
C    *
C    *   DETERMINE THE VALUES FOR THE COEFFICIENTS Y=A0+A1*X+A2*X*X
      A2 = ( (Y1-Y2)/(X1-X2) - (Y1-Y3)/(X1-X3) ) / (X2-X3)
      A1 = (Y1-Y2) / (X1-X2) - A2 * (X1+X2)
      A0 = Y1 - A1 * X1 - A2 * X1 * X1
      X = FLOATF(NEXT)
      YN(NEXT) = A0 + A1 * X + A2 * X * X
  100 CONTINUE
      RETURN
      END
      FUNCTION SIM( A, N, M, H )
C    *     SIMPSONS RULE INTEGRATION.  REF - NUMERICAL METHODS IN
C    *     ENGINEERING, SALVADORI + BARON, 1952, PAGES 72 - 75
C    *   A     THE ARRAY OF VALUES
C    *   N     THE STARTING ELEMENT WITHIN A
C    *   M     THE LAST ELEMENT OF A TO BE INTEGRATED
C    *   H     THE STEP SIZE ( WIDTH OF VERTICAL STRIP OF HEIGHT A(I) )
      DIMENSION A(10)
      L = M - N
      I = L / 2
      L = L - 2 * I
      IF( L ) 1, 2, 1
    1 M = M - 1
    2 SUM = 0.0
      DO  3 I = N, M
      SUM = SUM + A(I)
    3 CONTINUE
      NS =  N + 1
      DO  4 I = NS,  M, 2
      SUM = SUM + A(I)
    4 CONTINUE
      SUM = ( SUM + SUM - A(N) - A(M) ) * H / 3.0
      IF(L) 5, 6, 5
    5 M = M + 1
      SUM = SUM + 0.5 * H * ( A(M) + A(M-1) )
    6 SIM = SUM
      RETURN
      END
      SUBROUTINE COMCC
      EQUIVALENCE                ( SS(10), ND       ), ( SS(20), A1       )
     1, ( SS( 1), INT      ), ( SS(11), ALPHA    ), ( SS(21), AREAX    )
     2, ( SS( 2), NOCH     ), ( SS(12), P        ), ( SS(22), VALUE1   )
     3, ( SS( 3), PCAP     ), ( SS(13), E        ), ( SS(23), KLANK    )
     4, ( SS( 4), TAU      ), ( SS(14), PINE     ), ( SS(24), KOUNT    )
     5, ( SS( 5), DT       ), ( SS(15), ALDER    ), ( SS(25), LL       )
     6, ( SS( 6), R        ), ( SS(16), BIRCH    ), ( SS(26), AREAZ    )
     7, ( SS( 7), DM       ), ( SS(17), TERM1    ), ( SS(27), EXPCT    )
```

```
     8, ( SS( 8), TD       ), ( SS(18), AREA1    ), ( SS(28), CEDAR, C )
     9, ( SS( 9), RHO      ), ( SS(19), A2       ), ( SS(29), TERM2    )
      EQUIVALENCE             ( SS(30), AREA2    ), (SS(31), VALUE2    )
     1, ( SS(  41), XN(1)  ), ( SS( 941), TN(1)  ), ( SS(1251), PC(1)  )
     2, ( SS( 341), YN(1)  ), ( SS(1241), MO(1)  ), ( SS(1351), HOL(1) )
     3, ( SS( 641), ZN(1)  ), ( SS(1246), MC(1)  ), ( SS(1361),BOSH(1) )
      COMMON  SS
      DIMENSION XN(300), YN(300),  ZN(300),  TN(300),  MO(5),  MC(5)
      DIMENSION PC(100), HOL(10),  BOSH(100), SS(1500)
C     THE ARRAY IJKLMN IS INTENDED TO BE USED AS A PATCHING AREA
      DIMENSION   IJKLMN(50)
C   *     COMPUTE EXPONENTIALLY CORRECTED COUNTS
   16 CEDAR =  0.000001 * P
      DO 17 I = 1, INT
      ZN(I) = YN(I) * EXPF( CEDAR * TN(I) )
   17 CONTINUE
C   *     COMPUTE EQUATION (2)
      EXPCT = EXPF( C * TN(1) )
      AREA2 =(A1*EXPCT*(TN(1)-1.0/C) + A1/C )/C   + A2 / C  *
     1 (EXPCT* ( (TN(1)-2.0/C)*TN(1) + 2.0/C/C ) - 2.0/C/C )
      TERM2 = YN(INT) * 1000000.0 * EXPF( CEDAR * TN(INT) )
     1        / ( ALPHA - P )
      AREA2 = SIM ( ZN, 1, INT, BIRCH )
      VALUE2 = AREA2 + AREA2 + TERM2
      RETURN
      END
```

Appendix V

ACCELERATOR OPERATION

A description of the KAMAN pulsed neutron source tube and the accelerator set up for use with the subcritical assembly, has been given in Chapter V. Schematic diagrams of the electronic circuits and the pulse-forming networks are on file in the MITR Electronics Shop. For the benefit of the prospective operator of this equipment, the normal operating procedures are summarized below:

1. All cables between control racks, transformer and source tube are connected before energizing the equipment.

2. The various controls are adjusted as follows:

Filament, Ion Source, Target and Field Power:	OFF
Deuterium Replenisher Current:	CCW* or previous setting
Oscilloscope power:	OFF
All adjustable High Voltages:	CCW*
Pulse Mode:	Continuous manual
Pulse Spacing:	1 sec

3. The power cord is connected.

4. The filament and 'scope power are turned ON.

5. Replenisher current is adjusted to about 1.1 amp or to previous setting.

6. The pressure is allowed to stabilize for several minutes. The pressure indicator is adjusted to $(18 \pm 3)\ \mu A$ by manipulating the replenisher current. This indicator must not be allowed to exceed full scale. The pressure responds very slowly, so changes

*Counter clockwise.

in replenisher current should be made in steps of 0.05 amp or less, allowing pressure to stabilize each time.

7. After a delay of about 7 minutes, the HVREADY light comes on.

8. The Ion Source supply is turned ON and adjusted to about 2.5 to 3.0 KV.

9. The Time Analyzer (TMC) unit is put on COUNT so that the source trigger is ON.

10. The oscilloscope is connected to ION SOURCE CURRENT and the manual push-button (on Tektronix 162 Waveform Generator) is depressed intermittently and the shape of the waveform on the 'scope is examined:

Proper waveform:

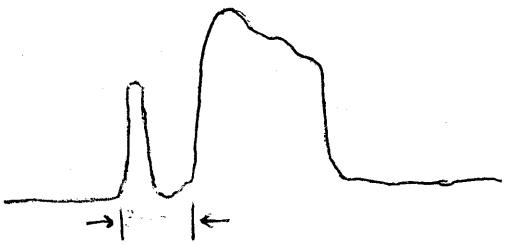

D_2 Pressure too low:

D_2 Pressure too high:

Note: The target voltage should not be run on if pressure is too high.

Observation of the Ion-Source current waveform gives running information on deuterium pressure. The pressure meter is inoperative during machine-pulsing.

11. The Target Supply is turned ON (one switch on the main rack and one on the Supply). Target supply voltage is run up slowly to about 3 KV.

12. The 'scope is connected to TARGET VOLTAGE through the 4 : 1 divider.

13. The manual push-button is again depressed to check target voltage waveform:

Proper Waveform:

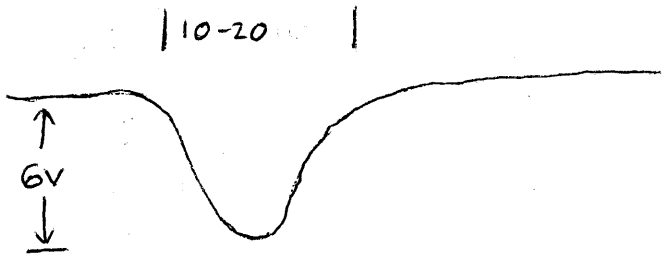

14. The D_2 pressure is rechecked and adjusted, if necessary.

15. The control on Tektronix 162 Waveform Generator is switched to RECURRENT PULSING.

16. Monitoring the Target Voltage on the 'scope, the voltage is slowly increased to about 5.5 KV or until the waveform indicates 100 KV peak, whichever is first. The calibration of the 'scope scale must be checked.

17. The Ion Source waveform is checked again and the deuterium pressure is adjusted, if necessary (the pressure meter should read ZERO during operation).

18. The pulsing conditions are selected and the experimental run may be begun.

The Ion Source voltage and the Target voltage are mutually adjusted so as to optimize neutron output as indicated by the rate of data collection in the analysis channels of the time analyzer. During the run, a periodic check is made of the deuterium pressure by monitoring the Ion Source current. The Target voltage should also be checked from time to time. If, at any stage during the run, the data accumulation has to be temporarily suspended or the Source

Trigger output is to be stopped, the Target voltage must first be lowered down to zero. Too long continuous runs tend to heat up the source tube; a check on the temperature can be kept by attaching a thermocouple to the housing of the tube.

19. On shutdown, first the Target Power supply and then the Ion Source Power supply are turned down and OFF. The deuterium current may be turned down to zero. The filament and 'scope power are switched OFF. A check should be made of radiation levels before entering the target area, although in pulsed operation, this is seldom of concern.